2021

Topics in Quantum Quench and Entanglement

Sinong Liu
University of Kentucky, snongliu@outlook.com
Author ORCID Identifier:
https://orcid.org/0000-0002-8338-8199
Digital Object Identifier: https://doi.org/10.13023/etd.2021.222

STUDENT AGREEMENT:

I represent that my thesis or dissertation and abstract are my original work. Proper attribution has been given to all outside sources. I understand that I am solely responsible for obtaining any needed copyright permissions. I have obtained needed written permission statement(s) from the owner(s) of each third-party copyrighted matter to be included in my work, allowing electronic distribution (if such use is not permitted by the fair use doctrine) which will be submitted to UKnowledge as Additional File.

I hereby grant to The University of Kentucky and its agents the irrevocable, non-exclusive, and royalty-free license to archive and make accessible my work in whole or in part in all forms of media, now or hereafter known. I agree that the document mentioned above may be made available immediately for worldwide access unless an embargo applies.

I retain all other ownership rights to the copyright of my work. I also retain the right to use in future works (such as articles or books) all or part of my work. I understand that I am free to register the copyright to my work.

REVIEW, APPROVAL AND ACCEPTANCE

The document mentioned above has been reviewed and accepted by the student's advisor, on behalf of the advisory committee, and by the Director of Graduate Studies (DGS), on behalf of the program; we verify that this is the final, approved version of the student's thesis including all changes required by the advisory committee. The undersigned agree to abide by the statements above.

Sinong Liu, Student

Dr. Sumit R. Das, Major Professor

Dr. Christopher Crawford, Director of Graduate Studies

TOPICS IN QUANTUM QUENCH AND ENTANGLEMENT

DISSERTATION

A dissertation submitted in partial
fulfillment of the requirements for
the degree of Doctor of Philosophy
in the College of Arts and Sciences
at the University of Kentucky

By
Sinong Liu
Lexington, Kentucky

Director: Dr. Sumit R. Das, Professor of Physics and Astronomy
Lexington, Kentucky
2021

https://orcid.org/0000-0002-8338-8199

ABSTRACT OF DISSERTATION

TOPICS IN QUANTUM QUENCH AND ENTANGLEMENT

The dissertation includes two parts.

In Part I, we study non-equilibrium phenomena in various models associated with global quantum quench. It is known that local quantities, when subjected to global quantum quench across or approaching critical points, exhibit a variety of universal scaling behaviors at various quench rates. To investigate if similar scaling holds for non-local quantities, we consider the scaling behavior of circuit complexity under quantum quench across the critical massless point in Majorana fermion field theory of the one-dimensional integrable transverse field Ising model and find it obeys such scaling. To investigate if similar scaling holds for non-relativistic theories, we test various solvable critical quantum quench protocols in a theory of fermions in a harmonic oscillator potential and find local quantities as well as entanglement entropy obeys different scaling behaviors at different quench rates. We study quantum quench in the $c = 1$ matrix model which is holographically dual to two-dimensional string theory. Unlike higher dimensional holographic setups where quantum quench leads to black holes, the emergent spacetime in this model generically develops cosmological singularities at late times.

In Part II, we expand the proposal that target space entanglement provides a precise notion of entanglement in the bulk gravitational duals of Dp brane theories, which was shown in a gauge fixed formalism. We developed a gauge invariant description of target space entanglement in these theories and derived path integral expressions for the entanglement entropy which can be used in numerical calculations.

KEYWORDS: Quantum Quench, Entanglement Entropy, Matrix Model, Circuit Complexity, Holography

Sinong Liu

June 16, 2021

TOPICS IN QUANTUM QUENCH AND ENTANGLEMENT

By
Sinong Liu

Sumit R. Das
Director of Dissertation

Christopher Crawford
Director of Graduate Studies

June 16, 2021

Dedicated to
my dearest
Ms. Jinru Chen, Ms. Xiaoyan Pan, and Mr. Tanqiang Liu.

ACKNOWLEDGMENTS

I am deeply grateful to my advisor, Sumit Das. Being his student is one of the luckiest things that have happened to me in my life. I learnt from him how beautiful physics can be and how much one can love physics. I will remember his advice and benefit from them in the rest of my life. The past five years mentored by him is the best five years I have experienced till now, for that I have been full of curious and hope every day, and have been feeling better everyday than yesterday.

I am also very grateful to my undergraduate supervisor, Ling-Yan Hung. It is Janet who brought me to this amazing theoretical physics world. Because of her I started to try any topic that interests me. Her comment on being a happy chimpanzee in physics world touched me a lot. I would like to spend the rest of my life learning how to be a chimpanzee that happily plays with physics.

I thank them for always being willing to trust me, encourage me, and let me try, especially when sometimes I cannot trust myself. I thank them for letting me realize that I also have potential. I thank them for changing my life by physics – They make my life though still tough, never frustrating.

I would like to thank all my graduate course instructors, Christopher Crawford, Anatoly Dymarsky, Michael Eides, Susan Gardner, Richard Hill, Ribhu Kaul, Ganpathy Murthy, Alfred Shapere, Douglas Strachan and Joseph Straley. Thank them for sharing their thoughts of physics, correcting my misunderstandings of physics, and giving me precious advice (on both career and life). I would also like to thank Diane, Libby and Suann, for helping me get familiar to the new enviroment step by step. That really means a lot to me, considering that I am such an idiot when it comes to the world without physics. More thanks for organizing online seminar and colloquium during the tough time. Not only have those activities enlightened me, but

they also prevent me from becoming the lonely experimental rodents (whose brains were inreversibly damaged, according to a recent science research, after a three-month quarantine).

I thank my collaborators Shaun Hampton, Ashish Kakkar, Anurag Kaushal, Gautam Mandal, Sandip P. Trivedi, Allic Sivaramakrishnan, Arpan Bhattacharyya and Long Cheng. Studying physics with them is a very happy thing.

Thank my academic brother Animik Ghosh, my peers Xingchen Li, and my colleagues Qing Chen and Xinshuai Yan for their support in the past five years (Indeed any of them have saved me from rolling in the deep at least twice). For me their friendship are very precious. It becomes more precious given that it is really hard to make new friends as we grow older.

From my undergraduate days I would like to thank my undergraduate course instructor Yongshi Wu, Zhifang Lin, Jianjun Xu, and Xuguang Huang for all the theoretical physics preparations. Thank my dorm-mate Run Wen, Tongtong Zhao and Tianyi Chen, and my undergraduate peers Yujiao Cao, Yun Huang, Xiuyun Jiang and Yuqi Shi. Six years ago they stayed with me when I wrote my undergraduate thesis. So do they now (though it might be partially because some of them are in GMT+8 time zone). Also thank Shangnan Zhou, Yixu Wang, Yikun Jiang and Yu Zhang. It is good to meet them again in TASI after I graduated. Thanks for the adventure with them in physics world as well as in Rocky Mountain. The snow there was so beautiful.

At last I want to thank my fate that has been entangled with physics since ten years ago. Thank her for having let me talk to so many beautiful minds. Thank her for letting me be able to continue my research for the next two years. From the depth of my heart, I hope I will still be working with physics two years, ten years, even fifty years later, as what I am doing today. I hope this hope will come true.

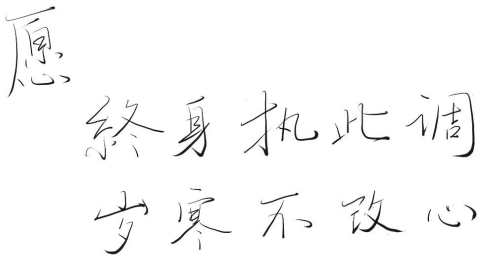

A particular thank goes to Shirley Chen (my dear Aunt Rui). We have celebrated four Chrismas holidays together since I started my doctoral program in US (Not five because of the pandemic). For me, where she lives is like another home of mine.

I dedicate this dissertation to my grandma, my mom and my dad, though none of them can read English. They were my first and only readers at very beginning. They will be my best readers forever.

TABLE OF CONTENTS

LIST OF FIGURES

Chapter 1
Introduction

Theoretical physicists have a long history in studying equilibrium[1] systems and have developed systematic methods to understand equilibrium phenomena. However, equilibrium is only an ideal situation. There are many natural phenomena which are far from equilibrium. One class of such phenomena involve systems in excited states which then relaxes to equilibrium: transport properties are examples of process which probe such out-of-equilibrium phenomena. Another class involve systems whose parameters vary in time. Our current understanding of non-equilibrium phenomena in the quantum regime is rather rudimentary. However recent progress in cold atom experiments has triggered a lot of interest in this field. A major part of this dissertation deals with studies of some aspects of quantum non-equilibrium behavior.

In many-body systems and quantum field theories, quantum quench describes a process during which a system, initially in equilibrium, is driven out of equilibrium by some external time-dependent coupling. Quantum quench is therefore a useful theoretical and experimental tool to study non-equilibrium phenomena. The first three papers on which this dissertation is based deals with aspects of quantum quench dynamics.

One important problem which is studied utilizing quantum quench is thermalization. Here thermalization means local correlators (as well as nonlocal quantities such as entanglement entropy of a subregion of the system) starting from a pure state, asymptotically approach their expectation values in grand canonical ensemble. While this is expected to happen in generic interacting systems, the process of how this happens is still not well understood. Also, there are some systems which do not thermalize such as integrable many-body systems and systems which exhibit many-body localization[1–3].

Another important problem which can be studied using quantum quench relates to critical dynamics. Here one starts with a gapped phase and then a time dependent parameter later takes it across a quantum critical point (gapless phase) or makes it approach a critical point. Such quench protocols are called critical quenches. In equilibrium, a critical point is characterized by universality. Near a critical point, various physical quantities scale as powers of the difference of the parameter from its critical value with exponents which are the same for a large class of microscopically different systems. The underlying mechanism for such universality is well understood. The exponents can be evaluated utilizing renormalization group. While one might expect that a similar universality should hold in critical quench, there is no general theoretical framework like the renormalization group which holds for such non-equilibrium situations. Over the past several decades theoretical research in this area has concentrated on studying a variety of models which can be investigated analytically or

[1] In this dissertation, equilibrium (system) means (a system) in a steady state unless otherwise stated explicitly.

numerically, and using simplifying (and sometimes drastic) assumptions to draw more general conclusions [4].

The earliest investigation on critical quench was done by T. Kibble in 1970s when studying defect formation in cosmology [5], and was later extended by W. Zurek in 1980s to condensed matter systems [6]. They considered systems driven through a critical point by a time-dependent source whose rate of change is slow compared to the initial energy gap. Initially the system evloves adiabatically. As the system approaches the critical point, the adiabatic approximation fails to describe the time evolution of the physical quantities. By making some perhaps drastic assumptions, Kibble and Zurek showed that certain universal properties hold. For example quantities like one- or two-point functions scales with the quench rate with exponents determined in terms of the equilibrium critical exponents of the critical point. This is called Kibble-Zurek scaling. Even though these conclusions were derived using rather drastic simplifying assumptions, the scaling behavior turns out hold in both analytic and numerical calculations in theoretical models where the quench process is studied without these assumptions. There are also indications that they hold in some recent experiments. This has motivated a lot of recent work aimed at a better understanding of the origin of this scaling.

It turns out that universal scaling, with different exponents, also hold when the quench rate is fast, as shown in [7–10]. In their investigation they proved that in a general relativistic field theory, the quantum quench with a rate fast compared to the initial energy gap but slow compared to the UV scale (e.g. lattice spacing), results in the renormalized quantities scaling with the quench rate with the exponents again determined by equilibrium critical exponents (different from slow quench ones). The mechanism of this scaling behavior is understood by utilizing the properties of relativistic theories, and the general results have been explicitly verified in many theoretical models where the exact quench dynamics can be studied.

Though these scaling behaviors are quite generic, explicit investigations have been mainly launched in solvable models subject to solvable quench protocols. Moreover, the physical quantities that have been most extensively investigated are local quantities such as one- or two-point functions. In comparison, much less is known about the scaling behaviors of non-local quantities such as entanglement entropy of a subregion or complexity of a quantum state (a measure of how difficult to prepare a quantum state). However, these non-local quantities actually characterize properties of a quantum state that are not easily captured by correlation functions. Therefore it is important to study if scaling holds for such quantities. Earlier studies by other authors have found evidence for scaling properties of entanglement entropy in both slow and fast quench regimes [11]. In this dissertation, we investigate whether the complexity of a quantum state produced by quantum quench also show similar behavior: We considered the simplest model of a quantum critical phase transition – the one-dimensional transverse field Ising model, and found that universality holds in both slow and fast quench regime. This is based on the paper [12].

Many interesting systems which are studied in condensed matter physics or cold atom physics are non-relativistic. In these theories, Kibble-Zurek scaling is expected to hold. However, the status of fast quench scaling in these theories is unclear, though

in specific models similar scaling behavior to relativistic systems is found due to the existence of an effective finite velocity of signal propagation. In this dissertation we study such a non-relativistic system which has direct relevance to experiments: one-dimensional non-relativistic fermionic field theory in external harmonic oscillator potential with time-dependent frequency. This part of the dissertation is based on [13]. Here we found quench protocols which are exactly solvable and showed that there is scaling behavior both for slow and fast quenches. For slow quenches, the result is consistent with Kibble-Zurek scaling. And the fast quench scaling is consistent with perturbation theory.

When quantum quench happens in a quantum field theory holographically dual to some gravitational theory, thermalization has an interesting dual interpretation. In such theories, the dynamics of the field theory is equivalently described by a gravitational theory living in one higher dimension. The additional dimension is "emergent". As a result, quantum quench in the quantum field theory also leads to a time-dependent geometry in the dual gravitational theory.

The most well-known example of holographic duality is the AdS/CFT correspondence [14]. It conjectures that a certain gravitational theory living on $(d+1)$-dimensional asymptotically anti-de Sitter spacetime is dual to some deformed conformal field theory (which does not contain gravity) on its d-dimensional boundary, where the additional dimension is identified with an energy scale in the field theory. Therefore the quench, acting on the conformal field theory, behaves as a time-dependent boundary condition in the AdS bulk. Usually, the resulting time-dependent geometry describes the formation of a black hole [15]. The black hole emits Hawking radiation, and simultaneously absorbs the Hawking radiation bounced back by the boundary, as well as the later gravitational radiation due to the quench. Eventually quantum quench leads to a steady black hole state in equilibrium[2] with the thermal environment outside the horizon. From the view of CFT side, this process is a thermalization.

However, in other well studied examples of holography this is not expected to happen. One example is the correspondence between the singlet sector of $(0+1)$-dimensional gauged quantum mechanics of a single $N \times N$ Hermitian matrix model, called $c = 1$ matrix model, and the $(1+1)$-dimensional critical string theory [16]– It is generally believed that the singlet sector in fact does not have a black hole. One evidence for this belief is that an incoming tachyon pulse does not produce a black hole [17]. However, quantum quench should lead to a time-dependent geometry. In a case like this, it is important to understand the nature of this emergent spacetime. To approach this goal, the nature of the time-dependent geometries produced by a quantum quench in matrix quantum mechanics is investigated in this dissertation (based on [18]). We found quench protocols for which the quantum dynamics can be studied exactly and the results could be used to determine the emergent spacetime. We found that unless the quench protocol is finely tuned, the spacetime has spacelike regions of large coupling in the gravity description at late times. A dual interpretation in terms of a smooth geometry however holds only when the bulk coupling is weak.

[2]The equilibrium here means thermal equilibrium.

Therefore in this region smooth spacetime interpretation fails, even though the time evolution of the underlying matrix quantum mechanics is well defined. This kind of scenario could have implications for higher dimensional models of holographic cosmologies.

The final part of this dissertation deals with a different subject: the role of entanglement in holography. It is widely believed that classical spacetime is an emergent description of some underlying microscopic quantum mechanical theory [19]. In particular, a smooth spacetime is rather an effective description (in the approximate semiclassical notion) of the entanglement structure between quantum degrees of freedom. A great amount of evidence has been found in the most widely known example of holography, AdS/CFT correspondence, to support this idea. The idea is that states which highly entangle in different spatial regions of the boundary field theory have dual description in terms of a smooth higher dimensional space-time.

However, there are examples of the holographic correspondence where the dual theory has no space at all. The earliest example of holography which predates the AdS/CFT correspondence of this type: this is the duality of the $c = 1$ matrix model mentioned above with string theory in two dimensions which contain gravity. Another example is the BFSS matrix model. It is natural to conjecture that in these examples, the emergence of a smooth dual space-time is related to entanglement in target space of the quantum mechanical system. More generally, even when the dual theory is a field theory, target space entanglement should play a key role.

This necessitates a precise understanding of entanglement in target space. Some formal properties of target space entanglement have been studied in [20].

Recently, [21] proposed a precise formalism to define and study target space entanglement in a class of holographic models arising in string theory. They argued that the target space entanglement in the gauge field theory on the boundary provides a precise and exact notion which reduces to the notion of entanglement between spatial regions of the gravitational dual in the semiclassical regime. This work, however, developed the notion of target space entanglement in a specific gauge of the gauge theory. In this dissertation, based on [22], I provide a completely gauge invariant definition of target space entanglement and study some of its properties. The connection of this to emergence of smooth space-time is under current study.

In the rest of this chapter we introduce relevant concepts. The outlines and a summary of this dissertation is in section 1.4.

1.1 Overview of Quantum Quench

Quench means rapid cooling, a heat treating process to obtain certain properties of materials. In quantum physics, a quantum quench is used to describe a process, during which a system is driven from equilibrium by a time-dependent coupling. To be concrete, one can consider a quantum field theory initially at ground state, with Hamiltonian containing a time-dependent parameter $\lambda(t)$. $\lambda(t)$ varies during a time scale δt and approaches some constant values, λ_0 and $\lambda_1 \equiv \lambda_0 + \delta\lambda$, at early and

late times, respectively, resulting in time-independent initial and final Hamiltonians. This is called a global quench.

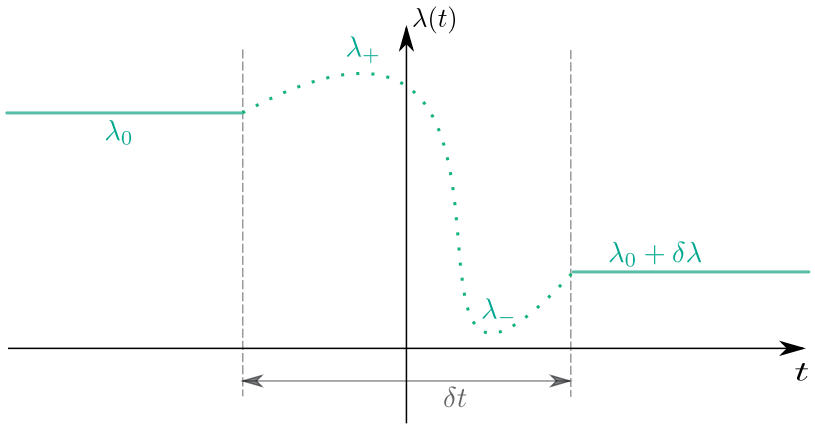

Figure 1.1: A typical global quantum quench protocol, described by time-dependent parameter $\lambda(t)$.

Quantum quench has attracted recent attention because it provides a possible way to study problems related to non-equilibrium phenomena – The ground state of initial Hamiltonian finally becomes an excited state of the new Hamiltonian at late times. Usually after a long time, the system thermalizes and we would like to understand the way this happens. The study of thermalization by means of quantum quench can be also experimentally studied – One may refer to the experiments with cold atom systems as examples.[3]

1.1.1 Scaling Behaviors at Critical Point with various Quench Rates

Apart from its use to understand thermalization, the study on quench-relevant problems is also motivated by efforts to understand critical dynamics, i.e. the universal scaling behaviors at critical points.[4] When the time-dependent coupling brings the system close to the critical point, e.g.

$$S = S_{critical} - \int \mathrm{d}t \int \mathrm{d}^{d-1}x \ \lambda(t)\mathcal{O}_\Delta(\vec{x}, t) \tag{1.1}$$

$$\lambda(t) = \lambda_0 + \delta\lambda \cdot F(t/\delta t) \tag{1.2}$$

where $\lambda(t) \to 0$ at some time and the theory becomes critical, the evolution of the system, as a response, is expected to follow the universal scaling laws. These universal scaling behaviors have been obeserved in expectation values of coupled observables $\langle \mathcal{O}_\Delta \rangle$, correlation functions, and entanglement entropy.

Different universal scaling are known to hold in different regimes characterized by the quench rate.

[3] Several experimental references could be found in [23–25].

[4] A review can be found in [26]

- **Slow quench** $\delta t \gg \lambda_0^{-1/(d-\Delta)}$

  In slow quench regime, the change rate of the energy gap is slow compared to the initial gap. Therefore the time evolution of the system should be adiabatic at early times. However, as the time-dependent parameter approaches critical point, the instantaneous energy gap $E_{gap}(t)$ becomes small. As a result the Landau criterion for adiabaticity

$$\frac{1}{E_{gap}(t)^2}\frac{\mathrm{d}E_{gap}(t)}{\mathrm{d}t}\bigg|_{t=t_{KZ}} \ll 1 \tag{1.3}$$

  is no longer satisfied and the adiabatic approximation is no longer a good one. It was assumed by Kibble and Zurek that soon after the time when the LHS of (1.3) is at the order 1, which is called Kibble-Zurek time t_{KZ}, the system becomes diabatic – all physical quantities remain unchanged since $t = t_{KZ}$. [5] Furthermore, they assumed that when the system is in diabatic regime, the instantaneous correlation length at Kibble-Zurek time, ξ_{KZ}, is the only length scale[6] in the problem. Then the universal scaling behaviors are entirely determined by powers of ξ_{KZ}. Here the power can be easily found via dimensional analysis. For example, after entering diabatic regime ($t > t_{KZ}$), one-point function $\langle \mathcal{O}_\Delta \rangle$ scales as

$$\langle \mathcal{O}_\Delta \rangle \sim \xi_{KZ}^{-\Delta} \tag{1.4}$$

  where Δ is the conformal dimension of operator $\mathcal{O}_\Delta$.

  It is remarkable that though Kibble and Zurek's assumptions are crude, the scaling behaviors predicted appear to be correct.

- **Abrupt/instantaneous quench**[7] $\delta t = 0$

  In the instantaneous quench regime, we consider the scaling behaviors of a system that will be relevant to this dissertation – the $1+1$-dimensional time-dependent system with Hamiltonian of the system abruptly switch from a gapped one, H_0, to a critical one $H \equiv H_{CFT}$. The Heisenberg picture state which is the ground state of the initial gapped Hamiltonian, $|\psi_0\rangle$ could be approximated, for long distance properties, by the form [27–29]

$$|\psi_0\rangle \propto e^{-\tau_0 H}|B\rangle \tag{1.5}$$

  where $|B\rangle$ is a conformally invariant state in the $(1+1)$-dimensional conformal field theory H_{CFT} called a "boundary state" (i.e. the state obtained by performing an euclidean path integral on a half plane with conformally invariant boundary condition on the boundary), and τ_0 is proportional to the correlation

[5] All physical quantities remain unchanged from $t = t_{KZ}$ till a future time when the Landau Criterion is satisfied again.

[6] The correlation length ξ_{KZ} satisfies $t_{KZ} \sim \xi_{KZ}^z$, where z is the dynamical critical exponent.

[7] Here "abrupt" or "instantaneous" means the quench rate is fast compared to all scales in the problem including the UV scale.

length (or inverse mass gap) of the initial state $\lambda_0^{-1/(d-\Delta)}$. Then the universal scaling laws of one-point and higher point functions are given by boundary conformal theory. For example, when $x, t \gg \tau_0$ the one-point function and two-point function of local primary scalar operators are

$$\langle \mathcal{O}_\Delta(t) \rangle \sim \exp\left(-\frac{\pi\Delta}{2\tau_0} t\right) \tag{1.6}$$

$$\langle \mathcal{O}_\Delta(x,t)\mathcal{O}_\Delta(0,0) \rangle \sim \exp\left(-\frac{\pi\Delta}{2\tau_0} \times \min\{t, x/2\}\right) \tag{1.7}$$

respectively.[8]

- **Fast quench** $\Lambda_{UV}^{-1} \ll \delta t \ll \lambda_0^{-1/(d-\Delta)}$

  Universal scaling law has also been found in intermediate quench regime when the field theory is relativistic [7–10]. Here "intermediate" means that the quench rate is fast compared to inverse physical mass scale $\lambda_0^{-1/(d-\Delta)}$ while slow compared to UV cutoff Λ_{UV}^{-1}. In such a regime the expectation value of observable, $\mathcal{O}_\Delta(\vec{x}, t)$, can be computed via perturbation theory, i.e.

$$\begin{aligned}\langle \mathcal{O}_\Delta(\vec{x},t) \rangle = \langle \mathcal{O}_\Delta(\vec{x},t) \rangle_{\lambda_0} - \delta\lambda \int_{-\infty}^{t} \mathrm{d}t' F(t/\delta t) \int \mathrm{d}^{d-1}x' G_{R,\lambda_0}(\vec{x},t;\vec{x'},t') \\ + \mathcal{O}(\delta\lambda^2) + ...\end{aligned} \tag{1.8}$$

  where the Green's function is given by

$$G_{R,\lambda_0}(\vec{x},t;\vec{x'},t') = i\Theta(t-t')\langle \Big[\mathcal{O}_\Delta(\vec{x},t), \mathcal{O}_\Delta(\vec{x'},t')\Big] \rangle_{\lambda_0} \tag{1.9}$$

  Now we turn on the quench at $t = 0$ and consider the late-time response at $t = \delta t$ such that $|t - t'| < \delta t$. Because 1) in the relativistic theories, Green's function should satisfy causality ($|\vec{x} - \vec{x'}| \leq |t - t'|$), and 2) in the limit $\lambda_0^{1/(d-\Delta)} \cdot \delta t \ll 1$, Green's function of the field theory is indistinguishable from that of a UV conformal field theory, we have

$$G_{R,\lambda_0}(\vec{x},t;\vec{x'},t') \approx G_{R,CFT}(\vec{x},t;\vec{x'},t') \sim \Big|(t-t')^2 - (\vec{x}-\vec{x'})^2\Big|^{-\Delta} \sim \delta t^{-2\Delta} \tag{1.10}$$

  Thus, the universal scaling behavior in fast quench regime is controlled by combinations of the scale of quench coupling $\delta\lambda$ and the quench rate δt, which could be figured out by dimensional analysis.

[8] For two-point function we assume that $\langle \mathcal{O}_\Delta \rangle \neq 0$ s.t. the boundary scaling dimension of the leading boundary operator to which $\mathcal{O}_\Delta$ couples, Δ_b, vanishes. This is in order to make it more clear that the scaling behavior of two-point function is related to the light-cone. The general scaling behavior when $t < x/2$ is $\sim \exp\left(-\frac{\pi\Delta t}{\tau_0}\right) \exp\left(\frac{\pi\Delta_b}{2\tau_0}(2t - x)\right)$. One can refer to [27, 28] for details.

1.1.2 Quantum Quench in Holographic Setup

The study of quantum quench problems in gauge theories also sheds light on gravitational theories via gauge/gravity duality. Gauge/gravity duality is a strong/weak correspondence motivated by string theory, which conjectures an equivalence between gauge theories and gravitational theories.[9] A typical example of gauge/gravity duality is AdS/CFT correspondence [14].

AdS/CFT correspondence is based on holographic principle. In particular, it is conjectured that a certain gravitational theory on $(d+1)$-dimensional AdS spacetime is dual to some conformal field theory on its d-dimensional boundary. If one adds a source $\phi_0(x) = \phi_0(\vec{x}, t)$ for some gauge invariant operator with conformal dimension Δ to the CFT action at the boundary, i.e.

$$S'_{CFT} = S_{CFT} - \int \mathrm{d}^d x \phi_0(x) \mathcal{O}_\Delta(x) \tag{1.11}$$

then in the regime where the bulk theory is weakly coupled while the boundary theory is strongly coupled, the AdS/CFT correspondence has the mathematical statement that [31]

$$\left\langle \exp \int \mathrm{d}^d x \phi_0(x) \mathcal{O}(x) \right\rangle_{CFT} = e^{-S_{SUGRA}[\phi]} \tag{1.12}$$

which relates the generating function of CFT to classical supergravity (or string theory) action. Note that the source is related to the boundary value of scalar field ϕ which has mass $m^2 = \Delta(d - \Delta)$ in AdS spacetime. To be concrete, one can consider the AdS spacetime near the boundary

$$\mathrm{d}s^2 = \frac{1}{z^2} \left(\mathrm{d}z^2 + g_{ij}(x, z) \mathrm{d}x^i \mathrm{d}x^j \right) \tag{1.13}$$

where $x = (\vec{x}, t)$, z is the radial coordinate of AdS spacetime, and the boundary of AdS is at $z = 0$. Then near the boundary the scalar field ϕ takes the form

$$\phi(\vec{x}, t, z) \sim z^{d-\Delta} \left[A(\vec{x}, t) + O(z^2) \right] + z^\Delta \left[B(\vec{x}, t) + O(z^2) \right] \tag{1.14}$$

The AdS/CFT correspondence claims that $A(\vec{x}, t)$ is identical to the source $\phi_0(\vec{x}, t)$. Also, $B(\vec{x}, t)$ is claimed to satisfy

$$\langle \mathcal{O}_\Delta \rangle_{CFT} = B(\vec{x}, t) + ... \tag{1.15}$$

where "..." depends on the theory we consider. Since for each primary operator in CFT there is a field in $(d + 1)$-dimensional bulk whose restriction to boundary is a source coupled to the operator, there are analogous asymptotic behaviors of vector current, metric, etc (with different exponents of z).

Now if we compared (1.11) with (1.1), one finds that the quench coupling $\lambda(t)$ can be regarded as a space-translation invariant source of the CFT on boundary (the critical action is chosen to be CFT now). Therefore, when the field theory has a

[9] For reviews one can see [30].

gravity dual, quantum quench becomes a time-dependent boundary condition in the bulk. When a quench in gauge boundary is turned on, it actually creates gravitational radiation that propagates from the boundary into the gravitational bulk. If the bulk is finite, the radiation usually results in the formation of a black hole horizon, which absorbs later radiations and increases the size of itself. However, the black hole, once formed, radiates. This effect is called Hawking radiation and leads to the evaporation of the black hole. Since AdS spacetime acts as a spatial box the two opposing processes will eventually leads to a balance and results in a static black hole.[10] In the boundary theory, this corresponds to a new equilibrium[11] after thermalization, i.e. the thermalization in the field theories usually corresponds to a black hole formation in their gravitational duals.[12]

The correspondence implies that difficult issues in the gravitational theories may be addressed by studying quantum quenches in the dual field theories or vice versa.

1.2 A bit of Quantum Entanglement

Quantum entanglement is a fundamental phenomenon in quantum systems. For a quantum system divided into two parts, the entanglement entropy of each subsystem gives a measure of entanglement between them.[13] In quantum mechanics, all information of the state is encoded in density matrix ρ, which is a semipositive-definite Hermitian operator with trace 1, such that the expectation value of an observable $\mathcal{O}$ is

$$\langle \mathcal{O} \rangle_\rho = \mathrm{Tr}(\mathcal{O}\rho) \tag{1.16}$$

If one is only interested in a subsystem A (not its complement $\bar{A}$), similar statement is still true for the density matrix ρ_A that encodes information of the state in the subsystem. ρ_A is called reduced density matrix, and it satisfies

$$\langle \mathcal{O}_A \rangle_{\rho_A} = \mathrm{Tr}(\mathcal{O}_A \rho_A) = \mathrm{Tr}\,(\mathcal{O}_A \rho) \tag{1.17}$$

where $\mathcal{O}_A$ is observable local to the subsystem A. Thus the reduced density matrix ρ_A is given by the partial trace of $\bar{A}$

$$\rho_A \equiv \mathrm{Tr}_{\bar{A}}\, \rho \tag{1.18}$$

Then the quantum entanglement can be quantified by von Neumann entropy of ρ_A, i.e.

$$S_A = -\,\mathrm{Tr}\, \rho_A \log \rho_A \tag{1.19}$$

[10] The Hawking radiation power is inverse proportional to the square of the mass of the black hole. This means that smaller black hole evaporates faster. Thus if the black hole formed by gravitational radiation is not large enough, the Hawking radiation will always dominate. In this case there will be no black hole eventually. In AdS the thermalization in the boundary theory usually leads to a stable black hole.

[11] The equilibrium here means thermal equilibrium.

[12] Examples can be found in [15, 32–45].

[13] For reviews, one can see [46].

Von Neumann entropy is a special case of Renyi entropies, which is a one-parameter entropy defined as

$$S_n \equiv \frac{1}{1-n} \log \operatorname{Tr} \rho_A^n \tag{1.20}$$

The $n \to 1$ limit is von Neumann entropy. Therefore Renyi entropies are sometimes treated as an intermediate step to obtain von Neumann entropy. The calculation of Renyi entropies can be performed by a replica trick and therefore by Euclidean path integral. In particular, the element of reduced density matrix ρ_A can be represented by a Euclidean path integral with proper boundary conditions (path ends in subregion A). Then the ingredient needed to compute n-th order Renyi entropy, $\operatorname{Tr} \rho_A^n$, is n copies of the path integral with the endpoint of each copy identified with the starting point of the next copy and integrated over subregion A. Thus, $\operatorname{Tr} \rho_A^n$ corresponds to a closed cyclic path integral with some constraints.

1.2.1 Many-Body Entanglement and Biparticle Fluctuations

For any reduced density matrix ρ_A, one can define modular Hamiltonian H_A

$$\rho_A \equiv \frac{1}{Z} e^{-H_A} \tag{1.21}$$

where Z is the partition function of the Gibbs state $Z = \operatorname{Tr} e^{-H_A}$. In quantum many-body system where Wick's theorem is satisfied, the correlation matrix C_A, which is the matrix of correlation functions in the subsystem A, also contains all information of the state ρ_A. Therefore one can represent von Neumann entropy, as well as Renyi entropies by correlation matrix C_A.

On the other hand, all the number distribution cumulants of particles, e.g. $\langle N_A \rangle$, $\langle (N_A - \langle N_A \rangle)^2 \rangle$, etc., are derivatives of a generating function

$$\chi(\lambda) = \operatorname{Tr} \rho_A e^{i\lambda N_A} \tag{1.22}$$

where N_A is the number operator in subsystem A. $\chi(\lambda)$ also encodes all information of the state, and can be expressed in terns of the correlation matrix C_A.

Thus, correlation matrix builds a bridge between entanglement entropies and number distribution cumulants

$$V_A^{(m)} \equiv (-i)^m \partial_\lambda^m \log \chi(\lambda) \big|_{\lambda=0} \tag{1.23}$$

In particular, for fermionic theory, one have von Neumann entropy [47, 48]

$$S_A = \sum_{k=1}^{\infty} \frac{(2\pi)^{2k} |B_{2k}|}{(2k)!} V_A^{(2k)} \tag{1.24}$$

where B_m are Bernoulli numbers. The leading order contribution is

$$S_A = \frac{\pi^2}{3} \left(\langle N_A^2 \rangle - \langle N_A \rangle^2 \right) \tag{1.25}$$

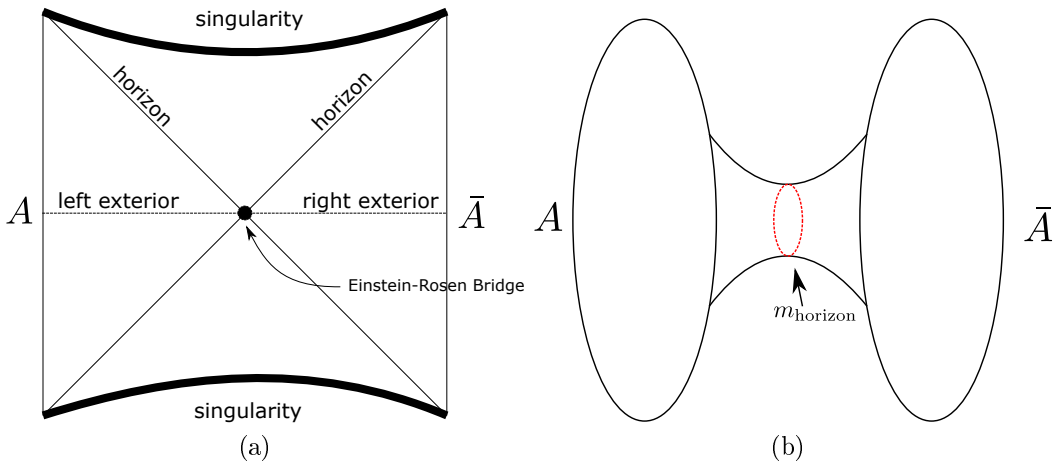

Figure 1.2: (1.2a) Penrose diagram of two-sided AdS black hole. The black dotted line is the Cauchy slice we consider. The thermal state lives on subregion A. (1.2b) The Einstein-Rosen bridge that connects the A and $\bar{A}$. The red dotted circle is the bifurcate horizon, which is the minimal surface between A and $\bar{A}$. The figures are based on figure 10 in [46].

1.2.2 Holographic Entanglement Entropy

Quantum entanglement in a quantum field theory may be quantified by extremal surfaces in the gravitational dual. In particular, for a conformal field theory, if one considers a Cauchy slice in its AdS bulk dual, it is conjectured that the von Neumann entropy of a subregion A in the boundary theory of the Cauchy slice is holographically determined by minimal codimension two surface with the same boundary in its bulk dual

$$S_A = \frac{\text{Area}(\gamma_A)}{4G_N} \tag{1.26}$$

where γ_A is the minimal surface in the bulk Cauchy slice with boundary ∂A, and G_N is Newton constant.

The holographic entanglement entropy formula (1.26) is known as Ryu-Takayanagi formula [49].[14] It is motivated by Bekenstein-Hawking entropy

$$S_{BH} = \frac{\text{Area}(m_{horizon})}{4G_N} \tag{1.27}$$

which relates the thermal entropy of a black hole to the area of black hole horizon. Though Bekenstein-Hawking entropy is a thermal entropy, it could be understood as an "entanglement" entropy. In particular, a static AdS black hole spacetime is holographically dual to a thermal state on boundary conformal field theory. The thermal state is a mixed state. However, one can always construct a pure state called thermofield double state via purification. Thermofield double state lives on a larger

[14] The Ryu-Takayanagi formula has an extension called HRT formula [50]. We will not discuss the latter here.

system that consists of two copies of Hilbert space on which the thermal state lives. As a result, the thermal state can be regarded as a state on the subsystem, and the (thermal) density matrix of the thermal state is understood as the reduced density matrix of the subsystem now. The thermofield double state is holographically dual to a two-sided extended black hole (See figure 1.2). The two copies of the original AdS black hole spacetime now become the two exterior regions. They are connected by a spatial section of the geometry at a special moment in time, called Einstein-Rosen bridge. The minimal surface in such a structure is the bifurcate horizon, which is the horizon of the original black hole spacetime. Thus the Bekenstein-Hawking entropy can be understood as a special case of Ryu-Takayanagi formula.

1.2.3 Target Space Entanglement

The partition of system considered above happens in the base space where the field lives. For example, it could happen in the spatial dimension of a $(1+1)$-dimensional quantum field theory. However, because $(1+1)$-dimensional quantum field theory is the second quantization of a $(0+1)$-dimensional quantum mechanics, one may ask what the corresponding partition and measure of entanglement are in this quantum mechanical system. Obviously the partition should not happen in base space because there is no spatial dimension for the theory to live on. Instead, it is a partition in target space where the field takes values in [20].

One can factorize the target (Hilbert) space by defining the subsystem A to be the sub-algebra $\mathcal{A}$ the operators $\mathcal{O}_A$ belong to. Then the reduced density matrix is determined via (1.17). According to Artin-Wedderburn theorem, the target (Hilbert) space and therefore the operators $\mathcal{O}_A$ can be decomposited into direct sums (called sectors) of tensor products of two parts, A and its complement $\bar{A}$, i.e.

$$\mathcal{H} = \bigoplus_k \mathcal{H}_{A,k} \otimes \mathcal{H}_{\bar{A},k} \tag{1.28}$$

$$\mathcal{O}_A = \bigoplus_k \mathcal{O}_{A,k} \otimes \mathbb{I}_{\bar{A},k} \tag{1.29}$$

Thus, a practical strategy to obtain reduced density matrix ρ_A is to find the projector of each sector first. The projector P_k belongs to the set of operators on $\mathcal{A}$ that commute with all operators in $\mathcal{A}$. It gives the density matrix of each sector

$$\rho = \bigoplus_k \rho_k, \qquad \rho_k = P_k \rho P_k \tag{1.30}$$

Then one can partially trace over the subsystem $\bar{A}$, and ρ_A will be the direct sum of the partial trace of each sector

$$\rho_A = \bigoplus_k \mathrm{Tr}_{\bar{A},k}\, P_k \rho P_k \tag{1.31}$$

There is a physics interpretation of sectors. Again take 1-particle quantum mechanics as an example. In this case the target space is actually the permitted position

of the particle. Thus, the possible two sectors are that particle is in A and that particle is in $\bar{A}$, respectively. This could be easily generalized to N-particle quantum mechanics and furtermore matrix models.

1.2.4 Quantum entanglement is not enough

Quantum entanglement is one quantity that captures global properties of a quantum state. There is another important property of a quantum state called complexity. For a (discrete) quantum system of size K (K qubits), a state $|\psi\rangle$ can be obtain from a simple state called reference state, e.g. $|000...0\rangle$, via a unitary transformation. The unitary transformation can be produced by a sequence of one- or two-qubit operators (gates). Then the complexity of $|\psi\rangle$ is the minimal number of gates that gives the unitary transformation. The motivation of introducing quantum complexity is that the estimated time for a quantum system of size K to reach its maximal complexity is e^K, which is much longer compared to thermalization, which takes some power of K. Note that complexity depends on the choice of the reference state.

It has been recently conjectured that when the quantum system has a gravitational holographic dual, complexity captures properties of the dual geometry which are not captured by e.g. Ryu-Takayanagi surfaces. This has motivated several authors to seek definitions of complexity in quantum field theories. One such definition involves circuit complexity [51]. Circuit complexity is defined to be the minimal geodesic between different states or operators on the manifold of unitary operators with metric determined by cost functional. The framework have been largely used for Gaussian-like state and therefore Gaussian unitary transformation.

1.3 Two Matrix Models

In this section we introduce two matrix models. They are examples of gauge/gravity duality.

1.3.1 $c = 1$ Matrix Model and 2D string theory

The partition function of 2-dimensional quantum gravity coupled to a scalar field can be described by a sum over random sufaces of all topologies, where the contribution from each random surface is given by a path integral of an action of a massless scalar field X that lives on 2-dimensional geometry described by metric g_{ab}. This action is indeed the worldsheet action of 1-dimensional noncritical string theory and is equivalent to 2-dimensional critical string theory. This is because one can choose a new gauge where $\hat{g}_{ab} = e^{\phi}\hat{g}_{ab}$. The field ϕ is called the Liouville mode. It has been shown that ϕ can be regarded as an extra target space spacelike dimension. In this description we have two scalar field X and ϕ that live on a fixed two-dimensional spacetime with a fixed metric $\hat{g}_{ab}$. As a result, one obtain a string theory embed-

ded in 2-dimensional target space (X, ϕ) that is Weyl-invariant (critical) under Weyl transformations of $\hat{g}$.[15]

To carefully define the continuum limit, the random surfaces are discretized by triangulation. Since the metric on the two dimensions is dynamical we have a dynamical triangulation. Such a dynamial triangulation is Hodge dual to a Feymann diagram of the quantum mechanics of a single $N \times N$ matrix $M(t)$, where the double-line Feymann diagram is used to show the orientation of random surface. Thus one can build a correspondence between 2-dimensional string theory and the $c = 1$ matrix model with action

$$S_{MM} = \beta \int \mathrm{d}t \mathrm{Tr} \left[\frac{1}{2} (\partial_t M)^2 - U(M) \right], \tag{1.32}$$

$$U(M) = -\frac{1}{2} M^2 + \frac{1}{3!} M^3 \tag{1.33}$$

where $\beta = N/g$ is a ratio of N and 't Hooft coupling g. In the continuum llimit, N is large and g is fixed.[16]

Indeed the duality between matrix model and 2-dimensional string theory can be seen in a more transparent way [16]. In the singlet sector, the matrix model is represented in terms of the eigenvalues of matrix M. The change of variables from the matrices to the eigenvalues leads to a Jacobian which is the square of the van der Monde determinant. Then by rescaling the wavefunction with van der Monde determinant, the theory becomes a theory of N fermions in one dimension (which is the space of eigenvalues) in the potential $U(\lambda)$, i.e.

$$\hat{H}_{ev} = \sum_i \left[-\frac{1}{2\beta} \frac{\partial^2}{\partial \lambda_i^2} + \beta U(\lambda_i) \right] \tag{1.34}$$

The second quantized discription involves a fermion field $\chi(\lambda, t)$ with a Hamiltonian

$$H = \int \mathrm{d}\lambda \left[\frac{1}{2\beta} |\partial_\lambda \chi|^2 + \beta U(\lambda) |\chi|^2 + \beta \mu_F |\chi|^2 \right] \tag{1.35}$$

where in the last term we have introduced a Lagrangian multiplier that enforces the condition that the number of fermions is N (from canonical ensemble to grand cannonical ensemble). In the double scaling limit

$$\beta \to \infty, \qquad \mu_F \to 0, \qquad g_s^{-1} \equiv 2\beta\mu_F \text{ is fixed} \tag{1.36}$$

if we rescale $\lambda = (\beta g_s)^{-1/2} x$, $\chi = (\beta g_s)^{1/4} \psi$, we can see that only quadratic term in the potential $U(\lambda)$ survives, which leaves us a theory of N non-relativistic fermions moving in an inverted harmonic oscillator potential [55–59]

$$H_F = \int \mathrm{d}x \left[\frac{g_s}{2} |\partial_x \psi|^2 - \frac{1}{2g_s} x^2 |\psi|^2 + \frac{1}{2g_s} |\psi|^2 \right] \tag{1.37}$$

[15] The procedure can be carried out for multiple scalar fields that define the worldsheet theory of noncritical strings in higher dimensions. For 25 scalar fields one gets the standard 26 dimensional bosonic string (the Liouville mode ϕ is regarded as a timelike dimension). For review, see [52].

[16] For reviews, see [53, 54].

Furthermore, one can consider the density of the eigenvalues of the matrix [16]

$$\partial_x \zeta(x,t) \equiv \mathrm{Tr}\,\delta(M - xI) = \psi^\dagger \psi(x,t) \tag{1.38}$$

This is a bosonic field called collective field, since the excitation of fermions is always in terms of productions of particle-hole pairs. Then by rewriting the theory one has completed a bosonization of the theory [60]. The classical action is

$$S_B = \frac{1}{g_s^2} \int \mathrm{d}t\mathrm{d}x \left[\frac{1}{2} \frac{(\partial_t \zeta)^2}{\partial_x \zeta} - \frac{\pi^2}{6} (\partial_x \zeta)^3 + \frac{1}{2} \left(x^2 - 1\right) (\partial_x \zeta) \right] \tag{1.39}$$

In the classical limit where g_s is small, one can expand around the saddle point solution (solution to equation of motion)

$$\partial_x \zeta_0 = \frac{1}{\pi} \sqrt{x^2 - 1} \tag{1.40}$$

and fluctuations $\eta(x,t)$ around the saddle point. In particular, the fluctuation field that satisfies

$$\zeta(x,t) = \zeta_0(x) + \frac{g_s}{\pi} \eta(x,t) \tag{1.41}$$

is subject to the action

$$S_B^{(2)} = \frac{1}{2\pi} \int \mathrm{d}x\mathrm{d}t \left[\frac{(\partial_t \eta)^2}{\partial_x \zeta_0} - 2 \frac{\partial_t \zeta_0}{(\partial_x \zeta_0)^2} (\partial_t \eta)(\partial_x \eta) + \left(\frac{(\partial_t \zeta_0)^2}{\partial_x \zeta_0)^3} - \pi^2 \partial_x \zeta_0 \right) (\partial_x \eta)^2 \right] \tag{1.42}$$

The fluctuation action $S_B^{(2)}$ describes a relativistic massless scalar in (1+1)-dimensional conformally flat spacetime if one transform the space coordinate x into

$$q \equiv \frac{1}{\pi} \int^x \frac{\mathrm{d}x'}{\partial_{x'} \zeta_0} \tag{1.43}$$

Now one have obtained an example of holography – the quantum mechanical description of N fermions in inverted harmonic oscillator potential which is dual to a field theory of $(1+1)$-dimensional relativistic massless scalar field. The latter indeed describes the $c = 1$ "tachyon", the only propagating mode in 2-dimensional string theory.[17] This is the earliest example of holography. Recently more evidences have been found to show the duality.

Unlike the generic cases where black holes are formed due to quench in the boundary, tachyonic matter seems not to form a black hole in singlet sector via collapsing pulse – the radiation bounces off before the black hole is about to form [17]. Actually it is widely believed that black holes that live in 2-dimensional gravity or 2-dimensional string theory are not contained in the singlet sector of this $c = 1$ matrix model [61].

[17] Tachyon has imaginary mass, therefore we use a quotation mark here. Indeed in 2d string theory, there is no transverse dimension. Thus one could find that the only dynamical mode is the motion of center of mass of the string, which is the massless scalar field called "tachyon". This means that though 2d string theory is called "string theory", it is not a real string theory since the oscillation of a string should have infinite modes.

1.3.2 D0-Brane Theory

A Dp-brane is a $(p+1)$-dimensional object in spacetime where open strings can end.[18] When the system has low energy, one only need to consider the open bosonic strings (as well as fermionic strings) in their lowest excited states, which can be reprensented by $(9+1)$-dimensional vector field operator. Among the 10 components of the vector field, $(p+1)$ of them parallel to Dp-brane are interpreted as $U(1)$ gauge field; the rest of them are the fluctuation of Dp brane in transverse directions, which become $9-p$ scalars on the Dp-brane worldvolume. The action is (supersymmetrized) Dirac-Born-Infeld action (with a Chern-Simons term). The induced metric of Dp-brane worldvolume is determined by $(9-p)$ scalar fields. Then in the low-energy limit, the DBI action turns into the $(p+1)$-dimensional $U(1)$ supersymmetric Yang-Mills theory, and the exponential of the expectation value of the dilaton is absorbed by Yang-Mills coupling g_{YM}.

For N parallel Dp-branes in low-energy system that dual to $U(1)^N$ supersymmetric Yang-Mills theory, the open bosonic strings that end on them have lowest energy proportional to the stretching length of the string. When the N Dp-branes are close, the stretching length and therefore the lowest energy of strings that end on different Dp-branes approach zero. This makes all open strings correspond to massless vector fields. Thus, it is robust to believe that a $U(N)$ symmetry should be restored from $U(1)$ symmetry in each Dp brane – the supersymmetric string theory of N Dp-branes is dual to $U(N)$ supersymmetric Yang-Mills theory [64].

An example of the gauge/gravity duality happens when $p=0$, in which all the N D-branes are points in the space. The action of dual supersymmetric Yang-Mills theory is given by

$$S=\frac{N}{2(g_sN)l_s}\,\mathrm{Tr}\int \mathrm{d}t\left[\sum_{I=1}^{9}(D_tX^I)^2-\frac{1}{l_s^4}\sum_{I\neq J=1}^{9}[X^I,X^J]^2\right]+\text{fermions} \tag{1.44}$$

In the action, g_s and l_s are the string coupling and string length, respectively. $X^I(t)$ where $I=1,2,...,9$ are nine $N\times N$ Hermitian matrices. The element of matrix $X^I_{ij}(t)$ represents the I-th transverse component of the string that ends on i-th and j-th D0-branes. D_t stands for the covariant derivative

$$D_tX^I=\partial_tX^I+i[A_t,X^I] \tag{1.45}$$

where A_t is the gauge field.

1.4 Outlines and Summary of the Dissertation

The dissertation includes two parts.

In Part I (Chapter 2, 3, and 4), we study non-equilibrium phenomena in various models associated with global quantum quench.

[18] For reviews see [62, 63].

It is known that quantities like one and two point correlation functions, as well as entanglement entropies, exhibit a variety of univeral scaling in global quantum quench across or approaching critical points (see section 1.1.1). It would be interesting to see if similar scaling holds for other quantum information theoretical quantities such as circuit complexity. In Chapter 2, we consider the scaling behavior of circuit complexity under quantum quench in free relativistic fermion field theory on a one dimensional spatial lattice with a time-dependent mass. This is equivalent to transverse field Ising chain with a time dependent transverse field. We find an exactly solvable quench protocol which asymptotes to massive phases at early and late times and crosses a critical point in between. We find a variety of scaling behavior as a function of the quench rate, starting with a saturation for quenches at the lattice scale, a "fast quench scaling" at intermediate rate and a Kibble Zurek scaling at slow rates. This chapter is based on [12].

To investigate fast scaling in non-relativistic theories, in Chapter 3 we investigate a class of exactly solvable quantum quench protocols with a finite quench rate in systems of one dimensional non-relativistic fermions in external harmonic oscillator or inverted harmonic oscillator potentials, with time dependent masses and frequencies. These hamiltonians arise, respectively, in harmonic traps, and the $c = 1$ Matrix Model description of two dimensional string theory with time dependent string coupling. We show how the dynamics is determined by a single function of time which satisfies a generalized Ermakov-Pinney equation. The quench protocols we consider asymptote to constant masses and frequencies at early times, and cross or approach a gapless potential. In a right side up harmonic oscillator potential we determine the scaling behavior of the one point function and the entanglement entropy of a subregion by obtaining analytic approximations to the exact answers. The results are consistent with Kibble-Zurek scaling for slow quenches and with perturbation calculations for fast quenches. For cis-critical quench protocols[19] the entanglement entropy oscillates at late times around its initial value. For end-critical protocols the entanglement entropy monotonically goes to zero inversely with time, reflecting the spread of fermions over the entire line. For the inverted harmonic oscillator potential, the dual collective field description is a scalar field in a time dependent metric and dilaton background. The chapter is based on a paper with Sumit R Das and Shaun Hampton [13].

A quantum quench in a boundary theory typically leads to black hole formation in the bulk in usual holographic correspondence like AdS/CFT [15] (see section 1.1.2). However, when it comes to $c = 1$ matrix model/$2D$ string theory duality, it is believed that the singlet sector of $c = 1$ matrix model does not contain the black hole of $2D$ string theory[17] (see section 1.3.1). It is therefore interesting to ask what is

[19] The definitions of different classes of quench protocols are given in Chapter 3. The three quench protocols referred to in this dissertation are: Trans-critical protocol (TCP) – the system begins in a gapped phase and the coupling varies monotonically across a critical value, and approaches a final value which also corresponds to a gapped phase. Cis-critical protocol (CCP) – the system starts from a gapped phase, approaches a critical point and reverts back to a constant value which also corresponds to a gapped phase. End-critical protocol (ECP) – the system begins in a gapped phase and monotonically approaches a critical point at infinitely late time.

the emergent bulk geometry produced by such a quench. In Chapter 4 we consider quantum quench in large-N singlet sector quantum mechanics of a single hermitian matrix in the double scaling limit. The time dependent parameter is the self-coupling of the matrix. We find exact classical solutions of the collective field theory of the eigenvalue density with abrupt and smooth quench profiles which asymptote to constant couplings at early and late times, and with the system initially in its ground state. With adiabatic initial conditions we find that adiabaticity is *always* broken regardless of the quench speed. In a class of quench profiles the saddle point solution for the collective field diverges at a finite time, and a further time evolution becomes ambiguous. However the underlying matrix model expressed in terms of fermions predict a smooth time evolution across this point. By studying fluctuations around the saddle point solution we interpret the emergent space-times. They generically have spacelike boundaries where the couplings of the fluctuations diverge and the semiclassical description fails. Only for very finely tuned quench profiles, the space-time is normal. The chapter is based on a paper with Sumit R Das and Shaun Hampton [18].

Part II (Chapter 5) is motivated by following question: Quantum entanglement plays a key role in gauge-gravity duality. There is some indication that if gauge-gravity duality is true, the properties of quantum entanglement of a quantum field theory is profoundly ingrained in the structure of gravity. For example, in AdS/CFT correspondence, theoretical physicists have learnt a lot about how to determine the entanglement entropy of boundary theory from its holographic dual utilizing Ryu-Takayanagi formula and its extensions [49, 50] (see section 1.2.2). However, to determine the entanglement in the bulk and its interpretation in its boundary dual is tricky since the bulk theory is gravitational.

It has been suggested in https://arxiv.org/abs/2004.00613 [21] that in Dp-brane holography, entanglement in the target space of the D-brane Yang-Mills theory provides a precise notion of bulk entanglement in the gravity dual. However this construction was done in a gauge-fixed description. In Chapter 5, we expand on this discussion by providing a gauge invariant characterization of operator sub-algebras corresponding to such entanglement. This is achieved by finding a projection operator which imposes a constraint characterizing the target space region of interest. By considering probe branes in the Coloumb branch we provide motivation for why the operator sub-algebras we consider are appropriate for describing a class of measurements carried out with low-energy probes in the corresponding bulk region of interest. We derive expressions for the corresponding Renyi entropies in terms of path integrals which can be directly used in numerical calculations. This chapter is based on a paper with Sumit R. Das, Anurag Kaushal, Gautam Mandal and Sandip P. Trivedi [22].

Technical details can be found in appendices.

Chapter 2
Complexity and scaling in quantum quench in $1+1$ dimensional fermionic field theories

2.1 Introduction

Quantum quench at finite quench rates which involve critical points are known to display universal scaling behavior in various regimes. For quench rates which are slow compared to physical mass scales local quantities in many systems obey Kibble Zurek scaling [5, 6, 65]. [1] In systems which have relativistic continuum limits there is a different scaling behavior for quench rates which are fast compared to physical mass scales, but slow compared to the UV scale [7–10, 71–74]. Finally at quench rates at the scale of a UV cutoff one expects that the response saturates as a function of the rate. These scaling behaviors are characteristic of early time response, i.e. for measurements made in the middle of the quench or soon after the quench is over.

While the scalings themselves are quite generic, explicit investigations typically involve solvable models and a lot has been learnt from exactly solvable quench protocols in these models. They have also been studied for models which have holographic descriptions via the AdS/CFT correspondence [26, 75–79]. In fact fast quench scaling was first discovered in holographic studies in [77–79]. They have been most extensively studied for local quantities like one point functions and correlation functions. For one dimensional harmonic chain scaling has also been found for the entanglement entropy [11, 80] and recently for circuit complexity [81].

Complexity in a field theory quantifies the difficulty in preparing a quantum state starting from some reference state. Study of such measures is motivated by ideas of holographic complexity [82–89]. Since this is a quantity which characterizes properties of a quantum state which are not easily captured by correlation functions, it is interesting to study its behavior in non-equilibrium situations. There are several proposals for quantifying complexity in field theories. The proposal we consider in this paper is "circuit complexity" which relates the length of the optimal circuit of unitary operations relating the reference state and a target state to a geometric quantity in the space of states parametrized in a suitable fashion [51, 90–98]. Clearly, because of the dependence on the reference state as well as the unitary gates used, this is not uniquely defined. Nevertheless such a definition is expected to capture the true complexity of a state and seems to agree with holographic expectations. For other approaches to field theoretic complexity, see [99–106].

In this paper we study scaling of circuit complexity in quantum quench for $1+1$ dimensional majorana fermions on a spatial lattice with a time (and momentum) dependent mass function - this is the fermionic description of a one dimensional transverse field Ising model with a time dependent transverse field. Following [71] we consider a time dependence for which the dynamics can be solved exactly - this corresponds to a transverse field which asymptotes to constant values at early and late

[1] For example, see the following reviews [66–70].

times and passes through the critical point at some intermediate time which we choose to be $t = 0$. The Heisenberg picture state of the system is chosen to be the "in" state, which approaches the ground state of the system at early times. This latter state is also chosen as the reference state. The Heisenberg picture state is then a Bogoliubov transformation of the reference state with time dependent Bogoliubov coefficients. As shown in [92] for such a free fermion theory, circuit complexity (as defined in that paper) can be expressed entirely in terms of these Bogoliubov coefficients. Using the exact expression for this quantity we study the complexity analytically in various regimes.

In the slow regime we use the standard adiabatic-diabatic sceneario underlying Kibble Zurek scaling to evaluate the complexity in the middle of the quench. We find a scaling behavior $\sim$ constant $+ (\delta t)^{-1/2}$ where δt denotes the time scale of the quench. We compare this result with a numerical evaluation of the integral involved in the exact result and find excellent agreement. Interestingly this comes mostly from contribution of modes which remain adiabatic. This is in contrast to what happens for the bosonic theory studied in [81] where the zero momentum modes in fact dominate the result.

In the fast regime, we can perform an expansion of the exact answer in a power series in $Jb\delta t$ where J denotes the mass scale of the theory and b is the quench amplitude. In this expansion, the complexity at $t = 0$ is proportional to δt for arbitrarily small δt. This agrees nicely with a numerical evaluation of the exact answer. The complexity at a slightly later time $t \ll \delta t$ shows a slightly different behavior : for δt smaller than a t-dependent threshold value the complexity saturates as a function of δt, while for δt larger than this threshold, the above mentioned linear behavior holds.

The content of the paper is as follows: In section 2.2, we summarize the definition of circuit complexity. In section 2.3, we introduce 1D Majorana fermion field theory and the derivation of complexity of its quench by considering Bogoliubov transformation. In section 2.4, we study the scaling of complexity with respect to quench rate. In section 2.5, we discuss the similarity and defference between 1D Majorana fermionic field theory and bosonic field theory in [81], then we show some numerical results of the late-time behaviors of complexity.

2.2 Complexity in Free fermionic theory

We follow the definiton of complexity in [51] and [92] which we summarize below: complexity is the minimal number of elementary unitary gates needed to prepare a certain target state $|\psi_T\rangle$ from a reference state $|\psi_R\rangle$

$$|\psi_T\rangle = U|\psi_R\rangle, U = \prod_{i=1}^{N} V_i. \tag{2.1}$$

In continuum limit, U takes a form of path-ordered exponential of the sum of products of control function $Y^I(s)$ and a basis of elementary gates $\mathcal{O}_I$

$$U(s) = \overleftarrow{\mathcal{P}} \exp\left[-i\int_0^s \mathrm{d}s \sum_I Y^I(s)\mathcal{O}_I\right], U = U(s=1) \tag{2.2}$$

And the complexity is defined to be the circuit that minimizes a cost

$$\mathcal{D}(U(t)) = \int_0^1 \mathrm{d}s F\left(U(s); Y^I(s)\right). \tag{2.3}$$

Notice that $Y^I(s)$ can be intepreted as the I^{th} component of the tangent vector of trajectory $U(s)$. The functional F is a measurement of "distance" from reference state at $U(0)$ to target state at $U(1)$: for example, if all classes of gates have equal cost, F can have a general form $F_\kappa(U; Y^I) = \sum_I |Y^I|^\kappa$. Then minimizing the cost is equivalent to looking for the shortest geodesic on the manifold formed by tangent vector $\vec{Y}(s)$.

When both the target state $|\psi_T\rangle$ and the reference state $|\psi_R\rangle$ are gaussian, there exist two pairs of sets of creation and annihiliation operators $\{a_T\}, \{a_T^\dagger\}$ and $\{a_R\}, \{a_R^\dagger\}$ s.t. $a_T|\psi_T\rangle = 0$ and $a_R|\psi_R\rangle = 0$. Then the transformation between the two states can be described by the transformation between the two pairs of creation and annihiliation operators. Most of time the transformation is a Bogoliubov transformation [2]. Below we give a rudimentary argument about fermions:

For a pair of fermions, the unitary operation U from reference state $|\psi_R\rangle$ to target state $|\psi_T\rangle$ is of the form

$$\begin{aligned} \tilde{a} &= \alpha a - \beta b^\dagger, \\ \tilde{b}^\dagger &= \alpha^* b^\dagger + \beta^* a, \end{aligned} \tag{2.4}$$

where operators a, b and $a^\dagger, b^\dagger$ are annihilation and creation operators of reference state, i.e. $a|\psi_R\rangle = b|\psi_R\rangle = 0$; Similarly, $\tilde{a}, \tilde{b}$ and $\tilde{a}^\dagger, \tilde{b}^\dagger$ are annihilation and creation operators of target state, i.e. $\tilde{a}|\psi_T\rangle = \tilde{b}|\psi_T\rangle = 0$. To preserve the anti-commutation relations, α and β satisfy

$$|\alpha|^2 + |\beta|^2 = 1. \tag{2.5}$$

The equation (2.5) implies that all of the possible target states form a unit sphere with the north pole the reference state. This is made explicit by writing α and β by two angles θ and ϕ, i.e.

$$\alpha = \cos\theta, \beta = e^{i\phi}\sin\theta. \tag{2.6}$$

[2] A single-fermion excited state $|k\rangle = a_k^\dagger|\mathrm{vac}\rangle$ with fermion momentum k can be expressed in the form "$f_p|k\rangle = 0, \forall p$" as well, i.e. one can find sets of creation and annihilation operators, $\{f_p\}$ and $\{f_p^\dagger\}$, to represent $|k\rangle$ as their vacuum state. This is because vacuum state $|\mathrm{vac}\rangle$ satisfies "$a_p|\mathrm{vac}\rangle = 0, \forall p$", and as a result one can always define $f_k \equiv a_k^\dagger$ (while for other p, $f_p \equiv a_p$). This implies that single-fermion excited state is gaussian. However, if we choose single-fermion excited state as the target state and vacuum state as the reference state, there is no Bogoliubov transformation between these two gaussian states.

Then a definition of the circuit complexity is the length of the geodesic from north pole to the position of the target state, i.e. $|\theta|$ gives the minimal cost. This can be generalized to N-pairs of free fermions. Since the Bogoliubov transformation does not mix operators with different momenta, it still takes the form in (2.4) and therefore (2.6) for each pair of fermion with momentum $\vec{k}, -\vec{k}$. On the other hand, to prepare the target state $|\psi_T\rangle$ from the reference state $|\psi_R\rangle$, one need to Bogoliubov transform all the independent (momentum) modes. As a result, the circuit complexity is the sum of geodesics $|\theta|(\vec{k})$ of all momenta, i.e.

$$\mathcal{C}^{(n)} = \sum_{\vec{k}} |\theta|^n(\vec{k}) \to V \int \frac{\mathrm{d}^d k}{(2\pi)^d} |\theta|^n(\vec{k}), \tag{2.7}$$

where

$$|\theta|\,(\vec{k}) = \tan^{-1}\frac{|\beta_{\vec{k}}|}{|\alpha_{\vec{k}}|} = \frac{1}{2}\tan^{-1}\frac{2|\alpha_{\vec{k}}||\beta_{\vec{k}}|}{\left||\alpha_{\vec{k}}|^2 - |\beta_{\vec{k}}|^2\right|}. \tag{2.8}$$

2.3 The model and quench dynamics

The model considered in this paper is Majorana fermion field theory of the one dimensional transverse field Ising model with a time dependent transverse field (The model is discussed in details in [71]). The Hamiltonian is given by

$$H = \int \frac{\mathrm{d}k}{2\pi} \chi^\dagger(k,t) \left[-m(k,t)\sigma_3 + G(k)\sigma_1\right] \chi(k,t). \tag{2.9}$$

where $\sigma_{1,3}$ are 2D Gamma matries and χ denotes the two component spinor field, i.e. $\chi = \begin{pmatrix} \chi_1(k) \\ \chi_2(k) \end{pmatrix}$.

The Heisenberg equation of motion for $\chi(k,t)$ is a superposition of two independent solutions $U(k,t)$ and $V(k,t)$,

$$i\partial_t \left(U(k,t), V(-k,t)\right) = \left[-m(k,t)\sigma_3 + G(k)\sigma_1\right] \left(U(k,t), V(-k,t)\right) \tag{2.10}$$

and

$$\chi(k,t) = a(k)U(k,t) + a^\dagger(-k)V(-k,t). \tag{2.11}$$

because of Majorana condition $\chi_2(k) = \chi_1^\dagger(-k)$. The operators $a(k)$ and $a^\dagger(k)$ satisfy the usual anti-commutation relations

$$\begin{aligned} \{a(k), a^\dagger(k')\} &= \quad \delta(k-k') \\ \{a(k), a(k')\} &= \{a^\dagger(k), a^\dagger(k')\} \quad = 0 \end{aligned} \tag{2.12}$$

We can relate the spinor to a scalar field $\phi(k,t)$ by letting

$$\begin{aligned} U(k,t) &= \begin{pmatrix} -i\partial_t + m(k,t) \\ -G(k) \end{pmatrix} \phi(k,t), \\ V(-k,t) &= \begin{pmatrix} G(k) \\ i\partial_t + m(k,t) \end{pmatrix} \phi^*(k,t), \end{aligned} \tag{2.13}$$

where $\phi(k,t)$ satisfies

$$\partial_t^2\phi + i\partial_t m\cdot\phi + (m^2+G^2)\phi = 0. \tag{2.14}$$

according to (2.10), and

$$|\partial_t\phi|^2 + (m^2+G^2)\,|\phi|^2 - 2m\cdot \mathrm{Im}\,(\phi\partial_t\phi^*) = 1 \tag{2.15}$$

to preserve anti-commutation relations and the orthonormality of $U(k,t)$ and $V(k,t)$.

An exactly solvable quench dynamics has been found in [71] which we use

$$m(k,t) = A(k) + B\tanh(t/\delta t), \tag{2.16}$$

and the rest of the parameters are

$$A(k) = 2J(a-\cos k), B = 2Jb, G(k) = 2J\sin k, \tag{2.17}$$

where J is the interaction strength between the nearest-neighbor spins in Ising model. It has dimension of energy. a is the lattice spacing of Ising model. b determines the mass gap.

In the rest of the paper we mainly consider the case $a = 1$, which describes a cross-critical-point (CCP) type-like potential at $k = 0$; another interesting case is when $a = 1-b$, which corresponds an end-critical-point (ECP) type-like potential at $k = 0$.

The Heisenberg picture state we use is the "in" state. This means that the spinors $U(k,t)$ should asymptote to the positive frequency solution of the equation in the infinite past. This "in" solution is given by (2.14) and (2.15) is

$$\begin{aligned}\phi_{in}(k,t) =& \frac{1}{|G(k)|}\sqrt{\frac{\omega_{in}+m_{in}}{2\omega_{in}}}\exp[-i\omega_+(k)t - i\omega_-(k)\delta t\log(2\cosh(t/\delta t))] \\ & {}_2F_1[1+i\omega_-(k)\delta t + iB\delta t, i\omega_-(k)\delta t - iB\delta t; 1-i\omega_{in}(k)\delta t; \frac{1}{2}(1+\tanh(t/\delta t))],\end{aligned} \tag{2.18}$$

where the frequencies $\omega_{in,out,\pm}$ are defined to be

$$\omega_{out,in} = \sqrt{G(k)^2 + (A(k)\pm B)^2}, \omega_\pm = \frac{1}{2}(\omega_{out}\pm\omega_{in}). \tag{2.19}$$

and $m_{in} = m(t\to-\infty) = A(k) - B$.

For the reference state we will choose the ground state of the system in infinite past, while the target state is the Heisenberg picture state. For some momentum k the former is annihilated by a set of fermionic oscillators $a_{-\infty}(k)$ and $a^\dagger_{-\infty}(k)$ defined by

$$\chi(k,t) = a_{-\infty}(k)U_{-\infty}(k,t) + a^\dagger_{-\infty}(-k)V_{-\infty}(-k,t) \tag{2.20}$$

where $U_{-\infty}(k,t)$ and $V_{-\infty}(k,t)$ are given by the expressions (2.13) using the asymptotic form $\phi_{-\infty}(k,t)$

$$\phi_{-\infty}(k,t) = \frac{1}{\sqrt{2\omega_{in}(\omega_{in}-m_{in})}}e^{-i\omega_{in}t} \tag{2.21}$$

The relationship between $a_{-\infty}(k), a^{\dagger}_{-\infty}(k)$ and $a(k), a^{\dagger}(k)$ then becomes a set of Bogoliubov transformations of the form (2.4)

$$\begin{aligned} a_{-\infty}(k,t) &= \alpha(k,t)a(k) - \beta(k,t)a^{\dagger}(-k), \\ a^{\dagger}_{-\infty}(-k,t) &= \beta^{*}(k,t)a(k) + \alpha^{*}(k,t)a^{\dagger}(-k), \end{aligned} \tag{2.22}$$

where $\alpha(k,t) = \alpha(-k,t)$ and $\beta(k,t) = -\beta(-k,t)$; anti-commutation relation requires $|\alpha(k,t)|^2 + |\beta(k,t)|^2 = 1$. Then $\alpha(k,t)$ and $\beta(k,t)$ can be expressed by $U(k,t), V(k,t)$:

$$\begin{aligned} \alpha(k,t) &= U^{\dagger}_{-\infty}(k,t)U(k,t) = V^{\dagger}(-k,t)V_{-\infty}(-k,t), \\ \beta(k,t) &= -U^{\dagger}_{-\infty}(k,t)V(-k,t) = U^{\dagger}(k,t)V_{-\infty}(-k,t), \end{aligned} \tag{2.23}$$

and therefore $\phi(k,t)$:

$$\begin{aligned} \alpha(k,t) &= \phi^{*}_{-\infty}(k,t)\left\{G^2(k) + (-\omega_{in} + m_{in})\left[-i\partial_t + m(k,t)\right]\right\}\phi(k,t) \\ \beta(k,t) &= \phi^{*}_{-\infty}(k,t)G(k)\left\{[i\partial_t + m(k,t)] - (-\omega_{in} + m_{in})\right\}\phi^{*}(k,t). \end{aligned} \tag{2.24}$$

In this paper we consider the measurement closest to the original definition of complexity in the discrete case, i.e. $F(U,\vec{Y}) = \sum_I \left|Y^I\right|$, therefore the circuit complexity of the model is

$$\mathcal{C}^{(1)} = V\int \frac{\mathrm{d}k}{2\pi}|\theta|(k,t), \tag{2.25}$$

where the integrand $\theta(k,t)$ is given by

$$\begin{aligned} |\theta|\,(k,t) \equiv& \tan^{-1}\frac{|\beta(k,t)|}{|\alpha(k,t)|} \\ =& \tan^{-1}\left|\frac{\phi_{-\infty}(k,t)G(k)\left\{[-i\partial_t + m(k,t)] - (-\omega_{in} + m_{in})\right\}\phi(k,t)}{\phi^{*}_{-\infty}(k,t)\left\{G^2(k) + (-\omega_{in} + m_{in})\left[-i\partial_t + m(k,t)\right]\right\}\phi(k,t)}\right| \end{aligned} \tag{2.26}$$

For practical reason, we ignore factor $\frac{V}{2\pi}$.

2.4 Scaling of Complexity

Now we want to see how circuit complexity scales with respect to quench rate. The behavior of $\mathcal{C}^{(1)}(t)$ as a function of δt is shown in Fig. 2.1 and Fig. 2.2. There are three regimes of the quench rate: slow quench, fast quench and instantaneous quench.

2.4.1 Slow quench

In slow quench region, $J\delta t \gg 1/b$, the asymptotic behavior of circuit complexity with respect to the quench rate is $\mathcal{C}^{(1)} \sim P' + Q'\delta t^{-1/2}$, where P', Q' are constants (Fig. 2.1). This behavior is consistent with Kibble-Zurek scaling. In particular, the system evolves adiabatically at the beginning because the rate of change of time-dependent coupling ($m(k,t)$ in this system) is much smaller than the square of the initial energy gap. However, the adiabaticity breaks down as one approaches the critical point

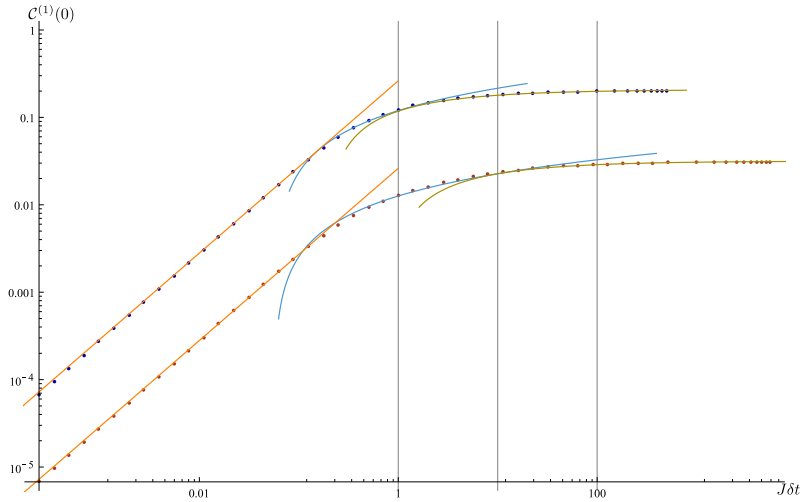

Figure 2.1: Exact $\mathcal{C}^{(1)}(0)$-δt relations in log-log scale. Red and blue dots correpond to $b = 0.01$ and $b = 0.1$ respectively. The orange, blue, and yellow fitting curve are $y = cx^d$, $y = P + Q \log x$, and $y = P' + Q' x^{-1/2}$, respectively. The linear fitting coefficient $d = 0.985146$ for $b = 0.1$ and $d = 0.984975$ for $b = 0.01$, which implies the linear relation between $\mathcal{C}^{(1)}(0)$ and δt in fast quench regime.

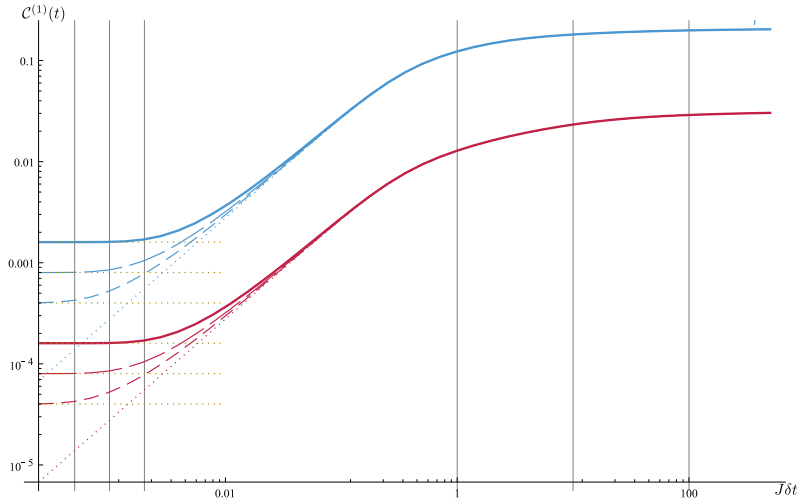

Figure 2.2: Exact $\mathcal{C}^{(1)}(t)$-δt relations in log-log scale. Red and blue lines correpond to $b = 0.01$ and $b = 0.1$ respectively. From solid to dashed, the curves correspond to $t = 0.002, 0.001$ and 0.0005, respectively. We can see the circuit complexity saturates around $\delta t \sim t$ (gridlines), and the saturation value is approximately $8Jbt$ (in yellow dotted lines). As reference, $\mathcal{C}^{(1)}(0)$-δt relations are in dotted lines.

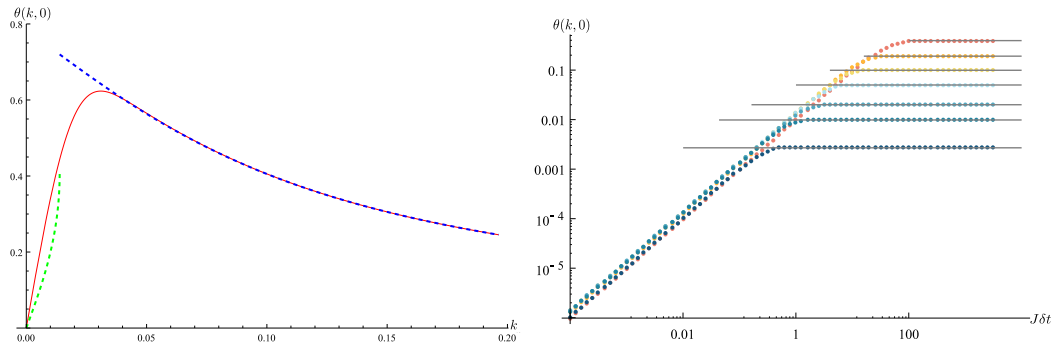

(a) (b)

Figure 2.3: 2.3a Relation between single-mode contribution $|\theta|(k,0)$ and momentum k: Red line shows the exact mode contribution to complexity $\theta(k,0)$; green and blue dashed lines are approximated complexity with KZ mass and critical mass, respectively. $b = 0.1$. 2.3b Relation between $|\theta|(k,0)$ and $J\delta t$: From dark blue to red, $k = 1.5, 0.5, 0.25, 0.1, 0.05, 0.025, 0.01$; the grey solid horizontal lines are adiabatic approximations (2.30) when $J\delta t > b\csc^2 k$. $b = 0.01$.

at a time called Kibble-Zurek time t_{KZ}, because of critical slowing down. Since the instantaneous energy gap scales with time-dependent coupling $m(k,t)$ with the correlation length exponent ν as $E_g \sim |m(k,t) - m_c|^\nu$. t_{KZ} can be found by using the Landau criterion

$$\frac{1}{E_g^2(t)} \frac{\mathrm{d}E_g(t)}{\mathrm{d}t}\bigg|_{-t_{KZ}} \sim 1, \tag{2.27}$$

where E_g is the instantaneous energy gap, and in the model we study,

$$E_g = \sqrt{m(k,t)^2 + G(k)^2}. \tag{2.28}$$

Adiabaticity holds when the quantity is much smaller than 1.

Clearly the Kibble-Zurek time depends on the momentum of the mode according to (2.27) and (2.28). In CCP type-like potential case, one can find that adiabaticity breaks down at $-t_{KZ}$ and reappears at t_{KZ}. On the other hand, in ECP type-like potential case, adiabaticity breaks down at t_{KZ}.

To make it clear, the circuit complexity is plotted mode by mode at $t = 0$ (See Fig. 2.3a). We find that the momentum-dependence of circuit complexity can be divded into two regions by Landau criterion. In particular, a critical momentum k_c exists, where

$$\sin k_c = \sqrt[4]{\frac{1}{27}}\sqrt{\frac{b}{J\delta t}}. \tag{2.29}$$

For $k < k_c$ the adiabatic approximation breaks down, and the system is frozen after $-t_{KZ}$. This implies that circuit complexity can be evaluated approximately by that at a fixed mass $m_{KZ} = m(-t_{\mathrm{KZ}})$, which can be treated as an effective mass of the frozen system. For $k > k_c$, adiabatic approximation is valid, and circuit complexity

can be evaluated by using the instantaneous mass at $t = 0$. Then in general, the approximation is

$$|\theta| \approx \frac{1}{2}\tan^{-1}\left|\frac{(m_{in}-m)G}{m_{in}\cdot m+G^2}\right|, \quad m=\begin{cases} m_{KZ}, & k<k_c \\ m(t=0), & k>k_c \end{cases}. \tag{2.30}$$

Therefore, by summing over all momenta ($k \in [0,\pi]$), an approximation of circuit complexity is

$$\begin{aligned}\mathcal{C}^{(1)}(0) \approx & \frac{1}{2}\int_0^{\pi} \mathrm{d}k \tan^{-1}\left|\frac{[m_{in}-m(t=0)]G}{m_{in}\cdot m(t=0)+G^2}\right| \\ & -\frac{1}{2}\int_0^{k_c} \mathrm{d}k \tan^{-1}\left|\frac{[m_{in}-m(t=0)]G}{m_{in}\cdot m(t=0)+G^2}\right| + \frac{1}{2}\int_0^{k_c} \mathrm{d}k \tan^{-1}\left|\frac{[m_{in}-m_{\mathrm{KZ}}]G}{m_{in}\cdot m_{\mathrm{KZ}}+G^2}\right|,\end{aligned} \tag{2.31}$$

where the 1st and the 2nd terms are the adiabatic approximation of $|\theta|$ for $k > k_c$, and the 3rd term is the response of the system at a constant mass equal to the Kibble-Zurek mass m_{KZ} when adiabaticity breaks down. Under the condition $J\delta t \gg 1/b$, we can simplify the complexity and determine the leading and subleading term of it:

$$\mathcal{C}^{(1)}(0) \sim \int_0^{\pi/2} \mathrm{d}x \tan^{-1}\left(\frac{b}{2-b}\cot x\right) + \mathcal{O}\left(\sqrt{\frac{b}{J\delta t}}\right). \tag{2.32}$$

Numerically we can find that leading term is 0.207762 when $b = 0.1$, which is close to the curve fitting result of exact $\mathcal{C}^{(1)}(0)$, $P' = 0.207605$ (yellow fitting in Fig. 2.1). Therefore, in the slow quench regime, circuit complexity follows the expectation of KZ.

2.4.2 Instantaneous quench

In the instantaneous quench regime, i.e. $J\delta t \ll 1$, we find that circuit complexity at time t shows linearity when $\delta t \gg t$ and saturation when $\delta t \ll t$; In both cases the circuit complexity is proportional to the gap of mass Jb (Fig. 2.2). One can see these features more clearly from the asymptotic behaviors of ϕ and β when $t, \delta t \ll 1$.

Notice that when $\delta t \gg t$, $\tanh(t/\delta t) \to t/\delta t$. Therefore we can expand solution $\phi_{in}(k,t)$ in (2.18) and find

$$\begin{aligned}\phi_{in}(\vec{k},t) \approx & \frac{1}{|G(k)|}\sqrt{\frac{\omega_{in}+m_{in}}{2\omega_{in}}}e^{-i\omega_+ t} \\ & \times\left\{2^{-i\omega_-\delta t}\frac{\omega_+ + B}{\omega_{out}}[1-i\delta t(\omega_- - B)\log(\frac{1}{2}(1+\frac{t}{\delta t}))]\right. \\ & \left.+2^{i\omega_+\delta t}(1-\frac{t}{\delta t})^{-i\omega_{out}\delta t}\frac{\omega_- - B}{\omega_{out}}[1+i\delta t(\omega_+ + B)\log(\frac{1}{2}(1+\frac{t}{\delta t}))]\right\} \\ & -\frac{1}{|G(k)|}\sqrt{\frac{\omega_{in}+m_{in}}{2\omega_{in}}}e^{-i\omega_+ t}\times t\delta t(\omega_+ + B)(\omega_- - B)\log 2 \\ & +(\text{higher order contributions}).\end{aligned} \tag{2.33}$$

Then the leading term of $\beta^*(k,t)$ (2.24) is now approximately

$$\beta^*(k,t) \approx \frac{1}{G}\frac{\omega_{in}+m_{in}}{2\omega_{in}} e^{-i\omega_+ t - i\omega_{in} t} \left\{ i2\delta t(\omega_+ + B)(\omega_- - B)\log 2 \right\}. \tag{2.34}$$

Since $J\delta t \ll 1$, circuit complexity $|\theta(k,0)| \approx |\beta|$ and as a result, we can plug $G(k)$ in and estimate the complexity to be

$$\mathcal{C}^{(1)}(0) \sim bJ\delta t \cdot 4\log 2 \approx 2.77 bJ\delta t. \tag{2.35}$$

when $b \ll 1$. This is close to the linear fitting of exact circuit complexity in Fig. 2.1, where the slopes are $c \approx 0.261913$ when $b = 0.1$ and $c \approx 0.0261736$ when $b = 0.01$.

When $\delta t \ll t$, $\tanh(t/\delta t) \to 1 - e^{-2t/\delta t}$. Again one can expand solutions and find

$$\begin{aligned} \phi_{in}(\vec{k},t) \approx & \frac{1}{|G(k)|}\sqrt{\frac{\omega_{in}+m_{in}}{2\omega_{in}}} \exp[-i\omega_- \delta t e^{-2t/\delta t}] \\ & \times \left\{ e^{-i\omega_{out} t}\frac{\omega_+ + B}{\omega_{out}} \left(1 + i\delta t(\omega_- - B)e^{-2t/\delta t}\right) \right. \\ & \left. + e^{i\omega_{out} t}\frac{\omega_- - B}{\omega_{out}} \left(1 - i\delta t(\omega_+ + B)e^{-2t/\delta t}\right) \right\}. \end{aligned} \tag{2.36}$$

Therefore $\beta(k,t)^*$ is approximately

$$\begin{aligned} \beta^*(k,t) \approx & -i\exp[-i\omega_- \delta t e^{-2t/\delta t}] \frac{G(m_{out}-m_{in})}{\omega_{in}\omega_{out}} e^{-i\omega_{in} t} \sin\omega_{out} t \\ & + \frac{1}{G}\frac{m_{in}+\omega_{in}}{2\omega_{in}} e^{-i\omega_{in} t} \exp[-i\omega_- \delta t e^{-2t/\delta t}] 4(\omega_- - B) e^{-2t/\delta t} e^{i\omega_{out} t}, \end{aligned} \tag{2.37}$$

and then the leading term and subleading term of the circuit complexity is

$$\mathcal{C}^{(1)}(t) \sim 8bJt + \mathcal{O}(te^{-2t/\delta t}). \tag{2.38}$$

Thus the leading term is δt-independent, and linearly increase as t increases, which corresponds to the saturation when $\delta t \ll t$ in Fig. 2.2.

Behavior of circuit complexity in instantaneous quench regime is consistent with the behavior when quench occurs instantaneously ($\delta t \to 0$). In the latter case the time-dependent mass in (2.16) can be described by

$$m(k,t) = A(k) + B\left(\Theta(t/\delta t) - 1/2\right) \tag{2.39}$$

where $\Theta(x)$ is the Heaviside step function. The circuit complexity can be exactly figured out. The exact "in" solution is

$$\phi(t) = \frac{1}{|G|}\sqrt{\frac{m_{in}+\omega_{in}}{2\omega_{in}}} \times \begin{cases} e^{-i\omega_{in} t}, & t < 0 \\ \frac{\omega_+ + B}{\omega_{out}} e^{-i\omega_{out} t} + \frac{\omega_- - B}{\omega_{out}} e^{i\omega_{out} t}. & t \geq 0 \end{cases} \tag{2.40}$$

and thus the circuit complexity

$$\mathcal{C}^{(1)}(t) = \int_0^\pi \mathrm{d}k \frac{2b\sin k}{\sqrt{\sin^2 k + (1-\cos k - b)^2}} \cdot 2Jt \approx \frac{8bJt}{\sqrt{1-b}} \approx 8bJt \tag{2.41}$$

when $b \ll 1$.

One can see that at $t = 0$ the circuit complexity $\mathcal{C}^{(1)}(0)$ does not saturate. This is different from $\langle \bar{\chi}\chi \rangle$, which saturates when $J\delta t < |b|$ ([71]).

2.4.3 Fast quench

Between slow quench $J\delta t \ll 1$ and instantaneous quench $J\delta t \gg 1/b$, we find a logarithmic dependence, i.e. $\mathcal{C}^{(1)}(0) \sim P + Q\log(J\delta t)$, where P, Q roughly linearly rely on b.

One can easily generalize the other definition of complexity in (2.8) to the time-dependent case, s.t.

$$|\theta|(k,t) \equiv \frac{1}{2}\tan^{-1}\frac{2|\alpha(k,t)||\beta(k,t)|}{\left||\alpha(k,t)|^2 - |\beta(k,t)|^2\right|} \tag{2.42}$$

Combined with ((2.13) and (2.23)), we can rewrite the denominator $\left||\alpha(k,t)|^2 - |\beta(k,t)|^2\right|$ in terms of the c-number $\bar{V}V \equiv V(-k,t)^\dagger \sigma_3 V(-k,t)$:

$$|\alpha(k,t)|^2 - |\beta(k,t)|^2 = \frac{m_{in}}{\omega_{in}}\bar{V}V + \frac{G}{\omega_{in}}\cos\gamma\sqrt{1-(\bar{V}V)^2} \tag{2.43}$$

where γ is the angular part of $-2G(k)\phi^*(-i\partial_t + m(k,t))\phi$.

On the other hand, the quench Hamiltonian (2.9) can be rewriten into the form

$$\begin{aligned} H =& \int \frac{\mathrm{d}k}{2\pi}\chi^\dagger(k,t)\left[-m_{in}\sigma_3 + G(k)\sigma_1\right]\chi(k,t) - \int \frac{\mathrm{d}k}{2\pi}\delta m(t)\bar{\chi}(k,t)\chi(k,t) \\ \equiv& H_{CFT} - \delta\lambda\int \mathrm{d}x F(t/\delta t)\mathcal{O}_\Delta, \end{aligned} \tag{2.44}$$

where $\delta\lambda = 2B$, $F(t/\delta t) = (1+\tanh(t/\delta t))/2$, and $\mathcal{O}_\Delta = \bar{\chi}(x.t)\chi(x,t)$ is an operator with comformal dimension Δ. Therefore one can use the Kubo formula to find the leading terms of $\langle\mathcal{O}_\Delta(t)\rangle \equiv \langle 0|\mathcal{O}_\Delta(t)|0\rangle$ when $t \ll \delta t$, where state $|0\rangle$ is the "in" vacuum that satisfies $a(k)|0\rangle = 0$ for all momentum k:

$$\langle\mathcal{O}_\Delta(x,t)\rangle = \langle\mathcal{O}_\Delta(x,t)\rangle_{m_{in}} - \delta\lambda\int_{-\delta t}^{t}\mathrm{d}t' F(t'/\delta t)\int \mathrm{d}x' G_{R,m_{in}}(x,t;x',t') + ... \tag{2.45}$$

where $G_{R,m_{in}}(x,t;x',t')$ is the retarded Green's function

$$G_{R,m_{in}}(x,t;x',t') = i\Theta(t)\langle[\mathcal{O}_\Delta(x,t),\mathcal{O}_\Delta(x',t')]\rangle_{m_{in}} \tag{2.46}$$

The argument in [26] [3] implies that one can use the Green's function in CFT as an approximation to the exact one when $\delta t \ll (\delta\lambda)^{-\frac{1}{d-\Delta}}, (m_{in})^{-\frac{1}{d-\Delta}}$, where d is the spacetime dimension. This is based on two facts: One is that the Green's function should satisfy causality. As a result the bound of integral over x is actually $(-t+t', t-t')$. The other is that when space and time scales are both much smaller than the correlation length $(m_{in})^{-\frac{1}{d-\Delta}}$, the commutator in CFT is a good approximation to the Green's function. The argument leads to the conclusion that the integrals in the Kubo formula scale with δt only, i.e.

$$\langle\mathcal{O}_\Delta(x,t)\rangle - \langle\mathcal{O}_\Delta(x,t)\rangle_{m_{in}} \sim \delta\lambda(\delta t)^{d-2\Delta} \tag{2.47}$$

[3] [26] considered a general continuous field theory instead of a lattice one. Here we follow the logic and argue in continuous case as well.

A more concrete calculation in [71] shows

$$\langle\bar{\chi}(x,t)\chi(x,t)\rangle - \langle\bar{\chi}(x.t)\chi(x,t)\rangle_{m_{in}} = \lim_{\eta\to 0} 2\pi\delta\lambda\log(\delta t/\eta)+..., \quad \delta t \ll \frac{1}{\delta\lambda}, \frac{1}{m_{in}} \tag{2.48}$$

Now, notice that $\bar{V}(-k.t)V(-k,t)$ is related to $\bar{\chi}_n(t)\chi_n(t)$ by a Fourier transform

$$\langle 0|\bar{\chi}_n\chi_n|0\rangle(t) = \int_{-\pi}^{\pi}\frac{\mathrm{d}k}{2\pi}e^{-in(k-k')}\langle 0|\bar{\chi}(k,t)\chi(k',t)|0\rangle = \int_{-\pi}^{\pi}\frac{\mathrm{d}k}{2\pi}\langle 0|\bar{V}(-k,t)V(-k,t)|0\rangle, \tag{2.49}$$

on the Ising model we consider. Momentum $k \in (-\pi,\pi]$ is independent from the scale $\delta\lambda$ and δt. Thus the order of $\delta\lambda$ and δt in the leading term and subleading term should not change. Figure out the leading term by plugging the $\phi_{-\infty}$ in, and we find

$$\bar{V}V = \langle 0|\bar{V}(-k,t)V(-k,t)|0\rangle \approx \frac{m_{in}}{\omega_{in}} + \mathcal{O}(b\log(\delta t/\eta)) \tag{2.50}$$

and leading term of $\cos\gamma$ is 1.

Therefore, (2.42) turns into

$$|\theta|(k,t) \approx \frac{1}{2}\tan^{-1}\frac{\mathcal{O}(b\log\delta t/\eta)}{1-\frac{1}{2}\left[\mathcal{O}(b\log\delta t/\eta)\right]^2} \sim b\log(\delta t/\eta) \tag{2.51}$$

Circuit complexity is therefore of the form $P + Q\log(J\delta t)$ as Fig. 2.1 shows.

Here we need to make a comment on the higher order terms of $\cos\gamma$. In the fast quench regime, it can be ignored because $b\log(\delta t)$ is the second lowest order. However, in instantaneous regime, subleading term of $\cos\gamma$ is at the order $\mathcal{O}(\delta t)$, which can be found by expanding the Hypergeometric function. This might explain why $\mathcal{C}^{(1)}(t)$-δt relation is not quadratic, though

$$\bar{V}V \approx \frac{m_{in}}{\omega_{in}} + \mathcal{O}((J\delta t)^2) \tag{2.52}$$

when $J\delta t \ll 1$ ([71]).

2.5 Discussions

In many ways the circuit complexity $\mathcal{C}^{(1)}(0)$ of relativistic fermionic Ising theory scales in a way similar to free bosonic oscillators [81]. In particular, like circuit complexity of free bosonic oscillators when $\omega_0\delta t \ll 1$, circuit complexity of free fermionic oscillators also shows linear behavior at $t = 0$ in instantaneous quench regime ($J\delta t \ll 1$). This is because the contribution from each single (momentum) mode, $|\theta|(k,0)$, scales linearly as δt varies (2.34). To explain the behavior of circuit complexity $\mathcal{C}(0)$ in bosonic theory when slow quenched, [81] analyzed the contributions from single modes C^k and found that C^k scales logarithmically when $\delta t < \frac{\omega_0}{4}\csc^2(\frac{k}{2})$ and saturates when $\delta t \geq \frac{\omega_0}{4}\csc^2(\frac{k}{2})$. Here we can draw a similar conclusion from (2.29) that single nonzero

mode contribution $|\theta|(k \neq 0, 0)$ saturates when $J\delta t \gg b \csc^2 k$ (See Fig. 2.3b). To be concrete, $k \gg k_c$ is the condition for $|\theta|(k, 0)$ to be adiabatic. Then by plugging in (2.29) one can find the inequality between k and δt

$$\sin k \gg \sin k_c = \sqrt[4]{\frac{1}{27}}\sqrt{\frac{b}{J\delta t}} \Longrightarrow J\delta t \gg \sqrt{\frac{1}{27}} b \csc^2 k \sim b \csc^2 k. \tag{2.53}$$

Given that adiabatic result (2.30) is independent of $J\delta t$ due to $m(t = 0) = A(k)$, when the inequality is satisfied, $|\theta|(k, 0)$ is independent of δt. [4]

However, the zero mode contribution $C^{k=0}$ in free bosonic theory is very different from $|\theta|(k = 0, 0)$ in free fermionic theory. In the free bosonic case, the contribution from zero-mode $C^{k=0} \sim \log \delta t$ in KZ regime due to the fact that the saturation happens when $\delta t \geq \frac{\omega_0}{4} \csc^2(\frac{k}{2}) \to \infty$. In the free fermionic case the contribution from zero-mode $|\theta|(k = 0, 0)$ is subtle. From (2.23) one may find that it is because when $k = 0$, $U_{-\infty}(k, t)$ and $V_{-\infty}(-k, t')$ are both zero vectors. A more profound reason might come from (2.22). When $k = 0$, (2.22) turns into

$$\begin{aligned} a_{-\infty}(0, t) &= \alpha(0, t)a(0) - \beta(0, t)a^\dagger(0), \\ a^\dagger_{-\infty}(0, t) &= \beta^*(0, t)a(0) + \alpha^*(0, t)a^\dagger(0). \end{aligned} \tag{2.54}$$

Then anticommutator $a(0)^2 = (a^\dagger(0))^2 = a_{-\infty}(0)^2 = (a^\dagger_{-\infty}(0))^2 = 0$ implies that

$$\alpha(0, t)\beta(0, t) \equiv 0 \tag{2.55}$$

Combined with (2.5), we find that $(|\alpha(0, t)|, |\beta(0, t)|) = (1, 0)$ or $(0, 1)$. Therefore the contribution from the zero-mode $|\theta|(0, t) = 0, \pi/2$ [92]. However, given that in the latter case (2.54) turns into

$$\left.\begin{aligned} a_{-\infty}(0, t) &= -e^{i\varphi(t)}a^\dagger(0), \\ a^\dagger_{-\infty}(0, t) &= e^{-i\varphi(t)}a(0). \end{aligned}\right\} \Longrightarrow \beta(0, t) \equiv e^{i\varphi} = 0, \tag{2.56}$$

i.e. the zero-mode contribution $|\theta|(k = 0, t)$ has to be zero in our case. The Bogoliubov transformation of the zero-mode is trivial, since Majorana fermions have an unpaired zero-mode.

As for nonzero-modes, Fig. 2.3a shows that single-mode contribution has a peak at some nonzero mode and it moves close to zero mode as quench becomes slower. Most of the contribution to complexity $\mathcal{C}^{(1)}(0)$ comes from modes that remain adiabatic, i.e. $|\theta|(k > k_c, 0)$. According to (2.29), when $J\delta t$ increases, k_c decreases, so that adiabaticity is moving toward $k = 0$. On the other hand, when $t = 0$, adiabatic contribution

$$|\theta|_{adia}(k, t = 0) \equiv \frac{1}{2} \tan^{-1} \left| \frac{(m_{in} - m(t = 0))G}{m_{in} \cdot m(t = 0) + G^2} \right| \tag{2.57}$$

[4] Here we cannot give a stronger condition such as $J\delta t \geq \sqrt{\frac{1}{27}} b \csc^2 k$ because according to Fig. 2.3a, adiabatic result does not match exact one when $J\delta t$ is slightly larger than $\sqrt{\frac{1}{27}} b \csc^2 k$.

monotonically decreases (as k increases). However, $|\theta|(k,t) \to 0$ when $k \to 0$ (2.23). Thus there exists a peak somewhere around k_c. As $J\delta t$ increases, the peak moves toward $k = 0$; more concretely, the peak of the exact $|\theta|$ moves along the curve of $|\theta|_{adia}$.

Now since $k_c \to 0$ when $J\delta t \to \infty$, all of the contributions from non-zero modes are adiabatic, i.e. $|\theta|(k,0) = |\theta|_{adia}(k,0)$ for all $k \neq 0$. This implies that circuit complexity $\mathcal{C}^{(1)}(0)$ saturates to a constant value

$$\int_0^\pi \mathrm{d}k |\theta|_{adia}(k,0)$$

given that $|\theta|_{adia}(k,0)$ is δt-independent. For a large δt that satisfies $J\delta t \gg 1/b$, the difference

$$\begin{aligned}\mathcal{C}^{(1)}(0)|_{\delta t} - \mathcal{C}^{(1)}(0)|_{\delta t\to\infty} &= \int_0^{k_c} \mathrm{d}k \left[|\theta|(k,0) - |\theta|_{adia}(k,0)\right] \\ &\leq \left[|\theta|(k,0) - |\theta|_{adia}(k,0)\right]|_{k\to 0} \times k_c = -|\theta|_{adia}(k\to 0,0) \times k_c\end{aligned} \tag{2.58}$$

since $|\theta|_{adia}(k,0)$ is monotonically decreases and $|\theta|(k,0)$ is non-negative. $|\theta|_{adia}(k \to 0,0)$ is δt-independent, and one can figure out that

$$|\theta|_{adia}(k \to 0,0) \to \pi/2.$$

On the other hand, according to (2.29), when δt is large, $k_c \sim \sin k_c \sim \delta t^{-1/2}$. Therefore, we can see

$$\mathcal{C}^{(1)}(0)|_{\delta t} = \int_0^\pi \mathrm{d}k |\theta|_{adia}(k,0) + \mathcal{O}(\delta t^{-1/2}) \tag{2.59}$$

This might explain why in slow quench regime ($J\delta t \gg 1/b$), $\mathcal{C}^{(1)}(0)$ in the fermionic theory saturates with the rate $\delta t^{-1/2}$. A more rigid argument is given in section 2.4.1.

The theory with ECP-type-like potential is slightly different when slow quenched (Fig. 2.5), complexity saturates much more quickly because the single-mode contribution saturates at large $J\delta t$ (Fig. 2.4a).

Finally, we numerically compare the late-time behaviors of circuit complexity ([107, 108] have studied circuit complexity at late time in the bosonic free field with smooth quench and fermionic free field with instantaneous quench, respectively) in ECP-type-like potential ($a = 1 - b$) and CCP-type-like one ($a = 1$), and the results are shown in Fig. 2.6. It shows that circuit complexity of ECP-type saturates without oscillation, unlike CCP-type potential. This is consistent to quantities such as $\langle\bar{\chi}\chi\rangle$ ([71]).

In conclusion, in this paper we have studied the scaling of circuit complexity in Majorana fermion field theory of 1D transverse field Ising model under quantum quench. It provides another evidence for the fact that just as correlation functions (e.g. $\langle\bar{\chi}\chi\rangle$) and entanglement entropy, complexity is a good quantity to see universal scaling in critical quench.

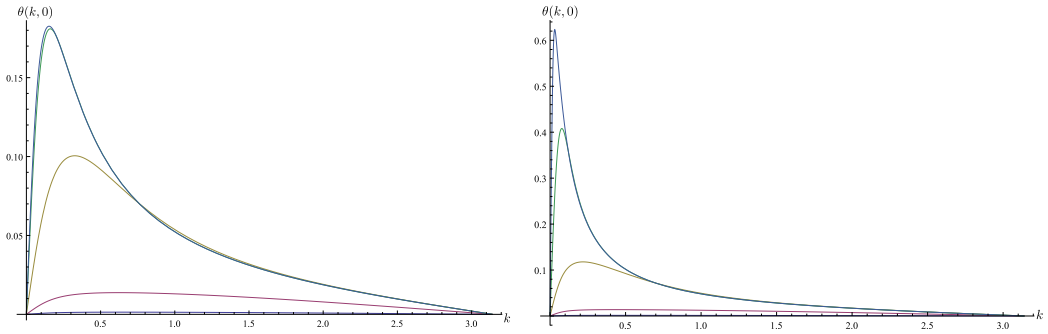

(a) ECP-type-like (b) CCP-type-like

Figure 2.4: Single-mode contribution to complexity at $t = 0$, $|\theta|(k, 0)$ in ECP and CCP-like potentials when $b = 0.01$. Purple, red, yellow, green and blue solid lines are $J\delta t = 0.01, 0.1, 1, 10, 100$, respectively.

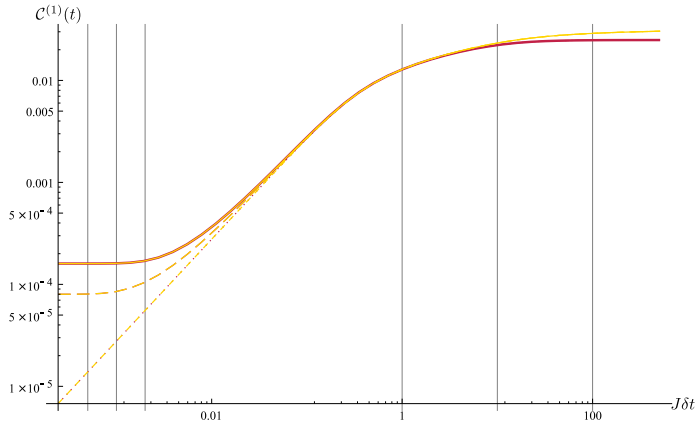

Figure 2.5: Exact $\mathcal{C}^{(1)}(t)$-$J\delta t$ relations in log-log scale when $b = 0.01$. Red and yellow lines correpond to ECP and CCP-type-like potential respectively. From solid to dashed, the curves correspond to $t = 0.002, 0.001$ and 0.0005, respectively. The plots differ at large $J\delta t$ (Red plots saturate more quickly).

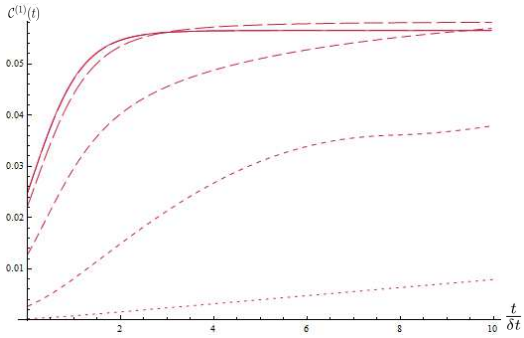

(a) ECP-type-like: from solid to dotted lines $J\delta t = 200, 100, 10, 1, 0.1, 0.01$, respectively

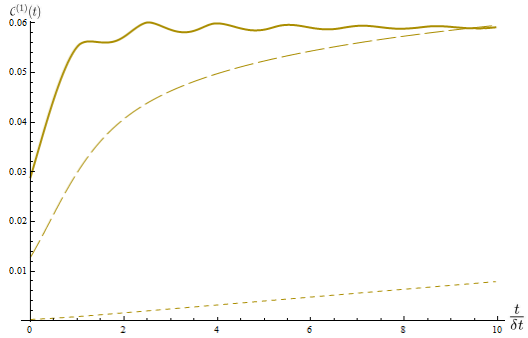

(b) CCP-type-like: from solid to dotted lines $J\delta t = 100, 1, 0.01$, respectively

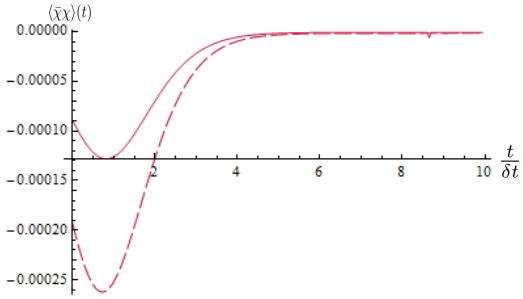

(c) ECP-type-like: from solid to dashed lines $J\delta t = 150, 100$, respectively

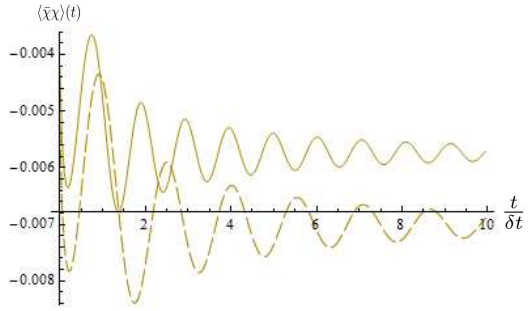

(d) CCP-type-like: from solid to dashed lines $J\delta t = 150, 100$, respectively

Figure 2.6: 2.6a&2.6b:Time evolution of complexity $\mathcal{C}^{(1)}(t)$ in ECP and CCP-like potentials; 2.6c&2.6d:Time evolution of $\langle\bar{\chi}\chi\rangle$ in ECP and CCP-like potentials. From thick solid lines to dotted lines $J\delta t$ decrease. Choose $b = 0.01$.

Chapter 3
Quantum Quench in Non-relativistic Fermionic Field Theory: Harmonic traps and 2d String Theory

3.1 Introduction

A common way to study non-equilibrium properties of quantum field theories is to subject them to a quantum quench, i.e. introduce an explicit time dependence to parameters which appear in the lagrangian. Among other things, this is interesting for several reasons. One motivation is to study equilibration and possible thermalization of these systems. Suppose the time dependent parameters approach constant values in the far past and future, and the system is initially in the ground state. The quench then excites the system. At late times, when the parameter again becomes a constant (which is generally different from the initial value), one would like to know the nature of the excited state, and if it is approximately described by a thermal state in some appropriate sense.

A second motivation - which is one of our main interests - is to study dynamics in critical phase transitions [66–70]. Suppose the initial hamiltonian is gapped, while the quench protocol crosses or approaches a critical point where the gap vanishes. On general grounds one expects that various observables would obey universal behavior.

An early example of such a universal behavior is Kibble Zurek scaling for global quenches [5, 6, 65] (where the parameters depend only on time). This holds in many systems when the time scale of the quench δt is large compared to the inverse of the initial energy gap E_g. In this case, the initial time evolution is adiabatic. However since the instantaneous gap is descreasing with time, adiabaticity breaks down at some time called the Kibble Zurek time t_{KZ}. This is typically determined by the Landau criterion,

$$\frac{1}{E_{gap}(t)^2}\frac{dE_{gap}(t)}{dt}|_{t=t_{KZ}} \sim 1 \tag{3.1}$$

where $E_{gap}(t)$ is the instantaneous energy gap. This equation then determines t_{KZ} in terms of δt. According to the assumptions of Kibble and Zurek, the system soon enters a *diabatic* regime, and the instantaneous correlation length at the Kibble Zurek time is the only length scale in the problem.

In the following we will follow standard nomenclature to distinguish several classes of quench protocols. The first protocol is called a trans-critical protocol (TCP). Here the system begins in a gapped phase and the coupling varies monotonically across a critical value, and approaches a final value which also corresponds to a gapped phase. The second is called a cis-critical protocol (CCP) where the time dependence is not monotonic. Here the system starts from a gapped phase, approaches a critical point and reverts back to a constant value which also corresponds to a gapped phase. The third protocol is called a end-critical protocol (ECP). Here the system begins in a gapped phase and monotonically approaches a critical point at infinitely late time. In TCP or CCP, the response at early times then scales as appropriate power of the

correlation length, leading to a scaling as some universal power of the quench time scale. For example the one point function of an operator $\mathcal{O}$ will scale as

$$\langle \mathcal{O} \rangle \sim \xi_{KZ}^{-\Delta} \tag{3.2}$$

where Δ is the dimension of $\mathcal{O}$. For ECP, the appropriate scaling variable is the energy scale at the Kibble Zurek time. At any given time the response will be adiabatic for sufficiently large δt, while for a small enough δt there will be a Kibble Zurek regime [11, 109–112].

Even though these assumptions appear to be drastic, such a scaling - together with an accompanying mechanism for defect formation in symmetry breaking transitions - appears to hold for many systems. Kibble Zurek scaling has been studied in a variety of solvable models and in holographic setups [75, 76, 113–116]. The latter provide some insight into the origins of universality. The best known results involve one point functions (e.g. defect density) and correlation functions. However similar scaling holds for the entanglement entropy of a subregion in some model $1+1$ dimensional systems.

At the other extreme is *instantaneous* quench where a sudden change of a parameter causes the system to go from a gapped phase to a critical point abruptly. In this case, universal results are known for correlators and entanglement entropies of $1+1$ dimensional systems [27–29]. Of particular interest is the spread of entanglement with time [27, 28] - this kind of spread has been conjectured to hold for higher dimensional systems [117–120] and there has been evidence for this in holographic calculations [117, 121–125] as well as in free field theories.

More recently it has been found that in a relativistic theory there is an intermediate regime where a different universal scaling holds [7–9]- a result which was first found in holographic calculations [77–79] and later found to hold quite generally. Consider a relativistic quantum field theory in d dimensional space-time which is obtained by the RG flow from a UV fixed point. The action can be then written as

$$S = S_{CFT} - \int dt \int d^{d-1}x \ \lambda(t) \mathcal{O}_\Delta(\vec{x}, t) \tag{3.3}$$

Here S_{CFT} stands for the conformal field theory action at the UV fixed point and Δ denotes the conformal dimension of the operator $\mathcal{O}_\Delta(\vec{x}, t)$ in this CFT. The time dependent coupling $\lambda(t)$ goes from a constant value λ_0 in the infinite past some other value λ_1 in the distant future, and the time dependence is in some time interval of size δt. Then this regime is defined by

$$\Lambda_{UV}^{-1} \ll \delta t \ll (\delta\lambda)^{-\frac{1}{d-\Delta}}, (\lambda_{0,\pm})^{-\frac{1}{d-\Delta}} \tag{3.4}$$

where $\lambda_\pm$ denote the largest and smallest value of the coupling and $\delta\lambda$ is the excursion of the coupling during the quench process. In this regime the one point function soon after the quench is over scales as

$$\langle \mathcal{O}_\Delta \rangle \sim (\delta t)^{d-2\Delta} \tag{3.5}$$

This is a result in *any* relativistic field theory, and follows from two basic properties [7–9]. The first is causality. The second property is that the causal Green's functions of a massive theory become those of the UV conformal theory for space-time separations which are small compared to the inverse mass gap. Once these properties hold, it turns out that the dimensionless parameter which controls time dependent perturbation theory is the combination of the coupling with an appropriate power of δt, and all other scales go away. This combination is small in the fast quench limit and the result (3.5) follows from the lowest order perturbation theory. This regime of scaling has been investigated explicitly in free field theories with time dependent masses and in conformal field theories with relevant and marginal deformations [72–74]. In continuum free theories there appears to be a smooth transition between Kibble-Zurek and Fast scaling regimes [10], while in lattice theories this connects to the abrupt quench regime at quench rates at the scale of the lattice spacing [71]. Apart from one point functions, the whole range of scaling behavior is visible in quantities like the entanglement entropy [11] as well as circuit complexity [12, 81] [1].

In many situations, particularly in experimental setups, one is interested in non-relativistic systems. Our ultimate goal is to investigate whether there are universal scaling laws which hold in non-relativistic systems. While Kibble Zurek scaling is expected to hold, the status of fast quench scaling is unclear. In specific models where non-relativistic Lifshitz type dispersion relations appear, e.g. the anisotropic critical points of the Kitaev model one indeed finds fast quench scaling with appropriate scaling dimensions [71]. More generally, Lieb Robinson bounds [127] for lattice non-relativistic systems may provide the necessary ingredient. Indeed in recent work in lattice models with dynamical exponent $z \neq 1$ it has been found that the spread of entanglement following a sudden quench indeed has an effective finite velocity [128]. However, such a finite speed has been also observed in non-relativistic systems which do not obey Lieb-Robinson bound [129, 130].

In this work we study the issue of scaling in a specific solvable system : a system of N mutually non-interacting non-relativistic fermions in a harmonic or inverted harmonic potential with a time dependent frequency and a time dependent mass. Using the results of [131–133] will show how the problem of quantum quench with some *smooth quench profile* in such systems can be solved analytically once one can solve a nonlinear equation (Ermakov-Pinney (EP) equation). The solutions of this equation can be in turn determined in terms of the solutions of the *classical* equation of motion of a single particle in the same harmonic potential.

Indeed harmonic traps are of considerable interest in experimental cold atom physics : quantum quench experiments often involve release of particles from harmonic traps.

Our interest in the inverted harmonic oscillator potential on the other hand stems from its connection to two dimensional string theory [52, 53, 134, 135]. As is well known, the double scaled limit of the singlet sector of the quantum mechanics of a single hermitian matrix reduces to a set of fermions in an inverted harmonic oscil-

[1] Other aspects of time dependence of complexity following a quench have been studied earlier in [107, 126].

lator potential. The string coupling appears as the mass of the fermion. Thus two dimensional string theory with a time dependent coupling reduces to the problem of fermions with time dependent mass in such a potential [2]. String theory with time dependent string couplings have been studied extensively in the context of AdS/CFT to investigate thermalization via black hole formation [15, 37]. In a different context these have been used as models of AdS cosmology [139–150], but the outcome has been rather inconclusive. Here we hope to obtain exact results in a simplified situation.

In this paper we will set up the formalism necessary to solve both the harmonic and inverted harmonic potential problems. We present detailed results for the problem in harmonic trap : the problem of two dimensional string theory will appear in a future publication [18].

We will solve the quantum mechanical time evolution of such a system for interesting time dependent frequencies of the CCP and ECP type and calculate the early time response of one point functions as well as entanglement entropies for a sub-region for arbitary quench rates to find the scaling behavior in various regimes. We will also explore the late time behavior of the entanglement entropy. We find Kibble-Zurek scaling for slow quenches, while for fast quenches we show that the result scales in a way which is consistent with time dependent perturbation theory. At late times the entanglement entropy in a CCP oscillates with an amplitude which appears to remain constant in time. This reflects the lack of thermalization of the system. For the ECP the entanglement entropy monotonically goes to zero as a power law in time, reflecting the fact that the particles can now spread all over space.

Such solvable systems have played a major role in providing insight into scaling properties of quantum quench in continuum relativistic theories and in spin systems which can be reduced to lattice versions of relativistic fermions [7–10, 71]. As we will see, our example may not be the appropriate setup to explore a possible universal scaling at fast rates. Neverthless, we hope that these exact solutions will provide some insight into the general problem.

Abrupt quantum quench in a system of free non-relativistic fermions which arise from Matrix Quantum Mechanics with various potentials has been investigated in several papers [151–161]. In particular [151, 152] has extensively studied the problem in terms of the dynamics of the Wigner phase space density, investigated approach to a generalized Gibbs ensemble and discovered interesting dynamical phase transitions. The papers [153–158, 160, 161] deal with the fermion problem directly in the presence of various kinds of abrupt quenches. Other aspects of the dynamics in such fermion systems (e.g. shock wave formation) have been studied in [162, 163].

The paper [159] considers the dynamics of the Wigner phase space density as well as a system of bosons and fermions using methods similar to us, in particular the EP equation. The paper [164] considers slow smooth quenches for bosons also using the

[2]Fermions in harmonic oscillator potentials also appear in the description of special states in the AdS/CFT correspondence [136–138]. Introducing a time dependent mass for such fermions naively corresponds to a time dependent coupling of the Yang-Mills theory. However this breaks supersymmetries : the truncation of matrix models and therefore fermions do not hold any more.

EP equation. The EP equation has also been used to study entanglement dynamics following an abrupt quench in a harmonic chain in [165].

Our work is complementary to these papers. We are interested in studying scaling of various quantities as functions of the quench rate. We have been able to find exact analytic solutions to several smooth quench protocols which we use for this purpose.

In section 3.2 we set up the second quantized fermion field theory and show how this can be solved exactly for $\pm x^2$ potentials in terms of a function $\rho(t)$ which satisfies generalized Ermakov-Pinney equation and show how to obtain its solutions. In section 3.3 we quantize these theories in the Heinsenberg picture "in" state and show how observables can be expressed entirely in terms of $\rho(t)$. In section 3.4 we provide exact solutions for some CCP and ECP quench protocols for the harmonic problem. Sections 3.5 - 3.7 contain our results for the one point function of the quenched operator and the entanglement entropy for these protocols and their scaling as functions of the quench rate. Section 3.8 deals with comments about the behavior of the phase space density.

3.2 Fermion field theory

Consider a system of N non-relativistic fermions in $1+1$ dimensions with a hamiltonian given by

$$H = \int dx\ \psi^\dagger(x) \left[-\frac{\hbar}{2m(t)} \frac{\partial^2}{\partial x^2} \pm \frac{1}{2\hbar} m(t) \nu^2(t) x^2 \right] \psi(x) \tag{3.6}$$

where $m(t), \nu(t)$ are real smooth functions. The Schrodinger picture fermion field operators above satisfy the usual anti-commutation relations

$$\begin{aligned} \{\psi(x), \psi^\dagger(x')\} &= \delta(x-x') \\ \{\psi(x), \psi(x')\} &= \{\psi^\dagger(x), \psi^\dagger(x')\} = 0 \end{aligned} \tag{3.7}$$

The condition that the total number of fermions is N then leads to the constraint

$$\int_{-\infty}^{\infty} dx\ \psi^\dagger(x,t)\psi(x,t) = N \tag{3.8}$$

The plus sign in (3.6) is the hamiltonian of particles with a time dependent mass in a harmonic trap with a time dependent frequency. The minus sign with $\nu = 1$ is the hamitonian of the singlet sector of the double scaled single hermitian matrix quantum mechanics which is dual to two dimensional string theory with a time dependent string coupling $g_s(t) = m(t)$. The Heisenberg picture equation of motion is the Schrodinger equation

$$i\frac{\partial \psi(x,t)}{\partial t} = \left[-\frac{\hbar}{2m(t)} \frac{\partial^2}{\partial x^2} \pm \frac{1}{2\hbar} m(t) \nu^2(t) x^2 \right] \psi(x,t) \tag{3.9}$$

In the following we will set $\hbar = 1$.

3.2.1 The general solution

In terms of a new time variable τ

$$d\tau = \frac{dt}{m(t)} \tag{3.10}$$

we can transfer the time dependence of the mass to the frequency term and (3.9) becomes

$$i\frac{\partial\psi(x,\tau)}{\partial\tau} = \left[-\frac{1}{2}\frac{\partial^2}{\partial x^2} \pm \frac{1}{2}\omega^2(\tau)x^2\right]\psi(x,\tau) \tag{3.11}$$

where

$$\omega(\tau) = m(t)\nu(t) \tag{3.12}$$

A solution to the equation (3.11) can be obtained in terms of the solution of the Schrodinger equation with a constant mass and a constant frequency as follows [131–133]. First define a new field $\Phi(x,\tau)$ by

$$\psi(x,\tau) = \exp[-\alpha(\tau)x^2 - \beta(\tau)]\ \Phi(x,\tau) \tag{3.13}$$

Secondly, make a change of variables

$$\begin{aligned} \tau \to T &= \int^{\tau} \frac{d\tau'}{\rho(\tau')^2} \\ x \to y &= \frac{x}{\rho(\tau)} \end{aligned} \tag{3.14}$$

Then $\Phi(y,T)$ satisfies

$$i\frac{\partial\Phi(y,T)}{\partial T} = \left[-\frac{1}{2}\frac{\partial^2}{\partial y^2} \pm \frac{1}{2}y^2\right]\Phi(y,T) \tag{3.15}$$

provided

$$\beta(\tau) = \log[\rho(\tau)]^{1/2} \qquad \alpha(\tau) = -i\partial_\tau\beta(\tau) \tag{3.16}$$

and the function $\rho(\tau)$ satisfies a generalization of the Ermakov-Pinney equation [166, 167]

$$\partial_\tau^2\rho(\tau) \pm \omega(\tau)^2\rho(\tau) = \pm\frac{1}{\rho(\tau)^3} \tag{3.17}$$

Here the positive sign refers to the right-side up harmonic oscillator while the negative sign refers to the inverted harmonic oscillator of relevance to the hermitian matrix model. The latter case will be discussed in detail in [18].

In the adiabatic approximation the function $\rho(\tau)$ is simply $\frac{1}{\sqrt{\omega(\tau)}}$. A departure from this value denotes a departure from adiabaticity and describes the exact response.

Furthermore the most general solution of (3.17) is given by

$$\rho(\tau)^2 = Af(\tau)^2 + 2Bf(\tau)g(\tau) + Cg(\tau)^2 \tag{3.18}$$

where A, B, C are constants and $f(\tau), g(\tau)$ are two linearly independent solutions of the *classical* equation of motion of a single particle moving in a harmonic (inverted harmonic) potential with the same time dependent frequency $\omega(\tau)$

$$\partial_\tau^2 X \pm \omega(\tau)^2 X = 0 \tag{3.19}$$

Furthermore A, B, C must satisfy

$$AC - B^2 = \pm \frac{1}{Wr(f,g)^2} \tag{3.20}$$

where $Wr(f,g) = f\partial_\tau g - g\partial_\tau f$ is the wronskian of the two solutions. By the equations of motion this is a constant in time and can be therefore evaluated at any time.

The problem of fermions with a time dependent mass in a harmonic (or inverted harmonic) potential with a time dependent frequency can be therefore reduced to a problem with a constant mass and a constant frequency. The only equation one needs to solve is the classical equation (3.19). As we will see below, many quantities of physical interest can be expressed entirely in terms of the function $\rho(t) = \rho(\tau)$.

A general solution of the equation (3.15) has the form

$$\Phi_n(y,T) = N_n \; e^{-i\lambda(n)T} \phi_n(y) \tag{3.21}$$

where ϕ_n denote a complete orthonormal set of eigenfunctions of the hamiltonian given by the right hand side of (3.15) with eigenvalue $f(n)$. Then the above discussion implies that a general solution of the equation (3.11) may be written as

$$\psi_n(x,\tau) = \frac{1}{\sqrt{\rho(\tau)}} \exp\left[\frac{i}{2}\frac{\partial_\tau \rho(\tau)}{\rho(\tau)} x^2\right] \; \Phi_n\left(\frac{x}{\rho(\tau)}, T\right) \tag{3.22}$$

The orthonormality conditions for the eigenfunctions $\phi_n(y)$ then imply the orthonormality conditions for the solution (3.22).

The form of the solution (3.22) reveals another physical meaning for the function $\rho(\tau)$. In the wavefunctions of a harmonic oscillator at fixed frequency ω, one can rescale out the frequency by $x \to \sqrt{\omega} x$ and $\tau \to \omega\tau$. The normalization of the wavefunction also involves $\omega^{1/4}$, as would be required by the rescaling of x. In our problem $\rho(\tau)$ *almost* plays the role of such a time dependent rescaling. The term which spoils this is the phase factor which involves $\partial_\tau \rho(\tau)$. This is of course consistent with the fact that in lowest order of adiabatic approximation $\rho(\tau) = \frac{1}{\sqrt{\omega(\tau)}}$.

The function $\rho(\tau)$ is given by (3.18). The independent solutions $f(\tau), g(\tau)$ and the constants A, B, C have to be chosen so that the solutions (3.22) satisfy the correct initial condition.

3.2.2 Solution in terms of Phase Space Density

It will be useful to think in terms of the Wigner phase space density operator

$$u(q,p,t) = \int dx e^{ipx/\hbar} \psi^\dagger(q - x/2)\psi(q + x/2) \tag{3.23}$$

The condition (3.7) then becomes

$$u(q,p,t) \star u(q,p,t) = u(q,p,t) \tag{3.24}$$

while (3.8) becomes

$$\int \frac{dqdp}{2\pi\hbar} u(q,p,t) = N \tag{3.25}$$

where $\star$ denotes the Moyal star product. As shown in [168–170] the fermion field theory can be expressed as a path integral in terms of these variables with a co-adjoint orbit action. Formulating the theory in terms of $u(p,q,t)$ is particularly useful in the classical limit $\hbar \to 0, N \to \infty$ with $N\hbar$ held fixed. In this limit the Moyal product reduces to an ordinary product.

In this limit the operator $u(p,q,t)$ satisfies the equation

$$[\partial_\tau + p\partial_q \mp \omega^2(\tau) q\partial_p] u(p,q,\tau) = 0 \tag{3.26}$$

If we make the change of variables

$$\begin{aligned} \tau \to T &= \int^\tau d\tau' \frac{1}{\rho(\tau')^2} \\ q \to Q &= \frac{q}{\rho(\tau)} \\ p \to P &= p\rho(\tau) - q\partial_\tau \rho(\tau) \end{aligned} \tag{3.27}$$

the function

$$U(P,Q,T) = u(p,q,t) \tag{3.28}$$

satisfies

$$[\partial_T + P\partial_Q \mp Q\partial_P] U(P,Q,T) = 0 \tag{3.29}$$

provided (3.18) holds.

This transformation is in fact a canonical transformation. Therefore the condition (3.25) that $u(p,q,t)$ describes N fermions transforms into the condition

$$\int dPdQ\ u(P,Q,T) = N \tag{3.30}$$

The equation (3.29) is the equation satisfied by the phase space density operator for a system of fermions which is in an external harmonic (or inverted harmonic) potential with unit mass and unit frequency. Therefore once we know the solution for this latter case, we can find a solution of the time dependent case in terms of a solution of the equation (3.17).

3.3 Quantization and the "in" state

The quantization of the fermionic field theory proceeds in a standard fashion. Given a complete set of modes $\{\psi_n(x,\tau)\}$ which solve the equations of motion the Heisenberg

picture field operators may be expressed as

$$\begin{aligned}\psi(x,\tau) &= \sum_{n=0}^{\infty} a_n\ \psi_n(x,\tau) \\ \psi^\dagger(x,\tau) &= \sum_{n=0}^{\infty} a_n^\dagger\ \psi_n^*(x,\tau)\end{aligned} \tag{3.31}$$

where the oscillators satisfy the standard anti-commutation relations

$$\{a_m, a_n^\dagger\} = \delta_{mn} \quad \{a_n, a_m\} = \{a_m^\dagger, a_n^\dagger\} = 0 \tag{3.32}$$

Different choices of modes determine different inequivalent quantizations related by Bogoliubov transformations.

We will be interested in profiles of $m(t), \nu(t)$ such that they approach constant values m_{in} and ν_{in} as $t \to -\infty$, and their time derivatives approach zero. Furthermore we will have choices of $m(t)$ such that when $t \to -\infty$, one also has $\tau \to -\infty$. In particular our choices of $m(t)$ are such that as $t \to -\infty$, we have $m(t) \to m_{in}$ so that $\tau \to \frac{1}{m_{in}} t$. The equation (3.17) means that $\rho(t) = \rho(\tau)$ has the initial condition

$$\lim_{\tau \to -\infty} \rho(\tau) = \rho_{in} = \frac{1}{\sqrt{m_{in}\nu_{in}}} = \frac{1}{\sqrt{\omega_{in}}} \tag{3.33}$$

The corresponding solution ψ_n in (3.31) must then have the property that this is positive frequency in the far past,

$$\lim_{\tau \to \infty} \psi_n(x,\tau) \sim e^{-i\alpha\tau} \qquad \alpha > 0 \tag{3.34}$$

We will consider the Heisenberg picture state which is the "in" ground state,

$$\begin{aligned} a_n|in\rangle &= 0 \qquad n \geq N \\ a_n^\dagger|in\rangle &= 0 \qquad 0 \leq n \leq N-1 \end{aligned} \tag{3.35}$$

3.3.1 Observables

The observables we will be interested in are the expectation value of the quenched operator and the entanglement entropy. We will now show that both these quantities can be expressed in terms of the corresponding quantities in the time independent problem and the function $\rho(\tau)$.

In the following we will consider the expectation value of the operator

$$\mathcal{O}(\tau) = \int_{-\infty}^{\infty} dx\ x^2 \psi^\dagger(x,\tau)\psi(x,\tau) \tag{3.36}$$

This is the operator which comes multiplied by the time dependent coupling $\omega^2(\tau)$ once the theory is expressed in the time variable τ. In the spirit of response theory, the expectation value then measures the response of the system to the external driving. $\langle \mathcal{O}(\tau) \rangle$ of our problem can be expressed simply in terms of the expectation value

of the quenched operator in an auxiliary problem of a harmonic oscillator with unit mass and frequency, using (3.22)

$$\langle in|\mathcal{O}(\tau)|in\rangle = \sum_{n=0}^{N-1} \int_{-\infty}^{\infty} dx\ x^2\ \psi_n^*(x,\tau)\psi_n(x,\tau) \tag{3.37}$$

Using (3.21) and (3.22) this becomes, after a change of variables,

$$\langle in|\mathcal{O}(\tau)|in\rangle = \rho^2(\tau) \sum_{n=0}^{N-1} \int_{-\infty}^{\infty} dY Y^2 \phi_n^*(Y)\phi_n(Y) = \rho(\tau)^2 \sum_{n=0}^{N-1}(n+1/2) = \frac{N^2}{2}\rho(\tau)^2 \tag{3.38}$$

where we have used the fact that the integral on the right hand side is the expectation value of the potential energy of a single harmonic oscillator with unit frequency in the state with quantum number n, and used the standard result.

For fermionic systems, the entanglement entropy of a subregion A has an expansion in terms of cumulants of the particle number distribution [47, 48, 171–174]. In the leading order of large N the dominant term is the variance of the expectation value of the particle number in A,

$$S_A(\tau) = \frac{\pi^2}{3}[\langle N_A(\tau)^2\rangle - \langle N_A(\tau)\rangle^2] \tag{3.39}$$

where the operator N_A is given by

$$N_A(\tau) = \int_A dx \psi^\dagger(x,\tau)\psi(x,\tau) \tag{3.40}$$

where the integral is over the region A.

This simplifies for the "in" state. Using the mode expansion (3.31) and the state defined in (3.35) it may be easily shown that

$$S_A(\tau) = \langle in|N_A(\tau)|in\rangle - \int_A dx \int_A dy |C(x,y,\tau)|^2 \tag{3.41}$$

where

$$C(x,y,\tau) = \langle in|\psi^\dagger(x,\tau)\psi(y,\tau)|in\rangle \tag{3.42}$$

This quantity can be also expressed entirely in terms of the expectation value of the phase density operator as follows

$$\begin{aligned} S_A =& \frac{1}{2\pi}\int_{-\infty}^{\infty} dp \int_A dx\, \langle in|u(p,x,\tau)|in\rangle \\ &- \frac{1}{(2\pi)^2}\int_{-\infty}^{\infty} dp_1 dp_2 \int_A dx dy\ e^{-i(p_2-p_1)(x-y)}\ \langle in|u(p_1,(x+y)/2,\tau)|in\rangle \\ &\qquad \times \langle in|u(p_2,(x+y)/2,\tau)|in\rangle \end{aligned} \tag{3.43}$$

Expressing the above expectation values in terms of the mode functions one has

$$\begin{aligned} \langle in|N_A(\tau)|in\rangle &= \int_A dx \sum_{n=0}^{N-1} \psi_n^*(x,\tau)\psi_n(x,\tau) \\ C(x,y,\tau) &= \sum_{n=0}^{N-1} \psi_n^*(x,\tau)\psi_n(y,\tau) \end{aligned} \tag{3.44}$$

Using (3.22) it then follows that the entanglement entropy can be expressed in terms of the entanglement entropy of a rescaled region in the ground state of the theory with a constant mass and frequency. If the subregion A is defined by $a \leq x \leq b$ then the rescaled subegion is defined by

$$S_A[\omega(\tau)] = S_{A_P}[\omega = 1] \qquad A_P : \frac{a}{\rho(\tau)} \leq x \leq \frac{b}{\rho(\tau)} \tag{3.45}$$

3.4 Results for fermions in Harmonic Oscillator Potential

For the right side up harmonic oscillator, the two independent solutions of the equation (3.19) may be therefore chosen to be such that

$$\lim_{\tau\to-\infty} f(\tau) = \frac{1}{\sqrt{2\omega_{in}}} e^{-i\omega_{in}\tau} \qquad g(\tau) = [f(\tau)]^* \tag{3.46}$$

To ensure that $\rho(\tau)$ is real we then need to choose

$$A = C = 0 \qquad B = 1 \tag{3.47}$$

Therefore for this solution we have

$$\rho(\tau) = \sqrt{2}\ |f(\tau)| \tag{3.48}$$

This yields the final form of the solution

$$\begin{aligned} \psi_n(x,\tau) = \frac{1}{\sqrt{2^n n!}} \left[\frac{1}{\pi\rho(\tau)^2}\right]^{1/4} \exp\left[-i(n+1/2)\int^\tau \frac{dt'}{\rho(\tau)^2}\right] \\ \exp\left[\frac{i}{2}\left(\partial_\tau \log\rho(\tau) + \frac{i}{\rho(\tau)^2}\right)x^2\right]\ H_n(x/\rho(\tau)) \end{aligned} \tag{3.49}$$

where $H_n(x)$ denotes the n-th order Hermite polynomial. This solution approaches the normalized solutions of the Schrodinger equation with a frequency ω_{in} as $\tau \to -\infty$. The oscillators in (3.31) with these modes are in the "in" oscillators.

We now provide exactly solvable quench protocols for fermions with a fixed mass m in a harmonic oscillator potential with time dependent frequencies. The two times t and τ are then related by $\tau = t/m$.

3.4.1 Cis-Critical Protocol

The first protocol is a cis-critical-protocol (CCP). As described in the introduction in such a protocol the system starts from a gapped phase, approaches a critical point and then turns back to another constant value. In this work we choose a protocol where the initial and the final values are the same. More specifically we choose

$$\omega(\tau)^2 = \omega_0^2 \ \tanh^2(\tau/\delta t) \tag{3.50}$$

This corresponds to a trap which is smoothly removed for a finite interval of time and then re-introduced.

The solution to the equation (3.19) which behaves as $e^{-i\omega_0\tau}$ is then given by

$$\begin{aligned} f_{CCP}(\tau) =& \frac{1}{\sqrt{2\omega_0}} \frac{2^{i\omega_0\delta t}\cosh^{2\alpha}(\tau/\delta t)}{E_{1/2}\tilde{E}'_{3/2} - E'_{1/2}\tilde{E}_{3/2}} \times \\ & \left\{ \tilde{E}'_{3/2} \ {}_2F_1(a, b; \frac{1}{2}; -\sinh^2\frac{\tau}{\delta t}) + E'_{1/2}\sinh\frac{\tau}{\delta t} \ {}_2F_1(a+\frac{1}{2}, b+\frac{1}{2}; \frac{3}{2}; -\sinh^2\frac{\tau}{\delta t}) \right\} \end{aligned} \tag{3.51}$$

where we defined

$$\begin{aligned} \alpha &= \frac{1}{4}[1 + \sqrt{1 - 4\omega_0^2\delta t^2}] \\ a = \alpha - \frac{i}{2}\omega_0\delta t, b &= \alpha + \frac{i}{2}\omega_0\delta t \\ E_{1/2} = \frac{\Gamma(1/2)\Gamma(b-a)}{\Gamma(b)\Gamma(1/2-a)}, \tilde{E}_{3/2} &= \frac{\Gamma(3/2)\Gamma(b-a)}{\Gamma(b+1/2)\Gamma(1-a)} \\ E'_c &= E_c(a \leftrightarrow b) \end{aligned} \tag{3.52}$$

The key function $\rho(\tau)$ is then given by (3.48) with $f(\tau)$ given by (3.51).

3.4.2 End Critical Protocol (ECP)

Another solvable quench protocol is the end critical protocol where the initial theory is a harmonic oscillator with a frequency ω_0 which monotonically descreases smoothly to a vanishing frequency at infinitely late times. This corresponds to a *smooth* release from a harmonic trap.

Consider the slightly more general protocol

$$\omega^2(\tau) = \omega_0^2 \left(a + b\tanh\frac{\tau}{\delta t}\right) \tag{3.53}$$

with the real constants a, b chosen such that $a > b$ to ensure reality of $\omega(\tau)$. Then the "in" solution of the equation (3.19) is given by

$$\begin{aligned} f_{ECP} = \frac{1}{\sqrt{2\omega_{in}}} & \exp[-i\omega_+\tau - i\omega_-\delta t\log(2\cosh(\tau/\delta t))] \\ & {}_2F_1[1 + i\omega_-\delta t, i\omega_-\delta t; 1 - i\omega_{in}\delta t; \frac{1}{2}(1+\tanh(\tau/\delta t))] \end{aligned} \tag{3.54}$$

where we defined

$$\begin{aligned} \omega_{in} &= \omega_0\sqrt{a-b}, \\ \omega_{out} &= \omega_0\sqrt{a+b}, \\ \omega_{\pm} &= \frac{1}{2}(\omega_{out} \pm \omega_{in}) \end{aligned} \tag{3.55}$$

The end critical protocol we consider has $a = -b = \frac{1}{2}$. The function $\rho(\tau)$ which determines the time dependence of the observables considered above is shown in Figure 3.1 for both these types of protocol.

At early times $\rho(-\infty) = \frac{1}{\sqrt{2\omega_{in}}}$. For ECP $\rho(\tau)$ monotonically increases and behaves as $\rho(\tau) \sim \tau$ at large τ. For CCP $\rho(\tau)$ initially increases and then starts oscillating. At late times these oscillations are around a mean value which is roughly the initial value $\frac{1}{\sqrt{2\omega}}$ with an amplitude which remains constant in time and with a frequency approximately given by ω_0.

3.5 The response and scaling : CCP

In this section we present the results of the expectation value of the quenched operator $\mathcal{O} = \int dx x^2 \psi^\dagger \psi$ at early times for CCP (equation (3.50)) and investigate their scaling behavior in various regimes. The details of the analytic approximations which lead to these results are given in Appendix A.

3.5.1 Slow Quench Regime

In the slow quench regime $\omega_0 \delta t \gg 1$ we can use the asymptotic form of gamma functions

$$\Gamma(z) \sim \sqrt{2\pi} e^{-z+(z-\frac{1}{2})\log z}, z \to \infty \tag{3.56}$$

to obtain $\rho(\tau = 0)$. The leading expression for the one point function $\langle \mathcal{O} \rangle$ at $\tau = 0$ is, using (3.38),

$$\langle \mathcal{O}(0) \rangle \sim \frac{\sqrt{\pi}}{2} N^2 \sqrt{\frac{\delta t}{\omega_0}} \tag{3.57}$$

This result is consistent with Kibble-Zurek scaling. The Landau criterion with the instantaneous frequency given by (3.50) leads to

$$\frac{1}{\omega_0 \delta t} \text{cosech}^2(\tau_{KZ}/\delta t) = 1 \tag{3.58}$$

which defines the Kibble-Zurek time τ_{KZ}. We expect a scaling behavior only when $\tau_{KZ} \ll \delta t$. In this regime (3.58) leads to

$$\tau_{\text{KZ}} = \sqrt{\frac{\delta t}{\omega_0}} \tag{3.59}$$

The condition $\tau_{KZ} \ll \delta t$ then becomes consistent with the slow quench condition $\omega_0 \delta t \gg 1$. This leads to the instantaneous frequency at the Kibble-Zurek time,

$$\omega_{KZ}^2 = \frac{\omega_0}{\delta t} \tag{3.60}$$

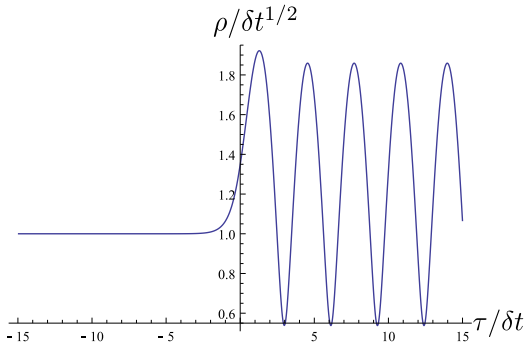

(a) $\omega_0\delta t = 1$(CCP)

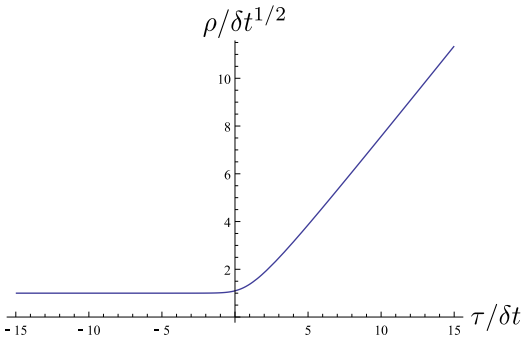

(b) $\omega_0\delta t = 1$(ECP)

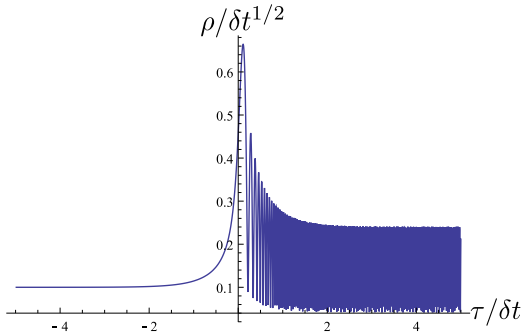

(c) $\omega_0\delta t = 100$(CCP)

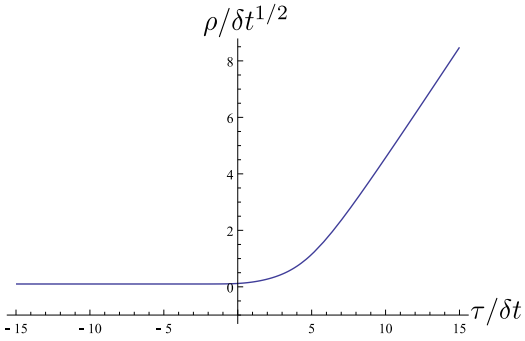

(d) $\omega_0\delta t = 100$(ECP)

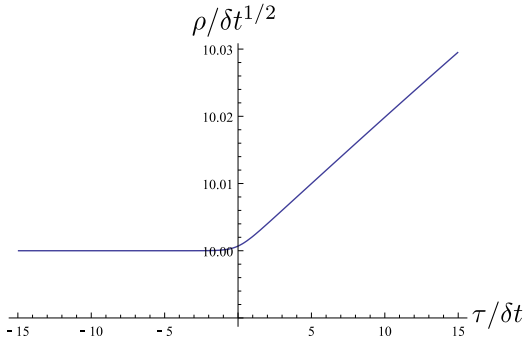

(e) $\omega_0\delta t = 0.01$(CCP)

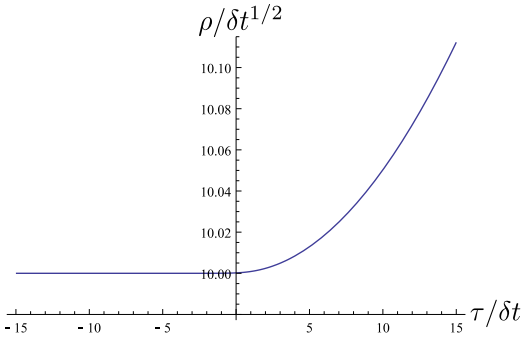

(f) $\omega_0\delta t = 0.01$(ECP)

Figure 3.1: relation between $\rho(\tau)$ and τ in various $\omega_0\delta t$ cases.

According to the Kibble-Zurek argument $\rho(\tau)$ in the middle of the quench (which is $\tau = 0$) is roughly equal to its value at $\tau = \tau_{KZ}$. Since the system is approximately adiabatic at $\tau = \tau_{KZ}$ this is in turn roughly equal to $\rho_{adia}(\tau_{KZ})$, the value of ρ for the fermions in a harmonic oscillator potential with a constant frequency ω_{KZ}. From (3.17) this is simply

$$\rho(\tau_{KZ}) \sim \rho_{adia}(\tau_{KZ}) = \frac{1}{\sqrt{\omega_{KZ}}} \tag{3.61}$$

leading to

$$\langle \mathcal{O} \rangle \sim \frac{N^2}{2}\sqrt{\frac{\delta t}{\omega_0}} \tag{3.62}$$

which is in agreement with the result from the exact solution (3.57) upto a numerical factor.

3.5.2 Fast Quench Regime

We now consider the regime $\omega_0 \delta t \ll 1$. While we have the exact answer anyway, we are able to approximate the answer by suitable expansions and obtain analytic expressions when we have in addition $\omega_0 \tau \ll 1$. The latter are useful to make a comparison with perturbation calculations.

First consider the response at a time τ which is in the range

$$\omega_0 \tau \ll \omega_0 \delta t \ll 1 \tag{3.63}$$

In this case, for the CCP (equation (3.50) we get an expression (see Appendix A.1, equations (A.8)-(A.18),

$$\langle \mathcal{O}(\tau) \rangle \approx \frac{N^2}{2\omega_0}\left\{1 + 2\log 2 \cdot \omega_0^2 \delta t^2 + 2\omega_0^2 \delta t \cdot \tau + \mathcal{O}(\omega_0^4 \delta t^4, \frac{\tau^2}{\delta t^2})\right\} \tag{3.64}$$

This is the response at early times. At late times, (see equations (A.19) to (A.28))

$$\omega_0 \delta t \ll \omega_0 \tau \ll 1 \tag{3.65}$$

one gets instead

$$\langle \mathcal{O} \rangle \sim \frac{N^2}{2\omega_0}\left(1 + 2\omega_0 \delta t \sin 2\omega_0 \tau + \mathcal{O}(\omega_0^2 \delta t^2)\right) \tag{3.66}$$

These results should also follow from usual time dependent perturbation theory. Let us discuss this for a general perturbation $\delta\omega(\tau)^2$ from the initial value. The leading term in the perturbation expansion is

$$\begin{aligned} &\langle \mathcal{O}(\tau) \rangle \\ =&\langle \mathcal{O}(-\infty) \rangle \\ &+ \frac{1}{2}\int_{-\infty}^{\tau} d\tau' \int dx \int dx' (xx')^2 \delta\omega(\tau')^2 \langle 0|[\psi^\dagger(x,\tau)\psi(x,\tau), \psi^\dagger(x',\tau')\psi(x',\tau')]|0\rangle_{\omega_0} \end{aligned} \tag{3.67}$$

where $\langle\rangle_{\omega_0}$ denotes the expectation value in the ground state of the theory at $\tau \to -\infty$ which is the harmonic oscillator with a constant frequency ω_0 and

$$\delta\omega(\tau)^2 = \omega(\tau)^2 - \omega_0^2 \tag{3.68}$$

The Green's function which appears in the linear response can be calculated. The result is

$$\begin{aligned} G(\tau,\tau') &= \theta(\tau-\tau')\int dx \int dx'\ x^2\ (x')^2\ \langle 0|[\psi^\dagger(x,\tau)\psi(x,\tau),\psi^\dagger(x',\tau')\psi(x',\tau')]|0\rangle_{\omega_0} \\ &= -\theta(\tau-\tau')\frac{N^2}{\omega_0^2}\sin[2\omega_0(\tau-\tau')] \end{aligned} \tag{3.69}$$

Now consider evaluating the response at a time which is of the order of $\tau \sim +\delta t$. In the fast quench regime $\omega_0\delta t \ll 1$. The limits of the integral in (3.69) can be replaced by $(-\delta t, \delta t)$. Suppose the form of $\delta\omega(\tau)^2$ is $\delta\omega(\tau)^2 = \delta\omega_0^2 f(\tau/\delta t)$ where δt is the time scale of the quench and $f(x)$ some smooth function. Using the above form of the Green's function the linear response becomes in the fast quench regime

$$\begin{aligned} \langle\mathcal{O}(\tau)\rangle - \langle\mathcal{O}(-\infty)\rangle &\sim \delta\omega_0^2\frac{N^2}{2\omega_0^2}\int_{-\delta t}^{\delta t} d\tau'\ f(\tau'/\delta t)\sin[2\omega_0(\tau-\tau')] \\ &\sim \delta\omega_0^2\frac{N^2}{2\omega_0^2}\omega_0\delta t^2 \end{aligned} \tag{3.70}$$

In the protocol we are using $\delta\omega_0^2 = \omega_0^2$ and $f(\tau/\delta t) = \mathrm{sech}^2(\tau/dt)$. We therefore reproduce the scaling in (3.64).

3.5.3 The exact response

The exact response for CCP is shown in Figure 3.2. This shows that the analytic approximatations in the fast and slow regime agree very well with the exact answer, and the transition between the two regimes is rather sharp.

3.6 The response and scaling : ECP

The investigation of the scaling behavior for the ECP case (3.53) follows along lines similar to CCP.

3.6.1 Slow Quench Regime

In the slow quench regime ($\omega_0\delta t \gg 1$) one expects a Kibble Zurek scaling. For the protocol (3.53) the Landau criterion determining the Kibble-Zurek time t_{KZ} becomes

$$\frac{1}{\cosh^2(\tau_{KZ}/\delta t)(1-\tanh(\tau_{KZ}/\delta t))^{3/2}} \sim \omega_0\delta t \tag{3.71}$$

For $\omega_0\delta t \gg 1$ the solution can appear only at late times. This yields

$$\tau_{KZ} \sim \delta t\log(\omega_0\delta t) \tag{3.72}$$

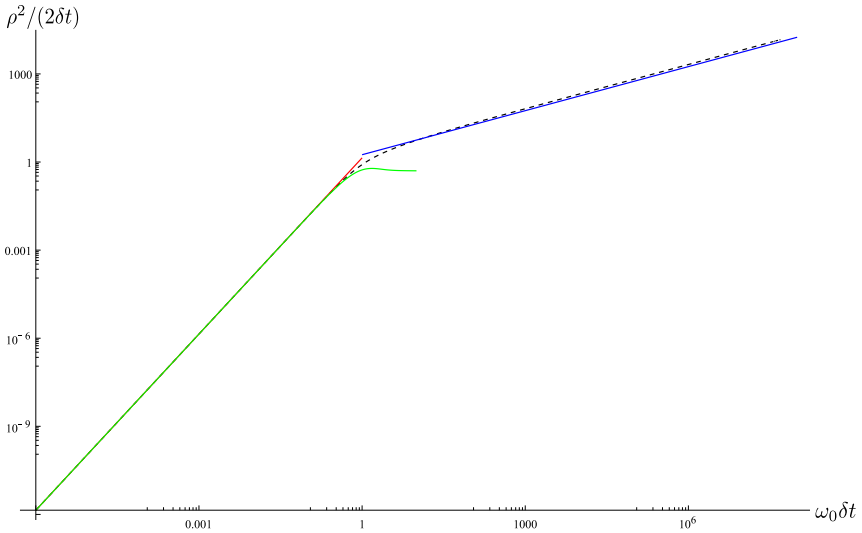

Figure 3.2: (Colour online) The response $\rho^2/(2\delta t) = \langle \mathcal{O} \rangle/(N^2\delta t)$ as a function of $\omega_0\delta t$ for CCP when $\tau = 0$. The black dashed curve is the exact result obtained by using (3.51). The blue curve is the leading Kibble Zurek result for $\omega_0\delta t \gg 1$, i.e. Eq. (3.62). The red curve is the leading behavior when $\omega_0\delta t \ll 1$, i.e. Eq. (3.64). The green curve is the perturbation expansion result i.e. Eq. (3.70).

In this case the instantaneous gap vanishes in the infinite future. This means that in the slow quench regime adiabaticity will fail at late times. The frequency at this time is

$$\omega_{KZ} = \omega_0 \sqrt{\frac{1 - \tanh(\tau_{KZ}/\delta t)}{2}} \sim \frac{1}{\delta t} \tag{3.73}$$

Therefore the standard Kibble Zurek argument would predict that the response at late times is given by

$$\langle \mathcal{O} \rangle \sim \frac{1}{2} N^2 \rho(\tau_{KZ})^2 = \frac{N^2}{2\omega_{KZ}} \sim \frac{1}{2} N^2 \delta t \tag{3.74}$$

At a time earlier than the Kibble Zurek time i.e. when

$$\tau < \delta t \log(\omega_0 \delta t), \tag{3.75}$$

the adiabatic approximation is valid. Therefore if one measures the response at some fixed value of $\tau/\delta t = \zeta$ we should have

$$\langle \mathcal{O} \rangle \sim \frac{N^2}{2\omega_0 \sqrt{\frac{1-\tanh(\tau/\delta t)}{2}}} \sim \frac{N^2}{\sqrt{2}\omega_0 \sqrt{1 - \tanh \zeta}} \tag{3.76}$$

This expectation needs refinement. Using the exact solution we can perform an expansion for $\omega_0\delta t \gg 1$ and for $\tau \gg \delta t \log \omega_0 \delta t$. We find that the leading term of $\rho^2(\tau)$ is

$$\rho^2(\tau) \sim \delta t \left[\frac{2}{\pi} \left(-\log \omega_0 \delta t + \log 2 - \gamma_E + \frac{\tau}{\delta t} \right)^2 + \frac{\pi}{2} \right] \sim \mathcal{O}(1) \tag{3.77}$$

The additional logarithmic dependence is not easily visible from the naive Kibble-Zurek argument.

3.6.2 Fast Quench Regime

In the fast quench regime one can get an analytic expression

$$\rho^2(\tau) \sim \omega_0 \delta t^2 \left(-\frac{\zeta(3)}{4} \omega_0^2 \delta t^2 + \frac{\tau}{\delta t} \right)^2 + \frac{1}{\omega_0} = \frac{1}{\omega_0} + \omega_0 \tau^2 - \frac{\zeta(3)}{2} (\omega_0 \delta t)^3 \tau. \tag{3.78}$$

at late times, i.e. $\omega_0 \delta t \ll \omega_0 \tau \ll 1$. Details of calculation which leads to (3.78) are summarized in Appendix A.2.

The limit $\delta t \to 0$ is smooth. In this limit the expression (3.78) reduces to the result which is obtained in an abrupt quench where the frequency suddenly changes from ω_0 to zero,

$$\rho^2_{abrupt}(\tau) = \frac{1}{\omega_0} [1 + (\omega_0 \tau)^2] \tag{3.79}$$

In relativistic theories this limit is non-trivial because of UV divergences, as discussed in [7–9].

Once again the answer should be obtainable by a perturbation expansion in $\omega_0 \delta t$. Again let $\delta\omega(\tau)^2 = \omega_0^2 f(\tau/\delta t)$, where

$$f(x) = \begin{cases} 0, & x < -1; \\ \frac{1+x}{2}, & -1 \le x \le 1; \\ 1, & x > 1. \end{cases} \tag{3.80}$$

Then at late times,

$$\begin{aligned} \langle \mathcal{O}(\tau) \rangle - \langle \mathcal{O}(-\infty) \rangle &\sim \omega_0^2 \frac{N^2}{2\omega_0^2} \int_{-\delta t}^{\tau} d\tau' \; f(\tau'/\delta t) \sin[2\omega_0(\tau - \tau')] \\ &\sim \frac{N^2}{2\omega_0} \sin^2 \omega_0 \tau. \end{aligned} \tag{3.81}$$

Thus $\omega_0 \tau \ll 1$ the perturbation expansion gives a good approximation.

3.6.3 The exact response

The above discussion shows that for the ECP it is useful to look at the response for a *fixed* value of $\tau/\delta t = \zeta$. Our analytic approximations then predict

$$\frac{2\langle \mathcal{O} \rangle}{N^2 \delta t} = \begin{cases} \frac{1}{\omega_0 \delta t} + (\omega_0 \delta t) \zeta^2 & : \omega_0 \delta t \ll 1 \\ \text{constant} & : 1 \ll \omega_0 \delta t \ll e^{\zeta} \\ \frac{\sqrt{2}}{(\omega_0 \delta t)\sqrt{1 - \tanh(\zeta)}} & : \omega_0 \delta t \gg e^{\zeta} \end{cases}$$

Figure 3.3 shows how the exact result compares with the above expectations. Here we plot the quantity $\rho^2/\delta t = 2\langle \mathcal{O} \rangle / (N^2 \delta t)$ as a function of $\omega_0 \delta t$ for different values of ζ. For very small $\omega_0 \delta t$ one reproduces the abrupt quench result. For slightly

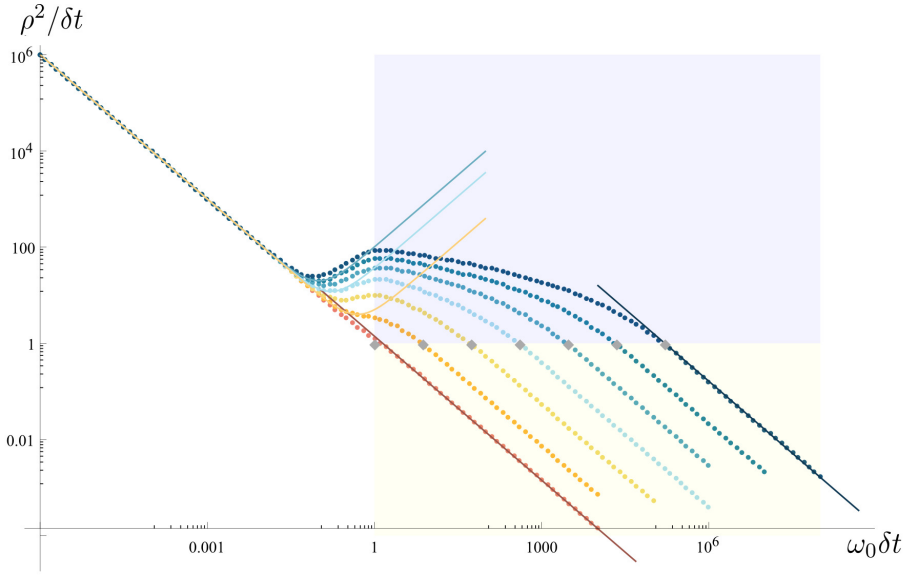

Figure 3.3: (Colour online) The response $\rho^2(\tau)/\delta t$ as a function of $\omega_0\delta t$ for ECP. The dots are the exact results obtained by using (3.54) for fixed values of $\zeta = \tau/\delta t = 0, 2, 4, 6, 8, 10, 12$ which are colored from red to blue respectively. The grey dot on each curve corresponds to $\omega_0\delta t = e^\zeta$ for that particular ζ. Thus all points in the yellow shaded region are in the adiabatic regime. The points which lie in the blue shaded region have $1 < \omega_0\delta t < e^\zeta$. For larger values of ζ there is a small window in this regime where $\rho^2(\tau)/\delta t$ is roughly constant which is the expectation from Kibble Zurek scaling. The slight increase is consistent with the logarithmic term in (3.77). The dark red and dark blue solid lines are the linear fitting ($\log y = P \log x + Q$) results of red ($\tau/\delta t = 0$) and blue dots ($\tau/\delta t = 12$) when $\omega_0\delta t \gg e^{\tau/\delta t}$ (yellow region), respectively. Both the slopes P are approximately -1. The orange, blizzard blue and light blue solid curves in the fast quench regime ($\omega_0\delta t \ll 1$) are the sudden quench result (3.79) for $\tau/\delta t = 2, 6, 10$, respectively. For $\omega_0\delta t < 1$ the data points lie on these solid lines. For $\omega_0\delta t > 1$ they continue to lie on the solid lines for a while and then depart from them, reflecting the $O(\omega_0^3\delta t^3)$ terms in (3.78).

larger $\omega_0\delta t$ we can see the fast quench correction predicted in (3.78). To investigate the behavior in the fast quench regime, it is useful to subtract the abrupt quench response. The quantity $|\rho^2(\tau) - \rho^2_{abrupt}(\tau)|/\delta t$ is plotted in Figure 3.4. This quantity is close to zero (and slightly negative) for sufficiently small $\omega_0\delta t$. For larger $\omega_0\delta t$ this becomes positive and in a reasonable range of $\omega_0\delta t$ this is consistent with the $(\omega_0\delta t)^3$ term in the fast quench response, equation (3.78) which are shown by solid lines. Note that the cusps in the data appear because the quantity $\rho^2(\tau) - \rho^2_{abrupt}(\tau)$ changes sign and we are plotting the absolute value - there is nothing singular here.

For sufficiently large values of $\omega_0\delta t$ this quantity is proportional to $1/(\omega_0\delta t)$ with a proportionality constant which depends on ζ, as expected from an adiabatic response. There is a small window in the intermediate regime where $\rho^2(\tau)/\delta t$ is roughly constant upto a logarithmic dependence as in (3.77).

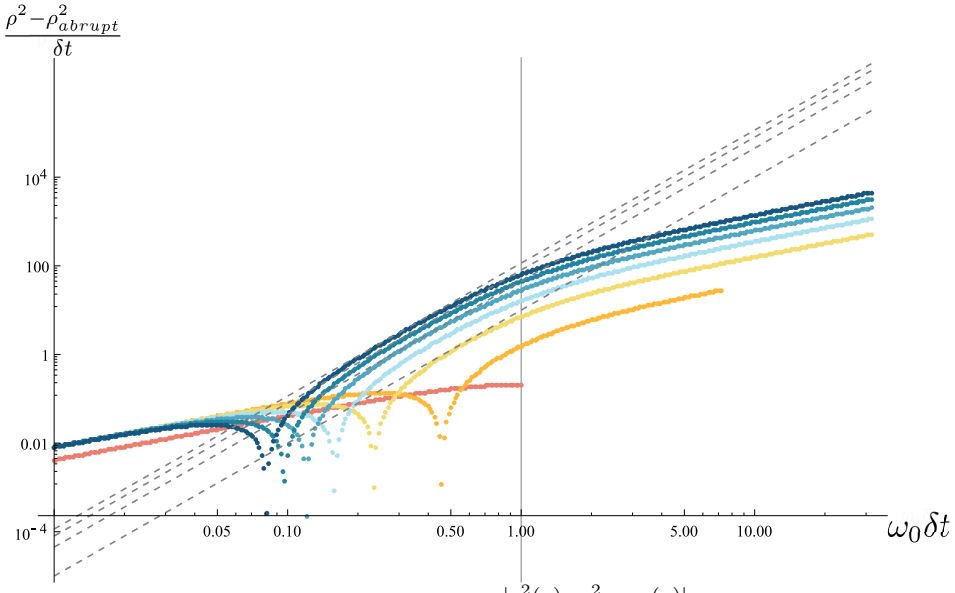

Figure 3.4: (Colour online) The response $\frac{|\rho^2(\tau)-\rho^2_{abrupt}(\tau)|}{\delta t}$ as a function of $\omega_0\delta t$ for ECP. The dots are the exact results obtained by using (3.54) for fixed values of $\zeta = \tau/\delta t = 0, 2, 4, 6, 8, 10, 12$ which are colored from red to blue respectively. The vertical gridline $\omega_0\delta t = 1$ is the threshold between fast quench and slow quench. The dashed lines are a set of cubic functions $y = ax^3$, where $a = 10, 45, 80, 115$ from the lowest one to the highest one, respectively to compare with the leading term in (3.78).

3.7 Entanglement Entropy

In this section we present the results for the entanglement entropy of a subregion, its scaling at early times and the time dependence at late times. As argued above, the entanglement entropy in a given subregion for a time dependent frequency can be expressed entirely in terms of the entanglement entropy of a *scaled* subregion for the system at fixed unit frequency, with the scaling factor given by $\rho(\tau)$ (eqn (3.45)). In the following we will examine the behavior of the entanglement entropy for a subregion $-a \leq x \leq a$. We will also be interested in the limit $N \gg 1$ so that we can use the expression (3.41).

We will be interested in the entanglement entropy for a subregion size

$$\frac{a}{\rho(\tau)} \ll \sqrt{N} \tag{3.82}$$

For ECP the function $\rho(\tau)$ monotonically increases with time, so this condition is equivalent to the condition $\sqrt{\omega_0}a \ll 1$ since $\rho(-\infty) = \frac{1}{\sqrt{\omega_0}}$ - the monotonicity then implies that once we impose (3.82) at the initial time, this will continue to hold for all times. For CCP the function $\rho(\tau)$ oscillates roughly around $\rho(-\infty)$ with an amplitude which is roughly constant in time : once we pick a value of a such that this condition is satisfied at some sufficiently large time, this will continue to be satisfied for all times.

The expression for entanglement entropy at large N can be written down using (3.41, 3.42) and (3.45) by using the Christoffel-Darboux formula for orthogonal polynomials

$$\sum_{k=0}^{n} \frac{H_k(x)H_k(y)}{k!2^k} = \frac{1}{n!2^{n+1}} \frac{H_n(y)H_{n+1}(x) - H_n(x)H_{n+1}(y)}{x-y}. \tag{3.83}$$

This leads to

$$\langle N_A \rangle = \frac{1}{\Gamma(N)2^N\sqrt{\pi}} \int_{A_P} d\xi e^{-\xi^2} \left[H_{N-1}(\xi)H'_N(\xi) - H'_{N-1}(\xi)H_N(\xi)\right] \tag{3.84}$$

$$\int_{A_P \times A_P} \mathrm{d}x\mathrm{d}y |C(x,y)|^2$$

$$= -\frac{1}{\pi 2^{2N}(\Gamma(N))^2} \int_{A_P \times A_P} d\xi d\eta e^{-(\xi^2+\eta^2)} \left(\frac{H_{N-1}(\eta)H_N(\xi) - H_{N-1}(\xi)H_N(\eta)}{\xi - \eta}\right)^2 \tag{3.85}$$

where the notation $A_P \times A_P$ means that the integrals go over the range defined by A_P. These expressions simplify in two regimes. First consider the regime

$$\frac{1}{\sqrt{N}} \ll \frac{a}{\rho(\tau)} \ll \sqrt{N} \tag{3.86}$$

Then one gets, using (3.41)

$$S_A \propto \frac{1}{\pi^2} \left\{1 + \gamma_E + \log\left[4\sqrt{2N}\frac{a}{\rho(\tau)}\right]\right\} \tag{3.87}$$

where γ_E is Euler's constant. The derivation (3.87) is given in Appendix B.

The logarithmic dependence on the subsystem size is characterisic of $1+1$ dimensional systems. For relativistic systems the scale is provided by a UV cutoff. For free non-relativistic fermions on a line the entanglement entropy is finite with the UV cutoff replaced by N [175, 176]. A similar result holds for fermions in an invererted harmonic oscillator potential [175–177]. For fermions in a harmonic oscillator potential with a constant frequency this logarithmic dependence has been shown in the so called "bulk limit" in [178].

For CCP protocols, $\rho(\tau)$ oscillates and the condition (3.86) continues to hold once it is imposed at early times. However for the ECP $\rho(\tau)$ monotonically increases so that at very late times the condition $\frac{1}{\sqrt{N}} \ll \frac{a}{\rho(\tau)}$ will be violated. It turns out, however, that for the regime

$$\frac{a}{\rho(\tau)} \ll \frac{1}{\sqrt{N}} \tag{3.88}$$

one can use a different approximation which yields

$$S_A \propto \frac{\sqrt{N}}{\pi} \frac{a}{\rho(\tau)} \tag{3.89}$$

Note that the entanglement entropy is now proportional to a. However the proportionality constant decreases steadily as $\frac{1}{\tau}$ since the function $\rho(\tau) \sim \tau$ at late times. The derivation of (3.89) is given in Appendix B.

Plots of the time dependence of the entanglement entropy in various cases are shown in Figure 3.5. For the cis-critical protocol, the function $\rho(\tau)$ oscillates after an initial increase, so that the effective size of the interval in the equivalent constant frequency problem also oscillates. This would lead to oscillations in the entanglement entropy as well.

For ECP, however, $\rho(\tau)$ decreases continuously. This means that for a given a the effective value of the interval in the equivalent constant frequency problem keeps decreasing with time. This should also mean that the entanglement entropy keeps desceasing with time. This is basically because as the fermions are released from the trap they simply spread out : both $\langle N_A \rangle$ and $\langle (\Delta N_A)^2 \rangle$ keep decreasing leading to a loss of entanglement. It follows from (3.89) that at late times the entanglement entropy goes to zero as a power law $\sim \frac{1}{\tau}$.

3.8 Phase Space Density for Harmonic Oscillator Potential

In this section we present the time evolution of the Wigner Distribution function, also called the phase space density, $u(x, p, \tau)$, under CCP and ECP quench protocols in a right side up harmonic oscillator potential. In the classical limit, which is given by $\hbar \to 0, N \to \infty$ with $N\hbar =$ fixed, $u(x, p, \tau)$ can only take values of 0, 1 since no two fermions can occupy the same position and momentum. A value of 1 corresponds to the presence of one fermion within a phase space volume between q and $q + dq$ and p and $p + dp$.

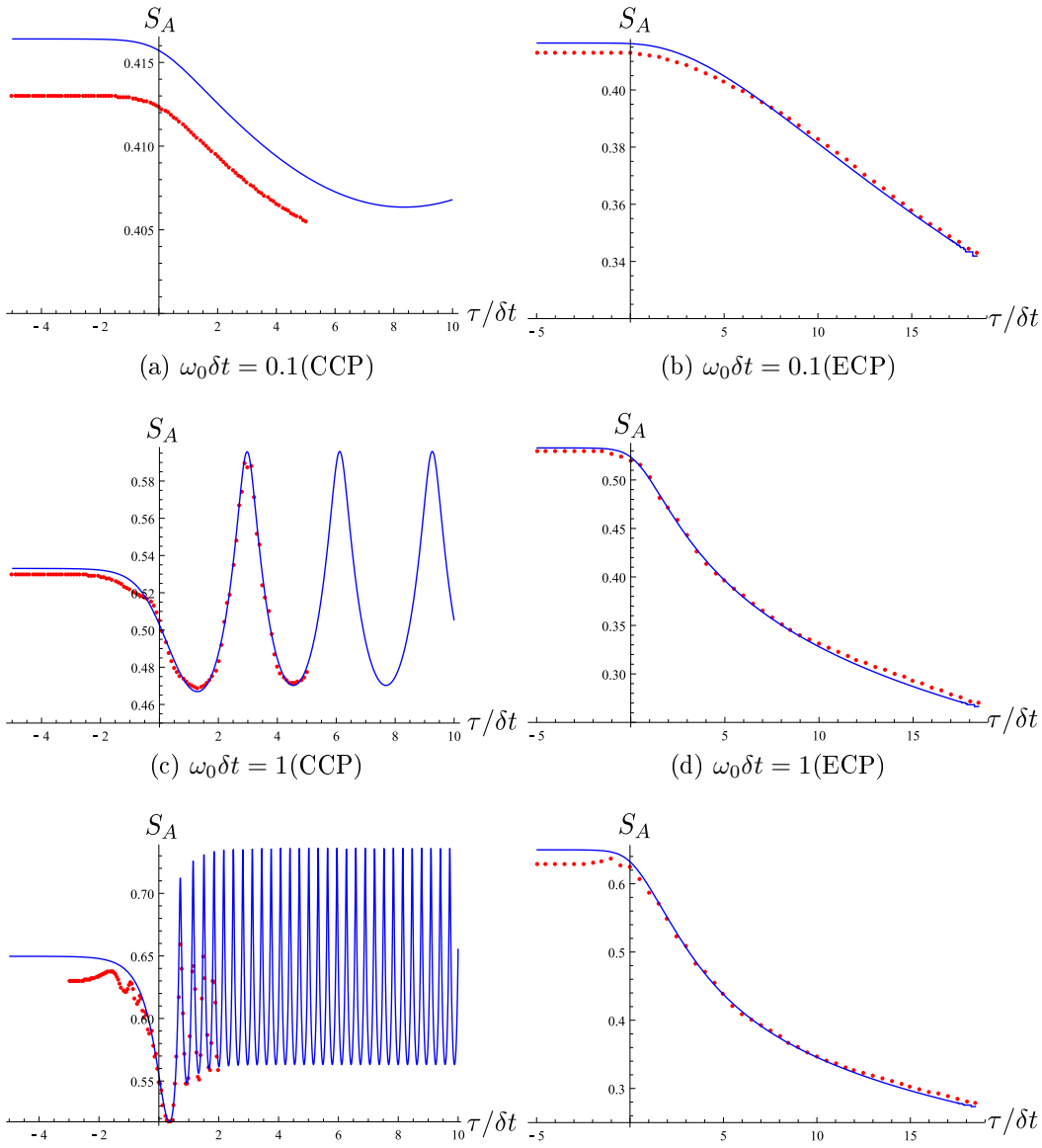

(a) $\omega_0\delta t = 0.1$(CCP) (b) $\omega_0\delta t = 0.1$(ECP)

(c) $\omega_0\delta t = 1$(CCP) (d) $\omega_0\delta t = 1$(ECP)

(e) $\omega_0\delta t = 10$(CCP) (f) $\omega_0\delta t = 10$(ECP)

Figure 3.5: Time evolution of Entanglement Entropy $S_A(\tau)$ in various cases. Red dots are exact large N result from (3.85). Blue solid lines are results (3.87) in the regime (3.86). $N = 50$, $a = 1$.

Using the canonical transformations in (3.27), we can write the time evolved phase space density as a function of the original coordinates as

$$u\left(\frac{q}{\rho}, p\rho - q\dot{\rho}, \tau\right) = \theta\left(2E_f - \left((\frac{q}{\rho})^2 + (p\rho - q\dot{\rho})^2\right)\right) \tag{3.90}$$

Here E_f is the fermi level and defines the boundary of the phase space density, i.e. the fermi surface. θ is the Heaviside step function which satisfies the relations

$$\theta(x) \;=\; \begin{cases} 1, & x \geq 0 \\ 0, & x < 0 \end{cases} \tag{3.91}$$

Equation (3.90) takes a value of 1 for q, p which satisfy the relation $2E_f \geq (\frac{q}{\rho})^2 + (p\rho - q\dot{\rho})^2$. This will produce what we call a phase space 'droplet'. As time evolves, the shape of this 'droplet' will evolve according to the chosen quench protocol. We present the results for the ECP and CCP cases.

3.8.1 ECP case

Here we discuss the time evolution of (3.90) for the ECP case that has a ρ which is given in (3.48) and (3.54).

In Figure 3.6 we see that the phase space 'droplet' spreads out in the upper right and lower left quadrants. This corresponds to motion along both directions of the infinite line. Since we are quenching to zero potential, we are 'freeing' the fermions from the harmonic trap and they begin to spread over the real line. The rate at which the 'droplet' spreads is related to δt, the timescale of the quench protocol.

3.8.2 CCP case

Here we discuss the time evolution of (3.90) for the CCP case that has a ρ which is given in (3.48) and (3.51).

In Figure 3.7 we see that the phase space 'droplet' initially spreads out and then begins to rotate in a clockwise fashion. This rotation comes from the oscillatory nature of ρ in the CCP case for $\tau > 0$. We can understand the physical origin of this rotation. We are quenching from a potential of frequency ω_0, to 0, back to ω_0 over a timescale of δt. The fermions initially just spread along the real line as the potential barrier goes to zero just as in the ECP case. However, when the barrier is restored to its original value, the fermions hit the edge of the restored barrier and then reflect back. This reflection is indicated by the rotation of the stretched droplet in a clockwise fashion. As time evolves the stretched droplet will continue to rotate indefinitely as the electrons keep reflecting off the walls of the potential barrier.

3.8.3 Time evolution of perturbations along fermi surface

In the previous subsection, we demonstrated the time evolution of a phase space 'droplet' under the influence of a right side up harmonic oscillator potential with a

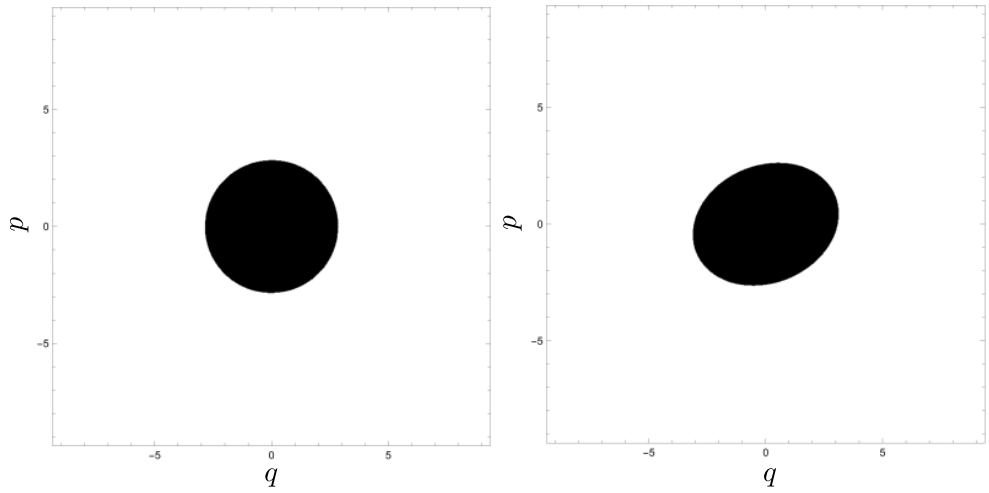

(a) $\tau = -2$ (b) $\tau = 0$

(c) $\tau = 2$ (d) $\tau = 4$

Figure 3.6: Time evolution of a contour plot of the Wigner Distribution function in the classical limit for the ECP case. The black region corresponds to $u = 1$ and the white region corresponds to $u = 0$. We have taken $\delta t = 1$, $\omega_0 = 1$. The radius of the initial droplet is $\sqrt{2E_f} = 2\sqrt{2}$ and the area, which is conserved in time, is $N\hbar = 2\pi E_f$.

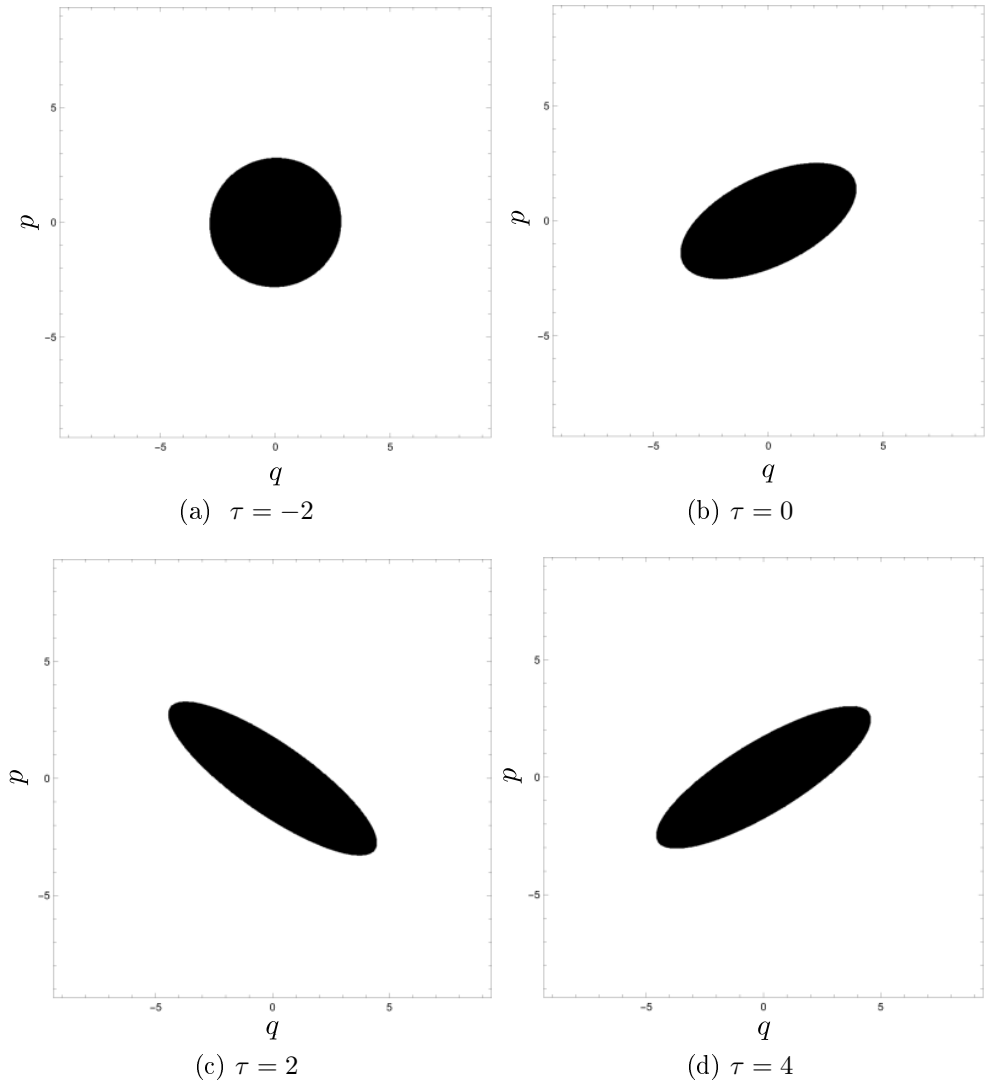

(a) $\tau = -2$ (b) $\tau = 0$

(c) $\tau = 2$ (d) $\tau = 4$

Figure 3.7: Time evolution of the Wigner Distribution function in the classical limit for the CCP case. We have taken $\delta t = 1$, $\omega_0 = 1$. The radius of the initial droplet is $\sqrt{2E_f} = 2\sqrt{2}$ and the area, which is conserved in time, is $N\hbar = 2\pi E_f$.

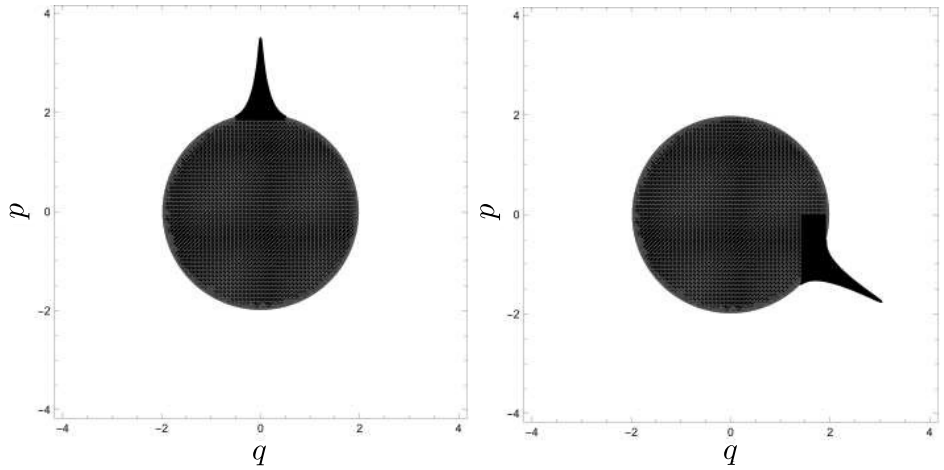

(a) $\tau = 0$ (b) $\tau = \frac{2\pi}{3}$

(c) $\tau = \frac{4\pi}{3}$ (d) $\tau = 2\pi$

Figure 3.8: Time evolution of a perturbation of the fermi surface for a time independent harmonic oscillator potential. We have taken $\omega_0 = 1$.

time dependent frequency. In this subsection we consider the time evolution of a perturbation of the fermi surface of this 'droplet'. We would like to know how this perturbation evolves in time. To gain a better understanding of what happens in this case, let us first consider the time evolution under a harmonic oscillator potential with a time independent frequency. In figure 3.8 we plot this evolution. As expected, we find that the perturbation maintains its shape throughout all of time. This is a consequence of the harmonic oscillator frequency being time independent. As a result, all points of an initial perturbation of the fermi surface will move at the same angular frequency for all subsequent times leaving its shape unaltered.

Now consider the case where an initial perturbation of the fermi surface of a phase space 'droplet' evolves under the influence of a right side up harmonic oscillator potential with a time dependent frequency. In particular, we consider the ECP quench protocol. We plot this evolution in Figure's 3.9, 3.10. In this case we find something

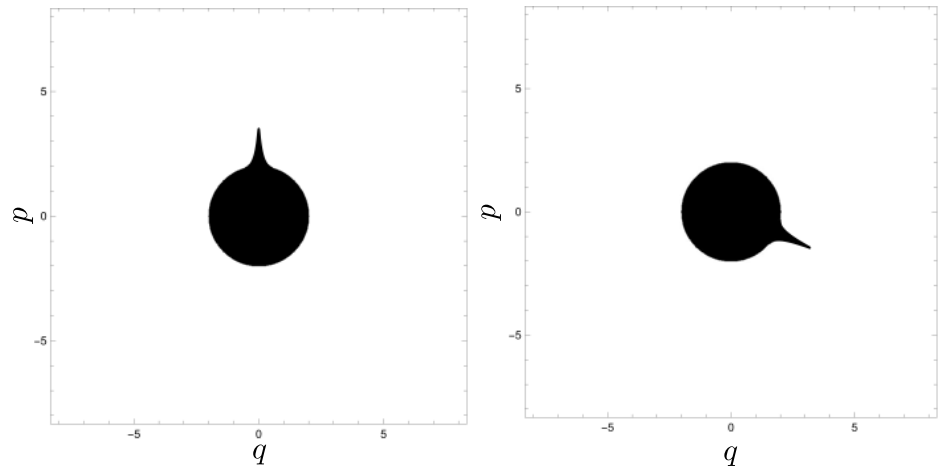

(a) $\tau = -5$ (b) $\tau = -3$

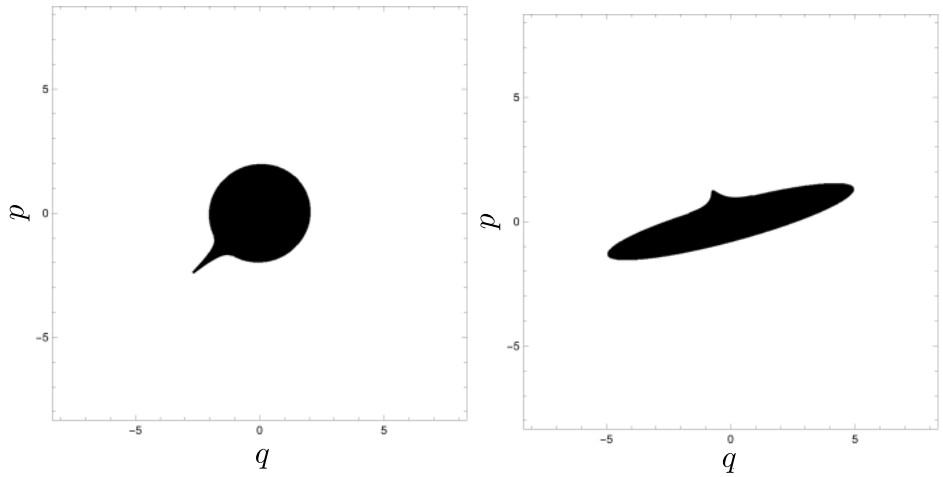

(c) $\tau = 0$ (d) $\tau = 3$

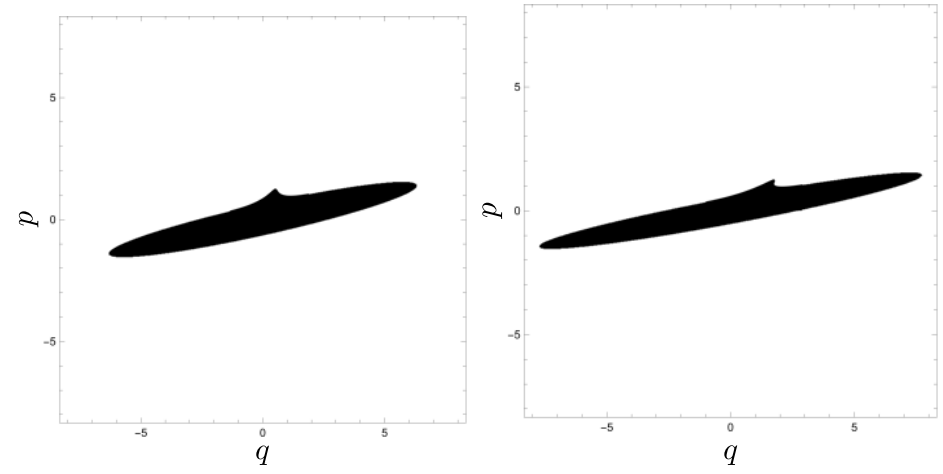

(e) $\tau = 4$ (f) $\tau = 5$

Figure 3.9: Time evolution of a perturbation of the fermi surface for the ECP case. We have taken $\delta t = 1$, $\omega_0 = 1$.

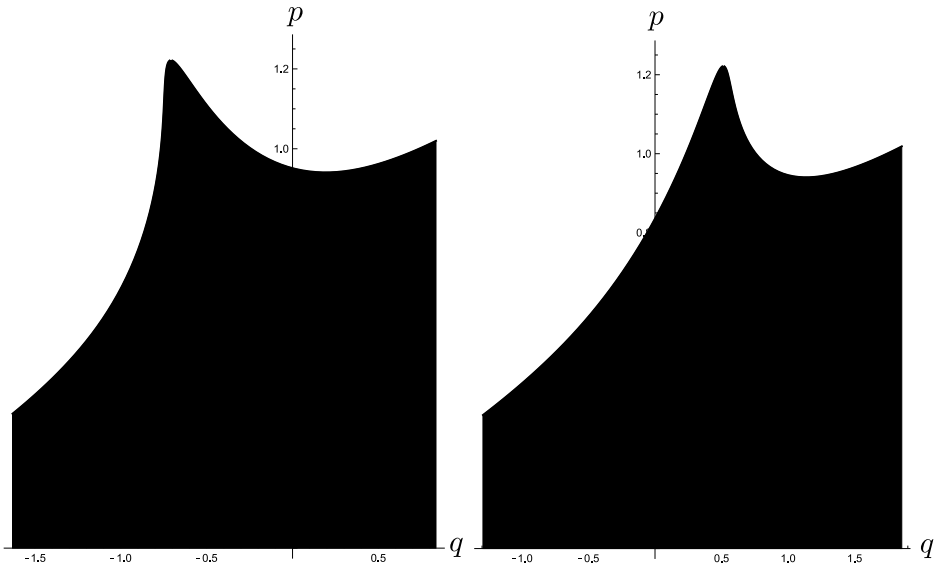

(a) $\tau = 3$ (b) $\tau = 4$

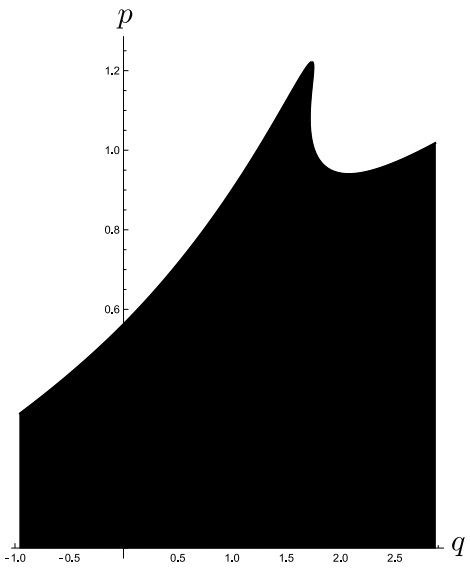

(c) $\tau = 5$

Figure 3.10: We zoom in to the region of the perturbation of the fermi surface to clearly see a 'fold' forming as time evolves.

quite interesting. We see that the perturbation develops what we call a 'fold'. This is a phenomenon in which a phase space point which is further from the fermi surface moves faster than a phase space point which is closer to the fermi surface. As a result, at some time later than the initial time, the outer most phase space points begin 'folding' over towards the fermi surface.

The feature of an initial perturbation developing a fold is characteristic of a system evolving under the influence of a harmonic oscillator potential with any arbitrary time dependent frequency. One can rewrite the phase space coordinates q, p in terms of polar coordinates r, θ. One can then show that $\frac{d\theta}{d\tau} \propto f(\theta, \omega(\tau), \dot{\omega}(\tau))$ and is therefore not constant in time. On the contrary, if $\frac{d\theta}{d\tau} = \text{const}$, then all the phase space points rotate with the same angular frequency. This is exactly the case for the harmonic oscillator potential with a time independent frequency.

3.9 Discussion

In this paper we considered quantum quench in a nonrelativistic field theory of fermions in an external harmonic oscillator or an invererted harmonic oscillator potential with time dependent mass and frequency. While the strategy we outlined to obtain exact solutions hold for both these potentials, we gave results for the right side harmonic potential in this paper. Explicit solutions for the inverted oscillator potential, which corresponds to quantum quench in the Matrix Model description of two dimensional string theory, will be presented in a future publication [18].

We examined scaling behavior of observables in the slow and fast quench regime. We found that the slow quench scaling is consistent with Kibble Zurek, and the fast quench scaling is a result of perturbation theory. This system is, however, not suitable to explore if there is a universal fast quench scaling. For the latter we would need to examine a translationally invariant system with an upper bound on the energy spectrum (for example a lattice system) so that a Lieb Robinson bound is possible. We are currently investigating the quench problem in situations like this.

Chapter 4
Quantum Quench in $c = 1$ Matrix Model and Emergent Space-times

4.1 Introduction

In the usual AdS/CFT correspondence, quantum quench [1] in a non-gravitational field theory is described as a time dependent boundary condition in the gravitational dual. When the system is initially in a nice state (e.g. the ground state) and the time dependence causes an energy injection over a finite time period, the usual outcome is black hole formation in the bulk [15, 32–45]. This manifests as thermalization in the field theory. Such quantum quenches have been accordingly used extensively to investigate thermalization in strongly coupled theories. In other situations where the quench takes the system across, or approaches a critical point this holographic connection has been used to understand universal scaling and dynamical phase transitions [75–79, 113–116, 179].

There are, however, other examples where holographic quenches lead to time dependent bulk backgrounds which resemble cosmologies [139–142, 144–150, 180–186] [2]. When the coupling of the boundary theory goes through a small value, the bulk develops a space-like or null region of high curvature, physically resembling a cosmological singularity. In this region the classical gravity approximation fails and it is interesting to ask if the dual field theory can provide an unambigious time evolution. While there are indications that *some* of these examples may indeed involve smooth time evolutions (especially for a null time dependence or a sufficiently slow time dependence), the nature of the final state is not clear : this possibly contains a black hole. Neverthless these examples have been useful in understanding boundary signatures of bulk singularities.

In this paper we will investigate quantum quench in the earliest example of holography which predates the AdS/CFT correspondence : duality of double scaled Matrix Quantum Mechanics and two dimensional non-critical string theory.[3] This is a model of holography where both sides of the duality are understood quantitatively : as such this could have lessons for the general question discussed above. The singlet sector of this model can be written exactly in terms of a theory of non-relativistic fermions in an inverted hamonic oscillator potential [55–59] and at large N it is more useful to write the model as a collective field theory of the density of eigenvalues [187]. The space on which these fermions live is the space of eigenvalues of the matrix. The fluctuations of the collective field around the large N saddle point solution is a massless scalar which is related to the single dynamical degree of freedom of two dimensional string theory [16]. The saddle point itself is related to a classical tachyon background of the

[1] In this paper we will use "quantum quench" to describe a time dependent coupling, typically with a finite rate of change

[2] In these examples the time dependence turns off in the inifinite past but in an exponential fashion, rather than at some finite past time

[3] For reviews see [52, 53, 134, 135].

string theory [188]. In fact a precise relationship involves a spatial transformation whose kernel is nonlocal at the string scale [189]. There is no propagating graviton, and the emergent space and gravitational effects are figured out by examining the propagation and scattering of collective field fluctuations. Recent work has made the relationship between two dimensional string theory in worldsheet formalism and the matrix model results even more precise [190–193]. The way holography works in this case is somewhat different from the usual AdS/CFT correspondence, even though the origins come from the physics of D-branes in either case [194, 195]. In particular this not really a "bulk-boundary correspondence". Nevertheless the description in terms of the collective field in $1+1$ dimension is a "bulk" description, while the description in terms of N^2 matrix degrees of freedom is the analog of the boundary description.

In two dimensional string theory, gravity and the higher string modes are not propagating degrees of freedom. Nevertheless there can be distinct *backgrounds* with different metrics and other fields. Indeed, the low energy description in terms of dilaton gravity has a well known black hole background and there is worldsheet theory in this background [196–199] - this led to significant insights in the issue of black hole evaporation. [4] Despite many decades of effort, this black hole background is not understood in the matrix model description. It is generally believed that the singlet sector in fact does not have a black hole. One evidence for this belief is that an incoming tachyon pulse does not produce a black hole [17]. The non-formation of black holes is related to the presence of an infinite number of W_∞ charges in the theory. It has been speculated that the non-singlet sector does contain a black hole [61]- however the status of this speculation is not clear at the moment. This naturally raises the question : what happens when we subject the matrix model (restricted to the singlet sector) to a quantum quench ?

We perform quantum quench in this model by introducing a *time dependent self-coupling* of the matrix which interpolates between constant values at early and late times. As we will show, in the singlet sector and in the double scaling limit, this model maps to a system of N fermions in an inverted harmonic oscillator potential with a time dependent coefficient of the potential (We will call this coefficient "frequency" below). Using standard methods, the collective field description can be written down.

We show that the action of the collective field theory with time dependent frequency can be mapped to one with a constant frequency plus a boundary term by a transformation involving a single function of time $\rho(t)$ which satisfies a generalization of nonlinear Ermakov-Pinney (EP) equation [167, 203]. Thus, in the classical limit, the response of the collective theory can be obtained once we know the solution of the EP equation with appropriate initial conditions. Actually what determines the solution is $\rho^2(\tau)$ and this quantity can be both positive and negative. The EP equation can be solved in terms of the independent solutions of the *classical* equations of motion of a single particle moving in the inverted harmonic potential with a time dependent frequency $f(t)$. Our method is adapted from known methods of solving the single particle Schrodinger equation in the presence of a harmonic potential with a time dependent frequency[132, 133, 204]. This technique has been used to under-

[4] For reviews and references to the original papers see [200–202].

stand aspects of the quantum quench problem for N non-relativistic fermions in such a potential [13, 159, 164] as well for quench in a harmonic chain in [165].

We discuss exact solutions for several quench protocols. These include abrupt quenches with piecewise constant frequencies, where the frequency increases or decreases in a single step, and a "pulse" or "dip" where the frequency rises or dips down for a finite period of time, and becomes a constant after that. For smooth quenches, our solvable examples include those which monotonically interpolate between constant values at early and late times with a time scale δt, as well as cases where the frequency starts with some constant value and ends up at the same constant value after dipping down for some time. The quench starts off with the system in a ground state at large negative times where the energy levels on both sides of the inverted harmonic potential are occupied upto some fermi energy.

The initial conditions are such that the collective field and its time derivative match the adiabatic solution in the far past. The initial time evolution is then adiabatic. The collective field has a cut (i.e. it vanishes inside a finite interval in eigenvalue space) which changes with time. However, in contrast to the right side up harmonic oscillator, we find that with these initial conditions adiabaticity is always broken at some finite time, regardless of the speed of the quench. This can be qualitatively understood by casting the generalized EP equation in terms of a potential problem : this analog potential is unstable which renders an adiabatic expansion invalid. As a result, the qualitative aspects of the solution are well approximated by similar profiles with abrupt changes.

We show that generically at late times the function $\rho^2(\tau)$ becomes infinitely large positive or negative. However, there are *finely tuned* pulse or dip protocols for which $\rho(\tau)^2$ approaches a constant value.

For the case where ρ^2 goes to negative infinity, it crosses zero at a *finite time* $\tau = \tau_0$: at this time the saddle point solution for the collective field diverges, and the equations cannot predict a further time evolution unambigously. This is therefore a situation where the "bulk" equations of motion fail. However, the underlying fermion description remains well-defined even at the classical level and predicts a smooth time evolution across this time. For $\tau > \tau_0$ the fermions in the initial fermi sea cross over to the other side of the potential. Using the fermion picture one can now define a different collective field (which is no longer the fermion density), but nevertheless obeys the same equations of motion. At infinite matrix model time, this new collective field vanishes everywhere.

We then seek a space-time interpretation of the model by considering fluctuations around the saddle point solution. The fluctuation action is that of a massless scalar field in a relativistic two dimensional space-time with couplings which are space and time dependent. Since the scalar is massless, we can read off the metric from the quadratic action only upto a conformal factor. However, this can be used to derive the Penrose diagram showing the global properties of the emergent spacetime. We do this in detail for abrupt quenches.

For a single step quench where the frequency increases, this semi-classical spacetime terminates on a spacelike boundary. At this boundary the cubic couplings of the fluctuations of the collective field diverge : this is like a space-like singularity. Of

course what this means is that the semiclassical collective theory used to obtain the space-time interpretation fails as we approach this time. The matrix model time at this point is $\tau = \infty$. To determine if the matrix model time evolution is smooth at these late times, one would need to use an exact non-perturbative treatment of the fermionic theory, perhaps along the lines of [205]. In view of the above discussion this would be the general feature of any smooth quench which leads to an increasing $\rho(\tau)^2$.

An interesting feature of this emergent relativistic space-time is that the space of eigenvalues, x, does not remain a space-like coordinate for all times. Constant x lines are timelike before the quench, but can become null or space-like after the quench. The signature of the emergent metric does not change.

For a single step quench where the frequency decreases, the time $\tau = \tau_0$ discussed above becomes a null $\mathcal{I}^{\pm}$. Normally this would be the boundary of space-time. However, the matrix model provides a smooth time evolution beyond this : we therefore need to append another piece of space-time. The infinite future in matrix model time $\tau = \infty$ corresponds to a space-like line in this additional piece where the cubic couplings of the fluctuations diverge. Once again all constant x lines do not remain time-like.

It is only in the very fine tuned situation where $\rho(\tau)$ asymptotes to a constant in the far future that the emergent space-time is "normal".

Time dependent solutions of the matrix model with *constant couplings* have been studied earlier as models of matrix cosmology [206–210]. These solutions are generated by the underlying W_∞ algebra. It turns out that for profiles of the first class where the frequency changes suddenly from one value to another, the solutions are identical to one class of such solutions [211, 212]. We do not understand why a quench produces precisely these kinds of states.

Quantum quench in unitary and hermitian matrix models was first investigated in [151], and followed up in a related recent paper [152]. These papers deal with abrupt quenches and address questions of relaxation to a Generalized Gibbs Ensemble and dynamical phase transitions, with several novel results. Our interest is complementary : we concentrate on the question of emergent space-time.

In section 4.2 we describe the model and set up the notation. Section 4.3 deals with the method of solving the dynamics following a general quench. Section 4.4 deals will explicit solutions of the collective field with various quench profiles. In section 4.5 we discuss the nature of the solutions in the fermion picture. Section 4.6 discusses the nature of the emergent space-time. Section 4.7 contains conclusions. The appendices provide details of some of the pertinent results.

4.2 The $c = 1$ Matrix Model with a time dependent coupling

The action of our model is

$$S = \beta_0 \int dt\ f(t)\ \mathrm{Tr}\ [\frac{1}{2}\dot{M}^2 - U(M)] \tag{4.1}$$

where M stands for a $N \times N$ hermitian matrix, and $f(t)$ is a specified function of time which goes to constant values at early and late times. $U(M)$ is a potential which has a maximum at $M = 0$, e.g.

$$U(M) = -\frac{1}{2}M^2 + \frac{1}{4}M^4 + \cdots \tag{4.2}$$

If we write $\beta_0 = \frac{N}{g}$, g is the 't Hooft coupling. We now define a new time variable τ by

$$d\tau = \frac{dt}{f(t)} \tag{4.3}$$

so that the action becomes

$$S = \beta_0 \int d\tau \mathrm{Tr}\, [\frac{1}{2}(\partial_\tau M)^2 - f(\tau)^2\, U(M)] \tag{4.4}$$

where $f(\tau) = f(t)$. We will consider $f(\tau)$ which remains positive for all times. Therefore τ is a monotonically increasing function of t.

We will consider a gauged version of the model where the $U(N)$ symmetry of (4.1) is gauged. Since there is no dynamics of a gauge field in 0+1 dimension this essentially means a restriction to the singlet sector. In this sector one can replace the N^2 degrees of freedom with the N eigenvalues $\lambda_i(t)$. The jacobian of the change of variables to λ_i is a van der Monde determinant. One can then redefine the wavefunction by absorbing a factor of the square root of this determinant - the new wavefunction is then a Slater determinant, so that we have a theory of N fermions moving in the space of eigenvalues in the presence of an external potential. The second quantized hamiltonian of the fermion field $\chi(\lambda, t)$ is given by

$$H = \int d\lambda \left[\frac{1}{2\beta_0}|\partial_\lambda \chi|^2 + \beta_0 f(\tau)^2 U(\lambda)|\chi|^2 + \beta_0 \mu_F |\chi|^2\right] - \beta_0 \mu_F N \tag{4.5}$$

where we have used a Lagrange multiplier μ_F to impose the constraint which sets the total number of fermions to N,

$$\int d\lambda |\chi|^2 = N \tag{4.6}$$

The double scaling limit of this model is then defined by

$$\beta_0 \to \infty \qquad \mu_F \to 0 \qquad g_s = \frac{1}{2\beta_0 \mu_F} = \text{fixed} \tag{4.7}$$

In this limit the model simplifies considerably. This is seen by rescaling

$$\lambda = (\beta_0 g_s)^{-1/2} x \qquad \chi = (\beta_0 g_s)^{1/4} \psi \tag{4.8}$$

and retaining the $O(1)$ terms. The final double-scaled hamiltonian is

$$H = \int dx \left[\frac{g_s}{2}|\partial_x \psi|^2 - \frac{f(\tau)^2}{2g_s} x^2 |\psi|^2 + \frac{1}{2g_s}|\psi|^2\right] \tag{4.9}$$

where we have ignored a constant additive term. The"Planck constant" of the problem is g_s.

If we think of this arising from e.g. a potential as in (4.2), the quartic terms become $O(1)$ when $x \sim \mu_F^{-1/2}$. Since g_s is held fixed this corresponds to $x \sim \sqrt{N}$. Because of this, a regulated version of this model can be written down with a hard wall at $|x| \sim \sqrt{N}$.

Alternatively the singlet sector of the matrix model can be expressed in terms of a collective field $\rho(x,\tau)$ which is the density of eigenvalues, or the fermion density in eigenvalue space

$$\rho(x,\tau) = \partial_x \zeta(x,\tau) = \mathrm{Tr}\delta(M(\tau) - xI) = \psi^\dagger \psi(x,\tau) \tag{4.10}$$

The dynamics of $\zeta(x,\tau)$ can be derived using the method of [16, 187]. For small g_s one can alternatively use the classical bosonization relations of [60]. The action is

$$S = \frac{1}{g_s^2}\int dx d\tau \ \left[\frac{1}{2}\frac{(\partial_\tau \zeta)^2}{\partial_x \zeta} - \frac{\pi^2}{6}(\partial_x \zeta)^3 + \frac{1}{2}[f(\tau)^2 x^2 - 1](\partial_x \zeta)\right] \tag{4.11}$$

In the time independent situation, $f(\tau) = \omega_0$, the ground state classical solution is given by

$$\partial_x \zeta_0(x) = \frac{\omega_0}{\pi}\left[x^2 - \frac{1}{\omega_0}\right]^{1/2} \qquad |x| \leq 1 \tag{4.12}$$

and zero in the interval $-\frac{1}{\sqrt{\omega_0}} \leq x \leq \frac{1}{\sqrt{\omega_0}}$. Fluctuations of the collective field becomes related to the"massless tachyon" of two dimensional string theory. The coordinate x which arose out of the space of eigenvalues plays the role of space.

4.3 Response to a Quantum Quench

We aim to find solutions of the equations of motion with appropriate initial conditions for a given quench profile $f(\tau)$. This is facilitated by a remarkable property of the theory. Consider a transformation of $(x,\tau) \to (y,T)$

$$y = \frac{x}{\rho(\tau)} \qquad T = \int^\tau \frac{d\tau'}{\rho(\tau')^2} \tag{4.13}$$

where $\rho(\tau)$ is some function, under which ζ transforms as a scalar,

$$\partial_\tau \zeta = \frac{1}{\rho^2}\partial_T \zeta - y\frac{\partial_\tau \rho}{\rho}\partial_y \zeta \tag{4.14}$$

If the function satisfies the nonlinear equation

$$\frac{d^2\rho}{d\tau^2} - f^2(\tau)\rho = -\frac{1}{\rho^3} \tag{4.15}$$

the action in (4.11) then becomes

$$\begin{aligned} S =& \frac{1}{g_s^2}\int dydT\ \left[\frac{1}{2}\frac{(\partial_T\zeta)^2}{\partial_y\zeta} - \frac{\pi^2}{6}(\partial_y\zeta)^3 + \frac{1}{2}(y^2-1)(\partial_x\zeta)\right] + \\ & \frac{1}{g_s^2}\int dydT\left[\partial_y\left(-\frac{1}{2}y^2\zeta + \frac{1}{2}f(\tau)^2y^2\rho^4\zeta + \frac{1}{2}y^2\rho^2(\partial_\tau\rho)^2\zeta\right) - \partial_T\left(y\rho\partial_\tau\rho\zeta\right)\right] \end{aligned} \tag{4.16}$$

This means the equations of motion map to those with a constant frequency $f = 1$, so that a solution of the equations of motion of the action with a constant frequency can be lifted to a solution of the equations of motion with a time dependent frequency using a solution of (4.15). The equation (4.15) is a generalization of Ermakov-Pinney equation [167, 203]. The latter has a plus sign in front of f^2 and $1/\rho^3$.

As we will see soon, the function which appears in our discussion is actually $\rho^2(\tau)$, and this can be a both positive and negative real quantity. It is therefore useful to consider the equation for this quantity,

$$\partial_\tau^2\rho^2 - \frac{1}{2\rho^2}(\partial_\tau\rho^2)^2 - 2\omega(\tau)^2\rho^2 = -\frac{2}{\rho^2} \tag{4.17}$$

In fact we will find that it is *necessary* to have negative values of ρ^2. It is therefore useful to define the quantity

$$\tilde{\rho}(\tau) \equiv +\sqrt{|\rho(\tau)^2|} \tag{4.18}$$

The rescaling involved is then really

$$y = \frac{x}{\tilde{\rho}(\tau)} \tag{4.19}$$

To get an intuition about the solutions, it is useful to rewrite the generalized EP equation (4.15) as the equation of motion of a particle in a potential,

$$\frac{d^2\rho}{d\tau^2} = -\frac{\partial V(\rho,\tau)}{\partial\rho} \tag{4.20}$$

where the potential is

$$V(\rho,\tau) = -\frac{1}{2}\left[f(\tau)^2\rho^2 + \frac{1}{\rho^2}\right] \tag{4.21}$$

When $f(\tau) = \omega_0$ for all τ the ground state solution is given by (4.12). This means that in this case we need to choose a constant solution of the generalized EP equation (4.15), $\rho^2 = \frac{1}{\omega_0}$.

The quench profile we are interested in asymptotes to a constant value ω_0 at $t \to -\infty$. Therefore if we start out the system in its ground state we need to solve the equation (4.15) such that it asymptotes to a constant value at early times. We will in fact use profiles which are either piecewise constant or become constant exponentially at early and late times. Thus the time evolution near $\tau = -\eta$ for large

enough positive η should be adiabatic. This means we need to find solutions of (4.15) which match on to the adiabatic solution

$$\rho_{ad}(\tau)^2 = \frac{1}{f(\tau)} \tag{4.22}$$

at some very early time. These conditions are, for a large negative T

$$\rho^2(T) = \frac{1}{f(T)} \qquad \partial_\tau \rho^2(\tau) = -\frac{\partial_\tau f(\tau)}{f(\tau)^2}|_{\tau=T} \tag{4.23}$$

Given such a solution, the time dependent classical solution for the original action can be easily written down using (4.13)

$$\partial_x \zeta_0(x,\tau) = \frac{1}{\pi\rho(\tau)^2}\left[x^2 - \rho(\tau)^2\right]^{1/2} \tag{4.24}$$

$$\partial_\tau \zeta_0(x,\tau) = -\frac{\partial_\tau \rho(\tau)^2}{2\rho(\tau)^2} x \partial_x \zeta(x,\tau) \tag{4.25}$$

It can be easily checked that these satisfy the consistency condition

$$\partial_x \partial_\tau \zeta_0(x,\tau) = \partial_\tau \partial_x \zeta_0(x,\tau) \tag{4.26}$$

There is a well known way to find solutions of the EP equation which we adapt to the generalized equation [132, 133, 204]. The most general solution of (4.15) is given by

$$\rho(\tau)^2 = Au(\tau)^2 + 2Bu(\tau)v(\tau) + Cv(\tau)^2 \tag{4.27}$$

where A, B, C are constants and $u(\tau), v(\tau)$ are two linearly independent solutions of the *classical* equation of motion of a single particle moving in an inverted harmonic potential with the same time dependent frequency $f(\tau)$

$$\partial_\tau^2 X - f(\tau)^2 X = 0 \tag{4.28}$$

Furthermore A, B, C must satisfy

$$AC - B^2 = -\frac{1}{Wr(u,v)^2} \tag{4.29}$$

where $Wr(u,v) = u\partial_\tau v - v\partial_\tau u$ is the wronskian of the two solutions. By the equations of motion this is a constant in time and can be therefore evaluated at any time.

Given a classical solution of the action (4.11), $\zeta_0(x,t)$, the next step is to obtain the action for small fluctuations by expanding

$$\zeta(x,t) = \zeta_0(x,t) + \frac{g_s}{\sqrt{\pi}}\eta(x,t) \tag{4.30}$$

The action for the fluctuations will clearly be nonpolynomial in η. The quadratic part of the fluctuation action is

$$S^{(2)} = \frac{1}{2\pi}\int dx d\tau \left[\frac{(\partial_\tau\eta)^2}{\partial_x\zeta_0} - 2\frac{(\partial_\tau\zeta_0)}{(\partial_x\zeta_0)^2}(\partial_\tau\eta)(\partial_x\eta) + \left(\frac{(\partial_\tau\zeta_0)^2}{(\partial_x\zeta_0)^3} - \pi^2\partial_x\zeta_0\right)(\partial_x\eta)^2\right] \tag{4.31}$$

while the cubic interaction part is

$$S^{(3)} = \\ -\frac{1}{\pi^{3/2}}\times \\ \int dxd\tau \left[\frac{1}{2}\frac{1}{(\partial_x\zeta_0)^2}(\partial_\tau\eta)^2(\partial_x\eta) - \frac{\partial_\tau\zeta_0}{(\partial_x\zeta_0)^3}(\partial_\tau\eta)(\partial_x\eta)^2 + \left(\frac{(\partial_\tau\zeta_0)^2}{(\partial_x\zeta_0)^4} + \frac{\pi^2}{6}\right)(\partial_x\eta)^3\right] \tag{4.32}$$

The quadratic action shows that the fluctuation field is a *relativistic* massless field which is propagating on a $1+1$ dimensional space-time with a metric which is conformal to

$$ds^2 = -d\tau^2 + \frac{(dx + \frac{\partial_\tau\zeta_0}{\partial_x\zeta_0}d\tau)^2}{(\pi\partial_x\zeta_0)^2} \tag{4.33}$$

Since we are dealing with a massless field in $1+1$ dimensions the quadratic action is insensitive to a conformal transformation of the metric. Note that the signature of the metric (4.33) remains negative at all times since $\det(g) = -\frac{1}{\pi^2(\partial_x\zeta)^2}$.

4.4 Solutions for some quench profiles

In this section we find solutions of the generalized EP equation for physically interesting quench profiles.

4.4.1 Abrupt Quenches

Consider first abrupt quenches. The first case we consider is a single step quench, where the function $f(\tau)$ appearing in e.g. (4.11) is given by

$$f(\tau) = \begin{cases} \omega_0 & : \tau < 0 \\ \omega_1 & : \tau > 0 \end{cases} \tag{4.34}$$

In this case the two linearly independent solutions to the classical equations of motion (4.28) may be chosen to be

$$\begin{aligned} u(\tau) &= \theta(-\tau)e^{\omega_0\tau} + \theta(\tau)\frac{1}{2}\left[(1+\frac{\omega_0}{\omega_1})e^{\omega_1\tau} + (1-\frac{\omega_0}{\omega_1})e^{-\omega_1\tau}\right] \\ v(\tau) &= \theta(-\tau)e^{-\omega_0\tau} + \theta(\tau)\frac{1}{2}\left[(1-\frac{\omega_0}{\omega_1})e^{\omega_1\tau} + (1+\frac{\omega_0}{\omega_1})e^{-\omega_1\tau}\right] \end{aligned} \tag{4.35}$$

Using (4.27) and (4.29) we need to find a solution for ρ^2 which is $\frac{1}{\omega_0}$ for $\tau < 0$. This clearly requires a choice $A = C = 0$ in (4.27). Then (4.29) requires $B = \frac{1}{\omega_0}$. This leads to the solution for $\rho^2(\tau)$

$$\rho^2(\tau) = \frac{1}{\omega_0}\left[\theta(-\tau) + \theta(\tau)\cosh^2\omega_1\tau\left(1 - \frac{\omega_0^2}{\omega_1^2}\tanh^2\omega_1\tau\right)\right] \tag{4.36}$$

The function $\rho^2(\tau)$ is shown in Figure 4.1. This monotonically increases for $\omega_0 < \omega_1$, while for $\omega_0 > \omega_1$ this montonically decreases, crossing a zero at a finite time τ_0 given by

$$\tanh \omega_1 \tau_0 = \frac{\omega_1}{\omega_0} \tag{4.37}$$

At this point the saddle point solution $\partial_x \zeta_0$ (4.25) diverges. Note that $\partial_\tau \rho^2$ is finite here - this implies that the ratio $(\partial_\tau \zeta_0)/(\partial_x \zeta_0)$ diverges as well.

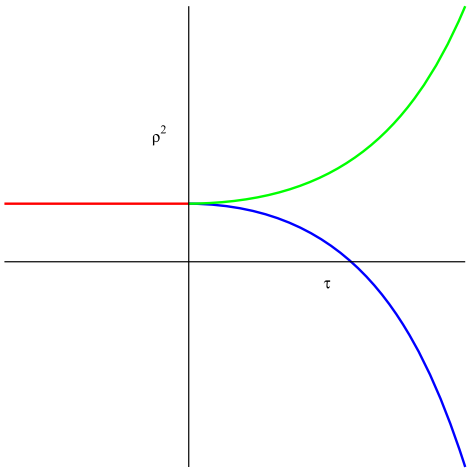

Figure 4.1: $\rho^2(\tau)$ for abrupt quench. We have chosen $\omega_0 = 1$. The green line has $\omega_1 = \sqrt{2}$ while the blue line has $\omega_1 = 1/\sqrt{2}$

The behavior of $\rho(\tau)$ can be understood from the analog potential $V(\rho)$ (4.21) which appears in the generalized EP equation. In Figure 4.2 the red curve is the potential for $\tau < 0$, the green curve is the potential for $\tau > 0$ in the case $\omega_0 < \omega_1$. For $\tau < 0$ our initial conditions mean that the analog particle starts off at the maximum of the red potential, $\rho = \frac{1}{\sqrt{\omega_0}}$. Thus the initial position is to the right of the maximum of the new potential and therefore the particle rolls down to large ρ, reaching $\rho = \infty$ at $\tau = \infty$.

In Figure 4.3 the red curve is the potential for $\tau < 0$, the blue curve is the potential for $\tau > 0$ in the case $\omega_0 > \omega_1$. Now the initial position is to the left of the maximum of the new potential and therefore the particle rolls down towards $\rho = 0$. It may be easily checked that it reaches $\rho = 0$ at a finite time $\tau = \tau_0$. This analog problem does not tell us what to do after this time. However, as explained above, the relevant quantity is not $\rho(\tau)$ itself, but $\rho(\tau)^2$. The solution (4.36) continues to hold for $\tau > \tau_0$ and satisfies all the continuity requirements for the equation (4.17).

For quench profiles which are not monotonic, the late time behavior can be more interesting. Consider a series of abrupt quenches given by

$$f(\tau) = \begin{cases} \omega_0 : & -\infty < \tau < -T/2 \\ \omega_2 : & -T/2 < \tau < T/2 \\ \omega_1 : & T/2 < \tau < \infty \end{cases}$$

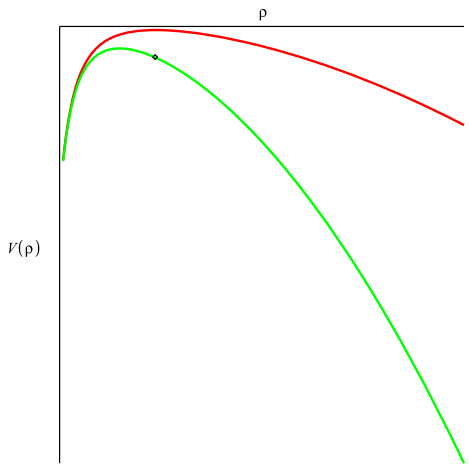

Figure 4.2: The potential in the Ermakov-Pinney analog potential problem for abrupt quench for $\omega_0 < \omega_1$. The red curve is the potential for $\tau < 0$, while the green curve is the potential for $\tau > 0$. The black dot is the position of the analog particle at $\tau = 0$.

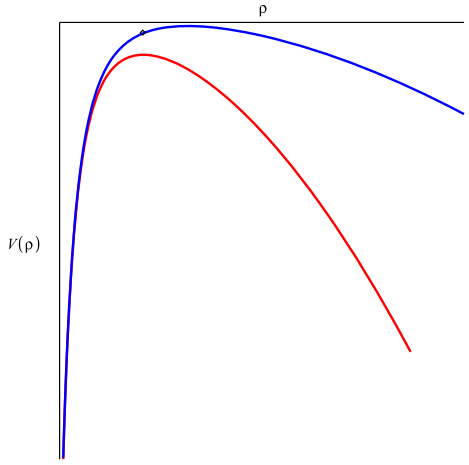

Figure 4.3: The potential in the Ermakov-Pinney analog potential problem for abrupt quench for $\omega_0 > \omega_1$. The red curve is the potential for $\tau < 0$, while the green curve is the potential for $\tau > 0$. The black dot is the position of the analog particle at $\tau = 0$.

Here $\omega_0, \omega_1, \omega_2$ are positive and nonzero. When $\omega_0 > \omega_2$ we will call this a "dip", while the $\omega_0 < \omega_2$ will be called a "pulse".

The details of the solution for $\rho^2(\tau)$ are given in appendix C. The solution to $\rho^2(\tau)$

is given by

$$\rho^2 = \begin{cases} \frac{1}{\omega_0}, & \tau \le -\frac{T}{2} \\ \frac{1}{\omega_0}\big(AA'e^{2\omega_2\tau} + BB'e^{-2\omega_2\tau} + AB' + A'B\big), & -\frac{T}{2} \le \tau \le \frac{T}{2} \\ \frac{1}{\omega_0}\big(CC'e^{2\omega_1\tau} + DD'e^{-2\omega_1\tau} + CD' + C'D\big), & \tau \ge \frac{T}{2} \end{cases} \quad (4.38)$$

where $A, A', B, B', C, C', D, D'$ are integration constants which are functions of $\omega_0, \omega_1, \omega_2$ which are given explcitly in Appendix C.

In this case, $\rho(\tau)^2$ can be non-monotonic, and generically diverges as $\tau \to \infty$, approaching either $+\infty$ or $-\infty$. An example of a non-monotonic solution is given in Figure 4.4.

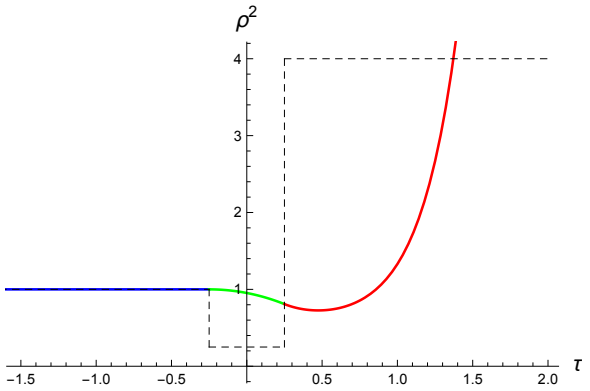

Figure 4.4: A non-monotonic $\rho^2(\tau)$ for an abrupt dip profile with $\omega_0 = 1, \omega_2 = 1/2$ and $\omega_1 = 2$ with $T = 1/2$. The dashed line is the profile of $f(\tau)^2$.

However there are finely tuned profiles for which $\rho^2(\tau)$ approaches a constant at late times. The generalized EP equation of course determines this constant to be $\frac{1}{\omega_1}$. To explore the late time behavior we need to look at the solution in the region $T/2 \le \tau < \infty$. This is given by the last equation of (4.38). For the discussion below we need the explicit forms of C, C' given below

$$C = \frac{e^{-\frac{T}{2}(2\omega_2+\omega_1+\omega_0)}}{4\omega_1\omega_2}\left[(\omega_2-\omega_0)(\omega_1-\omega_2) + e^{2T\omega_2}(\omega_2+\omega_1)(\omega_2+\omega_0)\right] \quad (4.39)$$

$$C' = \frac{e^{-\frac{T}{2}(2\omega_2+\omega_1-\omega_0)}}{4\omega_1\omega_2}\left[(\omega_2+\omega_0)(\omega_1-\omega_2) + e^{2T\omega_2}(\omega_2+\omega_1)(\omega_2-\omega_0)\right] \quad (4.40)$$

If $\rho(\tau)^2$ approaches a constant (which must be $\frac{1}{\omega_1}$) at late times either C or C' must vanish. It is straightforward to see that C cannot vanish since $e^{2\omega_2 T} > 1$, while one can find a nonzero finite value of T when $C' = 0$ both for a pulse $\omega_2 > \omega_0 > \omega_1$, as well for a dip $\omega_1 > \omega_0 > \omega_2$. The corresponding $\rho(\tau)^2$ are shown in Figures 4.5 and 4.6.

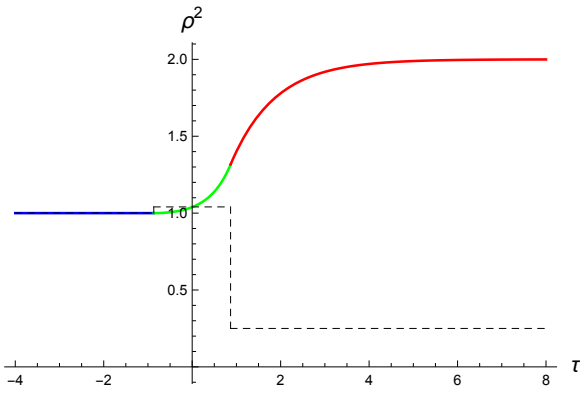

Figure 4.5: $\rho(\tau)^2$ for a fine-tuned pulse quench with $\omega_0 = 1, \omega_2 = 51/50, \omega_1 = 1/2$. The blue part of the curve corresponds to $\tau < -T/2$, the green part for $-T/2 < \tau < T/2$ and the red part is $\tau > T/2$. The quench profile is shown by dashed lines.

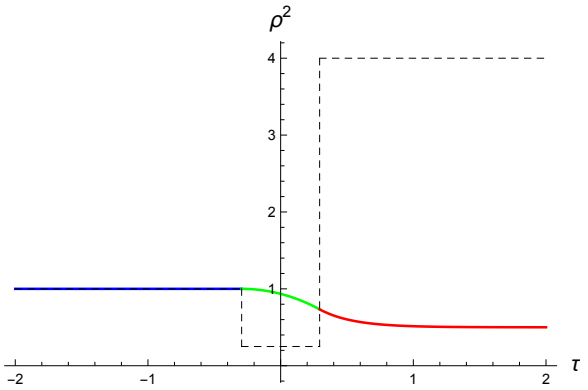

Figure 4.6: $\rho(\tau)^2$ for a fine-tuned dip quench with $\omega_0 = 1, \omega_2 = 1/2, \omega_1 = 2$. The blue part of the curve corresponds to $\tau < -T/2$, the green part for $-T/2 < \tau < T/2$ and the red part is $\tau > T/2$. The quench profile is shown by dashed lines.

4.4.2 Smooth Quenches

Consider now a smooth quench profile given by

$$f(\tau)^2 = \frac{\omega_1^2 + \omega_0^2 e^{-\frac{\tau}{\delta t}}}{1 + e^{-\frac{\tau}{\delta t}}} \tag{4.41}$$

The quench profiles are shown in Figure 4.7.

In this case the equation (4.28) admits analytic solutions in terms of hypergeometric functions. When $\omega_0 \delta t$ is not a half integer, a choice of the two independent solutions is

$$\begin{aligned} u(\tau) &= e^{\omega_0 \tau}{}_2F_1[\delta t(\omega_0 - \omega_1), \delta t(\omega_0 + \omega_1), 1 + 2\delta t \omega_0, -e^{\frac{\tau}{\delta t}}] \\ v(\tau) &= e^{-\omega_0 \tau}{}_2F_1[-\delta t(\omega_0 + \omega_1), \delta t(-\omega_0 + \omega_1), 1 - 2\delta t \omega_0, -e^{\frac{\tau}{\delta t}}] \end{aligned} \tag{4.42}$$

Since the frequency approaches a constant exponentially at early times, the intial time evolution is adiabatic. We need to find linear combinations of $u(\tau)$ and $v(\tau)$ in

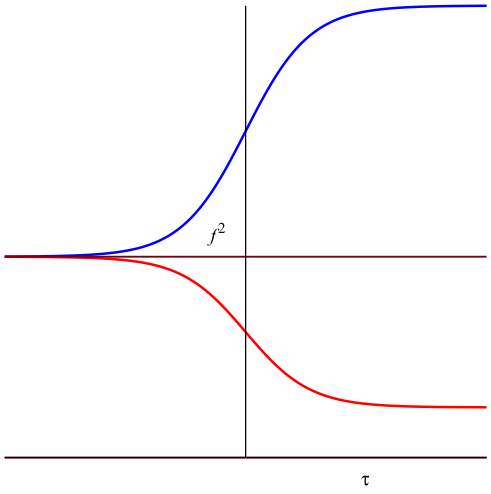

Figure 4.7: The function $f(\tau)$. The red curve has $\omega_0 > \omega_1$ and the blue curve has $\omega_0 < \omega_1$

(4.42) such that the function $\rho(\tau)$ constructed out of these solutions satisfy adiabatic initial conditions at an early time. The adiabatic solutions are given by

$$\begin{aligned} v_{ad}(\tau) &= \frac{C_v}{\sqrt{f(\tau)}} \exp\left[-\int^\tau f(\tau')d\tau'\right] \\ u_{ad}(\tau) &= \frac{C_u}{\sqrt{f(\tau)}} \exp\left[\int^\tau f(\tau')d\tau'\right] \end{aligned} \tag{4.43}$$

where the constants of integration C_u, C_v are chosen such that as $\tau \to -\infty$ these solutions behave as

$$\begin{aligned} v_{ad}(\tau) &\sim \frac{1}{\sqrt{\omega_0}} \exp\left[-\omega_0\tau\right] \\ u_{ad}(\tau) &\sim \frac{1}{\sqrt{\omega_0}} \exp\left[\omega_0\tau\right] \end{aligned} \tag{4.44}$$

Adiabatic initial conditions mean that at time $t = T$ where T is very large and negative,

$$\begin{bmatrix} u(T), \partial_\tau u(T) \\ v(T), \partial_\tau v(T) \end{bmatrix} \to \begin{bmatrix} u_{ad}(T), \partial_\tau u_{ad}(T) \\ v_{ad}(T), \partial_\tau v_{ad}(T) \end{bmatrix} \tag{4.45}$$

The specific linear combinations which satisfy this are given in the Appendix D.

The function $\rho(\tau)$ is then constructed by choosing $A = C = 0$ and $B = \frac{1}{2}$ in (4.27),

$$\rho(\tau)^2 = u(\tau)v(\tau) \tag{4.46}$$

At early times, this leads to the correct adiabatic initial conditions (4.23) .

An important aspect of the subsequent time evolution is that *regardless of the value of* δt, adiabaticity is always broken. This fact can be again understood from the feature of the potential of the analog problem.

Again, we regard Ermakov-Pinney equation as the equation of motion of an analog particle on potential (4.21). At a very early time, the analog particle is the maximum of the initial potential, $\rho = \frac{1}{\sqrt{\omega_0}}$. Then, at an early stage of a smooth quench, a slight variation of $f(\tau)$ causes a perturbation on the analog particle from this (unstable) equilibrium point, in a way similar to what is shown in figures 4.2 and 4.3. Although the equilibrium point is unstable, the particle can still move back to the new equilibrium point if the initial velocity $\partial_\tau \rho$ is finely tuned, otherwise it will either pass the new equilibrium point (when $\partial_\tau \rho$ is too large), or be bounced back (when $\partial_\tau \rho$ is too small). In both cases the analog particle moves away from equilibrium point.

Another way to see the failure of adiabaticity is to go back to the independent solutions in (4.42). The solutions $u(\tau), v(\tau)$ describe the motion of classical particles in inverted harmonic oscillator potential $-\frac{1}{2}f(\tau)^2 x(\tau)^2$. When particles move in such a potential with a cutoff x_b as boundaries, particles with negative energy $E = -\nu$ move between the boundary and the potential. Then we can figure out the adiabatic invariant of the system at $\tau \to -\infty$

$$I = \frac{1}{2\pi}\oint p\mathrm{d}x = \frac{1}{2\pi}\oint \sqrt{-2\nu + \omega_0^2 x^2}\mathrm{d}x \tag{4.47}$$

and therefore the period of the particle is

$$T = 2\pi\frac{\partial I}{\partial E} = \frac{1}{\omega_0}\left[-\log 2\nu + 2\log\left(\omega_0 x_b + \sqrt{\omega_0^2 x_b^2 - 2\nu}\right)\right] \tag{4.48}$$

The adiabatic approximation holds when

$$T\frac{\mathrm{d}f(\tau)}{\mathrm{d}\tau} \ll f(\tau) \tag{4.49}$$

The solutions $u(\tau)$ and $v(\tau)$ however represent trajectories which have zero energy at infinite past, and these have infinitely large T, which violate the condition (4.49). Thus, the adiabatic approximation fails for $u(\tau), v(\tau)$ and therefore for $\rho(\tau)$.

There is of course a solution which is fine-tuned by specifying initial and final conditions for $u(\tau), v(\tau)$ which lead to $\rho \to \frac{1}{\sqrt{\omega_0}}$ in the infinite past and $\rho \to \frac{1}{\sqrt{\omega_1}}$ in the infinite future [5]. The initial value of $\partial_\tau \rho$ at some $\tau = -\eta$ will be different from (4.23).

[5] We found the finely-tuned solutions

$$\begin{aligned} v_{finely-tuned} =& \left(\frac{\Gamma(1+2\omega_1\delta t)\Gamma(2\omega_0\delta t)}{\delta t(\omega_0+\omega_1)\Gamma(\delta t(\omega_0+\omega_1))^2}\right)^{-1} \\ & \times \frac{1}{\sqrt{\omega_0}} e^{-\omega_1\tau}{}_2F_1(-\delta t(\omega_0-\omega_1), \delta t(\omega_0+\omega_1); 1+2\delta t\omega_1; -e^{-\tau/\delta t}), \\ u_{finely-tuned} =& \frac{1}{\sqrt{\omega_0}} e^{\omega_0\tau}{}_2F_1([\omega_0-\omega_1]\delta t, [\omega_0+\omega_1]\delta t, 1+2\omega_0\delta t, -e^{\tau/\delta t}) \end{aligned} \tag{4.50}$$

Only when $\delta t \gg \eta \to \infty$, $\partial_\tau^2 \rho \to 0$ will the adiabatic approximation become the exact finely-tuned solution given that $\mathrm{d}\omega/\mathrm{d}\tau \propto \delta t^{-1}$. Now, because the generalized Ermakov-Pinney equation describes a Lyapunov unstable system, according to the definition of Lyapunov stability, there exists a value ϵ, for all exact solutions with initial adiabatic condition at $\tau = -\eta$ that satisfy $|\rho_{finely-tuned}(-\eta) - \rho_{ad}(-\eta)| < \delta$, where δ is a function of ϵ and time τ, we can find there exists some $\tau > -\eta$ where $|\rho_{finely-tuned}(\tau) - \rho_{ad}(\tau)| > \epsilon$; i.e. at some late time, finely-tuned solution and exact solution with adiabatic initial condition are no longer close no matter how large η is. This explains why we cannot find an exact adiabatic solution or even an exact finely-tuned solution with adiabatic initial conditions at $\tau = -\eta$ (4.23).

Figure 4.8 shows the exact and adiabatic solutions to the EP equation for the profile (4.41), both for $\omega_1 < \omega_0$ and $\omega_1 > \omega_0$ together with the adiabatic solution (the dashed lines). The explicit solution for this case is given in Appendix D. Clearly the nature of the solutions are quite similar to those which result from abrupt quenches. In the following we will use the abrupt quench solutions to map out the emergent space-times

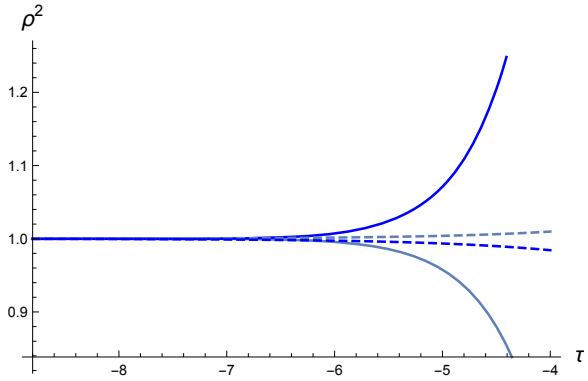

Figure 4.8: The solution for $\rho^2(\tau)$ for the smooth profile of the form (4.41). These have $\delta t = 1.1$ and the adiabatic condition is imposed at $T = -8.8$. The grey lines are for $\omega_0 = 1, \omega_1 = 0.5$ while the blue lines are for $\omega_0 = 1, \omega_1 = 1.5$. The dashed lines are the adiabatic solutions, while the solid lines are the exact solutions.

Another example of a solvable quench profile is give by a smooth dip or pulse,

$$f(\tau)^2 \;\; = \;\; \omega_1^2 + (\omega_0^2 - \omega_1^2) \tanh^2 \frac{\tau}{\delta t} \tag{4.51}$$

The results for this profile are presented in appendix E.

4.4.3 Collective Field Saddles

At $t \to -\infty$ the collective field in (4.25) vanishes in the interval $-\frac{1}{\sqrt{\omega_0}} < x < \frac{1}{\sqrt{\omega_0}}$ and monotonically increases with $|x|$. Given a solution $\rho(\tau)^2$ we can now substitute this in (4.25) to obtain a classical solution of the collective field. We saw that generically there can be three kinds of late time behavior for $\rho(\tau)^2$.

First, $\rho(\tau)^2$ can approach $+\infty$ at late times. In this case, the interval of x in which the collective field vanishes increases monotonically to arbitrarily large values, while the value of $\partial_x \zeta_0$ keeps decreasing till it vanishes for any finite $|x|$. This behavior is strictly for the inverted oscillator potential. For any finite but large β (or finite N) this potential needs to be regulated by some kind of wall at $x \sim \sqrt{\beta g_s}$. The modification which comes from this will be clear when we discuss the solutions in the fermion language.

Secondly, $\rho(\tau)^2$ can approach $-\infty$, crossing a zero value at a *finite time* $\tau = \tau_0$. At this time the collective field diverges. The collective field equations cannot be used to unambigously predict a future time evolution. As we will see, one needs to go back to the fundamental fermion description to figure out if there is anything singular going on here. In fact we will see that the fermion description provides a smooth time evolution and also provide us with a continuation of the collective field. Again, the divergence of the collective field is a feature of the strict double scaled limit. For finite large β this becomes at most of order $\sqrt{\beta}$ - see below. In any case this region is beyond the regime where we expect the classical collective description to be good.

Finally, there can be finely tuned profiles where $\rho(\tau)^2$ approaches a constant value. In this case, the collective field obtained from (4.25) is finite and well defined at all times and nothing special happens.

In the matrix model - 2d string theory duality the collective field description is the bulk description - what we are finding is that this bulk description becomes problematic except in a very finely tuned situation.

Remarkably the solutions for the single step abrupt quenches for $\tau > 0$ are exactly those which appeared earlier as time dependent solutions of the matrix model with a *time-independent* potential [211, 212]. The quench solutions for other quench profiles do not correspond to such solutions in a time independent potential.

4.5 The fermionic description

The fundamental description of the theory is given in terms of fermions. In the semiclassical limit of small g_s the fermionic theory can be understood in terms of the dynamics of the filled fermi sea in the single particle phase space. In this regime the density in phase space $u(x, p, \tau)$ is either 1 or zero, and satisfies the Euler equation

$$\left[\partial_\tau + p\partial_x + f(\tau)^2 x \partial_p\right] u(x, p, \tau) = 0 \tag{4.52}$$

There is a canonical transformation in the phase space

$$y = \frac{x}{\rho(\tau)} \qquad T = \int^\tau \frac{d\tau'}{\rho(\tau')^2} \qquad P = \rho(\tau)p - (\partial_\tau \rho)x \tag{4.53}$$

which transforms this equation to the one for a constant unit frequency

$$\left[\partial_T + P\partial_y + y\partial_P\right] u(y, P, T) = 0 \tag{4.54}$$

This may be used to write down the expression for the boundary of the filled fermi sea which corresponds to our solution for the collective field

$$x^2 - \left(\rho(\tau)^2 p - \frac{x}{2}\partial_\tau \rho^2\right)^2 = \rho(\tau)^2 \tag{4.55}$$

We have expressed this entirely in terms of ρ^2 since this is the quantity which appears in the solutions. There are two fermi seas corresponding to the two sides of the potential. The upper and lower edges of the fermi sea for a given value of x are then given by

$$p_\pm(x,\tau) = \frac{1}{\rho(\tau)^2}\left[\frac{x}{2}\partial_\tau\rho^2 \pm \sqrt{x^2-\rho(\tau)^2}\right] \tag{4.56}$$

In the following we will denote the points on the left branch by $p_\pm^<$ and the right branch by $p_\pm^>$.

The quantities $p_\pm(x,\tau)$ are related to the collective fields by the classical bosonization relations [60]

$$\partial_x\zeta^{>,<}(x,\tau) = \frac{1}{2\pi}\left[p_+^{>,<}(x,\tau) - p_-^{>,<}(x,\tau)\right] \tag{4.57}$$

$$\partial_\tau\zeta^{>,<}(x,\tau) = -\frac{1}{2}\partial_x\zeta^{>,<}\left[p_+^{>,<}(x,\tau) + p_-^{>,<}(x,\tau)\right] \tag{4.58}$$

These equations hold separately for each side of the potential, so that there are actually two collective fields.

We now determine the time evolution of the fermi surfaces using (4.56) for the various quench profiles. Since the qualitative behavior of the solution is similar to abrupt quenches,we will use the latter expressions.

Figure 4.9 shows the profile of the fermi surfaces for the quench profile (4.34) for $\omega_0 < \omega_1$. The solid curves are the functions $p_-^{>,<}$ for different values of the time τ while the dashed curves are the functions $p_+^{>,<}$. These two curves meet at $x = \rho(\tau)$. The red curves are for $\tau = 0$, and the blue and green curves are for later times. As time progresses the fermi surfaces fold onto themselves and receed from the potential on both sides.

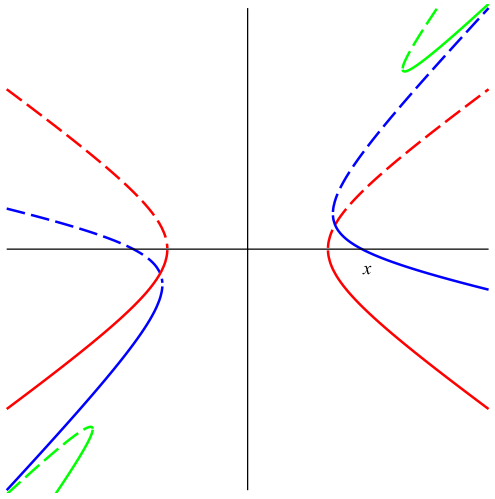

Figure 4.9: The fermi surface profiles for $\omega_0 < \omega_1$

Figure 4.10 shows the profile of the fermi surfaces for the quench profile (4.34) with $\omega_0 > \omega_1$. The solid curves are the functions $p_-^{>,<}$ for different values of the time τ while the dashed curves are the functions $p_+^{>,<}$. These two curves meet at $x = \rho(\tau)$. The red curves are for $\tau = 0$, and the blue, black and green curves are for later times. In particular the black curves correspond to $\tau \sim \tau_0$ while the green curves are for $\tau > \tau_0$. It is clear that the fermi surfaces evolve smoothly across $\tau = \tau_0$, the time at which the collective description becomes problematic. As we approach $\tau = \tau_0$ the meeting place of these curves is pushed off to infinity. For $\tau > \tau_0$ the fermions are pushed to the other side, and only $p_-^<$ and $p_+^>$ are visible. As $\tau \to \infty$ two fermi surfaces $p_-^<$ and $p_+^>$ come close to each other, and it appears that the whole phase space is filled.

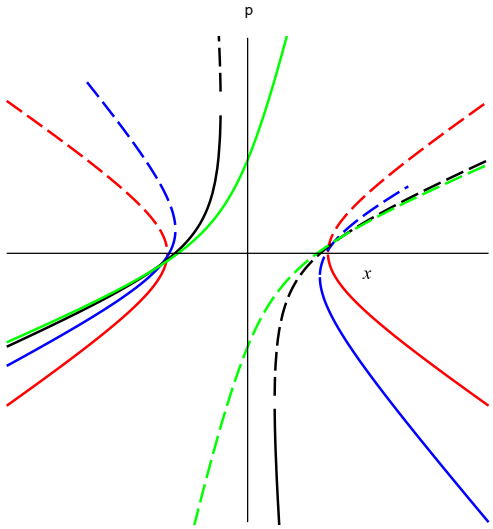

Figure 4.10: The fermi surface profiles for $\omega_0 > \omega_1$

The smooth time evolution of the fermion theory now provides a meaning for the continuation of the saddle point collective field for $\tau > \tau_0$. We now have a single collective field which is defined by

$$\partial_x \zeta_0 = \frac{1}{2\pi}\left[p_+^>(x,\tau) - p_-^<(x,\tau)\right] \tag{4.59}$$

$$= -\frac{1}{\tilde{\rho}(\tau)^2}\sqrt{x^2 + \tilde{\rho}(\tau)^2} \tag{4.60}$$

where $\tilde{\rho}$ is defined in (4.18).

These profiles are for the double scaled potential. For finite β (recall that $\beta \sim N$) the fermi surfaces are closed in phase space and the fermions cannot have arbitrarily large momenta and the entire phase space cannot be filled. In fact, for $\omega_0 > \omega_1$, the fermions which have large values of momenta as we approach $\tau = \tau_0$ come from the region of the original fermi sea which now lie above the ground state fermi level of the

new potential. Consider e.g. a fermion which has $x = x_0$ and $p = p_0$ at $\tau = 0$, with $\omega_0^2 x_0^2 - p_0^2 > \omega_0^2$. If $\omega_1^2 x_0^2 - p_0^2 < \omega_1^2$ these fermions are above the ground state fermi surface of the new potential. At $\tau = \tau_0 = \frac{1}{\omega_1} \tanh^{-1}(\frac{\omega_1}{\omega_0})$ the location and momentum of this fermion is

$$x(\tau_0) = \frac{\omega_0 x_0 + p_0}{\sqrt{\omega_0^2 - \omega_1^2}} \qquad p(\tau_0) = \frac{\omega_1^2 x_0 + \omega_0 p_0}{\sqrt{\omega_0^2 - \omega_1^2}} \tag{4.61}$$

Now consider a fermion which had a large negative x_0 and large positive p_0 at the time of the quench. Then $p_0 \approx -\omega_0 x_0$, and (4.61) yields $x(\tau_0) \approx 0$ and $p(\tau_0) \approx -x_0\sqrt{\omega_0^2 - \omega_1^2}$, which becomes arbitrarily large when x_0 becomes large. However, when β is finite one needs to modify the inverted harmonic potential at large values of x by e.g. imposing a hard wall at $|x| \sim \sqrt{\beta}$. This means that the maximum momenta are also of the order $\sqrt{\beta}$.

The fermi surface profiles for a potential with a cutoff are shown in figure 4.12 and figure 4.11 for various times. Here the filled regions of the phase space are shown in black. At an early time after abrupt quench, each fermi surface profile includes two parts: part of the fermi surface profile for potential without cutoff (shown in figure 4.9 and 4.10), and its reflection after hitting the cutoff. In figure 4.9, particles flow out of the imaginary cutoff while no particles flow in, thus the reflection fermi surface profile should make up the loss to keep the fermion number (the area of black region in figure 4.11) invariant. However, in figure 4.10, more particles with positive energy flow in than flow out, thus the filled fermi surface in the presence of a cutoff excludes these fermions. We explain the details of these two different cases and give the expression of the phase space density $u(x, p, \tau)$ in appendix F.

4.6 The emergent space-time

The nature of the emergent space-time is deduced from the fluctuation action. In particular the quadratic action for fluctuations (4.31) represents a massless scalar field in a $1+1$ dimensional space-time. Since a massless scalar field is insensitive to a conformal factor, we can only determine the conformal class of the metric. Equation (4.33) is one member of this class. The non-trivial features of the emergent space-time are its global aspects - this is what we need to determine.

For this purpose it is useful, as always, to find coordinates such that the metric becomes conformal to standard Minkowskian metric, which is always possible in $1+1$ dimensions. For an arbitrary quench profile, the Minkowskian coordinates (q, T) are given by,

$$x = \pm\tilde{\rho}(\tau)\cosh(q) \qquad T = \int^{\tau} \frac{d\tau'}{\rho(\tau)^2} \tag{4.62}$$

This is adequate for the single step abrupt quench with $\omega_0 < \omega_1$. In this case, we can

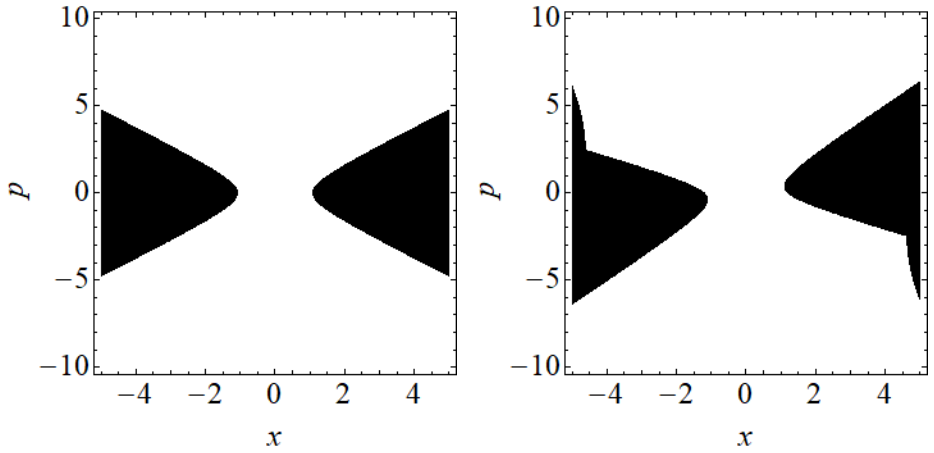

(a) $\tau = 0$ (b) $\tau = \frac{1}{8}$

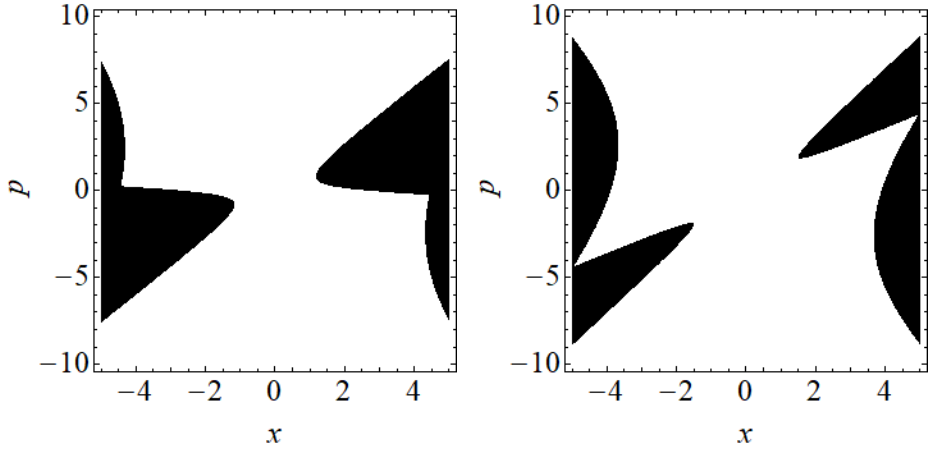

(c) $\tau = \frac{1}{4}$ (d) $\tau = \frac{1}{2}$

Figure 4.11: Time evolution of phase space density $u(x, p, \tau)$ for the potential with a cutoff at $x = \pm l/2$ after abrupt quench. Choose $\omega_0 = \frac{1}{2}, \omega_1 = 1$, $l/2 = 5$.

explicitly obtain, for $\tau > 0$

$$x = \pm \frac{1}{\sqrt{\omega_0}} \left[\cosh^2 \omega_1 \tau - \frac{\omega_0^2}{\omega_1^2} \sinh^2 \omega_1 \tau \right]^{1/2} \cosh q \tag{4.63}$$

$$T = \tanh^{-1} \left[\frac{\omega_0}{\omega_1} \tanh(\omega_1 \tau) \right] \tag{4.64}$$

Note that the forbidden values of x increase with time. As $0 < \tau < \infty$ we have $0 < T < \tanh^{-1} \frac{\omega_0}{\omega_1}$. The space-time appears to be geodesically incomplete, and normally one would have extended the time T further to ∞. However the underlying matrix model tells us that this extension does not make any sense, since the matrix model time τ ends at this point. In fact, on the space-like line $T = \tanh^{-1} \frac{\omega_0}{\omega_1}$, the cubic couplings of the fluctuation field diverge - in this sense this is a space-like singularity. As mentioned in the introduction this means that the semi-classical

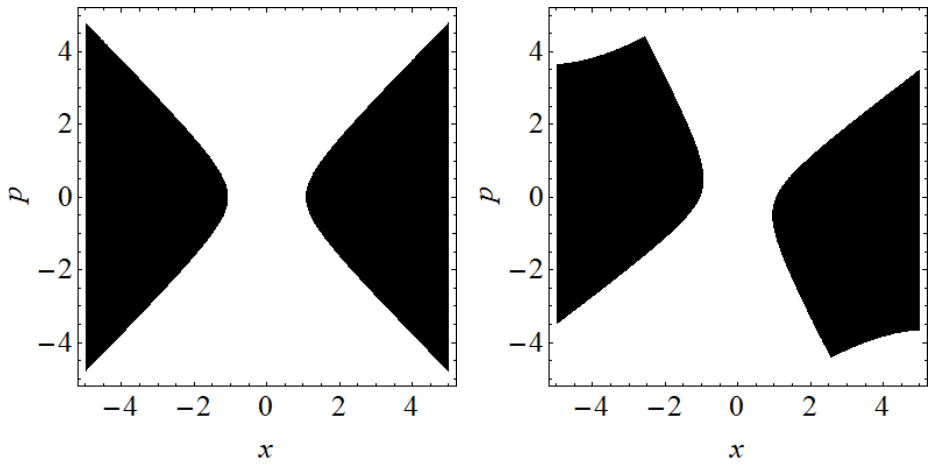

(a) $\tau = 0$

(b) $\tau = \frac{1}{2}\log 3 - 0.0001$

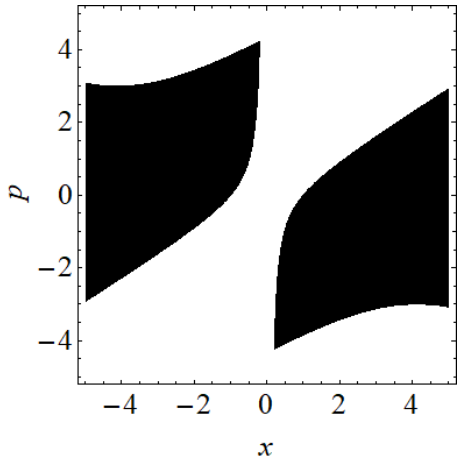

(c) $\tau = \log 3 - 0.001$

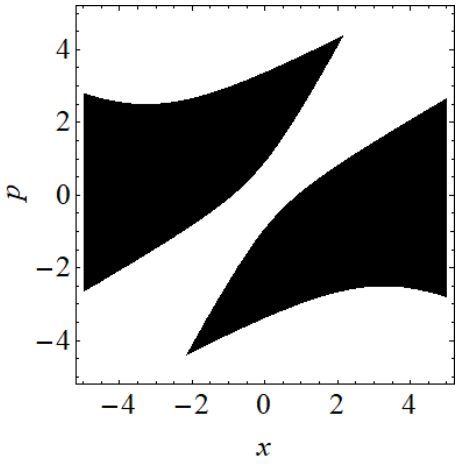

(d) $\tau = \frac{3}{2}\log 3 - 0.0001$

Figure 4.12: Time evolution of phase space density $u(x, p, \tau)$ for the potential with a cutoff at $x = \pm l/2$ after abrupt quench. Choose $\omega_0 = 2\omega_1 = 1$, $l/2 = 5$.

collective theory as well as the fermi fluid description are not valid anymore and strong coupling effects become important. The situation is similar to such singularities in GR which signal the breakdown of Einstein's equations.

An interesting feature of this space-time is that the x = constant lines do not remain time-like for all times. The Penrose diagram for the emergent space-time is shown in figure 4.13. In this figure the thick red solid line and the thick red dashed line seperate two different pieces of the space-time which are perceived by the fluctuations of the left and right fermi surfaces. The red dashed lines are constant x lines, while the blue dotted lines are constant τ lines. Clearly the constant τ lines are always spacelike. This can be seen from the form of the metric (4.33) since $ds^2 > 0$ for

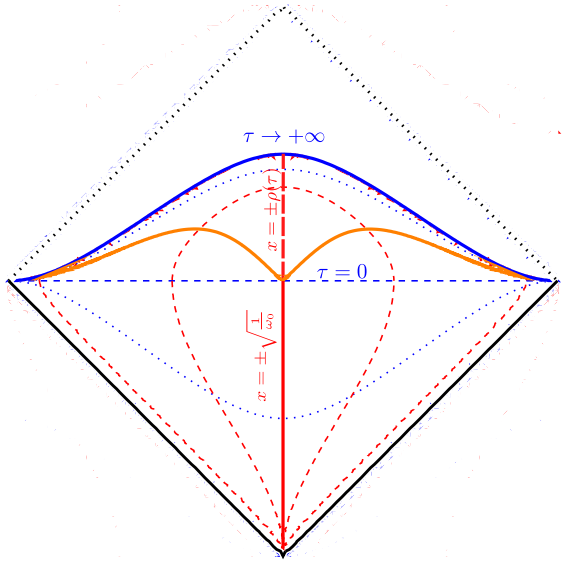

Figure 4.13: Penrose diagram for emergent space-time when $\omega_0 = \frac{1}{\sqrt{2}}\omega_1 = 1$. Blue dotted lines are constant τ lines; Specially, $\tau = 0$ when the abrupt quench occurs are plotted in blue dashed line; $\tau \to \infty$ i.e. infinite future is plotted in blue solid line. Red dashed lines are constant x lines. Special values of x, $x = \pm\sqrt{\frac{1}{\omega_0}}$ and $x = \pm\rho(\tau)$, is plotted in thick red solid line and thick red dashed line, respectively. The two sides of these lines are different disconnected space-times where the fluctuations of the left and right fermi surface propagate. The orange solid lines demarcate the regions in which constant x lines are spacelike from those where they are time-like.

$d\tau = 0$. However constant x lines are timelike only when

$$\frac{(\partial_\tau \zeta_0)^2}{\pi^2(\partial_x \zeta_0)^4} \leq 1 \tag{4.65}$$

They are null when the equality is satisfied and space-like otherwise.

For an abrupt quench with $\omega_0 > \omega_1$, the coordinates (T, q) defined in (4.64) cover only the region $\tau < \tau_0$, and the line $\tau = \tau_0$ has $T = \infty$, and is null. The red solid line is the line $x = \pm\frac{1}{\sqrt{\omega_0}}$. For $\tau \leq 0$ this is $q = 0$ which separates the two sides of the potential. For $\tau > 0$ excitations can propagate in the region $|x| < \frac{1}{\sqrt{\omega_0}}$, so this region is included in the Penrose diagram. The orange line demarcates the regions where constant x surfaces (denoted by red dashed lines) are space-like and time-like. Finally these constant x lines become null as they approach the $\tau = \tau_0$ lines. The part of the Penrose diagram for $\tau < \tau_0$ actually consists of two disconnected pieces (corresponding to the fluctuations of the left and right fermi surfaces) separated by the red solid line for $\tau < 0$ and the red dashed line for $\tau > 0$.

Normally $T = \infty$ or $\tau = \tau_0$ would be the future null boundary of two dimensional Minkowski space and there is no reason for continuing the space-time beyond this. However the matrix model predicts a smooth time evolution beyond $\tau = \tau_0$ - we therefore need to attach another piece of space-time. The Minkowskian coordinates

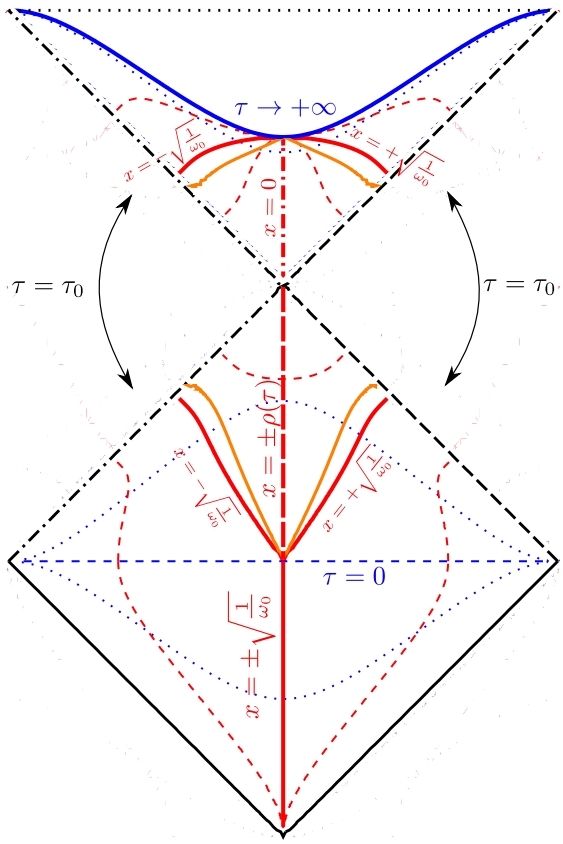

Figure 4.14: Penrose diagram for emergent space-time when $\omega_0 = \sqrt{2}\omega_1 = 1$. The black dot-dashed lines and dashed lines represent $\tau = \tau_0$ where τ_0 is defined in (4.37) and should be glued respectively. Blue dotted lines are constant τ lines; Specially, $\tau = 0$ when the abrupt quench occurs are plotted in the blue dashed line; $\tau \to \infty$ i.e. infinite future is plotted in blue solid line. Red dashed lines are constant x lines. The special value of x, $x = \pm\sqrt{\frac{1}{\omega_0}}$, is plotted in thick red solid lines; it splits into two lines at $\tau = 0$. $x = \pm\rho(\tau)$, is plotted in thick red dashed line. These separate two disconnected space-times corresponding to the fluctuations of the left and right fermi surfaces. These two pieces connect at $\tau = \tau_0$. $x = 0$ is plotted in the thick red dot-dashed line - this, however does not separate disconnected pieces. The orange solid lines demarcate the regions in which constant x lines are spacelike from those where they are time-like.

are now defined by

$$x = \tilde{\rho}(\tau)\sinh(q) \qquad T = -\coth^{-1}\left[\frac{\omega_0}{\omega_1}\tanh(\omega_1\tau)\right] \tag{4.66}$$

In the Penrose diagram this piece is given by the upper triangle. Note that the two disconnected pieces for $\tau < \tau_0$ have joined into a single connected space-time. Equation (4.66) shows that as τ ranges from τ_0 to ∞ the time T ranges from $-\infty$ to a finite value $\coth^{-1}\left(\frac{\omega_0}{\omega_1}\right)$. The matrix model tells us to end the space-time here. The cubic couplings diverge here - so this is like a space-like singularity. Again this means that our semi-classical treatment, together with the space-time interpretation of the model, breaks down here. The matrix model time evolution is possibly smooth, but this requires an exact treatment which we have not pursued.

Once again, the constant x lines are not always timelike. The resulting Penrose diagram is shown in figure 4.14.

For the finely tuned case, the space-time is geodesically complete : at late times ρ^2 saturates so that as $\tau \to \infty$ one also has $T \to \infty$.

4.7 Conclusions

In this work we explored the nature of emergent space-times in the $c = 1$ matrix model with a time dependent coupling. Our main finding is that generically such a quantum quench naturally leads to geodesically incomplete space-times with space-like boundaries where the coupling of the "bulk" theory diverges. Only for very finely tuned quenches, the emergent space-time is normal.

It will be interesting to understand the time dependence of the entanglement entropy of a region of the emergent space-time. In [13] it was shown that in a system of free fermions in an external potential, the entanglement entropy S_A of a region of the eigenvalue space A in the "in" state $|in\rangle$ (i.e. the Heisenberg picture state which is the ground state of the initial hamiltonian) can be expressed entirely in terms of the phase space density $u(x, p, \tau)$,

$$\begin{aligned} S_A =& \frac{1}{2\pi}\int_{-\infty}^{\infty} dp \int_A dx\, \langle in|u(p,x,\tau)|in\rangle - \\ & \frac{1}{(2\pi)^2}\int_{-\infty}^{\infty} dp_1 dp_2 \int_A dx dy \\ & \qquad \times e^{-i(p_2-p_1)(x-y)}\ \langle in|u(p_1,(x+y)/2,\tau)|in\rangle\langle in|u(p_2,(x+y)/2,\tau)|in\rangle \end{aligned} \tag{4.67}$$

The solutions for the phase space density for the various quench profiles studied in this paper can be then used to compute this quantity. For constant frequencies this bulk entanglement entropy has been investigated in [175–177] : one key result of this investigation is that this quantity is finite, with the string coupling replacing the usual UV cutoff. However the meaning of this quantity for our time dependent bulk space-time is unclear at the moment, since constant x lines do not remain time-like for all times. We are currently investigating this issue.

From the point of view of holography, the most interesting question is the relation of these to solutions to those of two dimensional string theory in the worldsheet or string field theory formulations. For the standard time independent case, this relationship involves a transformation whose kernel is non-local at the string scale, and obtained by a comparison on the S matrices obtained from the matrix model and worldsheet string theory. This is a manifestation of the "leg-pole" factors. One may be able to obtain a worldsheet description using the connection of the feynman diagrams of the matrix model with dynamical triangulations of the worldsheet. Naively this would lead to a time dependent dilaton and a time dependent worldsheet cosmological constant. However a precise relationship could be subtle and is under investigation. A precise connection to a worldsheet S-matrix can be then established. Assuming, however, that the non-locality continues to remain at the string scale, the space-time diagrams discussed above need to be smeared at this scale. As mentioned above, the single step abrupt quench results are identical to the time dependent solutions of the constant coupling matrix model considered in [211, 212] : this work contains some discussions of this issue.

Chapter 5
Gauge Invariant Target Space Entanglement in D-Brane Holography

5.1 Introduction

In quantum field theory on a fixed space-time background, entanglement between two regions of space has a well defined meaning in the presence of a UV cutoff and the corresponding entanglement entropy provides valuable information about the nature of the quantum state. In quantum gravity this is a tricky issue since space-time is dynamical. This becomes even more tricky in String Theory where the fundamental degrees of freedom are extended objects. Nevertheless, in a weakly coupled semi-classical regime there is an approximate notion which comes from thinking of gravity as a field theory of gravitons in a background. It is therefore interesting to ask if there is a precise notion of entanglement in a complete theory of gravity which reduces to the above approximate notion in the appropriate regime.

In [21] four of us proposed that in gravitational theories which have holographic duals, such as the ones which arise in String Theory, such a precise notion indeed exists. The proposal is that in Dp brane holography for $p < 3$ this notion is provided by entanglement in the target space of the Yang-Mills theory on the brane. The idea is that a suitable target space constraint can be associated with a co-dimension one spatial region in the bulk dual. In the Yang-Mills theory the target space constraint then leads to a sub-algebra of operators. The expectation values of operators in this sub-algebra can be obtained correctly using a reduced density matrix lying in the sub-algebra itself. The von-Neumann entropy for this reduced density matrix is the precise notion, sought above, of a geometric entropy of the bulk sub-region. When the entire system is in a pure state this entropy is entirely due to quantum entanglement. When the system is in a mixed state, this contains a classical piece.

We conjectured that when the state is the N brane bound state or its slightly heated up version, this von Neumann entropy is given by the Bekenstein formula $A/4G$ where A is the area of the entangling surface in the dual black brane geometry [1] . In a complete theory of gravity one would expect that in any definition of geometric entanglement entropy the UV cutoff is automatic. Our conjecture therefore implies that the UV cutoff is provided by Netwon's constant, and not by e.g. the string length. Indeed, for simple entangling surfaces for $p < 3$ our conjecture yields answers which scale as N^2 and are expressible purely in terms of the appropriate dimensionless quantities of the Yang-Mills theory - as one would expect.

The bulk entanglement we are considering is across *any* codimension two surface. This is distinct from the corrections to holographic entanglement entropy [49, 50] due to entanglement across extremal surfaces [214–217] or what would become a quantum extremal surface [218]. Note that the proposal discussed above, for Dp branes with

[1] For mixed states a spatial Bekenstein bound is not generally valid. In such situations one may need to consider the fine grained entropy of the degrees of freedom of a light sheet associated with a boundary of area A [213]

$p > 0$, considers the same target space constraint holding at all points on the Dp brane. The boundary of the corresponding codimension one spatial surface in the bulk then includes the entire spatial boundary of space-time. For $p > 0$ it is also possible to discuss a more general notion of entanglement which arises for a sub algebra of observables tied to a target space constraint that applies only to a part of the base space along which the Dp branes extend.

The fact that Newton's constant is the natural cutoff is consistent with the idea that the Bekenstein formula for black hole entropy involves a renormalized Newton constant [219–221]. Furthermore it has been argued in [222, 223] that this naturally happens in theories of induced gravity. In the past, [224–226] has argued that Einstein's equations follow from thermodynamics, provided the cutoff in the entanglement entropy in a theory of gravity is Newton's constant. [227] had also conjectured that the entanglement entropy across an arbitrary surface in a theory of gravity saturates the Bekenstein bound. The reasoning of [21] is initimately tied with the identification of bulk entanglement with target space entanglement and therefore differs from these other papers in an essential way.

The appearance of Newton's constant as the UV cutoff is also consistent with the calculation of the bulk entanglement entropy in the c=1 Matrix Model / 2d string theory duality [175–177]. The holographic theory is now gauged quantum mechanics of a single $N \times N$ hermitian matrix. In this case the space of eigenvalues can be interpreted as a bulk space and the only propagating mode of the two dimensional string is related to the density of eigenvalues or the collective field [16] [2] . The Matrix Model is described exactly by N free non-relativistic fermions in an inverted harmonic oscillator potential which can be rewritten as a second quantized field theory living in the eigenvalue space [58, 59]. Entanglement of a region of the eigenvalue space can be then defined in the usual way in this field theory. In fact, the c=1 theory provides the simplest example of target space entanglement, since the emergent space is the target space of the matrix model. In an approriate limit, the entanglement entropy agrees with what one would expect from the low energy effective field theory, but with the UV cutoff replaced by the position dependent string coupling. After incorporating the appropriate factor of N, the UV cutoff is identified with Newton's constant.

The target space entanglement explored in [21] is in a gauge fixed version of the holographic theory. This involves the temporal gauge for the gauge field, and a further gauge choice. For the c=1 model the latter is the gauge where the single matrix is diagonal. The remaining symmetries are Weyl transformations which permute the eigenvalues. In the Dp brane theories we have multiple matrices, and the remaining gauge freedom in the temporal gauge can be used to diagonalize a single matrix which needs to be chosen to express a desired target space constraint. The situation studied in detail in [21] involves diagonalization of one of the scalar fields. The target space constraint is then expressed in terms of an allowed range of the eigenvalues, e.g. requiring the eigenvalue to be larger than some number. This corresponds to

[2] The massless mode of two dimensional string theory is related to the density of eigenvalues by an integral transform with a kernel whose scale is the string scale [189, 228]. Strictly speaking, the entanglement entropy calculated here is in the eigenvalue space. However this would agree with a bulk notion in terms of usual string theory upto an uncertainty of the order of the string scale.

a bulk region characterized by one of the transverse coordinates being larger than some value and a spatial co-dimension one planar entangling surface which bounds this region. The full Hilbert space breaks up into a direct sum of superselection sectors characterized by the number of eigenvalues which satisfy the constraint. In each sector, the smaller Hilbert space is a direct product, which allows one to define a reduced density matrix in the usual fashion. Two possible versions of the proposal for a corresponding reduced density matrix were studied.

While [21] specified the general properties of the operators belonging to the subalgebra of operators associated with a given target space constraint, a procedure to obtain such operators in terms of the operators of the matrix theory was not specified. Furthermore, in this gauge fixed formalism, it is difficult (though not impossible) to describe general entangling surfaces.

In this paper we address both these issues by developing a *gauge invariant* description of target space entanglement. This will be achieved by constructing a projection operator appropriate for the desired target space constraint. Starting with a gauge invariant operator which contains a string of matrices, the subalgebra then consists of operators obtained by projecting each of these matrices. We show that in the gauge used in [21] these yield the correct class of operators in each superselection sector. Moreover, the gauge invariant construction enables us to easily formulate other target space constraints, e.g. those which correspond to entangling surfaces in the bulk at a given value of the radial coordinate in the transverse space of the D-branes - in this case we also show how the target space constraint can be implemented explicitly by developing a formalism for a polar decomposition of the matrices.

The proposed connection of a target space constraint with a bulk region is based on several ingredients of gauge-gravity duality and closely tied to the emergence of bulk locality. As is well known, the velocity dependent potential between two stacks of D0 branes in supergravity follows from an effective action calculation in the Coulomb branch of D0 brane quantum mechanics [229–235].[3] For example, one may consider a single D0 brane stripped off from a stack of N D0 branes in their bound state, corresponding to a point on the Coulomb branch of the D0 brane matrix theory. The Higgs vev at this point is then the transverse location of this probe D0 brane. This implies that a restriction to a region $\mathcal{R}$ of the bulk can be described as a restriction in the target space of the brane theory. In the 't Hooft limit, the gravity dual of the bound state of D0 branes is a non-trivial supergravity background [237], and the velocity dependent potential can be obtained from a DBI-CS action for the probe D0 brane moving in this background. It can also be calculated from the effective action evaluated at the corresponding point in moduli space in the gauge theory. Supersymmetry guarantees in fact that the leading terms in the effective action may be calculated perturbatively. We argue that the potential will also agree with the effective action for operators in the subalgebra, $\mathcal{A}_{\mathcal{R}}$, which we associate with the region $\mathcal{R}$, thereby arguing that the subalgebra contains operators needed to describe bulk measurements which can be carried out in $\mathcal{R}$.

A somewhat stronger connection comes from a point on the Coulomb branch

[3]For a review and references to the original literature see [236].

$SU(N) \to SU(N-2) \times U(1) \times U(1)$, which corresponds to two D branes stripped off from the rest. This situation has been studied in detail for D3 branes in [238–240]. In this case, when the two individual branes are excited, the lowest order terms in the effective action of the two $U(1)$'s agree precisely with a supergravity calculation of the potential between the two branes which follow from exchanges of supergravity modes propagating on the $AdS_5 \times S^5$ produced by the remaining $(N-1)$ branes. This agreement is more detailed than the single D0 DBI+CS action since the supergravity modes in this background mix non-trivially. There should be a similar agreement for D0 branes.

Going beyond the ground state, in an excited state of the gauge theory which corresponds to a modified supergravity background, also one expects that the potential experiences by a probe brane can be obtained from the DBI+CS action, and this potential should agree with an effective action calculation which can be carried out in the gauge theory keeping operators in the subalgebra $\mathcal{A}_{\mathcal{R}}$. Of course a perturbative calculation will no longer suffice to demonstrate this[4]. But one might hope to be able to check this as numerical techniques improve further. In fact some progress has already been made along these lines in obtaining the dynamics of probe branes at finite temperatures [242]. In these calculations some evidence was found that the supergravity fields couple to operators in the probe brane in a manner consistent with the generalized AdS/CFT correspondence discussed in [243, 244].

To summarize, the dynamics on the Coulomb branch should allow one to measure the local background, at least at the level of one point functions, for gravity and other supergravity modes, in a region $\mathcal{R}$. This dynamics we argue can be obtained in the gauge theory by studying the effective action for gauge invariant operators. If we are interested in measuring the supergravity fields *only in the region $\mathcal{R}$ of the bulk*, we argue that it is sufficient to only consider the operators in the subalgebra $\mathcal{A}_{\mathcal{R}}$ associated with $\mathcal{R}$. As mentioned above, this subalgebra contains gauge invariant operators obtained after carrying out a suitable projection determined by the target space constraint which corresponds to the bulk region $\mathcal{R}$.

While the discussion above pertains to the Coulomb branch, the considerations should be valid for a general *configuration* which appears in the wavefunction of the N D0 brane bound state. This motivates our identification of bulk entanglement with target space entanglement.

We should mention that we expect the effective action and the related correlation functions of the projected operators to provide only some and not *all* of the detailed information about supergravity modes and the dual boundary operators related to them via the BDHM-HKLL construction [245–247]. In particular, the energy momentum tensor is not contained in the sub-algebra, only its projected version is. We expect that this imposes important limitations on the extent to which we can learn about the stress energy tensor's correlation functions from the sub-algebra. In fact, as was importantly argued in [248, 249], if the sub-algebra would allow all information pertaining to the stress tensor to be obtained, then for an annular region adjacent to

[4]unless the excited state preserves a high degree of supersymmetry[241]

the boundary, the entanglement entropy would be exactly zero [5]. In this sense the association of a target space constraint with a bulk region is approximate.

An analytic calculation of the target space entanglement entropy requires an explicit expression for the wavefunction. Even in the simplest case of D0 branes, explicit expressions for the bound state wavefunction is not known, though the existence of bound states of D0 branes has been proven [250–252] [6]. There are candidates for approximate wavefunctions which can be in principle used to perform analytic computations of the von Neumann entropy [255, 256]. However, there has been substantial progress in numerical calculations of properties of D0 brane bound states at finite temperature: these calculations provide precision tests of the AdS/CFT correspondence [257–261]. These calculations deal with thermodynamic quantities, correlation functions [262, 263] and investigations of probe dynamics [242]. In this paper we derive path integral expressions for target space Renyi entropies which can be directly used to perform numerical calculations. Work in this direction is being developed currently [264]: these calculations should prove or disprove our conjecture about saturation of the Bekenstein bound.

The formalism of target space entanglement entropy has been developed in [265] and [20]. Notions similar to target space entanglement have been used to define entanglement in string theory in the worldsheet formalism [266–270] and in various explorations in holographic entanglement [271–274]. Another notion of entanglement of internal degrees of freedom (also combined with spatial degrees of freedom) called entwinement has been discussed in [275–277]. Notions of entanglement associated with other kinds of partitions of large-N degrees of freedom have been explored in [278, 279]. The proposal of [21] is distinct from these other works.

The paper [280] has explored general *extremal* surfaces in D brane geometries (as distinct from RT surfaces) and speculated on possible meanings of their areas with entanglement of degrees of freedom in the D0 brane quantum mechanics. In particular, these authors have considered subsets of operators consisting of linear combinations of traceless symmetric products of the matrices in the D0 brane theory which would correspond to functions which have support on some region of S^8 and speculated that an entropy can be associated with such a subset. Our proposal is quite different from this: we aim to describe bulk entanglement which involves the radial direction as well, and we associate an entropy with a closed subalgebra.

This paper is organized as follows. In section 5.2 we introduce the gauge invariant construction of operator algebras which define a target space entanglement. We show how this construction leads to the gauge fixed version discussed in [21] and review the proposed connection to bulk entanglement and our conjecture about the saturation of Bekenstein bound. We also discuss how to impose radial constraints in target

[5] The argument is as follows: if the energy-momentum tensor at all points on the boundary is included in the set of observables, so is the energy and the projector to the ground state. In the vacuum, the latter is the density matrix of the whole system. This would mean that the associated entanglement entropy must be exactly zero. In our case the energy, and therefore also the ground state projector, is not an element of the sub-algebra.

[6] For bosonic BFSS models, the existence of bound states has been proved both numerically [253] and analytically in the limit of large dimensions [254].

space by developing a polar decomposition of matrices. In section 5.3 we discuss the connection of target space entanglement and bulk entanglement. In section 5.4 we recapitulate the conjecture in [21] that the target space entanglement entropy saturates the Bekenstein bound. In section 5.5 we derive path integral expressions for target space Renyi entropies which can be directly used for numerical calculations. Section 5.6 contains concluding remarks. The Appendix G contains some details of the construction of projected operators. Appendix H provides details of matrix polar decompositions for multiple matrices. Appendix I deals with the DBI+CS action of a single D0 brane in the supergravity background produced by N other extremal branes and its comparison with D0 brane quantum mechanics effective action.

5.2 Gauge Invariant Target Space Entanglement

In this section we will show how target space entanglement in a theory of multiple matrices can be formulated in a gauge invariant fashion. A more detailed description appears in Appendix G.

5.2.1 Review of the gauge-fixed formulation

In a previous paper [21], we considered the $D0$ brane theory and discussed a bulk region specified by a condition on one of the spatial bulk coordinates, say x^1. The condition took the form,

$$x^1 > a, \tag{5.1}$$

for some real number a. We proposed that this condition mapped to a target space constraint in the quantum mechanical dual theory that lives on the boundary. And the bulk entanglement entropy maps to the entanglement entropy associated with this target space constraint in the boundary theory. The entanglement entropy defined in this way is manifestly finite when N is finite.

The action of D0 brane quantum mechanics is given by

$$S = \frac{N}{2(g_s N) l_s} \mathrm{Tr} \int dt \left[\sum_{I=1}^{9} (D_t X^I)^2 - \frac{1}{l_s^4} \sum_{I \neq J=1}^{9} [X^I, X^J]^2 \right] + \text{fermions} \tag{5.2}$$

where X^I are $N \times N$ hermitian matrices, and the covariant derivative is defined by

$$D_t X^I \equiv \partial_t X^I + i[A_t, X^I] \tag{5.3}$$

In the example above, the target space constraint involves the operator X^1 in the boundary theory. To specify the target space constraint, we worked in the gauge where $A_t = 0$. The remaining gauge freedom consists of time independent $SU(N)$ rotations, which we fixed by requiring X^1 to be diagonal. The corresponding operators and their canonical conjuagte momenta have the form

$$\begin{aligned} \hat{X}^1 &\rightarrow \mathrm{diag}\left(\hat{\lambda}_1, \cdots \hat{\lambda}_N\right) \\ \hat{\Pi}_1 &\rightarrow \mathrm{diag}\left(\hat{\pi}_1 \cdots \hat{\pi}_N\right) \end{aligned} \tag{5.4}$$

This does not fix the gauge completely: we are left with Weyl transformations,

$$\begin{aligned}(\hat{\lambda}_1, \hat{\lambda}_2, \cdots, \hat{\lambda}_N) &\mapsto (\hat{\lambda}_{\sigma(1)}, \hat{\lambda}_{\sigma(2)}, \cdots, \hat{\lambda}_{\sigma(N)}),\ \sigma \in S(N) \\ \hat{X}^L &\mapsto \sigma(\hat{X}^L),\ \sigma(\hat{X}^L_{ij}) = \hat{X}^L_{\sigma(i)\sigma(j)},\ L = 2, \cdots, 9. \end{aligned} \tag{5.5}$$

and $U(1)^N$ transformations which keep the diagonal matrix elements of all the matrices invariant and multiplies the off-diagonal elements by phases [7]

$$\hat{X}^L_{ij} \mapsto \hat{X}^L_{ij} e^{i(\theta_i - \theta_j)} \tag{5.6}$$

where θ_i are angles. The physical state is constructed by adding Weyl and $U(1)^N$ transforms. Let us work in a basis in the Hilbert space comprised of eigenvectors of the operators $\hat{\lambda}_i, \hat{X}^L_{ij}$ with eigenvalues λ_i, X^L_{ij}. As is well known the transformation to the eigenvalues of X^1 leads to a van der Monde factor in the measure of integration. In the following we will absorb a square root of this factor in the wavefunction so that the modified wavefunction is antisymmetric under an interchange of the eigenvalues. Then a Weyl and $U(1)^N$ symmetrized state is [8,9]

$$|\{\lambda_i\}, \{X^L_{ij}\}\rangle_W = \frac{1}{N!} \int \prod_{I=1}^{N} \frac{d\theta_i}{2\pi} \sum_{\sigma \in S_N} \mathrm{sgn}(\sigma) |\{\lambda_{\sigma(i)}\}, \{X^L_{\sigma(i)\sigma(j)} e^{i(\theta_{\sigma(i)} - \theta_{\sigma(j)})}\}\rangle \tag{5.7}$$

Note that this symmetrized state is not an eigenstate of the individual $\hat{\lambda}_i, \hat{X}^L_{ij}$'s. They are eigenstates of gauge invariant operators which are traces of products of $\hat{X}^I, \hat{\Pi}_I$ or products of these traces.

In this gauge, it was proposed that the required target space condition, corresponding to 5.1, on an eigenvalue λ_i, was

$$\lambda_i > a. \tag{5.8}$$

The target space constraint can be generalized trivially to

$$\lambda_i \in A \tag{5.9}$$

where A is some interval on the real line, with a corresponding change in the bulk region 5.1.

Since there are N eigenvalues the constraint gives rise to $N+1$ different possibilities depending on whether $0, 1, \cdots, N$, of the eigenvalues meet the constraint.

[7] In a previous version of this paper which appeared on the arXiv, we did not consider these $U(1)^N$ transformations. Subsequently the paper [281] appeared, where these remaining symmetries were emphasized.

[8] Our conventions for normalization of states is different from [21].

[9] Since the Weyl group elements g_W and the $U(1)^N$ group elements g_U do not commute, the combined action on a given state $|\psi\rangle$ depends on the order in which the group elements act. In 5.7 we have applied g_U followed by g_W. It is not difficult to see, however, the 'symmetrized' state, which involves sum over the entire set of transforms, does not depend on the order: $\sum_{W,U} g_W g_U \psi = \sum_{W,U} g_U g_W \psi$.

These different possibilities actually can be thought of as giving rise to different superselection sectors. The Hilbert space thus becomes a direct sum of Hilbert spaces,

$$\mathcal{H}_N = \oplus_k \mathcal{H}_{k,N-k} \tag{5.10}$$

where $\mathcal{H}_{k,N-k}$ denotes the sector where k of the eigenvalues of $\hat{X}^1$ are in the region of interest A and the rest in its complement $\bar{A}$.

The reduced density matrix in the k^{th} superselection sector, $\tilde{\rho}_{k,N-k}$, can be obtained by tracing out the degrees of freedom corresponding to the remaining $(N-k)$ eigenvalues. The corresponding target space entanglement entropy can then be obtained as the von Neumann entropy for this density matrix and the full entanglement entropy for all sectors can be obtained by adding the entropy from each sector [10]. Note that the density matrix in each individual sector is not normalized. Rather the trace $\mathrm{Tr}_k \tilde{\rho}_{k,N-k}$ is simply the probability that k of the eigenvalues are in the region of interest. The full reduced density matrix is block diagonal, where each block corresponds to a superselection sector

$$\rho = \begin{pmatrix} \tilde{\rho}_{0,N} & \mathbf{0} & \mathbf{0} & \cdots & \mathbf{0} \\ \mathbf{0} & \tilde{\rho}_{1,N-1} & \mathbf{0} & \cdots & \mathbf{0} \\ \cdots & \cdots & \cdots & \cdots & \cdots \\ \mathbf{0} & \mathbf{0} & \mathbf{0} & \mathbf{0} & \tilde{\rho}_{N,0} \end{pmatrix} \tag{5.11}$$

does have unit trace, so that

$$S = -\mathrm{Tr}(\rho \log \rho) = -\sum_{k=0}^{N} \mathrm{Tr}_k(\tilde{\rho}_{k,N-k} \log \tilde{\rho}_{k,N-k}) \tag{5.12}$$

is a legitimate von Neumann entropy.

Actually our proposal had two versions which arise when we think more precisely about tracing out the degrees of freedom corresponding to the remaining $N-k$ eigenvalues. By a suitable choice of gauge the eigenvalues of X^1 meeting the constraint can be taken to be the first k eigenvalues.

In the rest of the paper, the matrix indices $i, j, \cdots = 1 \cdots N$; the indices $a, b = 1 \cdots k$ and $\alpha, \beta = k+1 \cdots N$. In the rest of this subsection, we denote $X^2, X^3, ..., X^9$ by X^L, $L = 2, 3, ..., 9$.

1. In the first version, one traces out the degrees of freedom corresponding to the $(N-k)$ eigenvalues of X^1 which do not satisfy eq.(5.8), λ_α and the degrees of freedom in $(N-k) \times (N-k)$ block for the remaining spatial matrices, $X^2_{\alpha\beta}, X^3_{\alpha\beta}, \cdots X^9_{\alpha\beta}$. In addition, one also traces out the degrees of freedom corresponding to the off-diagonal elements $(X^2)_{a\alpha}, (X^2)_{\alpha a}$; and similarly for $X^3, X^4, \cdots X^9$. As a result the only degrees of freedom we retain are in the

[10] The sector with no eignvalues meeting the required condition is important to keep in mind. It is taken to be one dimensional and the density matrix is then a number corresponding to the probability of finding no eigenvalue meeting the constraint.

$k \times k$ block. In the basis we are using, the reduced density matrix for the k'th sector is then given by

$$\begin{aligned}
&\tilde{\rho}^{(1)}_{k,N-k}\left(\lambda_a, X^L_{ab}; \lambda'_a, X'^L_{ab}\right) \\
=&\binom{N}{k}\int [d\lambda_\alpha dX^L_{a\alpha} dX^L_{\alpha a} dX^L_{\alpha\beta}] \\
&\qquad \times \rho_{tot}\left(\lambda_a, X^L_{ab}, \lambda_\alpha, X^L_{a\alpha}, X^L_{\alpha a}, X^L_{\alpha\beta}; \lambda'_a, , X'^L_{ab}, \lambda_\alpha, X^L_{a\alpha} X^L_{\alpha a} X^L_{\alpha\beta}\right)
\end{aligned} \tag{5.13}$$

where ρ_{tot} is the density matrix of the state of the entire system.

2. In the second version, one traces out only the degrees of freedom which lie in the $(N-k)\times(N-k)$ blocks for all matrices and retains the remaining degrees of freedom. So for X^1 which is diagonal we retain the first k eigenvalues which meet the constraint, but for X^2 we retain not only the elements $(X^2)_{ab}$ but also the off-diagonal elements $(X^2)_{a\alpha}, (X^2)_{\alpha a}$ and similarly for $X^3, \cdots X^9$,

$$\begin{aligned}
&\tilde{\rho}^{(2)}_{k,N-k}\left(\lambda_a, X^L_{ab}, dX^L_{a\alpha} dX^L_{\alpha a}; \lambda'_a, X'^L_{ab} dX'^L_{a\alpha} dX'^L_{\alpha a}\right) \\
=&\binom{N}{k}\int [d\lambda_\alpha dX^L_{\alpha\beta}]\ \rho_{tot}\left(\lambda_a, X^L_{ab}, \lambda_\alpha, X^L_{a\alpha}, X^L_{\alpha a}, X^L_{\alpha\beta}; \lambda'_a, , X'^L_{ab}, \lambda_\alpha, X'^L_{a\alpha} X'^L_{\alpha a} X^L_{\alpha\beta}\right)
\end{aligned} \tag{5.14}$$

In each sector labelled by k, the corresponding density matrix evaluates expectation values of a closed subalgebra of operators which correspond to measurements on the variables which are retained. In the first version, the action of such an operator on a general Weyl and $U(1)^N$ symmetrized state of the form (5.7) has the form

$$\begin{aligned}
&\hat{\mathcal{O}}\ |\{\lambda_a, X^L_{ab}, X^L_{a\alpha}, X^L_{\alpha\beta}, \lambda_\alpha\}\rangle_W \\
&\quad = \int [d\lambda'_a][dX'^L_{ab}]\ \tilde{O}(\{\lambda'_a, X'^L_{ab})\}, \{\lambda_a, X^L_{ab}\})\ |\{\lambda'_a X'^L_{ab}\}; \{\lambda_\alpha, X^L_{a\alpha}, X^L_{\alpha\beta}\}\rangle_W
\end{aligned} \tag{5.15}$$

Operators which satisfy this form a subalgebra: $\tilde{O}(\{\lambda_a, X^L_{ab}\}, \{\lambda'_a, X'^L_{ab})\})$ then denote the matrix elements of an operator in the smaller Hilbert space in this sector. The reduced density matrix which evaluates expectation values of such operators is given by (5.13).

Similarly for the second version the action is given by

$$\begin{aligned}
&\hat{\mathcal{O}}\ |\{\lambda_a, X^L_{ab}, X^L_{a\alpha}, X^L_{\alpha\beta}, \lambda_\alpha\}\rangle_W \\
&\quad = \int [d\lambda'_a][dX'^L_{ab}][dX'^L_{a\alpha}][dX'^L_{\alpha a}]\ \tilde{O}(\{\lambda'_a, X'^L_{ab}, X'^L_{a\alpha}, X'^L_{\alpha a})\}, \{\lambda_a, X^L_{ab}, X^L_{a\alpha}, X^L_{\alpha a}\}) \\
&\qquad\qquad |\{\lambda'_a X'^L_{ab} X'^L_{a\alpha} X'^L_{\alpha a}\}, \{\lambda_\alpha X^L_{\alpha\beta}\}\rangle_W
\end{aligned} \tag{5.16}$$

It is clear that the density matrix is again of the form (5.11).

The associated entanglement entropy for a density matrix of the form eq.(5.11) is expressible in terms of the *normalized* density matrices of the subsectors, $\hat{\rho}_{k,N-k} =$

$\frac{1}{p_{k,N-k}}\tilde{\rho}_{k,N-k}$ as

$$S = -\sum_{k=0}^{N} [p_{k,N-k} \log p_{k,N-k} + p_{k,N-k} \mathrm{Tr}_k(\hat{\rho}_{k,N-k} \log \hat{\rho}_{k,N-k})] \tag{5.17}$$

The distillable part of the entanglement is only the second term in (5.17), while the first term is a classical piece which cannot be used as a quantum resource for teleportation [282, 283].

Before closing this subsection let us note that while we have focussed on bosonic operators above, a similar discussion also applies to fermionic operators in the theory. Depending on which version of our proposal we consider, the appropriate adjoint color degrees of freedom for fermonic operators are also to be retained in the sub-algebra.

5.2.2 Gauge-invariant formulation

A drawback of the discussion in the previous paper [21], and our discussion above, is that this description of the target space constraint and the related entropy has been given in a particular gauge, e.g., for the example above we worked in the gauge where X^1 is diagonal. Furthermore, while (5.15) and (5.16) describe the properties satisfied by operators belonging to the relevant subalgebra of observables, this does not tell us *what* these operators are in terms of the basic operators of the theory. In this subsection, we will address both these issues and give a gauge invariant description of the target space constraint; this will also allow us to generalise the discussion considerably to a much wider class of bulk regions.

In general, suppose we have a region in the bulk at time t specified by one condition among the 9 spatial coordinates,

$$f(x_i) > 0 \tag{5.18}$$

We would like to specify the target space constraint corresponding to this bulk region in a gauge invariant manner. For this purpose, instead of starting with a wave function, constructing the density matrix by a partial trace over some degrees of freedom and calculating its entropy, it is useful to think of the entanglement entropy as arising because one is dealing with a suitable *sub-algrebra* of the set of all observables. The sub-algebra corresponds to the operators whose expectation values can be obtained correctly from the reduced density matrix obtained after tracing out the unwanted degrees of freedom. Specifying the sub algebra is an equivalent way of specifying the tracing out procedure and implementing the target space constraint.

Note that when we think in this way, starting from a sub-algebra of all observables, the density matrix itself must lie in the sub-algebra of observables and, as mentioned, must give the correct expectation values for all operators in the sub-algebra. In addition the density matrix is normalised, as usual, to meet the condition, $\mathrm{Tr}\rho = 1$. This specifies the density matrix uniquely and the entanglement entropy is then the

von-Neumann entropy of this density matrix.[11] When there are superselection sectors, as in our current discussion, we found above a corresponding density matrix in each sector. However, as we will see, and this is one of the virtues of specifying a sub-algebra to implement the target space constraint, the sub-algebra of interest can in fact be *specified once and for all* in a gauge invariant manner regardless of the sector we are working in.

Before proceeding to a gauge invariant formulation let us first address the question; how do we determine the relevant subalgebra of operators even in a fixed gauge. To illustrate the procedure it is useful to consider the simple case of gauged quantum mechanics of a single matrix $\hat{M}$. In the gauge where the matrix is diagonal, this reduces to a theory of N fermions on a line. The position and momentum operators of individual fermions are the $\hat{\lambda}_i$ and $\hat{\pi}_i$. Consider a typical one body operator in this theory

$$\mathcal{C}_{n,m} = \sum_{i=1}^{N} \hat{\lambda}_i^n \hat{\pi}_i^m \tag{5.19}$$

We want to impose a target space constraint where the eigenvalues of $\hat{\lambda}_i$ lie in a certain interval on the line denotes by A. This corresponding subalegbra consists of operators which act only on the fermions which lie in this interval. Such an operator can be constructed as follows. Define a projection operator

$$(\hat{P}_A)_i = \int_A dx\ \delta(x - \hat{\lambda}_i) \tag{5.20}$$

where $A \subset R$. By considering matrix elements between arbitrary states it is clear that this operator indeed satisfies

$$(\hat{P}_A)_i^2 = (\hat{P}_A)_i \tag{5.21}$$

Now, starting from an operator (5.19) construct an operator by replacing each of the $\hat{\lambda}_i, \hat{\pi}_i$ by $(\hat{P}_A)_i \hat{\lambda}_i (\hat{P}_A)_i$ and $(\hat{P}_A)_i \hat{\pi}_i (\hat{P}_A)_i$ to get

$$(\mathcal{C}_{n,m})_A^P = \sum_{i=1}^{N} (\hat{P}_A)_i \hat{\lambda}_i^n (\hat{P}_A)_i \hat{\pi}_i (\hat{P}_A)_i \hat{\pi}_i (\hat{P}_A)_i \cdots (\hat{P}_A)_i \hat{\pi}_i (\hat{P}_A)_i \tag{5.22}$$

where we have used (5.21) and the fact $[(\hat{P}_A)_i, \hat{\lambda}_j] = 0$ to simplify the expression. It may be now easily checked that the expectation value of $(\mathcal{C}_{n,m})_A^P$ in a general many particle state becomes a sum of terms: each term corresponds to a sector with k particles in the interval A. The k-th term contains the contribution *only from the k particles in A*. This is discussed in more detail in Appendix G.

[11] The uniqueness can be easily seen. Suppose there are two possible density matrices, ρ and $\tilde{\rho}$, which satisfy $\mathrm{Tr}(\rho O) = \mathrm{Tr}(\tilde{\rho} O) = \mathrm{Tr}(\rho_{tot} O)$ for *all* operators O in the sub-algebra. Hence $\mathrm{Tr}[(\rho - \tilde{\rho}) O] = 0$ for all such operators; since both ρ and $\tilde{\rho}$ belong to the sub-algebra, this can only happen if $\rho = \tilde{\rho}$.

It is now straightforward to construct these operators in a gauge invariant fashion. In terms of the matrix valued operator $\hat{M}$ the projector is clearly given by

$$(\hat{P}_A) = \int_A dx\ \delta(x\mathbf{I} - \hat{M}) \tag{5.23}$$

where $\mathbf{I}$ is the $N \times N$ identity operator.This procedure generalizes to the D0 brane theory with multiple matrices as we now describe.

To obtain a sub-algebra which corresponds to the target space constraint following from eq.(5.18) we consider its target space analogue,

$$f(\hat{X}^I) > 0 \tag{5.24}$$

and the following projection operator which follows from this constraint

$$\hat{P}_1 = \int_{x>0} dx \delta(x\mathbf{I} - f(\hat{X}^I)) \tag{5.25}$$

where $\hat{X}^I$ are the operators in D0 brane quantum mechanics. Note that we have taken the function f here to be the same as in eq. (5.18) but its argument in eq.(5.25) are now operators [12]. The integral is over positive values of x which is a c number. We will choose the operator $f(X^I)$ to be hermitian.

In general there will be ordering ambiguities which will arise in going from the function f in the bulk to the corresponding function f of matrix operators which appears in eq.(5.25); we will comment on this issue further towards the end of this subsection.

By doing a unitary transformation and going to a basis in which $f(X^I)$ is diagonal one can easily check that $\hat{P}_1$ is a projection operator satisfying the condition

$$\hat{P}_1^2 = \hat{P}_1 \tag{5.26}$$

Gauge invariant operators can now be obtained by conjugating with $\hat{P}_1$ and taking a trace. For example, starting from $\hat{X}^I, I = 1, \cdots 9$, we construct the corresponding projected operators $\hat{P}_1\hat{X}^I\hat{P}_1, I = 1, \cdots 9$, and then take a trace over the color degrees to obtain gauge invariant operators from these projected operators $Tr(\hat{P}_1\hat{X}^1), Tr(\hat{P}_1\hat{X}^2), \cdots Tr(\hat{P}_1X^9)$ (here we have used cyclicity of the trace and the facts that $[\hat{P}_1, \hat{X}^I] = 0$ and $\hat{P}_1^2 = 1$ to drop one of the two $\hat{P}_1$ factors) .

More generally let $\mathcal{O}$ be any operator obtained by multiplying a string of $\hat{X}^I$'s and $\hat{\Pi}_I$'s where the $\hat{\Pi}_I$'s are the momenta conjugate to the $\hat{X}^I$'s. Schematically we can write $\mathcal{O} = \cdots \hat{X}^I \cdots \hat{\Pi}_J \cdots$ to depict the string of X^I's and $\hat{\Pi}_J$'s in some order. We can obtain a gauge invariant operator from $\mathcal{O}$ by taking the colour trace,

$$\hat{\mathcal{O}} = Tr(\mathcal{O}) = Tr(\cdots \hat{X}^I \cdots \hat{\Pi}_J \cdots). \tag{5.27}$$

Now to obtain elements of the desired sub-algebra we consider the projected operators,

$$\hat{X}^I \to (\hat{X}^I)^{P_1} = \hat{P}_1 X^I \hat{P}_1 \tag{5.28}$$

[12] More generally the target space constraint and bulk constraint could be related in a more complicated fashion, see below for further discussion of this point.

and

$$\hat{\Pi}_J \to (\hat{\Pi}_J)^{P_1} = \hat{P}_1 \hat{\Pi}_J \hat{P}_1 \tag{5.29}$$

and construct the string

$$\cdots (\hat{X}^I)^{P_1} \cdots (\hat{\Pi}_J)^{P_1} \cdots \tag{5.30}$$

by replacing every factor of $\hat{X}^I, \hat{\Pi}_J$ in $\mathcal{O}$ above with the projected counterpart. Then the projected operator corresponding to $\hat{\mathcal{O}}$ is given by taking the colour trace of eq.(5.30). We will use the notation $\hat{\mathcal{O}}^{P_1}$ for this operator below, so we have,

$$\hat{\mathcal{O}}^{P_1} = Tr(\cdots (\hat{X}^I)^{P_1} \cdots (\hat{\Pi}_J)^{P_1} \cdots). \tag{5.31}$$

It is important to note that the operator in eq.(5.31) is different from $Tr(P_1 \mathcal{O} P_1)$, where $\mathcal{O}$ is given by eq.(5.27). E.g., when $\mathcal{O}$ above is $X^I X^J$, $\hat{\mathcal{O}} = Tr(\hat{X}^I \hat{X}^J)$ and $Tr(P_1 \mathcal{O} P_1) = Tr(P_1 \hat{X}^I \hat{X}^J P_1)$. However the operator $\hat{\mathcal{O}}^{P_1} = Tr(P_1 \hat{X}^I P_1 \hat{X}^J)$ which is different.

The full sub -algebra we consider associated with the constraint eq.(5.18) involves all single trace operators obtained after projection in this manner and the multi trace operators obtained from products of such single trace projected operators.

Actually the projection operator P_1 above implements version 1) of the proposal, for a constraint specified by the function $f(X^I)$. To see this consider the case $f(X^I) = X^1 - a$, discussed above. Working in the gauge where X^1 is diagonal, let us consider the sector where the first k eigenvalues $x_i^1 > a, i = 1, \cdots k$ are in the region of interest. Then it is easy to see in this sector that the operator P_1 is the matrix

$$P_1 = \begin{pmatrix} \mathbf{I}_{k\times k} & \mathbf{0}_{k\times(N-k)} \\ \mathbf{0}_{(N-k)\times k} & \mathbf{0}_{(N-k)\times(N-k)} \end{pmatrix} \tag{5.32}$$

where $\mathbf{I}_{k\times k}$ denotes the identity in the $k \times k$ block and $\mathbf{0}$ denotes a matrix where all entries vanish. Projecting with this operator we retain for all matrix operators their upper left hand $k \times k$ block, as shown in detail in the Appendix G. Gauge invariant operators made out of such matrix operators are exactly the observables whose expectation values can be calculated using the density matrix obtained from the tracing out procedure described above for version 1) of the proposal.

More generally, for a constraint $f(x^I) > 0$ we can go to the gauge where $f(\hat{X}^I)$ is diagonal and in the sector where the first k eigenvalues satisfy the constraint find that multiplying with P_1 will retain similarly the upper left hand $k \times k$ block for all operators and thus give the correct sub-algebra associated with version 1).

Implementing the version 2) proposal in a gauge invariant manner is also similarly doable. We first consider the orthogonal projector

$$\tilde{P}_1 = \int_{x<0} dx \delta(x\mathbf{I} - f(\hat{X}^I)), \tag{5.33}$$

which involves the same argument for the delta function but with the range of the x integral now lying in the complementary region $x < 0$. It follows that $\tilde{P}_1^2 = \tilde{P}_1$ To implement version 2) we consider the operators, $\hat{X}^I$ and retain the elements corresponding to $\hat{X}^I - \tilde{P}_1 \hat{X}^I \tilde{P}_1$, so that

$$\hat{X}^I \to (\hat{X}^I)^{P_2} = \hat{X}^I - \tilde{P}_1 \hat{X}^I \tilde{P}_1 \tag{5.34}$$

and similarly for the momentum operators $\hat{\Pi}_I, I = 1, \cdots 9$,

$$\hat{\Pi}_I \to (\hat{\Pi}_I)^{P_2} = \hat{\Pi}_I - \tilde{P}_1 \hat{\Pi}_I \tilde{P}_1 \tag{5.35}$$

Then taking the trace of a string of such operators we obtain gauge invariant operators

$$\hat{\mathcal{O}}^{P_2} = Tr(\cdots (\hat{X}^I)^{P_2} \cdots (\Pi_J)^{P_2} \cdots) \tag{5.36}$$

which should be compared with eq.(5.31) obtained above for the version 1) case. It should be emphasised that the transformation $\hat{X}^I \to (\hat{X}^I)^{P_2}, \hat{\Pi}_J \to (\hat{\Pi}_J)^{P_2}$ also squares to itself, since

$$((\hat{X}^I)^{P_2})^{P_2} = (\hat{X}^I)^{P_2} - \tilde{P}_1 (\hat{X}^I)^{P_2} \tilde{P}_1 = (\hat{X}^I)^{P_2} \tag{5.37}$$

where we used the property $\tilde{P}_1^2 = \tilde{P}_1$. This transformation is therefore also a projection acting on the matrix operators $\hat{X}^i, \hat{\Pi}_J$. However, the transformation does not act by conjugation, unlike P_1 for version 1).

The notation we have adopted referring to the gauge invariant operators obtained in both cases, as $\hat{\mathcal{O}}^{P_1}, \hat{\mathcal{O}}^{P_2}$, allows for some simplification in the following discussion. We will often refer to the operators obtained in both versions as $\hat{O}^P$ without specifying which of the two cases P_1, P_2 we have in mind; where needed we will of course provide this clarification.

In the subsequent discussion we will also often denote the sub-algebra associated with a bulk region $\mathcal{R}$ which is obtained after projection, in either of the two versions as described above, as $\mathcal{A}_R$.

Let us end this subsection with two comments. First, in general, while passing from the constraint in terms of bulk coordinates, $f(x^I)$, eq.(5.18), to a constraint in terms of matrix operators, $f(\hat{X}^I)$, which appears in the target space constraint, we will encounter ordering ambiguities as was mentioned above. Note that in the matrix quantum mechanics, at any instant of time, the different matrix elements of the matrix operators commute, $[\hat{X}^I_{ij}, \hat{X}^J_{kl}] = 0$. However there are still matrix ordering ambiguities which are present since as matrices $[X^I, X^J] \neq 0$.

As we will soon discuss, the matrix model we are dealing with is formulated in terms of matrix operators $X^1, \cdots X^9$, which correspond to the poincare coordinates in supergravity. For a linear constraint in the bulk involving these coordinates, where $f(x^I) = \sum_{I=1}^9 c_I x^I - a$, it is straightforward to obtain the operator constraint $f(\hat{X}^I)$ to be the corresponding function involving the matrix operators, $f(\hat{X}^i) = \sum_{I=1}^9 c_I \hat{X}^I - a$. For some of the non-linear constraints also there is a natural way to find the corresponding operator constraints, for example $f(x^I) = \sum_{I=1}^9 c_I (x^I)^2 - a$, is mapped in a straightforward manner to $f(\hat{X}^I) = \sum_{I=1}^9 c_I (\hat{X}^I)^2 - a$. In fact, the last example can be extended to more general constraints which involve terms containing sums of monomials of individual coordinates, i.e.,

$$f(x^I) = \sum_I c_I (x^I)^{p_I} - a. \tag{5.38}$$

These are mapped to

$$f(\hat{X}^i) = \sum_I c_I (\hat{X}^I)^{p_I} - a. \tag{5.39}$$

However, more general non-linear constraints involving terms with multiple coordinates cannot be mapped to a matrix constraint unambiguously, e.g. take the case when $f(x^I) = x^1x^2 - a > 0$, this could be mapped to either to $\hat{X}^1\hat{X}^2 - a > 0$ or $\hat{X}^2\hat{X}^1 - a > 0$. Our discussion below will primarily focus on cases like eq.(5.38) where the map to the target space constraint eq.(5.39) is straightforward[13].

Second, it is easy to see that the operators contained in the subalgebra $\mathcal{A}_R$ for both versions 1) and 2) do not include the Hamiltonian of the system. Remaining in the temporal gauge, let us rescale the matrices in (5.2) and their conjugate momenta as

$$\hat{X}^I \to (g_sN)^{1/3} l_s \hat{X}^I \qquad\qquad \hat{\Pi}^I \to \frac{1}{(g_sN)^{1/3} l_s} \hat{\Pi}^I \tag{5.40}$$

the hamiltonian becomes

$$H = \frac{(g_sN)^{1/3}}{2l_s} \mathrm{Tr} \left[\frac{1}{N} \sum_{I=1}^{9} (\hat{\Pi}_I)^2 + N \sum_{I \neq J=1}^{9} [\hat{X}^I, \hat{X}^J]^2 \right] + \text{fermions} \tag{5.41}$$

Instead $\mathcal{A}_R$ contains the operator

$$H^P = \frac{(g_sN)^{1/3}}{2l_s} \mathrm{Tr} \left[\frac{1}{N} \sum_{J} [(\hat{\Pi}_J)^P]^2 + N \sum_{IJ} [(\hat{X}^I)^P, (\hat{X}^J)^P]^2 \right] + \text{fermions} \tag{5.42}$$

which is different.

In this paper we will consider gauge theories which involve matter fields in the adjoint representation. The main examples are gauged quantum mechanics of a single matrix, a particular example of which is the dual description of two dimensional strings, and Dp brane field theories. The $D0$ brane quantum mechanics is a particularly important example relevant for our discussion.

5.2.3 Implementing a non-linear target space constraint

As described above, the gauge invariant formulation of target space entanglement applies to any constraint characterized by a hermitian operator $f(\hat{X}^I)$. In a practical calculation, however, one would need to fix a gauge which diagonalizes this constraint. To perform a concrete calculation, however, one needs to make a change of variables to a set of *independent* variables which includes the eigenvalues. This is straightforward for a linear constraint, but becomes complicated very soon when we consider nonlinear constraints. In this subsection we explain how to do this for a constraint

$$f(\hat{X}^I) = \sum_{I=1}^{9} (\hat{X}^I)^2 \equiv \hat{R}^2 \tag{5.43}$$

The details of the procedure are given in the Appendix G. What we need is a "polar" decomposition for matrices.

[13]It could be that such operator ordering ambiguities give rise to differences in entanglement entropy which are subheading in N, we thank S. Minwalla for making this comment.

Two matrices

Let us begin with the simplest case of two matrices $\hat{X}^1$ and $\hat{X}^2$. In the following all the matrices are operators in the Hilbert space unless stated otherwise. We want to write this pair in terms of one hermitian matrix $\hat{R}$ and a unitary matrix $\hat{Q}$, where

$$\hat{R}^2 = (\hat{X}^1)^2 + (\hat{X}^2)^2 \tag{5.44}$$

Define the complex matrix

$$\hat{Z} = \hat{X}^1 + i\hat{X}^2 \tag{5.45}$$

Then it follows that

$$2\hat{R}^2 = \hat{Z}\hat{Z}^\dagger + \hat{Z}^\dagger\hat{Z} \tag{5.46}$$

Now consider a singular value decomposition

$$\hat{Z} = \hat{V}\hat{s}\hat{W}^\dagger \tag{5.47}$$

where $\hat{V}, \hat{W}$ are unitary matrices and $\hat{s}$ is a diagonal matrix. Using (5.46) we then get

$$\begin{aligned} 2(\hat{R}^2)_{ij} &= (\hat{V}\hat{s}^2\hat{V}^\dagger + \hat{W}\hat{s}^2\hat{W}^\dagger)_{ij} \\ &= [\hat{V}^\star \otimes \hat{V} + \hat{W}^\star \otimes \hat{W}]_{ij,kl}(\hat{s}^2)_{kl} \end{aligned} \tag{5.48}$$

where

$$[\hat{V}^\star \otimes \hat{V} + \hat{W}^\star \otimes \hat{W}]_{ij,kl} \equiv \hat{V}_{ik}\hat{V}^\star_{jl} + \hat{W}_{ik}\hat{W}^\star_{jl} \tag{5.49}$$

It is shown in the Appendix H that the direct product matrix appearing in (5.48) is invertible in the sense

$$[(\hat{V}^\star \otimes \hat{V} + \hat{W}^\star \otimes \hat{W})^{-1}]_{mn,ij}[(\hat{V}^\star \otimes \hat{V} + \hat{W}^\star \otimes \hat{W})]_{ij,kl} = \delta_{mk}\delta_{nl} \tag{5.50}$$

An explicit expression for the inverse is

$$[(\hat{V}^\star \otimes \hat{V} + \hat{W}^\star \otimes \hat{W})^{-1}]_{kl,rs} = \sum_{n=0}^{\infty}(-1)^n[\hat{V}^\dagger(\hat{Q}^\dagger)^n]_{kr}[\hat{V}^T(\hat{Q}^T)^n]_{ls} \tag{5.51}$$

where we have defined the unitary matrix $\hat{Q}$

$$\hat{Q} \equiv VW^\dagger \tag{5.52}$$

We can now invert (5.48) to write

$$\hat{s}^2 = 2\hat{V}^\dagger\left[\sum_{n=0}^{\infty}(-1)^n(\hat{Q}^\dagger)^n\hat{R}^2\hat{Q}^n\right]\hat{V} \tag{5.53}$$

In Appendix H we show that the matrix which appears in the square bracket in (5.53) is positive semi-definite, so that we can take the square root of this equation. Substituting this in (5.47) and using the definition of $\hat{Q}$ in (5.52) we finally get

$$\hat{Z} = (\mathfrak{L}_{\hat{Q}}\hat{R})\hat{Q} \tag{5.54}$$

where we have defined the hermitian matrix $\mathfrak{L}_{\hat{V}}\hat{M}$,

$$\mathfrak{L}_{\hat{V}}\hat{M} \equiv \sqrt{2}\left[\sum_{n=0}^{\infty}(-1)^n(\hat{V}^\dagger)^n\hat{M}^2\hat{V}^n\right]^{1/2} \tag{5.55}$$

where $\hat{V}$ is unitary and $\hat{M}$ is hermitian. This satisfies the equation

$$\hat{V}^\dagger(\mathfrak{L}_{\hat{V}}\hat{M})^2\hat{V} + (\mathfrak{L}_{\hat{V}}\hat{M})^2 = 2\hat{M}^2 \tag{5.56}$$

The matrices $\hat{X}^1, \hat{X}^2$ can be then expressed as

$$\begin{aligned}\hat{X}^1 &= \frac{1}{2}\left[(\mathfrak{L}_{\hat{Q}}\hat{R})\hat{Q} + \hat{Q}^\dagger(\mathfrak{L}_{\hat{Q}}\hat{R})\right] \\ \hat{X}^2 &= \frac{1}{2i}\left[(\mathfrak{L}_{\hat{Q}}\hat{R})\hat{Q} - \hat{Q}^\dagger(\mathfrak{L}_{\hat{Q}}\hat{R})\right]\end{aligned} \tag{5.57}$$

This is the matrix analog of a polar decomposition of cartesian coordinates in two dimensions $x^1 = r\cos\phi, x^2 = r\sin\phi$. For matrices we have the correspondence

$$re^{i\phi} \to (\mathfrak{L}_{\hat{Q}}\hat{R})\hat{Q} \tag{5.58}$$

To construct the relevant subalgebra of operators we then need to use the projector (5.25) with $f(X^I) = \hat{R}^2$, replace $\hat{X}^I, I = 1, 2$ using (5.57) by their projected versions (5.28) and express the $\hat{X}^I$ in terms of $\hat{Q}$ and $\hat{R}$ using (5.57).

An appropriate gauge-fixed version can be obtained by diagonalizing the matrix $\hat{R}$,

$$\hat{R} \to \mathrm{diag}[\hat{r}_1, \hat{r}_2, \cdots \hat{r}_N] \tag{5.59}$$

We can then proceed to work in a Hilbert space basis which are eigenstates of $\hat{r}_i$ and the $\hat{Q}_{ij}$ with eigenvalues r_i, Q_{ij}. The measure of integration then becomes

$$[dX^1 dX^2] = \mathbb{J}(r_i, Q_{ij})\prod_i dr_i \prod_{ij}[dQ_{ij}] \tag{5.60}$$

The jacobian $\mathbb{J}(r_i, Q_{ij})$ can be obtained in principle by using the explicit expressions (5.57). However this is rather complicated, and we have not been able to obtain compact expressions for this. To proceed further, it will be convenient to write the unitary matrix Q in terms of a unitary matrix U and a set of angles ϕ_i

$$Q = Ue^{i\Phi}U^\dagger, \qquad \Phi = \mathrm{diag}(\phi_1, \phi_2, \cdots \phi_N) \tag{5.61}$$

Defining

$$dS \equiv U^\dagger dU \tag{5.62}$$

the line element then becomes

$$\mathrm{Tr}(dQdQ^\dagger) = \sum_i d\phi_i^2 + 8\sum_{i<j}\sin^2(\frac{\phi_i - \phi_j}{2})dS_{ij}dS^\star_{ij} \tag{5.63}$$

which leads to the expression

$$[dX^1 dX^2] = \mathbb{J}(r_i, \phi_i, S_{ij}) \prod_i dr_i \prod_i d\phi_i \prod_{i<j} [4\sin^2(\frac{\phi_i - \phi_j}{2}) dS_{ij} dS^\star_{ij}] \tag{5.64}$$

As in the case of simple linear constraints the projector leads to restriction of the integration range of r_i.

The above construction is inspired by the work [284, 285] where the complex matrix $\hat{Z}$ was written as $\hat{Z} = \tilde{R}\tilde{U}$ where $\tilde{R}$ is a hermitian matrix operator and $\tilde{U}$ is a unitary operator. However in this decomposition $\tilde{R}^2 = (\hat{X}^1)^2 + (\hat{X}^2)^2 + i[\hat{X}^1, \hat{X}^2]$ rather than (5.44).

Multiple Matrices

The above polar decomposition can be extended to an arbitary number of matrices $\hat{X}^I$. To illustrate the procedure let us first consider the case of three matrices $\hat{X}^1, \hat{X}^2, \hat{X}^3$. The idea is to mimick the procedure to obtain spherical polar coordinates (r, θ, ϕ) from usual cartesian coordinates (x^1, x^2, x^3),

$$x^1 = r\cos\phi_1 \cos\phi_2, \quad x^2 = r\cos\phi_1 \sin\phi_2, \quad x^3 = r\sin\phi_1 \tag{5.65}$$

We want to make a change of variables from hermitian matrices $\hat{X}^I, I = 1, 2, 3$ to a hermitian matrix $\hat{R}$ and two unitary matrices $\hat{Q}_1, \hat{Q}_2$. Here the matrix $\hat{Q}_1$ generalizes $e^{i\theta}$, while $\hat{Q}_2$ generalizes $e^{i\phi}$. From (5.58) the necessary replacements are

$$\begin{aligned} re^{i\phi_1} &\rightarrow (\mathfrak{L}_{\hat{Q}_1}\hat{R})\hat{Q}_1 \\ r\cos\phi_1 e^{i\phi_2} &\rightarrow \frac{1}{2}\left[\mathfrak{L}_{\hat{Q}_2}\left((\mathfrak{L}_{\hat{Q}_1}\hat{R})\hat{Q}_1 + \hat{Q}_1^\dagger(\mathfrak{L}_{\hat{Q}_1}\hat{R})\right)\right]\hat{Q}_2 \end{aligned} \tag{5.66}$$

This leads to the final expressions

$$\begin{aligned} \hat{X}^1 =& \frac{1}{4}\left[\mathfrak{L}_{\hat{Q}_2}\left((\mathfrak{L}_{\hat{Q}_1}\hat{R})\hat{Q}_1 + \hat{Q}_1^\dagger(\mathfrak{L}_{\hat{Q}_1}\hat{R})\right)\right]\hat{Q}_2 + \frac{1}{4}Q_2^\dagger\left[\mathfrak{L}_{\hat{Q}_2}\left((\mathfrak{L}_{\hat{Q}_1}\hat{R})\hat{Q}_1 + \hat{Q}_1^\dagger(\mathfrak{L}_{\hat{Q}_1}\hat{R})\right)\right] \\ \hat{X}^2 =& \frac{1}{4i}\left[\mathfrak{L}_{\hat{Q}_2}\left((\mathfrak{L}_{\hat{Q}_1}\hat{R})\hat{Q}_1 + \hat{Q}_1^\dagger(\mathfrak{L}_{\hat{Q}_1}\hat{R})\right)\right]\hat{Q}_2 - \frac{1}{4i}Q_2^\dagger\left[\mathfrak{L}_{\hat{Q}_2}\left((\mathfrak{L}_{\hat{Q}_1}\hat{R})\hat{Q}_1 + \hat{Q}_1^\dagger(\mathfrak{L}_{\hat{Q}_1}\hat{R})\right)\right] \\ \hat{X}^3 =& \frac{1}{2i}\left((\mathfrak{L}_{\hat{Q}_1}\hat{R})\hat{Q}_1 - \hat{Q}_1^\dagger(\mathfrak{L}_{\hat{Q}_1}\hat{R})\right) \end{aligned} \tag{5.67}$$

Using (5.56) repeatedly it is easy to see that

$$(\hat{X}^1)^2 + (\hat{X}^2)^2 + (\hat{X}^3)^2 = \hat{R}^2 \tag{5.68}$$

However the domain of the unitary matrices need to be restricted. This is because in (5.65) one has $-\pi/2 < \phi_1 < \pi/2$ while $-\pi < \phi_2 < \pi$. To obtain the corresponding restriction on the domain of the unitary matrices Q_1, Q_2, we resort to the decomposition in (5.61) for each of these matrices.

$$Q_A = U_A e^{i\Phi_A} U_A^\dagger, \qquad \Phi_A = \text{diag}[(\phi_A)_1, \cdots (\phi_A)_N] \qquad A = 1, 2 \tag{5.69}$$

It is shown in the Appendix H that the requirement that the eigenvalues of $X^1 \cdots X^3$ should cover $\mathbb{R}^3$ once is equivalent to the requirement that

$$-\pi/2 < (\phi_1)_i < \pi/2 \qquad -\pi < (\phi_2)_i < \pi \tag{5.70}$$

The measure of integration is now

$$\begin{aligned}&[dX^1 dX^2 dX^3] \\ =&\mathbb{J}(r_i, (\phi_A)_i, (S_A)_{ij}) \prod_i dr_i \prod_{A=1}^{2} \left[\prod_i d(\phi_A)_i \prod_{i<j} [4 \sin^2(\frac{(\phi_A)_i - (\phi_A)_j}{2}) d(S_A)_{ij} d(S_A^\star)_{ij}] \right]\end{aligned} \tag{5.71}$$

where we have defined, in analogy with (5.62)

$$dS_A \equiv U_A^\dagger dU_A \tag{5.72}$$

It is now clear that this construction generalizes to arbitrary number of matrices $\hat{X}^I, I = 1 \cdots D$. Once again we start with the polar coordinats of $\mathbb{R}^D$ and generalize to matrix polar decompositions which generalize (5.66). Now we have a single hermitian matrix $\hat{R}$ and $(D-1)$ unitary matrices $Q_A, A = 1, \cdots (D-1)$. Once each of the Q_A's are decomposed as in (5.69) we have the domains

$$\begin{aligned} -\pi/2 &< (\phi_A)_i < \pi/2 \qquad A = 1 \cdots D-2 \\ -\pi &< (\phi_{(D-1)})_i < \pi \end{aligned} \tag{5.73}$$

The integration measure is as in (5.71) with $A = 1 \cdots (D-1)$.

As discussed below we would like to identify the entanglement entropy associated with a constraint which restricts the eigenvalues r_i to be in some range, e.g. $r_i > a$ in the dual supergravity background, at least for sufficiently large values of a.

5.2.4 Dp Branes

The above considerations generalize for Dp branes for $p < 3$. Now the matrices are scalar fields $X^I(\xi)$ and gauge fields $A_\mu(\xi)$. The target space restrictions are now on entire functions. The projector can be written in terms of a functional integral

$$\hat{P}_A = \int \mathcal{D}x(\xi) \prod_\xi \delta(x(\xi) - F[\hat{X}^I(\xi)]) \tag{5.74}$$

where the functional $F[\hat{X}^I(\xi)]$ needs to be chosen appropriately. For example, for a "planar" constraint we have $F[X^I(\xi)] = \hat{X}^1(\xi)$. Once again one can choose a gauge which is tailored to the constraint, e.g. for the planar constraint we can pick a gauge where $\hat{X}^1(\xi)$ is diagonal in matrix space. The discussion above can be now repeated and it follows that in this gauge one recovers the results of [21].

5.3 Target Space Entanglement as Bulk Entanglement

Some further remarks are called for at this stage. The purpose of our investigation is to try and obtain a precise version of bulk entanglement by mapping a bulk region to the target space in the boundary theory. Such an investigation is of course closely tied to understanding how approximate bulk locality arises in the boundary theory. In section 5.2 we showed how a sub-algebra of observables can be associated with the corresponding target space constraint. In this subsection we will discuss in what sense this subalgebra can probe supergravity fields in the region $\mathcal{R}$.

Our main reasoning comes from the bulk meaning of the Coulomb branch of the gauge theory. Let us start with the system being in the vacuum. For this case the map we are using between the bulk and target space is in agreement with what is well known about the system in the moduli space approximation. A single $D0$ brane moving in the supergravity bulk dual to the D0 brane ground state experiences a velocity dependent potential which depends on its bulk location.This may be calculated by considering the DBI + Chern Simons action in the non-trivial background of a large number of D0 branes (5.80). This calculation is summarized in Appendix I. For small velocities, the coefficient of v^2 is a constant, the next term goes like v^4/r^7, where v is its velocity and r the distance from the origin. Exactly the same potential follows from the gauge theory if the D brane location $(x^1, \cdots x^9)$ is mapped to a point in the Coulomb branch with one non-zero eigenvalue for the matrices $X^1, \cdots X^9$. For a D0 brane displaced along the x^1 direction and lying at x_0^1 the matrix X^1 has one non-zero eigenvalue,

$$X^1 = \begin{pmatrix} \mathbf{0}_{(N-1)\times(N-1)} & 0_{1\times(N-1)} \\ 0_{(N-1)\times 1} & x_0^1 = r + vt \end{pmatrix} \tag{5.75}$$

corresponding to $SU(N) \to SU(N-1) \times U(1)$. This represents stripping off a single D0 brane from a bunch of $N-1$ D0 branes which form a bound state. Non-renormalization theorems ensure the agreement, once this identification is made between the bulk and moduli space, see e.g., [234–236] and references therein.

At next order a two loop calculation in D0 brane quantum mechanics yields a term which behaves as v^6/r^{14}. This term can be also reproduced from the DBI+CS action as discussed in Appendix I [14]

We can think of the calculations in the gauge theory as a computation of the effective action for appropriate gauge invariant operators. In the example above, eq.(5.75) we calculate the effective action for the operators,

$$Tr(X^1), Tr(X^1)^2, \cdots Tr(X^1)^{N-1} \tag{5.76}$$

[14] A bulk calculation can also be done in M theory with a compact null direction where v is the relative velocity between two eleven dimensional gravitons with momenta $N_1/(g_s l_s)$ and $N_2/g_s l_s$ in the M theory direction for $N_2 \ll N_1$. The effect of the graviton with momentum $N_1/(g_s l_s)$ is to produce an Aichelburg-Sexl metric and the other graviton is considered as a probe in this background. The Aichelburg-Sexl metric results from an infinite boost of a 11 dimensional Schwarzschild black hole. We are interested in the extremal D0 brane background in 10 dimensions, which is obtainable from 11 dimensions by infinitely boosting a 11 dimensional black string along the string direction. While this looks like a different limiting procedure, the expansion of the DBI+CS action (see Appendix I) in the latter background is exactly identical to the particle action considered in [235].

and then evaluate this effective action by setting $Tr(X^1)^p = (x_0^1)^p$. The resulting value of the effective action as a function of x_0^1 then gives the effective potential for the probe $D0$ brane.

There is, conceptually speaking, another way to arrive at the same result in the gauge theory. Consider a region $\mathcal{R}$ which includes the location of the probe brane, i.e.,

$$(x_0^1, \vec{0}) \in \mathcal{R} \tag{5.77}$$

As discussed in Section 5.2.2, given some region $\mathcal{R}$ we can define a target space constraint and an associated projector, leading to a sub-algebra of operators $\mathcal{A}_\mathcal{R}$. This algebra also consists of gauge invariant operators and we can also obtain an effective action for operators in $\mathcal{A}_R$, i.e. obtain the Legendre transformation of the generating function for operators in $\mathcal{A}_R$. In this effective action we now set $Tr((X^1)^P))^m = (x_0^1)^m$, where the projector $P = P_1$ or P_2, depending on whether we are considering version 1) or 2) of our proposal. The result, as a function of x_0^1 will then agree with the effective action for the set of operators eq.(5.76), and therefore will correctly give the potential experienced by the probe brane in the bulk, as long as eq.(5.77) is met. This is manifestly clear if we think of calculating the effective action using the background field method in the gauge where X^1 is diagonal with background value given by eq.(5.75), since we will then be doing the same calculation in the two cases.

The force on the D0 brane in the bulk in the example above can be calculated by using a DBI +CS action which is sensitive to the local values of the metric, the 10 dimensional $U(1)$ RR gauge field and the dilaton. If the state is changed from the vacuum to some other coherent state $|s>$ which leads to a different background value of the metric and other bulk fields, we expect that the force that the probe D0 brane experiences can continue to be obtained in this way and will be sensitive to the local values of these bulk fields. For concreteness consider the state $|s>$ to contain a gravity wave. Now, one way to obtain the local value of the gravitational field can be to measure how the potential for a probe brane at the location changes due to the presence of this gravity wave. This should yield the same result as other methods which may not involve a probe brane.

In the gauge theory we expect that the potential for the probe brane continues to correspond to the effective action computed for suitable values of operators, i.e. the set eq.(5.76), now in the state $|s>$ of the type we are considering, and we also expect that this effective action is correctly obtained from the effective action for operators in $\mathcal{A}_\mathcal{R}$ as in the discussion above for the vacuum state. In this way we see that one expects to be able to obtain the one point function for the graviton, and some other supergravity modes, from operators contained in $\mathcal{A}_R$.

This reasoning above is in fact at the heart of our proposal for identifying the bulk and boundary target space regions and also identifying the algebra $\mathcal{A}_\mathcal{R}$ in the manner we have done. In the sector where k branes are present in $\mathcal{R}$ we keep the $k \times k$ block M_{ab} for all matrix operators but not the complementary $(N-k)\times(N-k)$ block which correspond to branes that are not present. In version 1) of our proposal we also keep the off diagonal blocks $M_{a\alpha}, M_{\alpha,a}$. The resulting algebra of observables

allows one to describe all measurements done on branes present in $\mathcal{R}$ and this should then be sufficient to also detect low-energy supergravity excitations in $\mathcal{R}$.

It is worth noting in this context that there is additional evidence, going beyond the moduli space approximation, that the map between the bulk and target space we are using continues to work. For example, one can consider two stacks of D0 branes one at the origin and the other displaced from it and excite open strings within branes in each set. This changes the potential between the two stacks, but one still finds agreement in the bulk and in the gauge theory for the resulting two-body interactions, after appropriately identifying operators in the gauge theory with their counterpart currents in the bulk, [236]. This suggests that the algebra $\mathcal{A}_{\mathcal{R}}$, which retains the appropriate operators for all the superselection sectors where different number of branes $k = 0, 1, \cdots N$ are present in the region of interest, should suffice for describing the results of all measurements made with local supergravity operators in $\mathcal{R}$.

Our intuition based on the above reasoning, can be extended to a given *configuration* in the bound state wavefunction for N D0 branes in the gauge where the constraint function is diagonal. Consider a configuration where k of these eigenvalues are in the region of interest $\mathcal{R}$. The degrees of freedom $M_{a\alpha}, M_{\alpha a}$ correspond to excitations in the bulk going between $\mathcal{R}$ and $\mathcal{R}^c$ or vice versa. If the state $|s>$ has some supergravity modes excited with support deep inside $\mathcal{R}$, by which we mean the excitations are localised many string lengths away from the boundary of $\mathcal{R}$, then neither the $M_{\alpha\beta}$ nor the $M_{a\alpha}, M_{\alpha a}$ degrees of freedom will be excited in $|s>$. The $M_{\alpha\beta}$ degrees will not be excited because the excitations in $|s>$ are localised in $\mathcal{R}$. The $M_{a\alpha}, M_{\alpha a}$ degrees will also not be excited because they would correspond to open strings which would have to stretch across the boundary across many string lengths and would therefore be very heavy.

As a result, one might expect that the full change in expectation values of any single trace operator $\hat{O}$ made out of a string of X^I, Π_J's schematically depicted in eq.(5.27) will be obtained to good approximation by the corresponding operator obtained after projection, $\hat{O}^P$, eq.(5.31), eq.(5.36) . Notice that at this level of admittedly imprecise arguments we cannot distinguish between version 1) and 2) of our proposal. Both contain the gauge invariant degrees of freedom coming from M_{ab}. In version 1) there are extra degrees of freedom coming from $M_{a\alpha}, M_{\alpha a}$ as well but as per the intuitive argument above they might not play an important role anyways.

However, there are reasons to believe that the sub-algebra we are considering will not provide all details of bulk fields as defined e.g. by the BDHM-HKLL map. In the low energy regime such a bulk field operator $\phi(r, \theta_i, t)$ is defined by

$$\phi(r, \theta_i, t) = \sum_{l_i, \omega_n} [\hat{O}_{l_i,\omega_n} f_{l_i,\omega_n}(r) Y_{l_i}(\theta_i) e^{-i\omega_n t} + cc] \tag{5.78}$$

where $\hat{O}_{l_i,\omega_n}$ are Fourier modes with frequency ω_n obtained from the time dependent operators $\hat{O}_{l_i}(t)$ (we are being schematic here, ω_n need not be discrete). Consider such a bulk operator with $(r, \theta_i) \in \mathcal{R}$. The expectation value of ϕ can be obtained if we know the expectation value of $\hat{O}_{l_i}(t)$ for all l_i and all times t. Now we can

regard $\hat{O}_{l_i}(t)$ as an operator acting on the Hilbert space of states at $t = 0$. Its expectation values can therefore be obtained, in principle, if the expectation values of all operators are known at time $t = 0$. In this way we see that the expectation value of $\phi(r, \theta_i, 0)$ in any state can be obtained once the expectation values of all operators in the corresponding state in the boundary theory are known at $t = 0$. One such bulk operator is the metric itself, for which the corresponding gauge theory operator is the energy momentum tensor.

Consider now a region $\mathcal{R}$ which is a small annular region near the boundary,

$$r_B^2 - \delta < r^2 < r_B^2, \tag{5.79}$$

where r_B is the boundary value of the radial variable $r^2 = \sum_i (x^i)^2$, and δ is small. It has been argued in [248], [249], that measurements carried out by observers in this region will allow detailed information about the state in the bulk to be obtained. It is crucial in these arguments that the observers close to the boundary have access to the full Hamiltonian of the system. In fact, having access to the Hamiltonian alone enables observers in $\mathcal{R}$ to reconstruct the full density matrix of the vacuum, $|0><0|$. As a result any algebra, which includes all operators corresponding to measurements bulk observers in the region eq.(5.79) can make, in particular which includes the Hamiltonian, would have a vanishing entanglement entropy for the vacuum state[15]. The subalgebra we are associating with the region $\mathcal{R}$ are the projected versions of the gauge theory operators, $\hat{\mathcal{O}}_{l_i \omega_n}$, which appear in (5.78). Thus, the bulk operators defined in eq.(5.78), with the restriction that $(r, \theta_i) \in \mathcal{R}$, are not contained in this subalgebra. In particular the Hamiltonian is not an element of this subalgebra, only its projected version is. We expect that this imposes significant restrictions on the amount of information which can be obtained for the bulk operators. In this sense our sub-algebra would only capture the notion of a local bulk region in an approximate sense. A more detailed investigation of how significant these restrictions are is left for the future.

Clearly, one would like a deeper understanding of the various issues discussed in this section. In particular, one would like a better understanding of how much information about the bulk region of information can actually be obtained from the sub-algebras we propose, and also whether there are refinements to our basic proposal, including an improved map between the constraint in the bulk eq.(5.18) and the corresponding one in the boundary eq.(5.24), that are needed. Since the issues at had are closely tied to how approximate bulk locality arises, as was mentioned above at the outset, it is unlikely though that we can make much progress through analytic methods alone . Numerical calculations hold considerable promise in this regard. Roughly speaking one wants to show that the change in the wave function which correspond to changes in some bulk region $\mathcal{R}$, arises mainly in the target space region associated with $\mathcal{R}$ and not its complement. This should also then shed light on which operators would be needed to determine this change in the boundary theory and whether a sub-algebra along the lines proposed here would suffice.

[15] We are grateful to Suvrat Raju for explaining this point to us.

5.4 Target Space Entanglement and Bekenstein Bound

In the 't Hooft limit the usual 't Hooft limit $g_s \to 0, N \to \infty$ with $(g_s N)$ held fixed, the bound state of N Dp branes is dual to a ten dimensional geometry. Our proposal implies that target space constraints correspond to regions in the transverse space to these Dp branes in this geometry and the target space entanglement entropy defined above provides a notion of a bulk entanglement entropy associated with this region. In [21] it was conjectured that for Dp brane matrix field theories, the target space entanglement entropy saturates the Bekenstein bound for this entangling surface. In this section we recapitulate the result for D0 branes.

We will be mostly interested in the bound state of N D0 branes which are slightly heated up to a temperature T. This is dual to the near-extremal black D0 brane geometry in supergravity. The string frame metric, dilaton and 1-form gauge fields are

$$\begin{aligned} ds^2_{string} &= -H_0(r)^{-1/2} g(r) dt^2 + H_0(r)^{1/2} [\frac{dr^2}{g(r)} + r^2 d\Omega_8^2] \\ e^{\phi} &= g_s H_0(r)^{3/4} \qquad\qquad A_0 = -\frac{1}{2}(H_0^{-1} - 1) \end{aligned} \tag{5.80}$$

where

$$g(r) = 1 - \left(\frac{r_H}{r}\right)^7 \qquad H_0(r) = \frac{R^7}{r^7}, \qquad r^2 = x_1^2 + \cdots x_9^2. \tag{5.81}$$

The horizon is at $r = r_H$. The Hawking temperature for this solution and the length scale R are given by

$$T = \frac{7}{4\pi R}\left(\frac{r_H}{R}\right)^{5/2} \qquad R^7 = 60\pi^3 l_s^7 (g_s N). \tag{5.82}$$

The supergravity solution above is valid in the regime

$$g_s^{\frac{1}{3}} N^{1/7} < r < (g_s N)^{1/3} l_s \qquad T\frac{l_s}{(g_s N)^{1/3}} \ll 1 \tag{5.83}$$

In D0 brane quantum mechanics consider the simple linear constraint, e.g. $f(X^I) = X^1 - a_0$. According to the proposal of [21] the bulk region of interest is simply $x^1 > a$. The relationship between the dimensionless a_0 and the dimensionful a can be read off from the rescaling (5.40)

$$a = a_0 (g_s N)^{\frac{1}{3}} l_s \tag{5.84}$$

This reflects the fact that in this holographic correspondence the transverse distance becomes the energy scale of the D0 brane quantum mechanics which is $\Lambda = (g_s N)^{1/3}/l_s$. Likewise the temperature appearing in (5.82) is related to a dimensionless temperature T_0 by $T = T_0 \Lambda$.

In [21] it was conjectured that this target space entanglement saturates the Bekenstein bound

$$S(a, T) = \frac{A_a(T)}{4G_N} \tag{5.85}$$

where A_a is the *Einstein Frame* area of the entangling surface $x^1 = a$ in the geometry (5.80) and $G_N = 8\pi^6 g_s^2 l_s^8$ is the ten dimensional Newton constant. The quantity $S(a,T)$ is actually divergent, the divergence coming from the large r region. The large r region is, however, beyond the regime of validity of supergravity: thus one may consider using a cutoff at $r = r_0$. However the difference $S(a,T) - S(a,T')$ is finite,

$$S(a,T) - S(a,T') = B_0 \; N^2 a_0^{-5/2} \left[(T_0)^{14/5} - (T_0')^{14/5} \right] \tag{5.86}$$

where B_0 is a number whose value is given in equation (29) of [21].

Note that the expression (5.86) the dimensionless quantities which characterize the state and the entangling region are those which are quantities which would appear in D0 brane quantum mechanics. The only other number which appears is N : the answer is proportional to N^2. This is what one expects if our proposal is correct. In particular all factors of g_s nicely cancel. The powers of T_0 and d_0 which appear in (5.86) does not follow from general considerations of target space entanglement. If a numerical calculation yields these powers we will have a very non-trivial evidence for our proposal.

Let us make one comment before ending this section. We have emphasised above that the discussion in this paper can be applied for constraints taking the general form, eq.(5.18). Instead of the linear constraint considered above suppose we take

$$f(x^1) = \sum_{i=1}^{9} (x^i)^2 > r_0^2 \tag{5.87}$$

where r_0 is some radius. In this case the Beckenstein- Hawking entropy which is given by

$$S = \Omega_8 \frac{R^{7/2} r_0^{9/2}}{4 G_N} \tag{5.88}$$

is a function of r_0 but is independent of the temperature T. As per our proposal we would like to equate this result with the entanglement entropy associated with the target space constraint

$$\sum_{I=1}^{9} (\hat{X}^I)^2 > r_0^2. \tag{5.89}$$

However it does seem rather strange then that the resulting entanglement entropy is independent of the temperature T. One reason could be that perhaps the map between a physical region in the bulk and the corresponding target space constraint is more complicated at finite temperature, i.e. the RHS in eq. (5.87) and eq.(5.89) are not equal but instead related by a temperature dependent function. This might also help explain why when we take $r_0 = r_H$ in eq.(5.87), we get the entanglement entropy to be the full entropy in the boundary theory and not a different value due to the additional target space constraint eq.(5.89) being present. We leave a more detailed investigation of such temperature dependent effects for the future.

5.5 Path Integral Expressions for Renyi Entropies

As discussed above, numerical calculations should be able to prove or disprove our conjecture that the target space von Neumann entropy saturates the Bekenstein bound. Recently there has been impressive advances in numerical calculations for D0 branes [259–261]. These calculations use euclidean path integrals to calculate finite temperature partition functions as well as some correlation functions. In this section we develop euclidean path integral expressions for target space Renyi entropies which can be used directly for numerical calculations. These expressions are in the gauge fixed formalism, and we will develop them for planar constraints.

Consider the D0 brane theory at some finite temperature $T = 1/\beta$. The density operator is given by $\hat{\rho}_0 = \exp[-\beta H]$ where the hamiltonian H is given by (5.41). As in the previous sections, we will fix the $A_0 = 0$ gauge, fix the time independent gauge transformations by diagonalizing one of the matrices X^1, and impose the remaining Weyl and $U(1)^N$ symmetries by explicitly summing over the corresponding transformations. The basis states are given by (2.40). In the following we will also ignore the fermions.

In the absence of any symmetrization the matrix elements of $\hat{\rho}$ can be written as a path integral as follows

$$\langle \lambda_i, X^L_{ij} | \hat{\rho}_0 | \lambda'_i, (X^L_{ij})' \rangle = \int_{\lambda_i(0)=\lambda'_i}^{\lambda_i(\beta)=\lambda_i} \mathcal{D}\lambda_i(\tau) \int_{X^L_{ij}(0)=(X^L_{ij})'}^{X^L_{ij}(\beta)=X^L_{ij}} \mathcal{D}X^L_{ij}(\tau) \exp[-S_\beta] \tag{5.90}$$

where the action S_β is the euclidean action

$$S = \frac{(g_s N)^{1/3} N}{2 l_s} \int_0^\beta d\tau \ \mathrm{Tr} \left[\sum_{I=1}^{9} (\partial_\tau X^I)^2 + \sum_{I \neq J=1}^{9} [\tilde{X}^I, \tilde{X}^J]^2 \right] \tag{5.91}$$

Weyl and $U(1)^N$ symmetries are then imposed by explicitly summing over the transformations, leading to braided boundary conditions. However, since the action is symmetric under these transformations, we need to sum over transforms of the boundary conditions at one of the ends of the euclidean time interval. We therefore have

$$\begin{aligned} & {}_W\langle \lambda_i, X^L_{ij} | \hat{\rho}_0 | \lambda'_i, (X^L_{ij})' \rangle_W = \rho_{tot}(\lambda_i, X^L_{ij}; \lambda'_i, (X^L_{ij})') \\ = \quad & \frac{1}{N!} \int \prod_{i=1}^{N} \frac{d\theta_i}{2\pi} \sum_{\sigma \in S(N)} (-)^\sigma \int_{\lambda_i(0)=\lambda'_i}^{\lambda_i(\beta)=\lambda_{\sigma(i)}} \mathcal{D}\lambda_i(\tau) \int_{X^L_{ij}(0)=(X^L_{ij})'}^{X^L_{ij}(\beta)=(X^L_{ij})^W} \mathcal{D}X^L_{ij}(\tau) \exp[-S_\beta] \end{aligned} \tag{5.92}$$

where we have introduced the notation

$$(X^L_{ij})^W \equiv X^L_{\sigma(i)\sigma(j)} e^{i(\theta_{\sigma(i)} - \theta_{\sigma(j)})} \tag{5.93}$$

which we will use in the following equations as well.

The construction for $N = 2$ and with two matrices X^1, X^2 is illustrated in Figure 5.1. Note that each term in the path integral is *not* a product of path integrals over

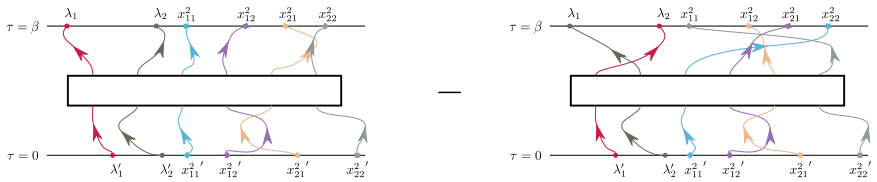

Figure 5.1: Path Integral Representation for the thermal density matrix for a model of two 2×2 matrices X^1 and X^2 in the gauge where X^1 is diagonal with eigenvalues λ_1 and λ_2. The blobs represent arbitrary number of interactions between the paths.

λ_i and X^L_{ij} since the interaction term in the action couple them. These interactions are symbolically drawn as rectangular boxes to emphasize this. The figure is meant to illustrate the boundary conditions.

To obtain the reduced density matrix in some sector $(k, N-k)$ one needs to integrate over the appropriate set of boundary values. Consider some interval A on the real line. As in the previous section we will split the matrix indices into two sets, $a, b = 1 \cdots k$ and $\alpha, \beta = k+1 \cdots N$ where the eigenvalues λ_a lie in A while the remaining λ_α lie in the complement $\bar{A}$. The boundary values of the matrix elements of X^L with $L = 2 \cdots 9$ are not constrained in any fashion. Then the expressions for the two proposals are given in (5.13) and (5.14).

In terms of the paths in the path integral this means the following. Along a given path parametrized by $0 < \tau < \beta$, the $\lambda_a(\tau)$ must begin and end in distinct points in the interval A. The eigenvalues $\lambda_\alpha(\tau)$ must begin and end at the *same point* in the complement $\bar{A}$, and there is an integral over this point. It is important to note that apart from these restrictions the paths are free to wander around anywhere in the λ space at intermediate times.

In proposal (1), the boundary values of $X^L_{\alpha\beta}, X^L_{a\alpha}, X^L_{\alpha a}$ are the same at $\tau = 0$ and $\tau = \beta$ and are integrated over, while the boundary values of X^L_{ab} are different. This leads to the following expression for the reduced density matrix:

$$\begin{aligned}
&\tilde{\rho}^{(1)}_{k,N-k}(\lambda_a, X^L_{ab}; \lambda'_a, (X^L_{ab})') \\
=&\frac{1}{N!}\binom{N}{k} \\
&\times \int_{\bar{A}} d\lambda_\alpha \int dX^L_{a\alpha} dX^L_{\alpha a} dX^L_{\alpha\gamma} \int \prod_{i=1}^{N} \frac{d\theta_i}{2\pi} \sum_{\sigma \in S(N)} (-)^\sigma \int_{\mathcal{A}_1} \mathcal{D}\lambda_i(\tau) \int_{\mathcal{B}_1} \mathcal{D}X^L_{ij}(\tau) \exp[-S_\beta]
\end{aligned} \tag{5.94}$$

where the boundary conditions are denoted by

$$\mathcal{A}_1 = \begin{pmatrix} \lambda_a(0) = \lambda'_a, & \lambda_{\sigma(a)}(\beta) = \lambda_a \\ \lambda_\alpha(0) = \lambda_\alpha, & \lambda_{\sigma(\alpha)}(\beta) = \lambda_\alpha \end{pmatrix} \tag{5.95}$$

$$\mathcal{B}_1 =$$
$$\begin{pmatrix} X^L_{ab}(0) = (X^L_{ab})', & X^L_{a\alpha}(0) = X^L_{a\alpha}, & X^L_{\alpha a}(0) = X^L_{\alpha a}, & X^L_{\alpha\gamma}(0) = X^L_{\alpha\gamma} \\ (X^L_{ab})^W(\beta) = X^L_{ab}, & (X^L_{a\alpha})^W(\beta) = X^L_{a\alpha}, & (X^L_{\alpha a})^W(\beta) = X^L_{\alpha a}, & (X^L_{\alpha\gamma})^W(\beta) = X^L_{\alpha\gamma} \end{pmatrix} \tag{5.96}$$

The Figures 5.2-5.4 show the paths for $N = 2$ in the various sectors for our first proposal, drawn as paths on a cylinder which is cut across the region A. In each sector there are two terms. In these figures we have represented only the boundary values of the eigenvalues of one of the matrices X^1. The other matrix elements are braided in the manner indicated in Figure 5.1. As in Figure 5.1 these diagrams are illustrative of the boundary conditions: the rectangular boxes represent interactions between the variables along the paths.

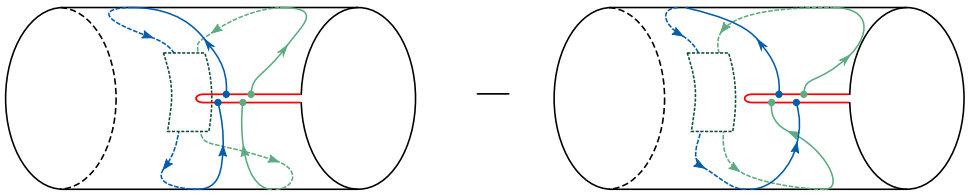

$(2, 0)$

Figure 5.2: Path Integral Representation for the reduced density matrix in the $(2, 0)$ sector for a model of two 2×2 matrices X^1 and X^2 in the gauge where X^1 is diagonal. The red cut represents the region of interest A. We have shown the end-point values only for the eigenvalues of X^1.

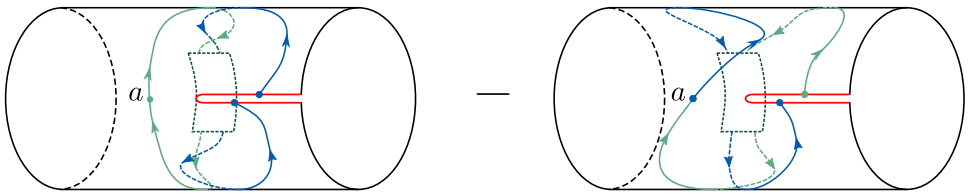

$(1, 1)$

Figure 5.3: Path Integral Representation for the reduced density matrix in the $(1, 1)$ sector for a model of two 2×2 matrices X^1 and X^2 in the gauge where X^1 is diagonal. The red cut represents the region of interest A. We have shown the end-point values only for the eigenvalues of X^1.

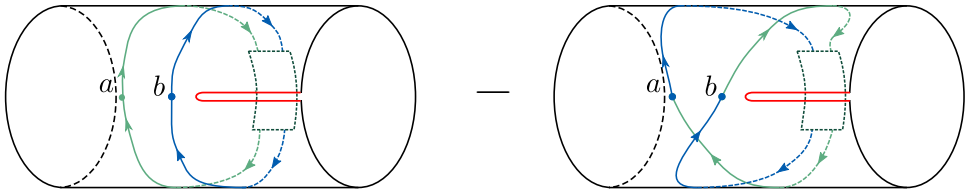

$(0,2)$

Figure 5.4: Path Integral Representation for the reduced density matrix in the $(0,2)$ sector for a model of two 2×2 matrices X^1 and X^2 in the gauge where X^1 is diagonal. The red cut represents the region of interest A. There are no specified boundary values.

In proposal (2), only the boundary values of $X^L_{\alpha\beta}$ are same and integrated over.

$$\begin{aligned}&\tilde{\rho}^{(2)}_{k,N-k}(\lambda_a, X^L_{ab}, X^L_{a\alpha}, X^L_{\alpha a}; \lambda'_a, (X^L_{ab})', (X^L_{a\alpha})', (X^L_{\alpha a})')\\ &= \frac{1}{N!}\binom{N}{k}\int_{\bar{A}} d\lambda_\alpha \int dX^L_{\alpha\gamma}\int \prod_{i=1}^{N}\frac{d\theta_i}{2\pi}\sum_{\sigma\in S(N)}(-)^\sigma \int_{\mathcal{A}}\mathcal{D}\lambda_i(\tau)\int_{\mathcal{B}_2}\mathcal{D}X^L_{ij}(\tau)\,\exp[-S_\beta]\end{aligned} \tag{5.97}$$

The boundary conditions for the λ_i remain the same as in (5.95) , while those for the X^L_{ij} are denoted by

$$\mathcal{B}_2 = \begin{pmatrix} X^L_{ab}(0) = (X^L_{ab})', & X^L_{a\alpha}(0) = (X^L)'_{a\alpha}, & (X^L)_{\alpha a}(0) = (X^L)'_{\alpha a}, & X^L_{\alpha\gamma}(0) = X^L_{\alpha\gamma} \\ (X^L_{ab})^W(\beta) = X^L_{ab}, & (X^L_{a\alpha})^W(\beta) = X^L_{a\alpha}, & (X^L_{\alpha a})^W(\beta) = X^L_{\alpha a}, & (X^L_{\alpha\gamma})^W(\beta) = X^L_{\alpha\gamma}\end{pmatrix} \tag{5.98}$$

The figures for paths for the second proposal can be drawn as in the earlier figures.

It is now straightforward to compute $\mathrm{Tr}\tilde{\rho}^n_{k,N-k}$ by taking powers of these expressions and tracing. For example, $\mathrm{Tr}\tilde{\rho}^2_{k,N-k}$ for Proposal (1) is

$$\begin{aligned}&\mathrm{tr}(\tilde{\rho}^{(1)}_{k,N-k})^2\\ &= \left[\frac{1}{N!}\binom{N}{k}\right]^2\int_A d\lambda_a d\lambda'_a\int dX^L_{ab}d(X^L_{ab})'\\ &\times\int_{\bar{A}} d\lambda_\alpha\int dX^L_{a\alpha}dX^L_{\alpha a}dX^L_{\alpha\beta}\int_{\bar{A}} d\lambda'_\alpha\int d(X^L_{a\alpha})'d(X^L_{\alpha a})'d(X^L_{\alpha\beta})'\\ &\times\int\prod_{i=1}^{N}d\theta_i\int\prod_{j=1}^{N}d\theta'_j\\ &\sum_{\sigma,\sigma'\in S(N)}(-)^{\sigma+\sigma'}\int_{\mathcal{C}_1}\mathcal{D}\lambda_i(\tau)\int_{\mathcal{C}_2}\mathcal{D}X^L_{ij}(\tau)\,\exp[-S_\beta]\int_{\mathcal{C}_3}\mathcal{D}\lambda_i(\tau)\int_{\mathcal{C}_4}\mathcal{D}X^L_{ij}(\tau)\,\exp[-S_\beta]\end{aligned} \tag{5.99}$$

where the periodicity conditions are

$$\mathcal{C}_1 = \begin{pmatrix} \lambda_a(0) = \lambda'_a, & \lambda_\alpha(0) = \lambda_\alpha \\ \lambda_{\sigma(a)}(\beta) = \lambda_a, & \lambda_{\sigma(\alpha)}(\beta) = \lambda_\alpha \end{pmatrix} \tag{5.100}$$

$$\mathcal{C}_2 = \begin{pmatrix} X^L_{ab}(0) = (X^L_{ab})', & X^L_{a\alpha}(0) = X^L_{a\alpha}, & X^L_{\alpha a}(0) = X^L_{\alpha a}, & X^L_{\alpha\gamma}(0) = X^L_{\alpha\gamma} \\ (X^L_{ab})^W(\beta) = X^L_{ab}, & (X^L_{a\alpha})^W(\beta) = X^L_{a\alpha}, & (X^L_{\alpha a})^W(\beta) = X^L_{\alpha a}, & (X^L_{\alpha\gamma})^W(\beta) = X^L_{\alpha\gamma} \end{pmatrix} \tag{5.101}$$

$$\mathcal{C}_3 = \begin{pmatrix} \lambda_a(0) = \lambda_a, & \lambda_\alpha(0) = \lambda'_\alpha \\ \lambda_{\sigma'(a)}(\beta) = \lambda'_a, & \lambda_{\sigma'(\alpha)}(\beta) = \lambda'_\alpha \end{pmatrix} \tag{5.102}$$

$$\mathcal{C}_4 = \begin{pmatrix} X^L_{ab}(0) = X^L_{ab}, & X^L_{a\alpha}(0) = (X^L_{a\alpha})', & X^L_{\alpha a}(0) = (X^L_{\alpha a})', & X^L_{\alpha\gamma}(0) = (X^L_{\alpha\gamma})' \\ (X^L_{ab})^{W'}(\beta) = (X^L_{ab})', & (X^L_{a\alpha})^{W'}(\beta) = (X^L_{a\alpha})', & (X^L_{\alpha a})^{W'}(\beta) = (X^L_{\alpha a})', & (X^L_{\alpha\gamma})^{W'}(\beta) = (X^L_{\alpha\gamma})' \end{pmatrix} \tag{5.103}$$

where in an obvious extension of the notation of (5.93)

$$(X^L_{ij})^{W'} \equiv X^L_{\sigma'(i)\sigma'(j)} e^{i(\theta'_{\sigma'(i)} - \theta'_{\sigma'(j)})} \tag{5.104}$$

The expression is invariant if we exchange $\sigma \leftrightarrow \sigma', \theta_i \leftrightarrow \theta'_i$. The expression for $\mathrm{Tr}\tilde{\rho}^n_{k,N-k}$ in Proposal (2) can be similarly written down. The Renyi entropies S_n can be then computed using these expressions,

$$S_n = \frac{1}{n-1} \log \left[\sum_{k=0}^{N} \mathrm{Tr}_k \tilde{\rho}^n_{k,N-k} \right] \tag{5.105}$$

These path integral expressions can be directly used in numerical calculations. It is difficult to take the $\beta \to \infty$ limit to recover a zero temperature answer. However it should be possible to compare the difference of the entropies at two different temperatures with the supergravity result.

5.6 Conclusions

In this paper we have have proposed that for near -horizon Dp brane backgrounds, target space entanglement in the boundary theory provides a precise version of bulk entanglement in the gravity dual. We have described how to obtain in a gauge invariant manner a sub -algebra related to a target space constraint. A Von-Neumann entropy can be associated with this sub-algebra in the standard manner and this then gives the target space entanglement entropy. Our paper builds on [21] which dealt with linear constraints in a gauge fixed formalism and we have provided here a general gauge invariant description of the target space entanglement.

We have also provided some arguments here, based on comparisons between the potential experienced by probe branes moving in some region of the bulk $\mathcal{R}$ and the effective potential in the boundary theory evaluated in the corresponding region of moduli space, to motivate why the sub-algebra of operators $\mathcal{A}_{\mathcal{R}}$ that we identify is sufficient to describe some local bulk measurements on gravitons and other supergravity modes, in addition to D branes, carried out by observers in $\mathcal{R}$.

We should emphasise that our arguments are not *completely* precise. One reflection of this is that there are in fact two versions of our proposal, which give rise to two different sub-algebras related to a target space constraint, and we cannot distinguish between them at our current level of understanding.

One source of imprecision in our proposal could be that the map between the bulk and target space constraints, eq.(5.18) and eq.(5.24), is more complicated than we have assumed. This could happen due to operator ordering ambiguities or for excited states, including at finite temperature, where some or all of the supersymmetries are broken. The target space function $f(\hat{X}^i)$ which appears in eq.(5.24) in such situations could be more non-trivially related to its bulk counterpart in eq.(5.18), with coupling constant and temperature dependent corrections, as was also discussed in section 5.4 above. By carrying out numerical calculations analogous to those in [242] one can try to determine the effective potential and equating these results to the potential obtained in the bulk for a probe brane, one can further hope to obtain the correct target space constraint corresponding to a bulk region. Our proposal would then be that the sub-algebra for this possibly modified target space constraint is the correct one to use for obtaining the bulk entanglement. Hopefully, further developments, especially in numerical methods will lead to concrete checks for our ideas and will allow them to be sharpened further. In fact, connecting with some of these recent developments has been one of our major motivations.

Our proposal for associating a target space constraint with a bulk region is most straightforward when the bulk region is bounded by a surface with a constant value of one of the cartesian coordinates. This is because the fields in the Dp brane field theory as written in (5.2) directly relate to cartesian coordinates in the geometry. For many physical questions, however, one would like to consider subregions which are bounded by constant values of the radial coordinate. A natural guess for the corresponding target space constraint is to require that the eigenvalues of the hermitian operator $\sum (X^I)^2$ are restricted to larger than some value. With this in mind, we have discussed in section 5.2.3 in some detail how to implement a constraint in the radial direction in the bulk. We have also derived path integral expressions for Renyi entropies in a gauge fixed description which can be directly used in numerical calculations.

There are several open questions which merit further study. As we have discussed above we expect that the sub -algebra of operators we are considering will allow one to determine the one- point function of the metric and some other supergravity fields in the vacuum and in excited coherent states. But we do not expect to be able to determine all correlators of supergravity modes in the bulk region of interest from the sub-algebra, in general. How much information can be extracted from the sub-algebra and how does this contrast with the measurements which bulk observers can do using supergravity probes restricted to the region of interest, is an important

issue which needs to be understood better. One would hope that bulk regions whose boundary is given by an RT extremal surface should correspond to rather special constraints in target space [16]. Unfortunately we do not see any evidence for this so far and leave it as an important question for further investigation. On a related note, one would think that area of extremal surfaces not of the RT type, as in D0 brane geometry [280] would also have some understanding in terms of target space entanglement entropy. Finally, for usual AdS/CFT duality there is evidence in favour of the conjecture that there is an intimate connection between entanglement in base space and emergence of a smooth AdS bulk with locality [286–288] . One would expect that in models of $AdS \times (\text{Sphere})/CFT$ there should be a similar connection between entanglement in color space and locality in the sphere factor of the bulk. Target space entanglement provides a concrete framework to study this connection. In particular in D0 brane holography there is no base space of the holographic theory: target space entanglement would entirely account for bulk locality. This deep connection is well worth understanding further as well.

[16] We are thankful to Shiraz Minwalla for emphasising this point.

Appendix A
Approximation of $\rho(\tau)^2$ in various limits

In this appendix we explicitly derive approximated $\rho(\tau)^2$ and therefore $\langle\mathcal{O}\rangle$ in various limits from the exact CCP solution (3.51) and ECP solution (3.54). In appendix A.1 we study the CCP case and in appendix A.2 we study the ECP case.

A.1 In CCP

Slow quench ($\omega_0\delta t \gg 1$) We consider the behavior at $\tau = 0$, in which case (3.51) can be simplified into

$$f(\tau=0) = \frac{1}{\sqrt{2\omega_0}} \frac{2^{i\omega_0\delta t}}{E_{1/2}\tilde{E}'_{3/2} - E'_{1/2}\tilde{E}_{3/2}} \tilde{E}'_{3/2}. \tag{A.1}$$

Notice that in (3.52), $\mathrm{Re}a = \mathrm{Re}b = \mathrm{Re}\alpha \in [1/4, 1/2]$, therefore we can utilize three identities of the Gamma function

$$\Gamma(z)\Gamma(1-z) = \pi \mathrm{csc}\pi z, 0 < \mathrm{Re}z < 1, \tag{A.2}$$

and

$$\begin{aligned} \Gamma(1+iy)\Gamma(1-iy) = |\Gamma(1+iy)|^2 = \frac{\pi y}{\mathrm{sinh}\pi y}, \\ \Gamma(1/2+iy)\Gamma(1/2-iy) = |\Gamma(1/2+iy)|^2 = \frac{\pi}{\mathrm{cosh}\pi y}, \end{aligned} \tag{A.3}$$

and simplify the denominator of (A.1) into

$$\begin{aligned} & E_{1/2}\tilde{E}'_{3/2} - E'_{1/2}\tilde{E}_{3/2} \\ &= \Gamma(1/2)\Gamma(3/2)|\Gamma(i\omega_0\delta t)|^2 \left(\frac{1}{\Gamma(a+1/2)\Gamma(1/2-a)\Gamma(b)\Gamma(1-b)} - (a \leftrightarrow b) \right) \\ &= \frac{1}{2\omega_0\delta t \mathrm{sinh}\pi\omega_0\delta t} \left(\mathrm{sin}\pi(1/2-a)\mathrm{sin}(\pi b) - \mathrm{sin}\pi(1/2-b)\mathrm{sin}(\pi a) \right) \\ &= \frac{1}{2\omega_0\delta t \mathrm{sinh}\pi\omega_0\delta t} \mathrm{sin}\pi(b-a) \\ &= \frac{i}{2\omega_0\delta t}. \end{aligned} \tag{A.4}$$

On the other hand, according to the asymptotic behavior of the Gamma function

$$\Gamma(z) \sim \sqrt{2\pi} e^{-z+(z-\frac{1}{2})\log z}, z \to \infty \text{ and } |\arg z| < \pi \tag{A.5}$$

we can find $[\Gamma(z)]^2 \sim \Gamma(z+1/4)\Gamma(z-1/4)$ under the condition. Therefore, the numerator of (A.1) satisfies

$$\begin{aligned}
&|\tilde{E}'_{3/2}|^2 \\
\approx&\frac{\pi}{4}\frac{\pi}{\omega_0\delta t \sinh\pi\omega_0\delta t}\left|\frac{1}{\Gamma(1+\frac{i}{4}\sqrt{4\omega_0^2\delta t^2-1}-\frac{i}{2}\omega_0\delta t)\Gamma(1-\frac{i}{4}\sqrt{4\omega_0^2\delta t^2-1}-\frac{i}{2}\omega_0\delta t)}\right| \\
&\times\left|\frac{1}{\Gamma(1/2+\frac{i}{4}\sqrt{4\omega_0^2\delta t^2-1}-\frac{i}{2}\omega_0\delta t)\Gamma(1/2-\frac{i}{4}\sqrt{4\omega_0^2\delta t^2-1}-\frac{i}{2}\omega_0\delta t)}\right| \\
=&\frac{1}{4}\frac{1}{\omega_0\delta t\sinh\pi\omega_0\delta t}\left\{\frac{\sinh\pi(\frac{1}{2}\sqrt{4\omega_0^2\delta t^2-1}-\omega_0\delta t)}{\frac{1}{2}\sqrt{4\omega_0^2\delta t^2-1}-\omega_0\delta t}\frac{\sinh\pi(\frac{1}{2}\sqrt{4\omega_0^2\delta t^2-1}+\omega_0\delta t)}{\frac{1}{2}\sqrt{4\omega_0^2\delta t^2-1}+\omega_0\delta t}\right\}^{1/2} \\
\to&\frac{1}{2}\frac{1}{\omega_0\delta t}\left\{\frac{\pi}{4\omega_0\delta t}\right\}^{1/2}
\end{aligned} \tag{A.6}$$

As a result,

$$\rho^2(\tau=0)=2|f|^2(\tau=0)=2\frac{1}{2\omega_0}\frac{1}{\frac{1}{(2\omega_0\delta t)^2}}\frac{1}{2}\frac{1}{\omega_0\delta t}\left\{\frac{\pi}{4\omega_0\delta t}\right\}^{1/2}=\sqrt{\pi}\sqrt{\frac{\delta t}{\omega_0}} \tag{A.7}$$

and thus (3.57).

Early time in fast quench ($\omega_0\tau \ll \omega_0\delta t \ll 1$) When $\omega_0\tau \ll \omega_0\delta t \ll 1$, in (3.52) $a=b^*$, thus the Hypergeometric functions in (3.51) are real. Therefore,

$$E_c^* = E_c(a\leftrightarrow b) = E'_c, \tag{A.8}$$

and

$$\begin{aligned}
&\rho^2(\tau) \\
=&\frac{1}{\omega_0}\frac{\cosh^{4\alpha}(\tau/\delta t)}{|E_{1/2}\tilde{E}'_{3/2}-E'_{1/2}\tilde{E}_{3/2}|^2} \\
\times&\left\{|\tilde{E}'_{3/2}|^2{}_2F_1{}^2(a,b;\frac{1}{2};-\sinh^2\frac{\tau}{\delta t})+|E'_{1/2}|^2\sinh^2\frac{\tau}{\delta t}{}_2F_1{}^2(a+\frac{1}{2},b+\frac{1}{2};\frac{3}{2};-\sinh^2\frac{\tau}{\delta t})\right. \\
&\left.+\left(\tilde{E}'_{3/2}E_{1/2}+\tilde{E}_{3/2}E'_{1/2}\right)\sinh\frac{\tau}{\delta t}{}_2F_1(a,b;\frac{1}{2};-\sinh^2\frac{\tau}{\delta t}){}_2F_1(a+\frac{1}{2},b+\frac{1}{2};\frac{3}{2};-\sinh^2\frac{\tau}{\delta t})\right\}.
\end{aligned} \tag{A.9}$$

Similar to the calculation of (A.4), we can find

$$E_{1/2}\tilde{E}'_{3/2}+E'_{1/2}\tilde{E}_{3/2}=\frac{1}{2\omega_0\delta t\sinh\pi\omega_0\delta t}\sin\pi(b+a)\to\frac{1}{2}+\mathcal{O}(\omega_0^4\delta t^4), \tag{A.10}$$

since $\alpha\sim\frac{1}{2}[1-\omega_0^2\delta t^2]$ when $\omega_0\delta t\ll 1$.

On the other hand, notice that

$$\Gamma(z+\epsilon) \approx \Gamma(z) + \Gamma'(z)\epsilon + \mathcal{O}(\epsilon^2) = \Gamma(z)(1+\epsilon\psi(z)) + \mathcal{O}(\epsilon^2), \tag{A.11}$$

where $\psi(z) \equiv \Gamma'(z)/\Gamma(z)$ is Digamma function. Moreover, the Gamma function satisfies duplication formula

$$\Gamma(2z) = \frac{1}{\sqrt{2\pi}} 2^{2z-1/2}\Gamma(z)\Gamma(z+1/2). \tag{A.12}$$

Then we can find

$$\begin{aligned}
|\tilde{E}'_{3/2}|^2 \approx & \frac{\pi}{4}|\Gamma(i\omega_0\delta t)|^2 \left| \frac{1}{\Gamma(1-1/2\omega_0^2\delta t^2 - \frac{i}{2}\omega_0\delta t)\Gamma(1/2+1/2\omega_0^2\delta t^2 - \frac{i}{2}\omega_0\delta t)} \right|^2 \\
\approx & \frac{\pi}{4} \frac{|\Gamma(i\omega_0\delta t)|^2}{|\Gamma(1-\frac{i}{2}\omega_0\delta t)|^2|\Gamma(1/2-\frac{i}{2}\omega_0\delta t)|^2} \\
& \times \frac{1}{\left[1-\omega_0^2\delta t^2 \mathrm{Re}\psi(1-\frac{i}{2}\omega_0\delta t)\right]\left[1+\omega_0^2\delta t^2\mathrm{Re}\psi(1/2-\frac{i}{2}\omega_0\delta t)\right]} \\
\approx & \frac{1}{4\omega_0^2\delta t^2} \frac{1}{1-\omega_0^2\delta t^2\mathrm{Re}\psi(\frac{i}{2}\omega_0\delta t) + \omega_0^2\delta t^2\mathrm{Re}\psi(1/2+\frac{i}{2}\omega_0\delta t)}
\end{aligned} \tag{A.13}$$

We can further simplify it since

$$\psi(2z) = \frac{1}{2}\psi(z) + \frac{1}{2}\psi(z+\frac{1}{2}) + \log 2 \tag{A.14}$$

and

$$\begin{aligned}
\mathrm{Re}\psi(iy) &= 1 - \gamma - \frac{1}{1+y^2} + \sum_{n=1}^{\infty}(-1)^{n+1}[\zeta(2n+1)-1]y^{2n}, (|y|<2) \\
&\to -\gamma + y^2 + (\zeta(3)-1)y^2 = -\gamma + \zeta(3)y^2, (|y| \ll 1)
\end{aligned} \tag{A.15}$$

and obtain

$$\begin{aligned}
|\tilde{E}'_{3/2}|^2 \approx & \frac{1}{4\omega_0^2\delta t^2} \frac{1}{1+2\omega_0^2\delta t^2\left[\mathrm{Re}\psi(i\omega_0\delta t) - \mathrm{Re}\psi(\frac{i}{2}\omega_0\delta t) - \log 2\right]} \\
\approx & \frac{1}{4\omega_0^2\delta t^2}\left\{1 + 2\log 2\cdot\omega_0^2\delta t^2 + \mathcal{O}(\omega_0^4\delta t^4)\right\}.
\end{aligned} \tag{A.16}$$

Similarly, we can find

$$|E'_{1/2}|^2 \approx \frac{1}{4}\left\{1 - 2\log 2\cdot\omega_0^2\delta t^2 + \mathcal{O}(\omega_0^4\delta t^4)\right\}. \tag{A.17}$$

Inserting the coefficients back into (A.9), we keep the results to order $\omega_0^2\delta t^2$ and $\tau/\delta t$, s.t. ${}_2F_1{}^2(\tilde{a},\tilde{b};\tilde{c};-\sinh^2\frac{\tau}{\delta t})\sim 1$ for arbitrary (a,b,c). We find

$$\begin{aligned}
&\rho^2(\tau)\\
=&\frac{1}{\omega_0}\cosh^{4\alpha}(\tau/\delta t)\times\\
&\left\{\left\{1+2\log 2\cdot\omega_0^2\delta t^2\right\}{}_2F_1{}^2(a,b;\frac{1}{2};-\sinh^2\frac{\tau}{\delta t})\right.\\
&+\omega_0^2\delta t^2\sinh^2\frac{\tau}{\delta t}{}_2F_1{}^2(a+\frac{1}{2},b+\frac{1}{2};\frac{3}{2};-\sinh^2\frac{\tau}{\delta t})\\
&\left.+2\omega_0^2\delta t^2\sinh\frac{\tau}{\delta t}{}_2F_1(a,b;\frac{1}{2};-\sinh^2\frac{\tau}{\delta t}){}_2F_1(a+\frac{1}{2},b+\frac{1}{2};\frac{3}{2};-\sinh^2\frac{\tau}{\delta t})+\mathcal{O}(\omega_0^4\delta t^4)\right\}\\
=&\frac{1}{\omega_0}\left\{1+2\log 2\cdot\omega_0^2\delta t^2+2\omega_0^2\delta t\cdot\tau+\mathcal{O}(\omega_0^4\delta t^4,\frac{\tau^2}{\delta t^2})\right\}
\end{aligned}\tag{A.18}$$

and therefore (3.64).

Late time in fast quench ($\omega_0\delta t\ll\omega_0\tau\ll 1$) Rewrite (3.51) by applying identity

$$\begin{aligned}
{}_2F_1(a,b;c;z)=&\frac{\Gamma(c)\Gamma(b-a)}{\Gamma(b)\Gamma(c-a)}(-z)^{-a}{}_2F_1(a,1-c+a;1-b+a;\frac{1}{z})\\
&+\frac{\Gamma(c)\Gamma(a-b)}{\Gamma(a)\Gamma(c-b)}(-z)^{-b}{}_2F_1(b,1-c+b;1-a+b;\frac{1}{z}).
\end{aligned}\tag{A.19}$$

to each Hypergeometric function on the RHS. When $\tau>0$, $(-z)^{1/2}=\sinh\frac{\tau}{\delta t}$, thus we can find

$$\begin{aligned}
f_{CCP}=&\frac{1}{\sqrt{2\omega_0}}\frac{2^{i\omega_0\delta t}\cosh^{2\alpha}(\tau/\delta t)}{E_{1/2}\tilde{E}'_{3/2}-E'_{1/2}\tilde{E}_{3/2}}\times\\
&\left\{\left(E_{1/2}\tilde{E}'_{3/2}+E'_{1/2}\tilde{E}_{3/2}\right)(-z)^{-a}{}_2F_1(a,1/2+a;1-b+a;\frac{1}{z})\right.\\
&\left.+2E'_{1/2}\tilde{E}'_{3/2}(-z)^{-b}{}_2F_1(b+\frac{1}{2},b;1-a+b;\frac{1}{z})\right\},
\end{aligned}\tag{A.20}$$

where $z\equiv-\sinh^2\frac{\tau}{\delta t}$.

Similar calculations to (A.13) show

$$
\begin{aligned}
&2E'_{1/2}\tilde{E}'_{3/2} \\
=&2\frac{\pi}{2}\Gamma(-i\omega_0\delta t)^2\cdot\frac{1}{\Gamma(a)\Gamma(a+1/2)\Gamma(1/2-b)\Gamma(1-b)} \\
=&2\frac{\pi}{2}\Gamma(-i\omega_0\delta t)^2\left(\frac{1}{\sqrt{2\pi}}2^{2a-1/2}\frac{1}{\Gamma(2a)}\cdot\frac{1}{\sqrt{2\pi}}2^{2(1/2-b)-1/2}\frac{1}{\Gamma(1-2b)}\right) \\
\approx&\frac{1}{2}\cdot 2^{-i2\omega_0\delta t}\frac{\Gamma(-i\omega_0\delta t)^2}{\Gamma(1-i\omega_0\delta t)\left(1-\omega_0^2\delta t^2\psi(1-i\omega_0\delta t)\right)\Gamma(-i\omega_0\delta t)\left(1+\omega_0^2\delta t^2\psi(-i\omega_0\delta t)\right)} \\
\approx&\frac{i}{2\omega_0\delta t}\cdot 2^{-i2\omega_0\delta t}\frac{1}{\left[1+\omega_0^2\delta t^2\left(\psi(-i\omega_0\delta t)-\psi(1-i\omega_0\delta t)\right)\right]}
\end{aligned}
\tag{A.21}
$$

We further simplify the equation by using relations

$$
\mathrm{Re}\psi(iy)=\mathrm{Re}\psi(-iy)=\mathrm{Re}\psi(1+iy)=\mathrm{Re}\psi(1-iy), \tag{A.22}
$$

and

$$
\mathrm{Im}\psi(iy)=\frac{1}{2y}+\frac{1}{2}\pi\mathrm{coth}\pi y, \tag{A.23}
$$

$$
\mathrm{Im}\psi(1+iy)=-\frac{1}{2y}+\frac{1}{2}\pi\mathrm{coth}\pi y. \tag{A.24}
$$

Then we see that

$$
\psi(-i\omega_0\delta t)-\psi(1-i\omega_0\delta t)=i\mathrm{Im}\psi(-i\omega_0\delta t)-i\mathrm{Im}\psi(1-i\omega_0\delta t)=-\frac{i}{\omega_0\delta t} \tag{A.25}
$$

thus

$$
2E'_{1/2}\tilde{E}'_{3/2}=\frac{i}{2\omega_0\delta t}\cdot 2^{-i2\omega_0\delta t}\frac{1}{1-i\omega_0\delta t} \tag{A.26}
$$

Notice that when $\tau\gg\delta t$, $-\sinh^2\frac{\tau}{\delta t}\to-\frac{e^{2\tau/\delta t}}{4}+\frac{1}{2}$, $\cosh^2\frac{\tau}{\delta t}\to\frac{e^{2\tau/\delta t}}{4}+\frac{1}{2}$, and therefore ${}_2F_1\to 1+\mathcal{O}(e^{-2\tau/\delta t})$. Thus, after inserting the coefficients into (A.20) and expanding the result to the order $\omega_0\delta t$, we obtain

$$
\begin{aligned}
f=&\frac{1}{\sqrt{2\omega_0}}\cosh^{2\alpha}(\tau/\delta t)\left\{-i\omega_0\delta t2^{i\omega_0\delta t}(-z)^{-a}{}_2F_1(a,1/2+a;1-b+a;\frac{1}{z})\right. \\
&\left.+(1+i\omega_0\delta t)2^{-i\omega_0\delta t}(-z)^{-b}{}_2F_1(b+\frac{1}{2},b;1-a+b;\frac{1}{z})\right\} \\
\to&\frac{1}{\sqrt{2\omega_0}}\left(\frac{e^{\tau/\delta t}}{2}\right)^{2\alpha}\left\{-i\omega_0\delta t2^{i\omega_0\delta t}\left(\frac{e^{\tau/\delta t}}{2}\right)^{-2a}\left(1+\mathcal{O}(e^{-2\tau/\delta t})\right)\right. \\
&\left.+(1+i\omega_0\delta t)2^{-i\omega_0\delta t}\left(\frac{e^{\tau/\delta t}}{2}\right)^{-2b}\left(1+\mathcal{O}(e^{-2\tau/\delta t})\right)+\mathcal{O}(\omega_0^2\delta t^2)\right\} \\
=&\frac{1}{\sqrt{2\omega_0}}\left\{e^{-i\omega_0\tau}+2\omega_0\delta t\sin\omega_0\tau+\mathcal{O}(\omega_0^2\delta t^2)\right\}.
\end{aligned}
\tag{A.27}
$$

i.e.

$$\rho^2(\tau) = 2|f|^2 \approx \frac{1}{\omega_0}\left(1 + 2\omega_0\delta t \sin 2\omega_0\tau + \mathcal{O}(\omega_0^2\delta t^2),\right) \tag{A.28}$$

and therefore (3.66).

A.2 In ECP

Late-time approximation ($\tau \gg \delta t$, and $\tau \gg \delta t \log \omega_0 \delta t$) According to identity

$$\begin{aligned}
&{}_2F_1(a,b;a+b;z)\\
=&\frac{\Gamma(a+b)}{\Gamma(a)\Gamma(b)}\sum_{n=0}^{\infty}\frac{(a)_n(b)_n}{(n!)^2}[2\psi(n+1)-\psi(a+n)-\psi(b+n)-\log(1-z)](1-z)^n,\\
&\qquad\qquad\qquad\qquad\qquad\qquad\qquad\qquad(|1-z|<1\&|\arg(1-z)|<\pi)
\end{aligned} \tag{A.29}$$

we can see that for large $\tau/\delta t$, in which case

$$z \equiv \frac{1+\tanh(\tau/\delta t)}{2} = 1 - e^{-2\tau/\delta t}, \tag{A.30}$$

(3.54) can be rewritten into

$$\begin{aligned}
&f_{ECP} \to\\
&\frac{1}{\sqrt{2\omega_0}}\exp\left[-\frac{i}{2}\omega_0\tau + \frac{i}{2}\omega_0\delta t\log(e^{\tau/\delta t})\right]{}_2F_1\left[1-\frac{i}{2}\omega_0\delta t, -\frac{i}{2}\omega_0\delta t; 1-i\omega_0\delta t; 1-e^{-2\tau/\delta t}\right]\\
=&\frac{1}{\sqrt{2\omega_0}}\frac{\Gamma(1-i\omega_0\delta t)}{\Gamma(1-\frac{i}{2}\omega_0\delta t)\Gamma(-\frac{i}{2}\omega_0\delta t)}\times\\
&\sum_{n=0}^{\infty}\frac{(1-\frac{i}{2}\omega_0\delta t)_n(-\frac{i}{2}\omega_0\delta t)_n}{(n!)^2}\\
&\qquad\times\left[2\psi(n+1)-\psi(1-\frac{i}{2}\omega_0\delta t+n)-\psi(-\frac{i}{2}\omega_0\delta t+n)+2\frac{\tau}{\delta t}\right](e^{-2\tau/\delta t})^n
\end{aligned} \tag{A.31}$$

When $\tau \gg \delta t \log \omega_0 \delta t$, one can keep the leading term[1], then by using Digamma function

$$\psi(1) = -\gamma_E \tag{A.32}$$

and

$$\psi(1-z) = \psi(z) + \pi\cot\pi z, \tag{A.33}$$

we find

$$\begin{aligned}
&f_{ECP} \to\\
&\frac{1}{\sqrt{2\omega_0}}\frac{\Gamma(1-i\omega_0\delta t)}{\Gamma(1-\frac{i}{2}\omega_0\delta t)\Gamma(-\frac{i}{2}\omega_0\delta t)}\left[-2\gamma_E - 2\mathrm{Re}\,\psi\left(\frac{i}{2}\omega_0\delta t\right) + i\pi\coth\frac{\pi\omega_0\delta t}{2} + 2\frac{\tau}{\delta t}\right]\\
&+\mathcal{O}(e^{-2\tau/\delta t})
\end{aligned} \tag{A.34}$$

[1] $\tau \geq \delta t \log \omega_0 \delta t$ is a sufficient condition to keep (A.31) to the leading term.

Therefore,

$$\begin{aligned}
&\rho^2(\tau)\\
\sim&\frac{1}{\omega_0}\left|\frac{\Gamma(1-i\omega_0\delta t)}{\Gamma(1-\frac{i}{2}\omega_0\delta t)\Gamma(-\frac{i}{2}\omega_0\delta t)}\right|^2\\
&\times\left[\left(-2\gamma_E-2\mathrm{Re}\,\psi\left(\frac{i}{2}\omega_0\delta t\right)+2\frac{\tau}{\delta t}\right)^2+\left(\pi\coth\frac{\pi\omega_0\delta t}{2}\right)^2\right]\\
=&\delta t\left(\frac{\pi}{2}\coth\frac{\pi\omega_0\delta t}{2}\right)^{-1}\left(-\gamma_E-\mathrm{Re}\,\psi\left(\frac{i}{2}\omega_0\delta t\right)+\frac{\tau}{\delta t}\right)^2+\delta t\left(\frac{\pi}{2}\coth\frac{\pi\omega_0\delta t}{2}\right).
\end{aligned}\tag{A.35}$$

One special case of $\rho^2(\tau)$ is when $\omega_0\delta t\ll 1$, in which $\frac{\pi}{2}\coth\frac{\pi\omega_0\delta t}{2}\sim\frac{1}{\omega_0\delta t}$. Therefore,

$$\rho^2(\tau)\sim\omega_0\delta t^2\left(-\frac{\zeta(3)}{4}\omega_0^2\delta t^2+\frac{\tau}{\delta t}\right)^2+\frac{1}{\omega_0}=\frac{1}{\omega_0}+\omega_0\tau^2+\mathcal{O}(\omega_0^3\delta t^3).\tag{3.78}$$

according to identity (A.15). Another case is when $\omega_0\delta t\gg 1$, in which $\coth\frac{\pi\omega_0\delta t}{2}\to 1$. Thus by using the identity

$$\mathrm{Re}\,\psi(iy)\approx\log y+\sum_{n=1}^{\infty}\frac{(-1)^{n-1}B_{2n}}{2ny^{2n}}\sim\log y+\mathcal{O}(y^{-2}),\ y\to\infty\tag{A.36}$$

we can find

$$\rho^2(\tau)\sim\delta t\left[\frac{2}{\pi}\left(-\log\omega_0\delta t+\log 2-\gamma_E+\frac{\tau}{\delta t}\right)^2+\frac{\pi}{2}\right]\tag{3.77}$$

Appendix B
Entanglement Entropy

In this appendix we explicitly derive the approximated Entanglement Entropy (3.87) and (3.89). In appendix B.1 we figure out $\langle N_A \rangle$ and in appendix B.2, we figure out $\int_{A_P \times A_P} \mathrm{d}x\mathrm{d}y|C(x,y)|^2$.

B.1 $\langle N_A \rangle$

First, we rewrite $\langle N_A \rangle$ into

$$\langle N_A \rangle = \frac{1}{\Gamma(N)2^N\sqrt{\pi}} \int_{A_P \times A_P} \mathrm{d}\xi\mathrm{d}\eta\delta(\xi-\eta)e^{-\frac{\xi^2+\eta^2}{2}} \frac{H_{N-1}(\eta)H_N(\xi) - H_{N-1}(\xi)H_N(\eta)}{\xi-\eta} \tag{B.1}$$

s.t. $\langle N_A \rangle$ has similar form to $\int_{A_P \times A_P} \mathrm{d}x\mathrm{d}y|C(x,y)|^2$ in (3.85). One can easily prove that (B.1) and (3.85) are identical.

In the large N limit, the Hermite polynomial shows the following asymptotic behavior

$$e^{-\frac{x^2}{2}} \cdot H_n(x) \sim \frac{2^n}{\sqrt{\pi}}\Gamma\left(\frac{n+1}{2}\right)\cos\left(x\sqrt{2n} - \frac{n\pi}{2}\right) \tag{B.2}$$

We use this to simplify the integrand on the RHS of (3.85) or (B.1),

$$\begin{aligned}
&\frac{1}{\Gamma(N)2^N\sqrt{\pi}}e^{-\frac{\xi^2+\eta^2}{2}}\left[H_{N-1}(\eta)H_N(\xi) - H_{N-1}(\xi)H_N(\eta)\right] \\
&\qquad = \frac{1}{2\pi}\left[-(-1)^N\sin\left(\eta\sqrt{2N-2}+\xi\sqrt{2N}\right) - \sin\left(\eta\sqrt{2N-2}-\xi\sqrt{2N}\right)\right. \\
&\qquad\qquad \left.+(-1)^N\sin\left(\xi\sqrt{2N-2}+\eta\sqrt{2N}\right) + \sin\left(\xi\sqrt{2N-2}-\eta\sqrt{2N}\right)\right].
\end{aligned} \tag{B.3}$$

Now, change the variables of integration by defining

$$u \equiv \frac{\xi+\eta}{\sqrt{2}}, v \equiv \frac{\xi-\eta}{\sqrt{2}}, \tag{B.4}$$

and we obtain

$$\begin{aligned}
\langle N_A \rangle = \frac{1}{2\pi}\int_{A_P \times A_P} \mathrm{d}u\mathrm{d}v\frac{\delta(v)}{v}\left\{-(-1)^N\cos\left[(\sqrt{N-1}+\sqrt{N})u\right]\sin\left[\frac{v}{\sqrt{N-1}+\sqrt{N}}\right]\right. \\
\left.+\cos\left[-\frac{u}{\sqrt{N-1}+\sqrt{N}}\right]\sin\left[(\sqrt{N-1}+\sqrt{N})v\right]\right\}.
\end{aligned} \tag{B.5}$$

Note that

$$\begin{aligned}&\int_{A_P\times A_P}\mathrm{d}u\mathrm{d}v\\&=\int_0^{\sqrt{2}\frac{a}{\rho}}\mathrm{d}u\int_{|v|\leq\sqrt{2}\frac{a}{\rho}-u}\mathrm{d}v+\int_{-\sqrt{2}\frac{a}{\rho}}^0\mathrm{d}u\int_{|v|\leq\sqrt{2}\frac{a}{\rho}+u}\mathrm{d}v=2\int_0^{\sqrt{2}\frac{a}{\rho}}\mathrm{d}u\int_{|v|\leq\sqrt{2}\frac{a}{\rho}-u}\mathrm{d}v\end{aligned}\tag{B.6}$$

since the integrand is even for both u and v. Moreover, because of the Dirac delta function,

$$\int_{A_P\times A_P}\mathrm{d}u\mathrm{d}v\to 2\int_0^{\sqrt{2}\frac{a}{\rho}}\mathrm{d}u\int_{-\epsilon}^{\epsilon}\mathrm{d}v,\tag{B.7}$$

and the integrand can be expanded around $v=0$:

$$\begin{aligned}\langle N_A\rangle=&\frac{1}{\pi}\int_0^{\sqrt{2}\frac{a}{\rho}}\mathrm{d}u\int_{-\varepsilon}^{\varepsilon}\mathrm{d}v\delta(v)\left\{-(-1)^N\cos\left[(\sqrt{N-1}+\sqrt{N})u\right]\frac{1}{\sqrt{N-1}+\sqrt{N}}\right.\\&\left.+\cos\left[-\frac{u}{\sqrt{N-1}+\sqrt{N}}\right](\sqrt{N-1}+\sqrt{N})\right\}\\=&\frac{1}{\pi}\left\{(-1)^{N-1}\sin\left[(\sqrt{N-1}+\sqrt{N})\sqrt{2}\frac{a}{\rho}\right]\frac{1}{(\sqrt{N-1}+\sqrt{N})^2}\right.\\&\left.+\sin\left[\frac{\sqrt{2}\frac{a}{\rho}}{\sqrt{N-1}+\sqrt{N}}\right](\sqrt{N-1}+\sqrt{N})^2\right\}\\\to&\frac{1}{\pi}(\sqrt{N-1}+\sqrt{N})\sqrt{2}\frac{a}{\rho}+\mathcal{O}\left(\frac{1}{N}\right)\end{aligned}\tag{B.8}$$

when

$$\frac{\sqrt{2}\frac{a}{\rho}}{\sqrt{N-1}+\sqrt{N}}\ll 1.\tag{3.82}$$

B.2 $\int_{A_P\times A_P}\mathbf{d}x\mathbf{d}y|C(x,y)|^2$

Similar to $\langle N_A\rangle$ (appendix B.1),

$$\begin{aligned}&\int_{A_P\times A_P}\mathrm{d}x\mathrm{d}y|C(x,y)|^2\\\approx&\frac{2}{\pi^2}\int_0^{\sqrt{2}\frac{a}{\rho}}\mathrm{d}v\int_0^{\sqrt{2}\frac{a}{\rho}-v}\mathrm{d}u\frac{1}{v^2}\left\{-(-1)^N\cos\left[(\sqrt{N-1}+\sqrt{N})u\right]\sin\left[\frac{v}{\sqrt{N-1}+\sqrt{N}}\right]\right.\\&\left.+\cos\left[\frac{u}{\sqrt{N-1}+\sqrt{N}}\right]\sin\left[(\sqrt{N-1}+\sqrt{N})v\right]\right\}^2.\end{aligned}\tag{B.9}$$

In the limit (3.82),

$$\sin\left[\frac{v}{\sqrt{N-1}+\sqrt{N}}\right] \sim \frac{v}{\sqrt{N-1}+\sqrt{N}} \ll 1 \sim \cos\left[\frac{u}{\sqrt{N-1}+\sqrt{N}}\right]. \tag{B.10}$$

This implies that we can ignore the 1^{st} term in the integrand of (B.9) and replace the cosine by 1. As a result,

$$\begin{aligned}
&\int_{A_P\times A_P} \mathrm{d}x\mathrm{d}y|C(x,y)|^2 \to \frac{2}{\pi^2}\int_0^{\sqrt{2}\frac{a}{\rho}} \mathrm{d}v \frac{1}{v^2}\sin^2\left[(\sqrt{N-1}+\sqrt{N})v\right]\left(\sqrt{2}\frac{a}{\rho}-v\right)\\
=&-\frac{1}{\pi^2}\left\{1+\gamma_E-\cos\left[(\sqrt{N-1}+\sqrt{N})2\sqrt{2}\frac{a}{\rho}\right]-\mathrm{Ci}\left[(\sqrt{N-1}+\sqrt{N})2\sqrt{2}\frac{a}{\rho}\right]\right.\\
&+\log\left[(\sqrt{N-1}+\sqrt{N})2\sqrt{2}\frac{a}{\rho}\right]\\
&\left.-\left[(\sqrt{N-1}+\sqrt{N})2\sqrt{2}\frac{a}{\rho}\right]\mathrm{Si}\left[(\sqrt{N-1}+\sqrt{N})2\sqrt{2}\frac{a}{\rho}\right]\right\}
\end{aligned} \tag{B.11}$$

The asymptotic behaviors of Trigonometric integrals are

$$\begin{aligned}
\mathrm{Si}(x) &= \frac{\pi}{2}-\frac{\cos x}{x}\left(1-\frac{2!}{x^2}+\frac{4!}{x^4}-\frac{6!}{x^6}\cdots\right)-\frac{\sin x}{x}\left(\frac{1}{x}-\frac{3!}{x^3}+\frac{5!}{x^5}-\frac{7!}{x^7}\cdots\right)\\
\mathrm{Ci}(x) &= \frac{\sin x}{x}\left(1-\frac{2!}{x^2}+\frac{4!}{x^4}-\frac{6!}{x^6}\cdots\right)-\frac{\cos x}{x}\left(\frac{1}{x}-\frac{3!}{x^3}+\frac{5!}{x^5}-\frac{7!}{x^7}\cdots\right)
\end{aligned} \tag{B.12}$$

when $x\to\infty$, and

$$\begin{aligned}
\mathrm{Si}(x) &= \sum_{n=0}^{\infty}\frac{(-1)^n x^{2n+1}}{(2n+1)(2n+1)!} = x-\frac{x^3}{3!\cdot 3}+\frac{x^5}{5!\cdot 5}-\frac{x^7}{7!\cdot 7}\pm\cdots\\
\mathrm{Ci}(x) &= \gamma_E+\ln x+\sum_{n=1}^{\infty}\frac{(-1)^n x^{2n}}{2n(2n)!} = \gamma_E+\ln x-\frac{x^2}{2!\cdot 2}+\frac{x^4}{4!\cdot 4}\mp\cdots
\end{aligned} \tag{B.13}$$

when $x\ll 1$. Thus (B.11) can be further simplified into

$$\begin{aligned}
&\int_{A_P\times A_P}\mathrm{d}x\mathrm{d}y|C(x,y)|^2\\
&\to -\frac{1}{\pi^2}\left\{1+\gamma_E+\log\left[(\sqrt{N-1}+\sqrt{N})2\sqrt{2}\frac{a}{\rho}\right]\right\}+\frac{1}{\pi}(\sqrt{N-1}+\sqrt{N})\sqrt{2}\frac{a}{\rho},
\end{aligned} \tag{B.14}$$

when

$$\sqrt{N-1}+\sqrt{N} \gg \frac{a}{\rho} \gg \sqrt{N}-\sqrt{N-1}; \tag{3.86}$$

and

$$\int_{A_P \times A_P} \mathrm{d}x\mathrm{d}y |C(x,y)|^2 \to 0 + \mathcal{O}\left(\frac{Na^2}{\rho^2}\right), \tag{B.15}$$

when

$$(\sqrt{N-1} + \sqrt{N})\frac{a}{\rho} \ll 1. \tag{3.88}$$

Inserting (B.14) and (B.15) back into (3.41) together with (B.8), one can get (3.87) and (3.89), respectively.

Appendix C
Abrupt Pulse and Dip protocols $\omega_0 \to \omega_2 \to \omega_1$

Here we compute analytic solutions for $\rho(\tau)^2$ for an abrupt pulse with $\omega_0 \to \omega_2 \to \omega_1$ with an $f(\tau)^2$ of

$$f(\tau)^2 = \begin{cases} \omega_0^2, & \tau < -\frac{T}{2} \\ \omega_2^2, & -\frac{T}{2} \le \tau < \frac{T}{2} \\ \omega_1^2, & \frac{T}{2} \le \tau \end{cases} \tag{C.1}$$

We know that the solution to the Pinney equation is given by

$$\rho^2(\tau) = Au(\tau)^2 + 2Bu(\tau)v(\tau) + Cv(\tau)^2 \tag{C.2}$$

where $u(\tau)$ and $v(\tau)$ are independent solutions which satisfy

$$\begin{aligned} \frac{d^2u}{d\tau^2} - f(\tau)^2 u &= 0 \\ \frac{d^2v}{d\tau^2} - f(\tau)^2 v &= 0 \end{aligned} \tag{C.3}$$

We require for $\tau < -\frac{T}{2}$ that $\rho^2 = \frac{1}{\omega_0}$. This requires $A = C = 0$ and by (4.29), $2B = \frac{1}{\omega_0}$. Therefore

$$\rho^2 = \frac{1}{\omega_0} u(\tau)v(\tau) \tag{C.4}$$

We look for solutions

$$\begin{aligned} \frac{d^2u}{d\tau^2} - f(\tau)^2 u &= 0 \\ \frac{d^2v}{d\tau^2} - f(\tau)^2 v &= 0 \end{aligned} \tag{C.5}$$

for $f(\tau)^2$ given in (C.1). A general solution for $u(\tau)$ in the three regions is given by

$$\begin{aligned} u_1(\tau) &= e^{\omega_0 \tau} \\ u_2(\tau) &= Ae^{\omega_2 \tau} + Be^{-\omega_2 \tau} \\ u_3(\tau) &= Ce^{\omega_1 \tau} + De^{-\omega_1 \tau} \end{aligned} \tag{C.6}$$

Enforcing boundary conditions at $\tau = -\frac{T}{2}$ and $\tau = \frac{T}{2}$, we find

$$\begin{aligned} e^{-\omega_0 \frac{T}{2}} &= Ae^{-\omega_2 \frac{T}{2}} + Be^{\omega_2 \frac{T}{2}} \\ \omega_0 e^{-\omega_0 \frac{T}{2}} &= \omega_2 (Ae^{-\omega_2 \frac{T}{2}} - Be^{\omega_2 \frac{T}{2}}) \\ Ae^{\omega_2 \frac{T}{2}} + Be^{-\omega_2 \frac{T}{2}} &= Ce^{\omega_1 \frac{T}{2}} + De^{-\omega_1 \frac{T}{2}} \\ \omega_2 (Ae^{\omega_2 \frac{T}{2}} - Be^{-\omega_2 \frac{T}{2}}) &= \omega_1 (Ce^{-\omega_1 \frac{T}{2}} - De^{\omega_1 \frac{T}{2}}) \end{aligned} \tag{C.7}$$

Solving for the coefficients yield

$$\begin{aligned}
A &= e^{\frac{1}{2}T(-\omega_0+\omega_2)}\frac{(\omega_0+\omega_2)}{2\omega_2} \\
B &= e^{-\frac{1}{2}T(\omega_0+\omega_2)}\frac{(-\omega_0+\omega_2)}{2\omega_2} \\
C &= e^{-\frac{T}{2}(\omega_0+\omega_1+2\omega_2)}\frac{((\omega_0-\omega_2)(-\omega_1+\omega_2)+e^{2T\omega_2}(\omega_0+\omega_2)(\omega_1+\omega_2))}{4\omega_1\omega_2} \\
D &= e^{-\frac{T}{2}(\omega_0-\omega_1+2\omega_2)}\frac{(e^{2T\omega_2}(\omega_0+\omega_2)(\omega_1-\omega_2)-(\omega_0-\omega_2)(\omega_1+\omega_2))}{4\omega_1\omega_2}
\end{aligned} \tag{C.8}$$

Similarly, for the other independent solution $v(\tau)$ we have

$$\begin{aligned}
v_1(\tau) &= e^{-\omega_0\tau} \\
v_2(\tau) &= A'e^{\omega_2\tau}+B'e^{-\omega_2\tau} \\
v_3(\tau) &= C'e^{\omega_1\tau}+D'e^{-\omega_1\tau}
\end{aligned} \tag{C.9}$$

and again applying boundary conditions

$$\begin{aligned}
e^{\omega_0\frac{T}{2}} &= A'e^{-\omega_2\frac{T}{2}}+B'e^{\omega_2\frac{T}{2}} \\
-\omega_0 e^{\omega_0\frac{T}{2}} &= \omega_2(A'e^{-\omega_2\frac{T}{2}}-B'e^{\omega_2\frac{T}{2}}) \\
A'e^{\omega_2\frac{T}{2}}+B'e^{-\omega_2\frac{T}{2}} &= C'e^{\omega_1\frac{T}{2}}+D'e^{-\omega_1\frac{T}{2}} \\
\omega_2(A'e^{\omega_2\frac{T}{2}}-B'e^{-\omega_2\frac{T}{2}}) &= \omega_1(C'e^{-\omega_1\frac{T}{2}}-D'e^{\omega_1\frac{T}{2}})
\end{aligned} \tag{C.10}$$

we find

$$\begin{aligned}
A' &= e^{\frac{1}{2}T(\omega_0+\omega_2)}\frac{(-\omega_0+\omega_2)}{2\omega_2} \\
B' &= e^{\frac{1}{2}T(\omega_0-\omega_2)}\frac{(\omega_0+\omega_2)}{2\omega_2} \\
C' &= e^{\frac{T}{2}(\omega_0-\omega_1-2\omega_2)}\frac{((\omega_0+\omega_2)(\omega_1-\omega_2)+e^{2T\omega_2}(-\omega_0+\omega_2)(\omega_1+\omega_2))}{4\omega_1\omega_2} \\
D' &= e^{\frac{T}{2}(\omega_0+\omega_1-2\omega_2)}\frac{(e^{2T\omega_2}(\omega_0-\omega_2)(-\omega_1+\omega_2)+(\omega_0+\omega_2)(\omega_1+\omega_2))}{4\omega_1\omega_2}
\end{aligned} \tag{C.11}$$

Therefore, inserting (C.6) and (C.9) into (C.4) with the coefficients defined in (C.8) and (C.11), $\rho^2(\tau)$ becomes

$$\rho^2(\tau) = \begin{cases} \frac{1}{\omega_0}, & \tau \le -\frac{T}{2} \\ \frac{1}{\omega_0}\big(AA'e^{2\omega_2\tau}+BB'e^{-2\omega_2\tau}+AB'+A'B\big), & -\frac{T}{2} \le \tau \le \frac{T}{2} \\ \frac{1}{\omega_0}\big(CC'e^{2\omega_1\tau}+DD'e^{-2\omega_1\tau}+CD'+C'D\big), & \tau \ge \frac{T}{2} \end{cases} \tag{C.12}$$

Appendix D
Smooth step protocols $\omega_0 \to \omega_1$

Here we compute analytic solutions for $\rho(\tau)^2$ for a smooth step for $\omega_0 \to \omega_1$ with an $f(\tau)^2$ of

$$\begin{aligned} f(\tau)^2 &= \omega_0^2 + \frac{\omega_1^2 - \omega_0^2}{1 + e^{-\frac{\tau}{\delta t}}} \\ &= \frac{\omega_1^2 + \omega_0^2 e^{-\frac{\tau}{\delta t}}}{1 + e^{-\frac{\tau}{\delta t}}} \end{aligned} \tag{D.1}$$

where in this case we choose

$$\rho^2(\tau) = u(\tau)v(\tau) \tag{D.2}$$

First we look for solutions to

$$\begin{aligned} \frac{d^2u'}{d\tau^2} - f(\tau)^2 u' &= 0 \\ \frac{d^2v'}{d\tau^2} - f(\tau)^2 v' &= 0 \end{aligned} \tag{D.3}$$

where in general our solution will be of the form

$$\begin{aligned} u(\tau) &= A'u'(\tau) + B'v'(\tau) \\ v(\tau) &= Au'(\tau) + Bv'(\tau) \end{aligned} \tag{D.4}$$

We find that the two independent solutions are given by

$$\begin{aligned} u'(\tau) &= e^{\omega_0\tau}{}_2F_1(\delta t(\omega_0 - \omega_1), \delta t(\omega_0 + \omega_1), 1 + 2\delta t\omega_0, -e^{\frac{\tau}{\delta t}}) \\ v'(\tau) &= e^{-\omega_0\tau}{}_2F_1(-\delta t(\omega_0 + \omega_1), \delta t(-\omega_0 + \omega_1), 1 - 2\delta t\omega_0, -e^{\frac{\tau}{\delta t}}) \end{aligned} \tag{D.5}$$

The v' solution is nonsingular for $\omega_0\delta t$ not a half integer.

D.1 Solution for u

Now we write the following adiabatic solution for u.

$$\begin{aligned} u_{ad}(\tau) &= \frac{1}{\sqrt{\omega(\tau)}} e^{-C(\delta t,\omega_0,\omega_1) + \int^\tau f(\tau')d\tau'} \\ &= \frac{1}{\sqrt{\omega(\tau)}} e^{-C(\delta t,\omega_0,\omega_1) + \int^\tau \left(\omega_0^2 + \frac{\omega_1^2-\omega_0^2}{1+e^{-\frac{\tau'}{\delta t}}}\right)^{\frac{1}{2}} d\tau'} \\ &= \frac{1}{\sqrt{\omega(\tau)}} e^{-C(\delta t,\omega_0,\omega_1) + F(\tau,\delta t,\omega_0,\omega_1)} \end{aligned} \tag{D.6}$$

where

$$C(\delta t, \omega_0, \omega_1) = -\delta t \omega_0 \log(4\omega_0^2) + \delta t \omega_1 \log(\omega_0 + \omega_1)^2$$

$$\begin{aligned} F(\tau, \delta t, \omega_0, \omega_1) = \\ \left(\omega_0 \left(\tau - \delta \mathrm{t} \log\left(2\omega_0 \sqrt{e^{\tau/\delta \mathrm{t}} + 1} \sqrt{\omega_1^2 e^{\tau/\delta \mathrm{t}} + \omega_0^2} + \left(\omega_0^2 + \omega_1^2\right) e^{\tau/\delta \mathrm{t}} + 2\omega_0^2\right)\right)\right. \\ \left. + \delta \mathrm{t} \omega_1 \log\left(\omega_1 \left(2\omega_1 e^{\tau/\delta \mathrm{t}} + 2\sqrt{e^{\tau/\delta \mathrm{t}} + 1} \sqrt{\omega_1^2 e^{\tau/\delta \mathrm{t}} + \omega_0^2} + \omega_1\right) + \omega_0^2\right)\right) \end{aligned}$$

The constant $C(\delta t, \omega_0, \omega_1)$ is chosen such that for $\tau \to -\infty$

$$u_{ad} \to \frac{1}{\sqrt{\omega_0}} e^{\omega_0 \tau} \tag{D.7}$$

Therefore, the coefficient C_u in (4.43), is given by

$$C_u = e^{-C(\delta t, \omega_0, \omega_1)} \tag{D.8}$$

The derivative of u_{ad} is given by

$$\partial_\tau u_{ad}(\tau) \quad = \quad \left(f(\tau) - \frac{\partial_\tau f(\tau)}{2f(\tau)}\right) u_{ad}(\tau) \tag{D.9}$$

Solving for the solution

$$u(\tau) = A' u'(\tau) + B' v'(\tau) \tag{D.10}$$

we impose the boundary conditions

$$\begin{aligned} u(T) &= u_{ad}(T) \\ \partial_\tau u(T) &= \partial_\tau u_{ad}(T) \end{aligned} \tag{D.11}$$

This yields an A' and B' of

$$
\begin{aligned}
&A' = \\
&\frac{1}{4} e^{-T\omega_0 - C(\delta t,\omega_0,\omega_1)+F(T,\delta t,\omega_0,\omega_1)} \left(\omega_1^2 + \frac{\omega_0^2-\omega_1^2}{1+e^{\frac{T}{\delta t}}}\right)^{\frac{3}{4}} \\
&\Bigg[\Bigg(4\delta t\omega_0^2\Bigg(-\omega_1 + \sqrt{\omega_1^2 + \frac{\omega_0^2-\omega_1^2}{1+e^{\frac{T}{\delta t}}}}\Bigg) + 4e^{2\frac{T}{\delta t}}\delta t\omega_1^2\Bigg(-\omega_1 + \sqrt{\omega_1^2 + \frac{\omega_0^2-\omega_1^2}{1+e^{\frac{T}{\delta t}}}}\Bigg) \\
&+ e^{\frac{T}{\delta t}}\omega_0^2\Bigg(1 + 4\delta t\Bigg(-\omega_1 + \sqrt{\omega_1^2 + \frac{\omega_0^2-\omega_1^2}{1+e^{\frac{T}{\delta t}}}}\Bigg)\Bigg) + e^{\frac{T}{\delta t}}\omega_1^2\Bigg(-1 + 4\delta t\Bigg(-\omega_1 + \sqrt{\omega_1^2 + \frac{\omega_0^2-\omega_1^2}{1+e^{\frac{T}{\delta t}}}}\Bigg)\Bigg)\Bigg) \\
&\times {}_2F_1(\delta t(-\omega_0+\omega_1), -\delta t(\omega_0+\omega_1), 1-2\delta t\omega_0, -e^{\frac{T}{\delta t}}) \\
&+ 4(1+e^{\frac{T}{\delta t}})\delta t(\omega_0+\omega_1)(\omega_0^2 + e^{\frac{T}{\delta t}}\omega_1^2){}_2F_1(1-\delta t(\omega_0+\omega_1), \delta t(-\omega_0+\omega_1), 1-2\delta t\omega_0, -e^{\frac{T}{\delta t}})\Bigg] \\
&\times \Bigg(\delta t(\omega_0^2 + e^{\frac{T}{\delta t}}\omega_1^2)^2\Bigg((\omega_0-\omega_1)\ {}_2F_1\left(\delta\mathrm{t}\,(\omega_0-\omega_1)+1, \delta\mathrm{t}\,(\omega_0+\omega_1); 2\delta\mathrm{t}\omega_0+1; -e^{T/\delta\mathrm{t}}\right) \\
&\qquad {}_2F_1\left(\delta\mathrm{t}\,(\omega_1-\omega_0), -\delta\mathrm{t}\,(\omega_0+\omega_1); 1-2\delta\mathrm{t}\omega_0; -e^{T/\delta\mathrm{t}}\right) \\
&+ (\omega_0+\omega_1)\ {}_2F_1\left(\delta\mathrm{t}\,(\omega_0-\omega_1), \delta\mathrm{t}\,(\omega_0+\omega_1); 2\delta\mathrm{t}\omega_0+1; -e^{T/\delta\mathrm{t}}\right) \\
&\qquad {}_2F_1\left(\delta\mathrm{t}\,(\omega_1-\omega_0), 1-\delta\mathrm{t}\,(\omega_0+\omega_1); 1-2\delta\mathrm{t}\omega_0; -e^{T/\delta\mathrm{t}}\right)\Bigg)\Bigg)^{-1}
\end{aligned}
$$

$$
\begin{aligned}
&B' = \\
&\frac{1}{4} e^{T\omega_0 - C(\delta t,\omega_0,\omega_1)+F(T,\delta t,\omega_0,\omega_1)} \left(\omega_1^2 + \frac{\omega_0^2-\omega_1^2}{1+e^{\frac{T}{\delta t}}}\right)^{\frac{3}{4}} \\
&\Bigg[\Bigg(4\delta t\omega_0^2\Bigg(\omega_1 - \sqrt{\omega_1^2 + \frac{\omega_0^2-\omega_1^2}{1+e^{\frac{T}{\delta t}}}}\Bigg) + 4e^{2\frac{T}{\delta t}}\delta t\omega_1^2\Bigg(\omega_1 - \sqrt{\omega_1^2 + \frac{\omega_0^2-\omega_1^2}{1+e^{\frac{T}{\delta t}}}}\Bigg) \\
&+ e^{\frac{T}{\delta t}}\omega_0^2\Bigg(-1 + 4\delta t\Bigg(\omega_1 - \sqrt{\omega_1^2 + \frac{\omega_0^2-\omega_1^2}{1+e^{\frac{T}{\delta t}}}}\Bigg)\Bigg) + e^{\frac{T}{\delta t}}\omega_1^2\Bigg(1 + 4\delta t\Bigg(\omega_1 - \sqrt{\omega_1^2 + \frac{\omega_0^2-\omega_1^2}{1+e^{\frac{T}{\delta t}}}}\Bigg)\Bigg)\Bigg) \\
&\times {}_2F_1(\delta t(\omega_0-\omega_1), \delta t(\omega_0+\omega_1), 1+2\delta t\omega_0, -e^{\frac{T}{\delta t}}) \\
&+ 4(1+e^{\frac{T}{\delta t}})\delta t(\omega_0-\omega_1)(\omega_0^2 + e^{\frac{T}{\delta t}}\omega_1^2){}_2F_1(1+\delta t(\omega_0-\omega_1), \delta t(\omega_0+\omega_1), 1+2\delta t\omega_0, -e^{\frac{T}{\delta t}})\Bigg] \\
&\times \Bigg(\delta t(\omega_0^2 + e^{\frac{T}{\delta t}}\omega_1^2)^2\Bigg((\omega_0-\omega_1)\ {}_2F_1\left(\delta\mathrm{t}\,(\omega_0-\omega_1)+1, \delta\mathrm{t}\,(\omega_0+\omega_1); 2\delta\mathrm{t}\omega_0+1; -e^{T/\delta\mathrm{t}}\right) \\
&\qquad {}_2F_1\left(\delta\mathrm{t}\,(\omega_1-\omega_0), -\delta\mathrm{t}\,(\omega_0+\omega_1); 1-2\delta\mathrm{t}\omega_0; -e^{T/\delta\mathrm{t}}\right) \\
&+ (\omega_0+\omega_1)\ {}_2F_1\left(\delta\mathrm{t}\,(\omega_0-\omega_1), \delta\mathrm{t}\,(\omega_0+\omega_1); 2\delta\mathrm{t}\omega_0+1; -e^{T/\delta\mathrm{t}}\right) \\
&\qquad {}_2F_1\left(\delta\mathrm{t}\,(\omega_1-\omega_0), 1-\delta\mathrm{t}\,(\omega_0+\omega_1); 1-2\delta\mathrm{t}\omega_0; -e^{T/\delta\mathrm{t}}\right)\Bigg)\Bigg)^{-1}
\end{aligned}
\tag{D.12}
$$

D.2 Solution for v

Similarly for v we write the following adiabatic solution

$$\begin{aligned} v_{ad}(\tau) &= \frac{1}{\sqrt{\omega(\tau)}} e^{C(\delta t,\omega_0,\omega_1)-\int^\tau \omega(\tau')d\tau'} \\ &= \frac{1}{\sqrt{\omega(\tau)}} e^{C(\delta t,\omega_0,\omega_1)-\int^\tau \left(\omega_0^2+\frac{\omega_1^2-\omega_0^2}{1+e^{-\frac{\tau'}{\delta t}}}\right)^{\frac{1}{2}} d\tau'} \\ &= \frac{1}{\sqrt{\omega(\tau)}} e^{C(\delta t,\omega_0,\omega_1)-F(\tau,\delta t,\omega_0,\omega_1)} \end{aligned} \tag{D.13}$$

Similarly, as $\tau \to -\infty$

$$v_{ad}(\tau) \to \frac{1}{\sqrt{\omega_0}} e^{-\omega_0 \tau} \tag{D.14}$$

$$C_v = \frac{1}{C_u} = e^{C(\delta t,\omega_0,\omega_1)} \tag{D.15}$$

The derivative of $v_{ad}(\tau)$ is given by.

$$\partial_\tau v_{ad}(\tau) = \left(- f(\tau) - \frac{\partial_\tau f(\tau)}{f(\tau)} \right) v_{ad}(\tau) \tag{D.16}$$

Solving for the solution

$$v(\tau) = Au'(\tau) + Bv'(\tau) \tag{D.17}$$

we impose the boundary conditions

$$\begin{aligned} v(T) &= v_{ad}(T) \\ \partial_\tau v(T) &= \partial_\tau v_{ad}(T) \end{aligned} \tag{D.18}$$

for T sufficiently less than 0. This yields an A and B of

$$
\begin{aligned}
&A = \\
&\frac{1}{4}e^{-T\omega_0+C(\delta t,\omega_0,\omega_1)-F(T,\delta t,\omega_0,\omega_1)}\left(\omega_1^2+\frac{\omega_0^2-\omega_1^2}{1+e^{\frac{T}{\delta t}}}\right)^{\frac{3}{4}} \\
&\Bigg[-\left(4\delta t\omega_0^2\left(\omega_1+\sqrt{\omega_1^2+\frac{\omega_0^2-\omega_1^2}{1+e^{\frac{T}{\delta t}}}}\right)+4e^{2\frac{T}{\delta t}}\delta t\omega_1^2\left(\omega_1+\sqrt{\omega_1^2+\frac{\omega_0^2-\omega_1^2}{1+e^{\frac{T}{\delta t}}}}\right)\right. \\
&\left.+e^{\frac{T}{\delta t}}\omega_0^2\left(-1+4\delta t\left(\omega_1+\sqrt{\omega_1^2+\frac{\omega_0^2-\omega_1^2}{1+e^{\frac{T}{\delta t}}}}\right)\right)+e^{\frac{T}{\delta t}}\omega_1^2\left(1+4\delta t\left(\omega_1+\sqrt{\omega_1^2+\frac{\omega_0^2-\omega_1^2}{1+e^{\frac{T}{\delta t}}}}\right)\right)\right) \\
&\times {}_2F_1(-\delta t(\omega_0+\omega_1),\delta t(-\omega_0+\omega_1),1-2\delta t\omega_0,-e^{\frac{T}{\delta t}}) \\
&+4(1+e^{\frac{T}{\delta t}})\delta t(\omega_0+\omega_1)(\omega_0^2+e^{\frac{T}{\delta t}}\omega_1^2){}_2F_1(1-\delta t(\omega_0+\omega_1),\delta t(-\omega_0+\omega_1),1-2\delta t\omega_0,-e^{\frac{T}{\delta t}})\Bigg] \\
&\times\Bigg(\delta t(\omega_0^2+e^{\frac{T}{\delta t}}\omega_1^2)^2\Bigg((\omega_0-\omega_1)\ {}_2F_1\left(\delta\mathrm{t}\,(\omega_0-\omega_1)+1,\delta\mathrm{t}\,(\omega_0+\omega_1)\,;2\delta\mathrm{t}\omega_0+1;-e^{T/\delta\mathrm{t}}\right) \\
&\qquad {}_2F_1\left(\delta\mathrm{t}\,(\omega_1-\omega_0)\,,-\delta\mathrm{t}\,(\omega_0+\omega_1)\,;1-2\delta\mathrm{t}\omega_0;-e^{T/\delta\mathrm{t}}\right) \\
&\quad+(\omega_0+\omega_1)\ {}_2F_1\left(\delta\mathrm{t}\,(\omega_0-\omega_1)\,,\delta\mathrm{t}\,(\omega_0+\omega_1)\,;2\delta\mathrm{t}\omega_0+1;-e^{T/\delta\mathrm{t}}\right) \\
&\qquad {}_2F_1\left(\delta\mathrm{t}\,(\omega_1-\omega_0)\,,1-\delta\mathrm{t}\,(\omega_0+\omega_1)\,;1-2\delta\mathrm{t}\omega_0;-e^{T/\delta\mathrm{t}}\right)\Bigg)\Bigg)^{-1}
\end{aligned}
$$

$$
\begin{aligned}
&B = \\
&\frac{1}{4}e^{T\omega_0+C(\delta t,\omega_0,\omega_1)-F(T,\delta t,\omega_0,\omega_1)}\left(\omega_1^2+\frac{\omega_0^2-\omega_1^2}{1+e^{\frac{T}{\delta t}}}\right)^{\frac{3}{4}} \\
&\Bigg[\left(4\delta t\omega_0^2\left(\omega_1+\sqrt{\omega_1^2+\frac{\omega_0^2-\omega_1^2}{1+e^{\frac{T}{\delta t}}}}\right)+4e^{2\frac{T}{\delta t}}\delta t\omega_1^2\left(\omega_1+\sqrt{\omega_1^2+\frac{\omega_0^2-\omega_1^2}{1+e^{\frac{T}{\delta t}}}}\right)\right. \\
&\left.+e^{\frac{T}{\delta t}}\omega_0^2\left(-1+4\delta t\left(\omega_1+\sqrt{\omega_1^2+\frac{\omega_0^2-\omega_1^2}{1+e^{\frac{T}{\delta t}}}}\right)\right)+e^{\frac{T}{\delta t}}\omega_1^2\left(1+4\delta t\left(\omega_1+\sqrt{\omega_1^2+\frac{\omega_0^2-\omega_1^2}{1+e^{\frac{T}{\delta t}}}}\right)\right)\right) \\
&\times {}_2F_1(\delta t(\omega_0-\omega_1),\delta t(\omega_0+\omega_1),1+2\delta t\omega_0,-e^{\frac{T}{\delta t}}) \\
&+4(1+e^{\frac{T}{\delta t}})\delta t(\omega_0-\omega_1)(\omega_0^2+e^{\frac{T}{\delta t}}\omega_1^2){}_2F_1(1+\delta t(\omega_0-\omega_1),\delta t(\omega_0+\omega_1),1+2\delta t\omega_0,-e^{\frac{T}{\delta t}})\Bigg] \\
&\times\Bigg(\delta t(\omega_0^2+e^{\frac{T}{\delta t}}\omega_1^2)^2\Bigg((\omega_0-\omega_1)\ {}_2F_1\left(\delta\mathrm{t}\,(\omega_0-\omega_1)+1,\delta\mathrm{t}\,(\omega_0+\omega_1)\,;2\delta\mathrm{t}\omega_0+1;-e^{T/\delta\mathrm{t}}\right) \\
&\qquad {}_2F_1\left(\delta\mathrm{t}\,(\omega_1-\omega_0)\,,-\delta\mathrm{t}\,(\omega_0+\omega_1)\,;1-2\delta\mathrm{t}\omega_0;-e^{T/\delta\mathrm{t}}\right) \\
&\quad+(\omega_0+\omega_1)\ {}_2F_1\left(\delta\mathrm{t}\,(\omega_0-\omega_1)\,,\delta\mathrm{t}\,(\omega_0+\omega_1)\,;2\delta\mathrm{t}\omega_0+1;-e^{T/\delta\mathrm{t}}\right) \\
&\qquad {}_2F_1\left(\delta\mathrm{t}\,(\omega_1-\omega_0)\,,1-\delta\mathrm{t}\,(\omega_0+\omega_1)\,;1-2\delta\mathrm{t}\omega_0;-e^{T/\delta\mathrm{t}}\right)\Bigg)\Bigg)^{-1}
\end{aligned}
\tag{D.19}
$$

D.3 Solutions for ρ^2

Let us check that the set of adiabatic initial conditions chosen for $u(\tau)$ and $v(\tau)$ in (D.6), (D.9), (D.13), and (D.16) and thus $\rho^2(\tau)$ in (D.2) are consistent with choosing adiabatic initial conditions for $\rho^2(\tau)$ without reference to $u(\tau)$ and $v(\tau)$. Since the equation for $\rho^2(\tau)$ is (D.2), when $\tau \to T$ we have the first initial condition

$$\rho^2(\tau) \to u_{ad}(T)v_{ad}(T) = \frac{1}{f(T)} = \rho^2_{ad}(T) \tag{D.20}$$

where

$$\rho^2_{ad}(\tau) \equiv \frac{1}{f(\tau)} \tag{D.21}$$

The second initial condition uses $\partial_\tau \rho^2(\tau)$ where

$$\partial_\tau \rho^2(\tau) \;\; = \;\; v(\tau)\partial_\tau u(\tau) + u(\tau)\partial_\tau v(\tau) \tag{D.22}$$

Taking $\tau \to T$ yields

$$\begin{aligned}
\partial_\tau \rho^2(\tau) \;\; &\to \;\; v_{ad}(T)\partial_\tau u(T) + u_{ad}(T)\partial_\tau v(T) \\
&= \;\; v_{ad}(T)\partial_\tau u_{ad}(T) + u_{ad}(T)\partial_\tau v_{ad}(T) \\
&= \;\; \left(f(T) - \frac{\partial_\tau f(T)}{2f(T)}\right)u_{ad}(T)v_{ad}(T) + \left(- f(T) - \frac{\partial_\tau f(T)}{2f(T)}\right)u_{ad}(T)v_{ad}(T) \\
&= \;\; -\frac{\partial_\tau f(T)}{f(T)^2} \\
&= \;\; \partial_\tau \rho^2_{ad}(T)
\end{aligned} \tag{D.23}$$

where

$$\partial_\tau \rho^2_{ad}(\tau) = -\frac{\partial_\tau f(\tau)}{f(\tau)^2} \tag{D.24}$$

Therefore, we see that the set of initial conditions for $u(\tau)$ and $v(\tau)$ respectively are consistent with choosing $\rho^2(T) = \rho^2_{ad}(T) = \frac{1}{f(T)}$ and $\partial_\tau \rho^2(T) = \partial_\tau \rho^2_{ad}(T) = -\frac{\partial_\tau f(T)}{f(T)^2}$ without referring to the functions $u(\tau), v(\tau)$. Therefore the solution for $\rho^2(\tau)$ is

$$\rho^2(\tau) = u(\tau)v(\tau) \tag{D.25}$$

with $u(\tau)$ and $v(\tau)$ given in (D.10), (D.17), (D.12), (D.19) and (D.7).

Appendix E
Smooth Pulse and Dip protocols $\omega_0 \rightarrow \omega_1 \rightarrow \omega_0$

Performing similar computations as for the smooth step protocols in the previous section we solve for $\rho^2(\tau)$ for a smooth pulse for $\omega_0 \rightarrow \omega_1 \rightarrow \omega_0$. $f(\tau)^2$ is given by

$$f(\tau)^2 = \omega_1^2 + (\omega_0^2 - \omega_1^2)\tanh^2 \frac{\tau}{\delta t} \tag{E.1}$$

We again apply adiabatic initial conditions for $u(\tau)$ and $v(\tau)$ at some early time T sufficiently smaller than 0. We obtain

$$\rho^2(\tau) = u(\tau)v(\tau) \tag{E.2}$$

The solutions for u, v are given

$$\begin{aligned} u(\tau) &= A'u'(\tau) + B'v'(\tau) \\ v(\tau) &= Au'(\tau) + Bv'(\tau) \end{aligned} \tag{E.3}$$

with

$$\begin{aligned} u'(\tau) &= P_\nu^\mu(\tanh \frac{\tau}{\delta t}) \\ v'(\tau) &= Q_\nu^\mu(\tanh \frac{\tau}{\delta t}) \end{aligned} \tag{E.4}$$

and

$$\begin{aligned} \mu &= \omega_0 \delta t \\ \nu &= \frac{1}{2}(-1 + \sqrt{1 + 4\delta t^2(\omega_0^2 - \omega_1^2)}) \end{aligned} \tag{E.5}$$

$u'(\tau)$ and $v'(\tau)$ are solutions of

$$\begin{aligned} \frac{d^2u'}{d\tau^2} - f(\tau)^2 u' &= 0 \\ \frac{d^2v'}{d\tau^2} - f(\tau)^2 v' &= 0 \end{aligned} \tag{E.6}$$

with $f(\tau)$ given in (E.1). $P_\nu^\mu(z)$ and $Q_\nu^\mu(z)$ are associated Legendre Polynomials of the first and second kind respectively. The coefficients A', B', A, B are given by the expressions

$$
\begin{aligned}
&A' = \\
&- e^{\tilde{F}(T,\delta t,\omega_0,\omega_1)} \\
&\Bigg[- \left(1 - 2\delta t\omega_0 + \sqrt{1 + 4\delta t^2(\omega_0^2 - \omega_1^2)}\right)\left(- \omega_0^2 + (\omega_0^2 - \omega_1^2)\mathrm{sech}^2\left(\frac{T}{\delta t}\right)\right) Q^{\mu}_{1+\nu}(\tanh\frac{T}{\delta t}) \\
&+ \Bigg(- \omega_0^2\left(1 + \sqrt{1 + 4\delta t^2(\omega_0^2 - \omega_1^2)}\right)\tanh\frac{T}{\delta t} + \mathrm{sech}^2\frac{T}{\delta t}\Bigg(- \delta t(\omega_0^2 - 2\omega_1^2)\sqrt{\omega_0^2 + (\omega_1^2 - \omega_0^2)\mathrm{sech}^2\frac{T}{\delta t}} \\
&\quad + \delta t\omega_0^2\cosh\frac{2T}{\delta t}\sqrt{\omega_0^2 + (\omega_1^2 - \omega_0^2)\mathrm{sech}^2\frac{T}{\delta t}} + (\omega_0^2 - \omega_1^2)\sqrt{1 + 4\delta t^2(\omega_0^2 - \omega_1^2)}\tanh\frac{T}{\delta t}\Bigg)\Bigg) Q^{\mu}_{\nu}(\tanh\frac{T}{\delta t})\Bigg] \\
&\times \Bigg[\left(1 - 2\delta t\omega_0 + \sqrt{1 + 4\delta t^2(\omega_0^2 - \omega_1^2)}\right)\left(\omega_0^2 + (-\omega_0^2 + \omega_1^2)\mathrm{sech}^2\frac{T}{\delta t}\right)^{\frac{5}{4}} \\
&\qquad \left(P^{\mu}_{1+\nu}(\tanh\frac{T}{\delta t})Q^{\mu}_{\nu}(\tanh\frac{T}{\delta t}) - P^{\mu}_{\nu}(\tanh\frac{T}{\delta t})Q^{\mu}_{1+\nu}(\tanh\frac{T}{\delta t})\right)\Bigg]^{-1}
\end{aligned}
$$

$$
\begin{aligned}
&B' = \\
&- e^{\tilde{F}(T,\delta t,\omega_0,\omega_1)}\mathrm{sech}^2\frac{T}{\delta t} \\
&\Bigg[2\left(1 - 2\delta t\omega_0 + \sqrt{1 + 4\delta t^2(\omega_0^2 - \omega_1^2)}\right)\left(- \omega_0^2 + 2\omega_1^2 + \omega_0^2\cosh\left(\frac{2T}{\delta t}\right)\right) P^{\mu}_{1+\nu}(\tanh\frac{T}{\delta t}) \\
&+ \Bigg(- \omega_0^2\sinh\frac{2T}{\delta t} - (\omega_0^2 - 2\omega_1^2)\Bigg(- \sqrt{1 + 4\delta t^2(\omega_0^2 - \omega_1^2)}\tanh\frac{T}{\delta t} + 2\delta t\sqrt{\omega_0^2 + (\omega_1^2 - \omega_0^2)\mathrm{sech}^2\frac{T}{\delta t}}\Bigg) \\
&\quad + \omega_0^2\cosh\frac{2T}{\delta t}\Bigg(- \sqrt{1 + 4\delta t^2(\omega_0^2 - \omega_1^2)}\tanh\frac{T}{\delta t} + 2\delta t\sqrt{\omega_0^2 + (\omega_1^2 - \omega_0^2)\mathrm{sech}^2\frac{T}{\delta t}}\Bigg)\Bigg) 2P^{\mu}_{\nu}(\tanh\frac{T}{\delta t})\Bigg] \\
&\times \Bigg[4\left(1 - 2\delta t\omega_0 + \sqrt{1 + 4\delta t^2(\omega_0^2 - \omega_1^2)}\right) \\
&\qquad \left(P^{\mu}_{1+\nu}(\tanh\frac{T}{\delta t})Q^{\mu}_{\nu}(\tanh\frac{T}{\delta t}) - P^{\mu}_{\nu}(\tanh\frac{T}{\delta t})Q^{\mu}_{1+\nu}(\tanh\frac{T}{\delta t})\right)\Bigg]^{-1}
\end{aligned}
\tag{E.7}
$$

$$
\begin{aligned}
&A = \\
&e^{-\tilde{F}(T,\delta t,\omega_0,\omega_1)}\mathrm{sech}^2\frac{T}{\delta t} \\
&\Bigg[-2\bigg(1-2\delta t\omega_0+\sqrt{1+4\delta t^2(\omega_0^2-\omega_1^2)}\bigg)\bigg(-\omega_0^2+2\omega_1^2+\omega_0^2\cosh\Big(\frac{2T}{\delta t}\Big)\bigg)Q^{\mu}_{1+\nu}(\tanh\frac{T}{\delta t}) \\
&+\bigg(-2\delta t\big(\omega_0^2-4\omega_1^2\big)\cosh\frac{T}{\delta t}\sqrt{\omega_0^2+(\omega_1^2-\omega_0^2)\mathrm{sech}^2\frac{T}{\delta t}}+2\delta t\omega_0^2\cosh\frac{3T}{\delta t}\sqrt{\omega_0^2+(\omega_1^2-\omega_0^2)\mathrm{sech}^2\frac{T}{\delta t}} \\
&\quad+2\sinh\frac{T}{\delta t}\bigg(-(\omega_0^2-2\omega_1^2)\sqrt{1+4\delta t^2(\omega_0^2-\omega_1^2)}+\omega_0^2\bigg(1+\bigg(1+\sqrt{1+4\delta t^2(\omega_0^2-\omega_1^2)}\bigg)\cosh\frac{2T}{\delta t}\bigg)\bigg)\bigg) \\
&\quad\times\mathrm{sech}\frac{T}{\delta t}Q^{\mu}_{\nu}(\tanh\frac{T}{\delta t})\Bigg] \\
&\times\Bigg[4\bigg(1-2\delta t\omega_0+\sqrt{1+4\delta t^2(\omega_0^2-\omega_1^2)}\bigg)\bigg(\omega_0^2+(\omega_1^2-\omega_0^2)\mathrm{sech}^2\frac{T}{\delta t}\bigg)^{\frac{5}{4}} \\
&\qquad\bigg(P^{\mu}_{1+\nu}(\tanh\frac{T}{\delta t})Q^{\mu}_{\nu}(\tanh\frac{T}{\delta t})-P^{\mu}_{\nu}(\tanh\frac{T}{\delta t})Q^{\mu}_{1+\nu}(\tanh\frac{T}{\delta t})\bigg)\Bigg]^{-1}
\end{aligned}
$$

$$
\begin{aligned}
&B = \\
&-e^{-\tilde{F}(T,\delta t,\omega_0,\omega_1)}\mathrm{sech}^2\frac{T}{\delta t} \\
&\Bigg[-2\bigg(1-2\delta t\omega_0+\sqrt{1+4\delta t^2(\omega_0^2-\omega_1^2)}\bigg)\bigg(-\omega_0^2+2\omega_1^2+\omega_0^2\cosh\Big(\frac{2T}{\delta t}\Big)\bigg)P^{\mu}_{1+\nu}(\tanh\frac{T}{\delta t}) \\
&+\bigg(-2\delta t\big(\omega_0^2-4\omega_1^2\big)\cosh\frac{T}{\delta t}\sqrt{\omega_0^2+(\omega_1^2-\omega_0^2)\mathrm{sech}^2\frac{T}{\delta t}}+2\delta t\omega_0^2\cosh\frac{3T}{\delta t}\sqrt{\omega_0^2+(\omega_1^2-\omega_0^2)\mathrm{sech}^2\frac{T}{\delta t}} \\
&\quad+2\sinh\frac{T}{\delta t}\bigg(-(\omega_0^2-2\omega_1^2)\sqrt{1+4\delta t^2(\omega_0^2-\omega_1^2)}+\omega_0^2\bigg(1+\bigg(1+\sqrt{1+4\delta t^2(\omega_0^2-\omega_1^2)}\bigg)\cosh\frac{2T}{\delta t}\bigg)\bigg)\bigg) \\
&\quad\times\mathrm{sech}\frac{T}{\delta t}P^{\mu}_{\nu}(\tanh\frac{T}{\delta t})\Bigg] \\
&\times\Bigg[4\bigg(1-2\delta t\omega_0+\sqrt{1+4\delta t^2(\omega_0^2-\omega_1^2)}\bigg)\bigg(\omega_0^2+(\omega_1^2-\omega_0^2)\mathrm{sech}^2\frac{T}{\delta t}\bigg)^{\frac{5}{4}} \\
&\qquad\bigg(P^{\mu}_{1+\nu}(\tanh\frac{T}{\delta t})Q^{\mu}_{\nu}(\tanh\frac{T}{\delta t})-P^{\mu}_{\nu}(\tanh\frac{T}{\delta t})Q^{\mu}_{1+\nu}(\tanh\frac{T}{\delta t})\bigg)\Bigg]^{-1}
\end{aligned}
\tag{E.8}
$$

where

$$
\begin{aligned}
&\tilde{F}(T,\delta t,\omega_0,\omega_1) = \\
&\delta t\bigg(\omega_0\sinh^{-1}(\frac{\omega_0}{\omega_1}\sinh(\frac{T}{\delta t}))+\sqrt{\omega_1^2-\omega_0^2}\tan^{-1}\bigg(\frac{\sqrt{-2\omega_0^2+2\omega_1^2}\sinh\frac{T}{\delta t}}{\sqrt{-\omega_0^2+2\omega_1^2+\omega_0^2\cosh(\frac{2T}{\delta t})}}\bigg)\bigg)
\end{aligned}
$$

Appendix F
Phase space density for a potential with a cutoff

In this part we explain in detail the fermi surface profiles for a potential with a cutoff at $x = \pm l/2$. Without loss of generality, we consider coordinate (x, p) on the left and up side of phase space.

After abrupt quench, the equi-energy trajectories become

$$\frac{1}{2}p^2 - \frac{1}{2}\omega_1^2 x^2 = E \tag{F.1}$$

which can be described by hyperbolic functions

$$\begin{cases} x = \frac{\sqrt{2E}}{\omega_1}\sinh(\omega_1\tau + \phi), \\ p = \sqrt{2E}\cosh(\omega_1\tau + \phi), \end{cases} (E > 0) \& \begin{cases} x = -\frac{\sqrt{-2E}}{\omega_1}\cosh(\omega_1\tau + \phi), \\ p = -\sqrt{-2E}\sinh(\omega_1\tau + \phi), \end{cases} (E < 0) \tag{F.2}$$

Here the energy E and phase ϕ are two independent parameters determined by the continuity of phase space trajectories, i.e. the continuity of (x, p) during the abrupt quench.

Now, because the potential has cutoffs at $x = \pm l/2$, all the classical particles should be bounced back. This implies that the $(x = \pm l/2, p)$ and $(x = \pm l/2, -p)$ are identical in phase space. In terms of E and ϕ, the reflection of particles at the boundary only change the phase ϕ, and the coordinates of the particle in phase space after reflection can be described by

$$\begin{cases} x = -\frac{\sqrt{2E}}{\omega_1}\sinh(\omega_1(\tau - \tau_l) - \phi_l), \\ p = -\sqrt{2E}\cosh(\omega_1(\tau - \tau_l) - \phi_l) \end{cases} (E > 0) \\ \& \begin{cases} x = -\frac{\sqrt{-2E}}{\omega_1}\cosh(\omega_1(\tau - \tau_l) - \phi_l), \\ p = -\sqrt{-2E}\sinh(\omega_1(\tau - \tau_l) - \phi_l), \end{cases} (E < 0) \tag{F.3}$$

where τ_l is the time the particle needs to reach the boundary to be reflected, and ϕ_l is the phase of the particle at the boundary before reflection (after reflection the phase becomes $-\phi_l$). Thus they satisfy the relation

$$\phi_l = \omega_1\tau_l + \phi \tag{F.4}$$

Therefore, we can simplify (F.3) and find that the reflection is equivalent to the transformation on E and ϕ:

$$E \to E, \quad \& \quad \phi \to \phi - 2\phi_l \tag{F.5}$$

Now we can rewrite the coordinates of the particle that bounced back as

$$\begin{cases} x_b = -x\cosh 2\phi_l + \frac{1}{\omega_1}p\sinh 2\phi_l \\ p_b = -p\cosh 2\phi_l + \omega_1 x\sinh 2\phi_l \end{cases} (E > 0) \\ \& \begin{cases} x_b = x\cosh 2\phi_l - \frac{1}{\omega_1}p\sinh 2\phi_l \\ p_b = p\cosh 2\phi_l - \omega_1 x\sinh 2\phi_l, \end{cases} (E < 0) \tag{F.6}$$

which implies a boost

$$K = \begin{pmatrix} \cosh 2\phi_l & -\sinh 2\phi_l \\ -\sinh 2\phi_l & \cosh 2\phi_l \end{pmatrix} \tag{F.7}$$

from $(x, p/\omega_1)$ to $(x_b, p_b/\omega_1)$. For $E > 0$, the boost is $-K$; for $E < 0$, it is K. The boost can be applied to the coordinates of the particles after the n-th reflection to obtain the coordinates after the $(n+1)$-th reflection. The inverse boost is

$$K^{-1} = \begin{pmatrix} \cosh 2\phi_l & \sinh 2\phi_l \\ \sinh 2\phi_l & \cosh 2\phi_l \end{pmatrix} \tag{F.8}$$

and therefore,

$$\begin{aligned} &\begin{cases} x = -x_b \cosh 2\phi_l - \frac{1}{\omega_1} p_b \sinh 2\phi_l \\ p = -p_b \cosh 2\phi_l - \omega_1 x_b \sinh 2\phi_l \end{cases} \quad (E > 0) \\ \& &\begin{cases} x = x_b \cosh 2\phi_l + \frac{1}{\omega_1} p_b \sinh 2\phi_l \\ p = p_b \cosh 2\phi_l + \omega_1 x_b \sinh 2\phi_l, \end{cases} \quad (E < 0) \end{aligned} \tag{F.9}$$

We can figure out the matrix element from $x = \pm l/2$

$$\begin{aligned} \left(\frac{l}{2}\right)^2 &= \frac{2E}{\omega_1^2} \sinh^2 \phi_l \Longrightarrow \cosh 2\phi_l = 1 + 2\sinh^2 \phi_l = 1 + \frac{\omega_1^2 l^2}{4E}, \quad (E > 0) \\ \left(\frac{l}{2}\right)^2 &= \frac{-2E}{\omega_1^2} \cosh^2 \phi_l \Longrightarrow \cosh 2\phi_l = 2\cosh^2 \phi_l - 1 = -1 - \frac{\omega_1^2 l^2}{4E}. \quad (E < 0) \end{aligned} \tag{F.10}$$

Notice that the Fermi surface for an unbounded potential satisfies (4.55), we can plug (F.9) in and obtain the relation satisfied by particle reflected back once:

$$\begin{aligned} &\left(x \cosh 2\phi_l + \frac{1}{\omega_1} p \sinh 2\phi_l\right)^2 \\ &- \left[\rho(\tau)^2 \left(p \cosh 2\phi_l + \omega_1 x \sinh 2\phi_l\right) - \frac{1}{2}\left(x \cosh 2\phi_l + \frac{1}{\omega_1} p \sinh 2\phi_l\right) \partial_\tau \rho^2\right]^2 = \rho(\tau)^2 \end{aligned} \tag{F.11}$$

Here we have omitted the lower index "b" since (F.11) represents part of the Fermi surface at τ. The complete Fermi surface after quench is a combination of (F.11) and (4.55) and $x = \pm l/2$.

Finally we consider two cases: $\omega_0 > \omega_1$ and $\omega_0 < \omega_1$. For $\omega_0 > \omega_1$, more particles flow in from the upper side (where $E > 0$) than flow out from the lower side (where $E > 0$) when there is no cutoff. This implies that when there is a cutoff, less particles should flow in and therefore, the Fermi surface due to reflection should give a third

bound for the Fermi surface. As a result, the phase space density should be

$$\begin{aligned} u =&\Theta\left(\frac{x^2}{\rho^2}-\frac{1}{\rho^2}\left(p\rho^2-\frac{1}{2}x\partial_\tau\rho^2\right)^2-1\right)\\ &\Theta\left(\frac{1}{\rho^2}\left(x\cosh 2\phi_l+\frac{1}{\omega_1}p\sinh 2\phi_l\right)^2\right.\\ &\left.-\frac{1}{\rho^2}\left(\left[p\cosh 2\phi_l+\omega_1 x\sinh 2\phi_l\right]\rho^2-\frac{1}{2}\left[x\cosh 2\phi_l+\frac{1}{\omega_1}p\sinh 2\phi_l\right]\partial_\tau\rho^2\right)^2-1\right) \end{aligned} \tag{F.12}$$

where $\cosh 2\phi_l = 1+\frac{\omega_1^2 l^2}{4E}$, $E>0$. The phase space density is shown in figure 4.12.

For $\omega_0 < \omega_1$, no particles flow in from the upper side (where $E<0$) while many particles flow out from the lower side (where $E<0$) when there is no cutoff. Therefore, when there is a cutoff, particles reflected should flow in from the upper side and occupy the empty space. As a result, the phase space density should be

$$\begin{aligned} u =&\Theta\left(\frac{x^2}{\rho^2}-\frac{1}{\rho^2}\left(p\rho^2-\frac{1}{2}x\partial_\tau\rho^2\right)^2-1\right)\\ &+\Theta\left(\frac{1}{\rho^2}\left(x\cosh 2\phi_l+\frac{1}{\omega_1}p\sinh 2\phi_l\right)^2\right.\\ &\left.-\frac{1}{\rho^2}\left(\left[p\cosh 2\phi_l+\omega_1 x\sinh 2\phi_l\right]\rho^2-\frac{1}{2}\left[x\cosh 2\phi_l+\frac{1}{\omega_1}p\sinh 2\phi_l\right]\partial_\tau\rho^2\right)^2-1\right)\\ &-\Theta\left(\frac{x^2}{\rho^2}-\frac{1}{\rho^2}\left(p\rho^2-\frac{1}{2}x\partial_\tau\rho^2\right)^2-1\right)\\ &\times\Theta\left(\frac{1}{\rho^2}\left(x\cosh 2\phi_l+\frac{1}{\omega_1}p\sinh 2\phi_l\right)^2\right.\\ &\left.-\frac{1}{\rho^2}\left(\left[p\cosh 2\phi_l+\omega_1 x\sinh 2\phi_l\right]\rho^2-\frac{1}{2}\left[x\cosh 2\phi_l+\frac{1}{\omega_1}p\sinh 2\phi_l\right]\partial_\tau\rho^2\right)^2-1\right) \end{aligned} \tag{F.13}$$

where $\cosh 2\phi_l = -1-\frac{\omega_1^2 l^2}{4E}$, $E<0$. The phase space density is shown in figure 4.11.

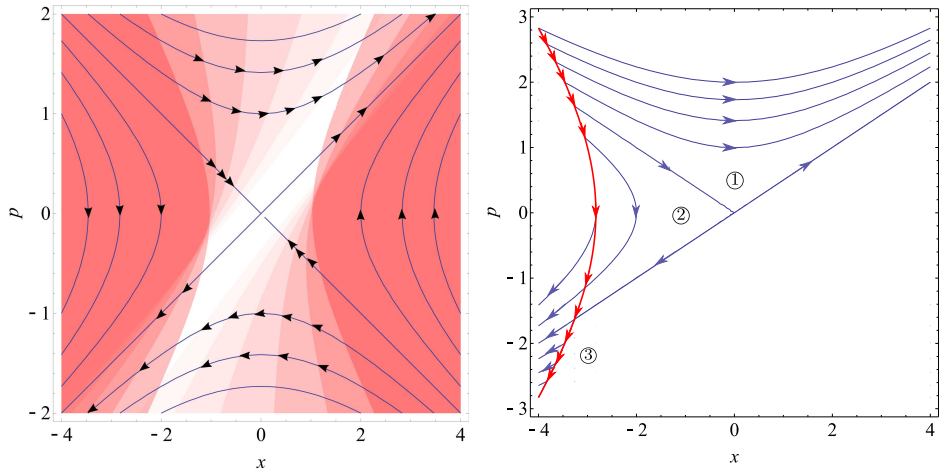

(a) $\omega_0 = 2\omega_1 = 1$

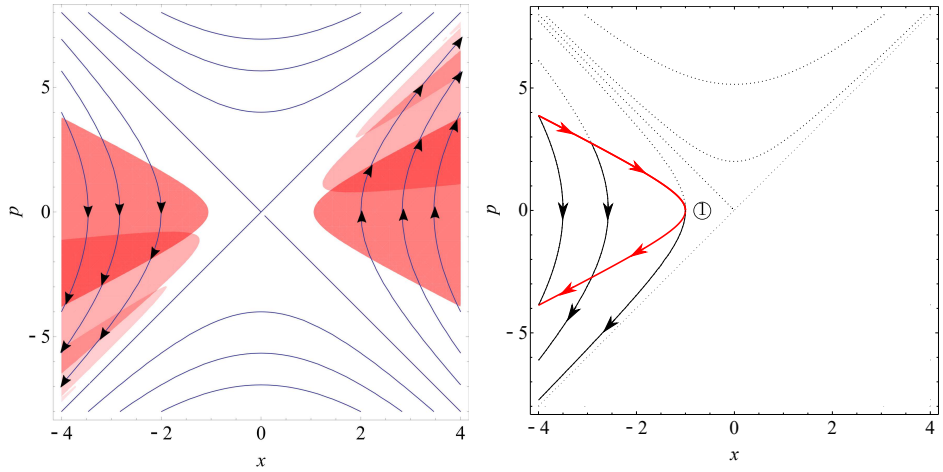

(b) $\omega_0 = \omega_1/2 = 1$

Figure F.1: The formation of Fermi surface (4.55). Left: the Fermi surfaces are plotted more transparently as time evolves. Solid lines are equi-energy surfaces i.e. the trajectories of classical particles after abrupt quench. The directions of particle motion are labeled by arrows. Right: the original Fermi surface when $\tau \leq 0$ is plotted in solid red with arrows pointing in the directions of classical particles. Blue or black solid lines are the trajectories of classical particles after abrupt quench. The orientations of motion are labeled by arrows. Dashed black lines are equi-energy surfaces.

Appendix G
Details of construction of sub-algebras

This appendix provides some details of the gauge invariant construction of the sub-algebra described in Section 5.2.

G.1 Single Matrix

First consider gauged matrix quantum mechanics of a single $N \times N$ matrix M. Gauge invariant single trace operators are of the form

$$\hat{C} = \mathrm{Tr}\left(\hat{M}^m \hat{\Pi}_M^n\right)_{\mathrm{order}} \tag{G.1}$$

Here $\hat{\Pi}_M$ denotes the conjugate momentum to $\hat{M}$ and the notation $()_{\mathrm{order}}$ means that the $\hat{M}$ and $\hat{\Pi}_M$'s are sprinkled in all possible orders. However we can use the commutation relations to bring e.g. all the $\hat{M}$'s together. The trace Tr is over matrix indices.

We want to construct a sub-algebra of operators which can be used to make measurements in a region A of the space of eigenvalues of $\hat{M}$. This is achieved by defining the projector (5.23). Then the operator which will belong to this algebra is of the form

$$\hat{C}_A = \mathrm{Tr}\left(\hat{P}_A M \hat{P}_A M \cdots \hat{P}_A M \hat{P}_A \hat{\Pi}_M \hat{P}_A \cdots \hat{\Pi}_M \hat{P}_A\right) \tag{G.2}$$

In writing (G.2) we have used $\hat{P}_A^2 = \hat{P}_A$ and the fact that in this particular case $\left[\hat{P}_A, \hat{M}\right] = 0$. The operators of the form (G.2) together with the identity operator form a sub-algebra of operators of the theory.

To see that gives us the right sub-algebra, fix a gauge where $\hat{M}$ is diagonal with its diagonal elements denoted by $\hat{\lambda}_i, i = 1 \cdots N$, while the diagonal elements of the conjugate momenta are denoted by $\hat{\pi}_i$. As explained in Section 5.2.1, the resulting constraint requires the states to be singlets. The remaining gauge freedom of Weyl transformations needs to be imposed by Weyl symmetrizing the states, and absorbing the standard van der Monde factor then makes $\hat{\lambda}_i$ coordinate operators of N fermions on a line. Let us begin by considering operators which do not contain the conjugate momenta, i.e.

$$\mathcal{O}_n = \mathrm{Tr}(\hat{M}^n) \tag{G.3}$$

The expectation value of the operator $\mathcal{O}_n$ in some pure state $|\Psi\rangle$ is given by

$$\sum_{i=1}^{N} \langle \Psi | \hat{\lambda}_i^n | \Psi \rangle \tag{G.4}$$

This measures the position of each of the fermions, takes its n-th power and then sums over all the particles. Similarly, the expectation value of $\mathrm{Tr}(\hat{\pi}_M^n)$ would measure

the sum of n-th power of the momenta of all the fermions. This is of course a standard measurement in a system of many identical particles. The projected version of the operator (G.3) is

$$\mathcal{O}_n^P = \sum_{i=1}^{N} \int_A [\prod_{s=1}^{n} dx_s][\prod_{s=1}^{n} \delta(x_s - \hat{\lambda}_i)]\hat{\lambda}_i^n \tag{G.5}$$

We will use the basis

$$|\lambda_1, \lambda_2, \cdots \lambda_N >_a = \frac{1}{N!} \sum_{\sigma \in S_N} \mathrm{sgn}(\sigma) |\lambda_{\sigma(1)}, \cdots \lambda_{\sigma(1)}\rangle \tag{G.6}$$

where $|\rangle_a$ denotes an anti-symmetrized ket. Note that this is *not* an eigenstate of each individual term in the sum in (G.5). However it *is* an eigenstate of the sum. This follows from the fact that the sum is symmetric under permutations.

Consider first the case $N = 2$. The expectation value of the operator $\mathcal{O}_3^P$ in a state with a wavefunction $\Psi(\lambda_1, \lambda_2)$ is given by

$$\begin{aligned}\langle\Psi|\mathcal{O}_3^P|\Psi\rangle = \int_A [dx_1 dx_2 dx_3] \int_R d\lambda_1 d\lambda_2 \; \Psi^\star(\lambda_1, \lambda_2)\{\lambda_1^3 \; \delta(x_1 - \lambda_1)\delta(x_2 - \lambda_1)\delta(x_3 - \lambda_1) \\ + \lambda_2^3 \; \delta(x_1 - \lambda_2)\delta(x_2 - \lambda_2)\delta(x_3 - \lambda_2)\}\Psi(\lambda_1, \lambda_2)\end{aligned} \tag{G.7}$$

where the wavefunction is $\Psi[\lambda_1 \cdots \lambda_N] = \langle\{\lambda_i\}|\Psi\rangle$. where we have used antisymmetry of the wavefunctions. The integrals over λ_1 and λ_2 are over the entire real line. Writing each of these integrals as a sum over an integral over A and an integral over the complement $\bar{A}$, and noting that the delta functions ensure that only the integrals over A contribute, it is straightforward to see that the result is

$$\begin{aligned}\langle\Psi|\mathcal{O}_3^P|\Psi\rangle = \int_A d\lambda_1 \int_A d\lambda_2 \Psi^\star(\lambda_1, \lambda_2)(\lambda_1^3 + \lambda_2^3)\Psi(\lambda_1, \lambda_2) \\ + 2\int_A d\lambda_1 \int_{\bar{A}} d\lambda_2 \Psi^\star(\lambda_1, \lambda_2)(\lambda_1^3)\Psi(\lambda_1, \lambda_2)\end{aligned} \tag{G.8}$$

The first term is the contribution from configurations when both the particles are in the region of interest, while the second term from configurations where one of the particles is in the region of interest. Clearly this expectation value is equal to the expectation value of the operator without the projection if the wavefunction is non-vanishing only when *both* the particles are in the region of interest A.

This result can be easily generalized for arbitrary N. Then the expectation value of the operator $\mathcal{O}_n^P$ becomes

$$\langle\Psi|\mathcal{O}_n^P|\Psi\rangle = \sum_{k=1}^{N} \binom{N}{k} \sum_{a=1}^{k} \int_A \prod_{a=1}^{k} d\lambda_a \int_{\bar{A}} \prod_{\alpha=k+1}^{N} d\lambda_\alpha \; (\Psi^\star[\{\lambda_i\}] \; \lambda_a^n \; \Psi[\{\lambda_i\}]) \tag{G.9}$$

The expression (G.9) is a sum over sectors specified by the number of the λ_i's in the region of interest. The expectation value then measures the sum of the n-th power

of the position of all particles *which are in the region of interest*. Equation (G.9) is simply a reflection of the decomposition of the Hilbert space into sectors, as in (5.10).

The action of our projected operator on a basis state is

$$\mathcal{O}_n^P|\{\lambda_i\}\rangle_a = \sum_{i=1}^{N}\int [\prod_{s=1}^{n} dx_s][\prod_{s=1}^{n}\delta(x_s-\lambda_i)]\lambda_i^n|\{\lambda_i\}\rangle_a \tag{G.10}$$

Suppose the state is in the $(k, N-k)$ sector, i.e. k of the λ_i's lie in the region of interest. We can choose these to be the $\lambda_a, a = 1\cdots k$. Consider a term in the sum in (G.10). This contains a product of delta functions, so this will be nonzero only when the corresponding λ_i lie in the region of interest A. This means that the sum over i is truncated to the first k terms,

$$\mathcal{O}_n^P|\{\lambda_i\}\rangle_a = \sum_{i=1}^{k}\lambda_i^m|\{\lambda_i\}\rangle_a \tag{G.11}$$

Thus this operator acting on a basis state in the $(k, N-k)$ sector has a trivial action on the eigenvalues which are in the complement $\bar{A}$. This is an example of an operator of the type $(k, N-k)$,

$$\mathcal{O}_{k,N-k}\ |\{\lambda_a\},\{\lambda_\alpha\}\rangle_a = \int\prod_{a=1}^{k}[d\lambda_a']\ \tilde{O}\left(\{\lambda_a'\},\{\lambda_a\}\right)\ |\{\lambda_a'\},\{\lambda_\alpha\}\rangle_a \tag{G.12}$$

Let us define a smaller Hilbert space of k particles which s spanned by

$$|\{\lambda_a\}\rangle_a \qquad a = 1\cdots k\ \ \lambda_a \in A \tag{G.13}$$

Then one can define an operator in this smaller Hilbert space,

$$\tilde{\mathcal{O}}_{k,N-k} = \int[\prod_{a=1}^{k} d\lambda_a d\lambda_a']\ \tilde{O}_{k,N-k}\left(\{\lambda_a\},\{\lambda_a'\}\right)\ |\{\lambda_a\}\rangle_a\ {}_a\langle\{\lambda_a'\}| \tag{G.14}$$

In the above discussion the sector $(0, N)$ did not enter in the expression (G.9). This simply reflects the fact that if we measure any operator involving the position and momenta in the region of interest A, we should get a non-zero answer only if there are particles in A. However since the identity operator is also a member of the sub-algebra, this sector needs to be included. In fact the identity operator is the only operator which will receive contributions from the $(0, N)$ sector.

Clearly the expression (G.9) can be written as a sum over traces in the smaller Hilbert spaces,

$$\langle\Psi|\mathcal{O}^P|\Psi\rangle = \sum_{k=1}^{N-1}\mathrm{Tr}_A\left[\tilde{\rho}_{k,N-k}\mathcal{O}_{k,N-k}\right] \tag{G.15}$$

where the density matrix $\tilde{\rho}_{k,N-k}$ is given by

$$\tilde{\rho}_{k,N-k} = \binom{N}{k}\int_A[\prod_{i=1}^{k} d\lambda_a d\lambda_a']\int_{\bar{A}}[\prod_{\alpha=k+1}^{N} d\lambda_\alpha]\ \Psi^\star[\{\lambda_a\},\{\lambda_\alpha\}]\ \Psi^\star[\{\lambda_a'\},\{\lambda_\alpha\}]|\{\lambda_a\}\rangle_a\ {}_a\langle\{\lambda_a'\}| \tag{G.16}$$

Note that this is an operator which lives in the k-particle sector of the small Hilbert space defined in (G.13). This decomposition of the whole hilbert space into sectors is exactly what appears in [21]. The projected operators therefore provide a gauge invariant formulation of the problem.

The above constructions easily generalize to the situation when the state of the entire system is a mixed state. Let the density matrix of the whole system be

$$\rho_{tot} = \int [\prod_{i=1}^{N} d\lambda_i d\lambda_i'] \ \rho_{tot}\left(\{\lambda_i\},\{\lambda_i'\}\right) \ |\{\lambda_i\}\rangle_a \ {}_a\langle\{\lambda_i'\}| \tag{G.17}$$

Then the reduced density matrix $\tilde{\rho}$ which evaluates expectation values of operators belonging to this subalgebra is obtained by tracing over $\bar{A}$,

$$\tilde{\rho}_{k,N-k} = \binom{N}{k} \int [\prod_{i=1}^{k} d\lambda_a d\lambda_a'][\prod_{\alpha=k+1}^{N} d\lambda_\alpha] \ \rho_{tot}\left(\{\lambda_a\},\{\lambda_\alpha\};\{\lambda_a'\},\{\lambda_\alpha\}\right) \ |\{\lambda_a\}\rangle_a \ {}_a\langle\{\lambda_a'\}| \tag{G.18}$$

This density matrix is not normalized. In fact the trace $\mathrm{Tr}_k\tilde{\rho}_k$ is the probability of k particles to be in the region of interest. Thus the density matrix in the Hilbert space which is a direct sum of all the sector is properly normalized.

The von Neumann entropy associated with the reduced density matrix $\mathrm{Tr}\tilde{\rho}_k$ is given by

$$S_{k,A} = -\mathrm{Tr}_{\mathcal{H}_{k,N-k}}(\tilde{\rho}_{k,N-k}\log\tilde{\rho}_{k,N-k}) \tag{G.19}$$

This quantifies the entanglement between the target space region A and its complement $\bar{A}$ in this sector. Following the above steps, we can easily see that a reduced density matrix $\rho_{_{RDM}}$ based on the gauge invariant subalgebra $\mathcal{A}$, defined by

$$\mathrm{Tr}(\rho_{_{RDM}}\mathcal{O}) := \mathrm{Tr}(\rho_{tot}\mathcal{O}) \quad \forall\mathcal{O}\in\mathcal{A}$$

satisfies

$$\rho_{_{RDM}} = \oplus_{k=0}^{N}\tilde{\rho}_{k,N-k}$$

The total target space entanglement entropy is then a sum over all sectors

$$S_A = \sum_{k=0}^{N} S_{k,A} \tag{G.20}$$

As shown in [21] this quantity satisfies the usual positivity properties and strong subadditivity. Similar sector-wise entanglement also appears in discussions of entanglement entropy in gauge theories [282, 283].

We have used a first quantized description of the system. However there is an equivalent second quantized description. In the latter, we have a conventional non-relativistic field theory of a fermion field $\psi(\lambda,t)$: the space of this theory is the space of eigenvalues. The target space entanglement we discussed above now becomes a conventional geometric entanglement in this field theory.

Momentum operators

Operators involving momenta are subtle and at a first sight, appear to require introduction of other sectors. This can be illustrated by a calculation of the expectation value of the projected version of an operator of the form (G.1) with $m = 0$ and $n = 2$, with the region of interest A being the positive real line $\lambda \geq 0$. The result of a calculation analogous to (G.8) is, for $N = 2$,

$$\begin{aligned}
&\langle\Psi|\,\mathrm{tr}(\hat{P}\hat{\Pi}_M\hat{P}\hat{\Pi}_M\hat{P})|\Psi\rangle \\
=&-\frac{1}{2}\int_0^\infty d\lambda_1\int_0^\infty d\lambda_2 \\
&\times\left[\Psi^*(\lambda_1,\lambda_2)\left(\frac{\partial^2}{\partial\lambda_1^2}+\frac{\partial^2}{\partial\lambda_2^2}\right)\Psi(\lambda_1,\lambda_2)+\Psi(\lambda_1,\lambda_2)\left(\frac{\partial^2}{\partial\lambda_1^2}+\frac{\partial^2}{\partial\lambda_2^2}\right)\Psi^*(\lambda_1,\lambda_2)\right] \\
&-\int_0^\infty d\lambda_1\int_{-\infty}^0 d\lambda_2\left[\Psi^*(\lambda_1,\lambda_2)\frac{\partial^2}{\partial\lambda_1^2}\Psi(\lambda_1,\lambda_2)+\Psi(\lambda_1,\lambda_2)\frac{\partial^2}{\partial\lambda_1^2}\Psi^*(\lambda_1,\lambda_2)\right] \\
&+\int_{-\infty}^\infty d\lambda\left(\frac{\partial}{\partial\lambda_1}|\Psi(\lambda_1,\lambda)|^2\right)\Big|_{\lambda_1=0}+2\delta(0)\int_{-\infty}^\infty d\lambda|\Psi(0,\lambda)|^2
\end{aligned} \tag{G.21}$$

The first and second lines of the RHS are analogous to what we got in G.8; the first line is the contribution from the $(2,0)$ sector, and the second line is the contribution from the $(1,1)$ sector. However, we appear to also have an extra line, the third line, which represents a sector that has one of the particles exactly at $\lambda = 0$.

Note that since these extra terms pertain to particles at the boundary, it is tied to the question of how one defines the region A precisely, e.g. as an open or a closed set, or in terms of a target space lattice etc. We suggest below an alternative treatment in terms of translation operators, rather than momenta, which provide a proof of principle how these problems can be avoided.

To explain this, let us start with the case of $N = 1$, that is, just the case of a single 1×1 matrix or equivalently the case of one particle. We now have just two sectors $(1,0)$ and $(0,1)$, in the first one the particle is in region A (which we will again define as $x > 0$) and in the second one it is outside.

Consider the traslation operator

$$O_a = \exp[-ia\hat{\Pi}] \tag{G.22}$$

with the action

$$O_a|x\rangle = |x + a\rangle \tag{G.23}$$

Clearly such operators can take states in $(1,0)$ to $(0,1)$ (if $a < 0$) or vice versa (if $a > 0$). In the following, we will take $a > 0$ to be specific; a similar analysis can be carried out with $a < 0$. To obtain operators acting within the sector $(1,0)$, let us use the projection $O_a \to O_a^P$. It is useful to represent G.22 in terms of the product of a large number n of exponentials (as in Feynman path integrals), with $a = n\epsilon$. In the limit of $\epsilon \to 0$, each exponential can be approximated as $\exp[-i\epsilon\hat{\Pi}] \approx 1 + (-i\epsilon)\hat{\Pi}$

whose projected version is $\hat{P}(1+(-i\epsilon)\hat{\Pi})\hat{P} \approx \hat{P}(\exp[-i\epsilon\hat{\Pi}])\hat{P}$. In short, we have

$$O_a \equiv \left(\exp[-i\epsilon\hat{\Pi}]\right)^n$$
$$O_a^P = \lim_{\epsilon\to 0}\left(\hat{P}\exp[-i\epsilon\hat{\Pi}]\hat{P}\right)^n$$

With the above expressions, it is easy to see that

$$\langle x'|O_a|x\rangle = \langle x'|x+a\rangle = \delta(x'-a-x) \tag{G.24}$$
$$\begin{aligned}\langle x'|O_a^P|x\rangle &= \lim_{\epsilon\to 0}\langle x'|\left(\hat{P}\exp[-i\epsilon\hat{\Pi}]\hat{P}\right)^n|x\rangle \\ &= \lim_{\epsilon\to 0}\theta(x')\langle x'-\epsilon|\theta(x'-\epsilon)\left(\hat{P}\exp[-i\epsilon\hat{\Pi}]\hat{P}\right)^{n-1}|x\rangle \\ &= \lim_{\epsilon\to 0}\theta(x')\theta(x'-\epsilon)\theta(x'-2\epsilon)...\theta(x'-a)\delta(x'-a-x)\end{aligned} \tag{G.25}$$

Note that unless x and x' are both in A, the above matrix element vanishes. This is because, say x is not in A while x' is in A, then at least $\theta(x) = \theta(x'-a)$ will vanish, making the entire product G.25 vanish.[1] On the other hand, if both x and x' *are* in A, then all the theta-functions in G.25 evaluate to 1 (since the arguments of the theta-functions are all located on a straight 'Feynman' path joining x and x' which are both in A which is convex). This leads to the original matrix element of O G.24 which described the case with no restrictions. There are no extra terms corresponding to particles located at $x = 0$.

Now, an observable corresponds to the hermitian operator is $\mathbf{O}_a = O_a + c.c.$, the projected operator being $\mathbf{O}_a^P = O_a^P + c.c.$. Their expectation values are given as follows. For a general wavefunction $\Psi(x)$

$$\begin{aligned}\langle\Psi|\mathbf{O}_a|\Psi\rangle &= \int_{-\infty}^{\infty} dx\,[\Psi^*(x)\Psi(x+a) + \Psi^*(x+a)\Psi(x)] \\ \langle\Psi|\mathbf{O}_a^P|\Psi\rangle &= \int_{0}^{\infty} dx\,[\Psi^*(x)\Psi(x+a) + \Psi^*(x+a)\Psi(x)]\end{aligned} \tag{G.26}$$

Note that the projected operator merely restricts the range of the integral to $x > 0$ as it should, and does not introduce any unwarranted boundary terms, unlike in G.21, corresponding to particles located at $x = 0$.

The generalization to $N > 1$ can be done as follows. Consider the translation operator $O_a = \exp[-ia\,\mathrm{Tr}\,\hat{\Pi}] = \exp[-ia\sum_{m=0}^{N}\hat{\Pi}_m]$. This operator is obviously gauge-invariant, since it involves $\mathrm{Tr}\,\hat{\Pi}$. In this case the above argument for $N = 1$ can be straightforwardly generalized. The position space matrix elements of O_a^P again involve a string of theta functions all located along a straight line from $X = (x_1, x_2, ...)$ to $X' = (x_1 + a, x_2 + a, ...)$, which all evaluate to 1 if both X and X' are in region A, i.e. both x_1 and $x_1 + a$ are positive.

[1] We avoid here the possibility $x = 0$ by assuming that the partition demarcating the region A does not fall on $x = 0$. This is equivalent to assuming a lattice structure of the real line such that none of the sites falls exactly on 0, which is possible for any lattice separation, however small. Presumably a similar reasoning can get rid of the boundary terms in G.21 as well.

Now the reader may justifiably point out that this is not the most general translation operator, since the above operator translates the point $(x_1, x_2, ...)$ by the same amount. This can be remedied by considering an operator $\exp[-i\,\mathrm{Tr}(A\hat{\Pi})]$ which evaluates to $\exp[-i\sum_{m=0}^{N} a_{mm}\hat{\Pi}_m]$. This clearly describes a most general translation. The operator is not gauge invariant, however, since A is a fixed matrix. To make it gauge invariant, one can sum over terms with Weyl-copies of A.[2]

We made these arguments in the context of a single matrix, but it is generalizable to multiple matrices too.

The above considerations provide a proof of principle that if we replace the momentum operators by appropriately defined 'translation' operators, then the problem pointed out at the beginning of this subsubsection can be taken care of.

G.2 Multiple Matrices

For multiple matrices we have two possible subalgebras which correspond to a given target space constraint.

A projector leading to the first sub-algebra is defined by (5.25), and the procedure to construct operators which belong to the sub-algebra is explained in section 5.2.2.The gauge choice which makes the physics most transparent is the one where the hermitian matrix $f(\hat{X}^I)$ is chosen to be diagonal. In this subsection we will discuss the simplest constraint where the function which appears in (5.25) is

$$F[\hat{X}] = X^1 \tag{G.27}$$

As in the single matrix example, we fix a $A_t = 0$ gauge and fix the remaining time independent gauge freedom by choosing $\hat{X}^1$ to be diagonal with diagonal elements are $\hat{\lambda}_i$. The remaining symmetries are Weyl transformations which permute the eigenvalues and the matrix elements of the other matrices, and $U(1)^N$ transformations as in (5.5) and (5.6). This symmetry is imposed by hand by adding the transforms in the states, as in (5.7). As in the single matrix case, this is an eigenstate of the traced operators of the form (5.31). Thus when $\hat{\mathcal{O}}^{P_1}$ acts on such a state, we can replace the operators appearing in (5.31) by their eigenvalues which we denote by the matrix without a hat.

Acting on a state where the λ_i for $i = 1 \cdots k$ are in the region A, the projected version of the operator $\hat{X}^I$ as defined in (5.28)

$$(X^I)_{ij}^{P_1} = \int dx_1 \delta(x_1 - \lambda_i) X_{ij}^I \int dx_2 (x_2 - \lambda_j) = \begin{cases} X_{ij}^I & \text{if } i,j = 1 \cdots k \\ 0 & \text{if otherwise} \end{cases}$$

Thus the projector projects each of the matrices to the $k \times k$ block, as depicted in (5.32).

[2] In the previous paragraph, $A = a\mathbf{1}$ which was automatically Weyl-invariant.

Consider, for example, an operator $\hat{\mathcal{O}}$ (as in (5.27) which is of the form $\mathcal{O} = \mathrm{Tr}(\hat{X}^I \hat{X}^J \hat{X}^K)$. The action of its projected version on a basis state is given by

$$\begin{aligned}\hat{\mathcal{O}}^{P_1} \; & |\{\lambda_a\}, \{\lambda_\alpha\}\{X^L_{ab}\}\{X^L_{a\alpha}\}\{X^L_{\alpha a}\}\{X^L_{\alpha\beta}\}\rangle_W \\ & = \sum_{a_1 \cdots a_3 = 1}^{k} X^I_{a_1 a_2} X^J_{a_2 a_3} X^K_{a_3 a_1} \; |\{\lambda_a\}, \{\lambda_\alpha\}\{X^L_{ab}\}\{X^L_{a\alpha}\}\{X^L_{\alpha a}\}\{X^L_{\alpha\beta}\}\rangle_W \end{aligned} \tag{G.28}$$

This is an example of an operator of type $(k, N-k)$ in the first proposal for a sub-algebra in [21]. An operator belonging to this first sub-algebra has a non-trivial action only on the $\lambda_a, X^L_{ab}, L \neq 1$ for $a, b = 1 \cdots k$, as shown in (5.15). The reduced density matrix which evaluates the expectation values of these operators is then obtained from the density matrix ρ_{tot} of the whole system by tracing over the variables $\lambda_\alpha, X^I_{a\alpha}, X^I_{\alpha\beta}$. This expression is given in (5.13)

A second sub-algebra was also defined which retains the off diagonal matrices of the type $X^L_{a\alpha}$. This is defined in equations (5.33) - (5.36) Acting on a state of the form (5.7) where $\lambda_i, i = 1 \cdots k$ we then have

$$(X^I)^{P_2}_{ij} = \begin{cases} X^I_{ij} & \text{if} \quad i = 1 \cdots k, j = 1 \cdots N \\ X^I_{ij} & \text{if} \quad i = 1 \cdots N, j = 1 \cdots k \\ 0 & \text{otherwise} \end{cases}$$

It is now straightforward to see that a projected operator has a non-trivial action only on $\lambda_a, X^I_{ab}, X^I_{a\alpha}$ and $X^I_{\alpha a}$. This is an operator of type $(k, N-k)$ in the second subalgebra defined in [21], whose action is given in (5.16) The corresponding reduced density matrix is given in (5.14)

Appendix H
Polar Decomposition of Matrices

In this appendix we provide the details of the polar decomposition of multiple matrices.

H.1 Two Matrices

For two matrices, the positive semi-definite matrix $\hat{R}$ given by (5.44) is expressed in terms of unitary matrices $\hat{V}, \hat{W}$ by (5.48). The inverse of the direct product matrix $\left[\hat{V} \otimes \hat{V}^* + \hat{W} \otimes \hat{W}^*\right]$ in terms of a infinite series as follows

$$\begin{aligned}\left(\hat{V}^* \otimes \hat{V} + \hat{W}^* \otimes \hat{W}\right)^{-1} =& \hat{V}^T \otimes \hat{V}^\dagger \left(\mathbb{I} \otimes \mathbb{I} + (\hat{W}\hat{V}^\dagger)^* \otimes \hat{W}\hat{V}^\dagger\right)^{-1} \\ =& \hat{V}^T \otimes \hat{V}^\dagger \sum_{n=0}^{\infty} (-1)^n \left[(\hat{W}\hat{V}^\dagger)^* \otimes \hat{W}\hat{V}^\dagger\right]^n\end{aligned} \tag{H.1}$$

which proves (5.51) with the matrix $\hat{Q}$ defined in (5.52).

Thus $(\hat{s}^2)_{kl}$ can be solved by applying the relation (5.51)

$$\begin{aligned}\left(\hat{s}^2\right)_{ij} =& \left[\left(\hat{V}^* \otimes \hat{V} + \hat{W}^* \otimes \hat{W}\right)^{-1}\right]_{ij,kl} 2\left(\hat{R}^2\right)_{kl} \\ =& 2\left[\sum_{n=0}^{\infty} (-1)^n \hat{V}^T \left[(\hat{W}\hat{V}^\dagger)^*\right]^n \otimes \hat{V}^\dagger \left[\hat{W}\hat{V}^\dagger\right]^n\right]_{ij,kl} \left(\hat{R}^2\right)_{kl} \\ =& 2\sum_{n=0}^{\infty} (-1)^n \left[\hat{V}^\dagger \left[\hat{W}\hat{V}^\dagger\right]^n\right]_{ik} \left(\hat{R}^2\right)_{kl} \left[\left[(\hat{W}\hat{V}^\dagger)^\dagger\right]^n \hat{V}\right]_{lj}\end{aligned} \tag{H.2}$$

which proves (5.53).

We now prove that the right hand side of (5.53) is positive semi-definite. Let $\{v_i\}$ be the set of eigenvectors of $\hat{Q}$. Because $\hat{Q}$ is unitary, the eigenvalues of $\hat{Q}$ take the form

$$\hat{Q}v_i = e^{i\phi_i} v_i \tag{H.3}$$

then we find the inner product

$$\begin{aligned}&\langle v_i, 2\left\{\sum_{n=0}^{\infty} (-1)^n \left[\hat{Q}^\dagger\right]^n \hat{R}^2 \hat{Q}^n\right\} v_i\rangle \\ =& 2\sum_{n=0}^{\infty} (-1)^n \langle v_i, \left(\hat{Q}^\dagger\right)^n \hat{R}^2 \hat{Q}^n v_i\rangle = 2\sum_{n=0}^{\infty} (-1)^n \langle \hat{Q}^n v_i, \hat{R}^2 \hat{Q}^n v_i\rangle \\ =& 2\sum_{n=0}^{\infty} (-1)^n \langle v_i, \hat{R}^2 v_i\rangle = \langle v_i, \hat{R}^2 v_i\rangle > 0\end{aligned} \tag{H.4}$$

since $\hat{R}^2$ is positive semi-definite according to (5.44).

Since $\hat{s}$ is positive semi-definite diagonal matrix, $(\hat{s}^2)_{ij} = \hat{s}_i^2 \delta_{ij}$, we can take the square root of both sides of (5.53) to get

$$\hat{s} = \sqrt{2}\hat{V}^\dagger \left\{ \sum_{n=0}^{\infty} (-1)^n \left[\hat{Q}^\dagger\right]^n \hat{R}^2 \hat{Q}^n \right\}^{1/2} \hat{V} \tag{5.53}$$

Plugging (5.53) back into (5.47) we obtain $\hat{Z}$,

$$\begin{aligned} \hat{Z} = \hat{V}\hat{s}\hat{W}^\dagger =& \sqrt{2} \left\{ \sum_{n=0}^{\infty} (-1)^n \left[\hat{Q}^\dagger\right]^n \hat{R}^2 \hat{Q}^n \right\}^{1/2} \hat{V}\hat{W}^\dagger \\ =& \sqrt{2} \left\{ \sum_{n=0}^{\infty} (-1)^n \left[\hat{Q}^\dagger\right]^n \hat{R}^2 \hat{Q}^n \right\}^{1/2} \hat{Q} \end{aligned} \tag{H.5}$$

This proves (5.54), where the operation $\mathfrak{L}_{\hat{V}}$ is defined in (5.55). In terms of matrix elements, the equation (5.54) can be written as

$$\hat{Z}_{ij} = \sqrt{2} \left\{ \left[\left(\mathbb{I} \otimes \mathbb{I} + \hat{Q}^T \otimes \hat{Q}^\dagger \right)^{-1} \right]_{il,mn} \left(\hat{R}^2 \right)_{mn} \right\}^{1/2} \hat{Q}_{lj}. \tag{H.6}$$

The identity (5.56) follows from the definition (5.55),

$$\begin{aligned} & \hat{V}^\dagger \left(\mathfrak{L}_{\hat{V}} \hat{M} \right)^2 \hat{V} + \left(\mathfrak{L}_{\hat{V}} \hat{M} \right)^2 \\ =& -2 \sum_{n=1}^{\infty} (-1)^n \left(\hat{V}^\dagger \right)^n \hat{M}^2 \hat{V}^n + 2 \sum_{n=0}^{\infty} (-1)^n \left(\hat{V}^\dagger \right)^n \hat{M}^2 \hat{V}^n = 2\hat{M}^2, \end{aligned} \tag{5.56}$$

we obtain (5.54).

We now explain the derivation of the integration measure (5.61). In the gauge where $\hat{R}$ is diagonal, as in (5.59), the expression for the complex matrix $\hat{Z}$ is given by (5.53) with $\hat{R}^2$ replaced by $\hat{r}^2$. In a Hilbert space basis where $\hat{r}_i$ and $\hat{Q}_{ij}$ are diagonal, the measure is given by (5.60). Parametrizing Q as in (5.61) we have

$$dQ = U \left(de^{i\Phi} - \left[e^{i\Phi}, U^\dagger dU \right] \right) U^\dagger \tag{H.7}$$

where we have used the identity $dU^\dagger = -U^\dagger dU U^\dagger$. Then define

$$dS \equiv U^\dagger dU \tag{5.62}$$

We can see that $dS^\dagger = -dS$. Then the line element becomes

$$\begin{aligned} \mathrm{tr}\left(dQ dQ^\dagger\right) =& \mathrm{tr}\left\{ de^{i\Phi} de^{-i\Phi} + \left[e^{i\Phi}, dS \right] \left[e^{-i\Phi}, dS \right] \right\} \\ =& \sum_i d\phi_i^2 + 2 \sum_{ij} e^{i\phi_i} dS_{ij} e^{-i\phi_j} dS_{ji} - 2 \sum_{ij} dS_{ij} dS_{ji} \\ =& \sum_i d\phi_i^2 + 8 \sum_{i<j} \sin^2 \frac{\phi_i - \phi_j}{2} dS_{ij} dS_{ij}^* \end{aligned} \tag{5.63}$$

This implies that we can choose $dS_{ii} = 0$. Now we have metric $ds^2 = g_{AB} d\bar{x}^A dx^B$ with $dx^A = \left(d\phi_i, dS_{ij(i<j)}, dS^*_{ij(i<j)}\right)$, where

$$g_{AB} = \begin{pmatrix} 1 & 0 & 0 \\ 0 & 4\sin^2\frac{\phi_i-\phi_j}{2} & \\ 0 & 0 & 4\sin^2\frac{\phi_i-\phi_j}{2} \end{pmatrix} \tag{H.8}$$

The determinant of g is

$$\det g_{AB} = \prod_{i<j} \left(4\sin^2\frac{\phi_i-\phi_j}{2}\right)^2 \tag{H.9}$$

Thus

$$\prod_{ij}[dQ_{ij}] = \sqrt{\det g_{AB}} \prod_i d\phi_i \prod_{i<j} dS_{ij} dS^*_{ij} \tag{H.10}$$

The final expression (5.64) follows when we use this in (5.60). To ensure that the variables r_i, ϕ_i cover the $\mathbb{R}^2$ formed by X^1, X^2 once we see that the ranges of the angles ϕ_i are

$$-\pi < \phi_i < \pi, \quad i = 1, \cdots, N \tag{H.11}$$

H.2 Three Matrices

Now consider three matrices $\hat{X}^1, \hat{X}^2, \hat{X}^3$, with $\hat{R}$ defined by (5.68). To obtain a polar decomposition we first form a complex matrix as follows

$$\hat{Y} \equiv \sqrt{(\hat{X}^1)^2 + (\hat{X}^2)^2} + i\hat{X}^3 \tag{H.12}$$

so that

$$2\hat{R}^2 = \hat{Y}\hat{Y}^\dagger + \hat{Y}^\dagger\hat{Y} \tag{H.13}$$

We can now use the procedure we used for two matrices to write

$$\hat{Y} = \sqrt{2}\left\{\sum_{n=0}^{\infty}(-1)^n \left(\hat{Q}_1^\dagger\right)^n \hat{R}^2 \hat{Q}_1^n\right\}^{1/2} \hat{Q}_1 = \left(\mathfrak{L}_{\hat{Q}_1}\hat{R}\right)\hat{Q}_1 \tag{H.14}$$

where $\hat{Q}_1$ is a unitary matrix. Therefore, in manner analogous to (5.57) we get

$$\sqrt{(\hat{X}^1)^2 + (\hat{X}^2)^2} = \frac{\hat{Y} + \hat{Y}^\dagger}{2} = \frac{\left(\mathfrak{L}_{\hat{Q}_1}\hat{R}\right)\hat{Q}_1 + \hat{Q}_1^\dagger\left(\mathfrak{L}_{\hat{Q}_1}\hat{R}\right)}{2} \tag{H.15}$$

$$\hat{X}^3 = \frac{\hat{Y} - \hat{Y}^\dagger}{2i} = \frac{\left(\mathfrak{L}_{\hat{Q}_1}\hat{R}\right)\hat{Q}_1 - \hat{Q}_1^\dagger\left(\mathfrak{L}_{\hat{Q}_1}\hat{R}\right)}{2i} \tag{H.16}$$

The next step is to consider the $\hat{X}^1, \hat{X}^2$ exactly as in the two matrix example in the previous subsection,

$$\hat{Z} \equiv \hat{X}^1 + i\hat{X}^2 \tag{H.17}$$

Then we have

$$(\hat{X}^1)^2 + (\hat{X}^2)^2 = \frac{\hat{Z}\hat{Z}^\dagger + \hat{Z}^\dagger\hat{Z}}{2} \tag{H.18}$$

Since (H.15) implies

$$(\hat{X}^1)^2 + (\hat{X}^2)^2 = \frac{1}{4}\left[\left(\mathfrak{L}_{\hat{Q}_1}\hat{R}\right)\hat{Q}_1 + \hat{Q}_1^\dagger\left(\mathfrak{L}_{\hat{Q}_1}\hat{R}\right)\right]^2 \tag{H.19}$$

it is clear we need to introduce another unitary matrix $\hat{Q}_2$ to write

$$\hat{Z} = \frac{1}{2}\left[\mathfrak{L}_{\hat{Q}_2}\left((\mathfrak{L}_{\hat{Q}_1}\hat{R})\hat{Q}_1 + \hat{Q}_1^\dagger(\mathfrak{L}_{\hat{Q}_1}\hat{R})\right)\right]\hat{Q}_2 \tag{H.20}$$

This construction is exactly like (5.54) with the replacements

$$\hat{Q} \to \hat{Q}_2 \qquad \hat{R} \to \frac{1}{2}\left[(\mathfrak{L}_{\hat{Q}_1}\hat{R})\hat{Q}_1 + \hat{Q}_1^\dagger(\mathfrak{L}_{\hat{Q}_1}\hat{R})\right] \tag{H.21}$$

Finally one can express $\hat{X}^1, \hat{X}^2$ in terms of $\hat{Z}$ and Q_2 and use (H.20) to rewrite these in terms of $\hat{R}, \hat{Q}_1, \hat{Q}_2$, while $\hat{X}_3$ is already expressed in terms of these in (H.16). This leads to (5.67). Finally one can check (5.68) directly,

$$\begin{aligned}(\hat{X}^1)^2 + (\hat{X}^2)^2 =& \frac{1}{2}\left[\mathfrak{L}_{\hat{Q}_2}\frac{\left(\mathfrak{L}_{\hat{Q}_1}\hat{R}\right)\hat{Q}_1 + \hat{Q}_1^\dagger\left(\mathfrak{L}_{\hat{Q}_1}\hat{R}\right)}{2}\right]^2 \\ &+ \frac{1}{2}\hat{Q}_2^\dagger\left[\mathfrak{L}_{\hat{Q}_2}\frac{\left(\mathfrak{L}_{\hat{Q}_1}\hat{R}\right)\hat{Q}_1 + \hat{Q}_1^\dagger\left(\mathfrak{L}_{\hat{Q}_1}\hat{R}\right)}{2}\right]^2\hat{Q}_2 \\ =& \left[\frac{\left(\mathfrak{L}_{\hat{Q}_1}\hat{R}\right)\hat{Q}_1 + \hat{Q}_1^\dagger\left(\mathfrak{L}_{\hat{Q}_1}\hat{R}\right)}{2}\right]^2\end{aligned} \tag{H.22}$$

Thus

$$\begin{aligned}(\hat{X}^1)^2 + (\hat{X}^2)^2 + (\hat{X}^3)^2 =& \left[\frac{\left(\mathfrak{L}_{\hat{Q}_1}\hat{R}\right)\hat{Q}_1 + \hat{Q}_1^\dagger\left(\mathfrak{L}_{\hat{Q}_1}\hat{R}\right)}{2}\right]^2 \\ &+ \left[\frac{\left(\mathfrak{L}_{\hat{Q}_1}\hat{R}\right)\hat{Q}_1 - \hat{Q}_1^\dagger\left(\mathfrak{L}_{\hat{Q}_1}\hat{R}\right)}{2i}\right]^2 \\ =& \frac{1}{2}\left(\mathfrak{L}_{\hat{Q}_1}\hat{R}\right)^2 + \frac{1}{2}\hat{Q}_1^\dagger\left(\mathfrak{L}_{\hat{Q}_1}\hat{R}\right)^2\hat{Q}_2 = \hat{R}^2\end{aligned} \tag{5.68}$$

To find the ranges of integration let us now work in a Hilbert space basis which are eigenstates of $\hat{r}_i$ and the $(\hat{Q}_1)_{ij}, (\hat{Q}_2)_{ij}$ with eigenvalues $r_i, (Q_1)_{ij}, (Q_2)_{ij}$. Unlike

the case of two matrices we now have additional constraints on Q_1. This is because $\sqrt{(X^1)^2+(X^2)^2}$ should be positive semi-definite. That is,

$$\frac{(\mathfrak{L}_{Q_1}R)\,Q_1+Q_1^\dagger\,(\mathfrak{L}_{Q_1}R)}{2}>0 \tag{H.23}$$

Now let the set of eigenvectors of Q_1 be $\{v_i\}$ so that $Q_1v_i=e^{i(\phi_1)_i}v_i$. Then

$$\begin{aligned}0<&\frac{1}{2}\langle v_i,\left[(\mathfrak{L}_{Q_1}R)\,Q_1+Q_1^\dagger\,(\mathfrak{L}_{Q_1}R)\right]v_i\rangle=\frac{1}{2}\left[\langle v_i,(\mathfrak{L}_{Q_1}R)\,Q_1v_i\rangle+\langle(\mathfrak{L}_{Q_1}R)\,Q_1v_i,v_i\rangle\right]\\=&\frac{1}{2}\left[e^{i(\phi_1)_i}\langle v_i,(\mathfrak{L}_{Q_1}R)\,v_i\rangle+e^{-i(\phi_1)_i}\langle(\mathfrak{L}_{Q_1}R)\,v_i,v_i\rangle\right]=\cos(\phi_1)_i\langle v_i,(\mathfrak{L}_{Q_1}R)\,v_i\rangle\end{aligned} \tag{H.24}$$

since $\mathfrak{L}_{Q_1}R$ is Hermitian. Given that $\mathfrak{L}_{Q_1}R$ is positive semi-definite, i.e. $\langle v_i,(\mathfrak{L}_{Q_1}R)\,v_i\rangle$, we have

$$\cos(\phi_1)_i>0 \tag{H.25}$$

for $i=1,\cdots,N$. This means we need to restrict the range of the $(\phi_1)_i$'s

$$-\frac{\pi}{2}\le(\phi_1)_i\le\frac{\pi}{2} \tag{H.26}$$

On the other hand, there is no condition on the eigenvalues of Q_2. These conditions lead to (5.70), and the measure of integration is (5.71).

H.3 More Matrices

Repeating using the strategy shown in (5.54), we can transfer matrices $\{\hat{X}^I\}_{I=1,\cdots,D}$ into $\{\hat{R};\hat{Q}_A\}_{A=1,\cdots,D-1}$. The transformation is similar to D-spherical coordinates

$$\begin{aligned}x_D&=r\sin(\varphi_1)\\x_{D-1}&=r\cos(\varphi_1)\sin(\varphi_2)\\x_{D-2}&=r\cos(\varphi_1)\cos(\varphi_2)\sin(\varphi_3)\\&\vdots\\x_2&=r\cos(\varphi_1)\cdots\cos(\varphi_{D-2})\sin(\varphi_{D-1})\\x_1&=r\cos(\varphi_1)\cdots\cos(\varphi_{D-2})\cos(\varphi_{D-1}).\end{aligned} \tag{H.27}$$

with

$$r\sin\varphi\to\frac{\left(\mathfrak{L}_{\hat{Q}}\hat{R}\right)\hat{Q}-\hat{Q}^\dagger\left(\mathfrak{L}_{\hat{Q}}\hat{R}\right)}{2i},\quad r\cos\varphi\to\frac{\left(\mathfrak{L}_{\hat{Q}}\hat{R}\right)\hat{Q}+\hat{Q}^\dagger\left(\mathfrak{L}_{\hat{Q}}\hat{R}\right)}{2} \tag{H.28}$$

In a Hilbert space basis which are eigenstates of $\hat{r}_i$ and the $(\hat{Q}_A)_{ij}$ with eigenvalues $r_i,(Q_A)_{ij}$, we still need to find out the constraints on $\{R;Q_A\}_{A=1,\cdots,D-1}$. Firstly, according to the argument in section H.1, we can always choose R to be positive

semi-definite since it appears in the form of R^2. Moreover, according to (H.4), we can always choose

$$\mathfrak{L}_{Q_1} R = \sqrt{2} \left\{ \sum_{n=0}^{\infty} (-1)^n \left(Q^\dagger\right)^n R^2 Q^n \right\}^{1/2} > 0 \tag{H.29}$$

Now we consider $\{Q_A\}_{A=1,\cdots,D-1}$. Notice that in (H.27) we have

$$\varphi_A \in \begin{cases} (-\pi/2, \pi/2) & A = 1, ..., D-2 \\ (-\pi, \pi) & A = D-1 \end{cases} \tag{H.30}$$

to avoid counting the space repeatedly. Then in matrix case, we should have similar conclusion that if we define

$$R_{A+1} \equiv \frac{(\mathfrak{L}_{Q_A} R_A) Q_A + Q_A^\dagger (\mathfrak{L}_{Q_A} R_A)}{2}, \quad A = 1, ..., D-2, \tag{H.31}$$

$$R_1 \equiv R, \tag{H.32}$$

then $R_A, A = 1, ..., D-1$ are all positive semi-definite.

We use Mathematical induction to derive the constraints on $Q_A, A = 1, ..., D-2$:

1. $R_1 = R$ is positive semi-definite;

2. Assume R_A is positive semi-definite. Then we have $\mathfrak{L}_{Q_A} R_A$ positive semi-definite according to (H.4).

   Now for R_{A+1}, let $\{(v_A)_i\}$ be the set of eigenvectors of Q_A, i.e. $Q_A (v_A)_i = q_A (v_A)_i$. Then for the complete set formed by $\{u_A\}$:

$$\begin{aligned} 0 <& \langle (v_A)_i, R_{A+1} (v_A)_i \rangle = \frac{1}{2} \langle (v_A)_i, (\mathfrak{L}_{Q_A} R_A) Q_A + Q_A^\dagger (\mathfrak{L}_{Q_A} R_A) (v_A)_i \rangle \\ =& \frac{1}{2} \langle (\mathfrak{L}_{Q_A} R_A) Q_A (v_A)_i, (v_A)_i \rangle + \frac{1}{2} \langle (v_A)_i, (\mathfrak{L}_{Q_A} R_A) Q_A (v_A)_i \rangle \\ =& \operatorname{Re} q_A \langle (v_A)_i, (\mathfrak{L}_{Q_A} R_A) (v_A)_i \rangle \end{aligned} \tag{H.33}$$

   Thus given that $\mathfrak{L}_{Q_A} R_A$ is positive semi-definite i.e. $\langle (v_A)_i, (\mathfrak{L}_{Q_A} R_A) (v_A)_i \rangle > 0$, we have $\operatorname{Re} q_A > 0$ i.e. Q_A is positively stable. Because the eigen-basis of Q_A forms a complete set, when R_{A+1}, R_A, Q_A are all $N \times N$ matrices, it should be a necessary and sufficient condition.

From 1° and 2°, we can show that $Q_A, A = 1, ..., D-2$ should be positively stable. Because Q_A are unitary matrices, their eigenvalues have the form

$$Q_A \equiv U_A e^{i\Phi_A} U_A^\dagger, \quad \Phi_A = \operatorname{diag}[(\phi_A)_1, (\phi_A)_2 ..., (\phi_A)_N] \tag{H.34}$$

Thus "positively stable" means that

$$\operatorname{Re} e^{i(\phi_A)_i} = \cos(\phi_A)_i > 0, \quad i = 1, ..., N; A = 1, ..., D-2 \tag{H.35}$$

The conditions of $\Phi^A, A = 1, ..., D-1$ are

$$\phi_i^A \in \begin{cases} (-\pi/2, \pi/2) & A = 1, ..., D-2 \\ (-\pi, \pi) & A = D-1 \end{cases} \qquad i = 1, ..., N \tag{5.73}$$

As a result, the measure of integration is

$$\begin{aligned} \left[\prod_I^D dX^I\right] =& \mathbb{J}(r_i, (\phi_A)_i, (S_A)_{ij}) \\ & \times \prod_i dr_i \prod_{A=1}^{D-1} \left[\prod_i d(\phi_A)_i \prod_{i<j} [4\sin^2(\frac{(\phi_A)_i - (\phi_A)_j}{2}) d(S_A)_{ij} d(S_A^\star)_{ij}]\right] \end{aligned} \tag{H.36}$$

where

$$dS_A \equiv U_A^\dagger dU_A, \quad A = 1, ..., D-1 \tag{H.37}$$

Appendix I
DBI+CS action for probe D0 brane

Consider a probe D0 brane moving in the near-horizon background (5.80) produced by a stack of N other D0 branes. The action is given by the Dirac-Born-Infeld and Chern-Simons action. In the static gauge this is given by

$$S = -\frac{1}{g_s l_s}\int dt\left[e^{-\phi}\sqrt{-g_{00}-g_{IJ}\dot{x}^I\dot{x}^J}+2A_0\right] \tag{I.1}$$

where the metric $g_{\mu\nu}$, the dilaton ϕ and the 1-form gauge fields are given in (5.80). Defining the velocity v by

$$v^2 \equiv \delta_{IJ}\partial_t x^I \partial_t x^J \tag{I.2}$$

we expand the action in powers of v. This gives

$$S = \int dt\left[\frac{1}{2R_s}v^2+\frac{15}{16}\frac{N}{R_s^3 M_p^9}\frac{v^4}{r^7}+\frac{225}{64}\frac{N^2}{R_s^5 M_p^{18}}\frac{v^6}{r^{14}}+\cdots\right]-\frac{1}{R_s}\int dt \tag{I.3}$$

where we have used (5.81) and (5.82) and expressed the coefficients in terms of M theory quantities

$$R_s = g_s l_s \qquad \ell_p = g_s^{1/3} l_s \qquad M_p^{-9} = (2\pi)^3 \ell_p^9 = (2\pi)^3 g_s^3 l_s^9 \tag{I.4}$$

The action (I.3) is in precise agreement with the action of a 11 dimensional graviton with light cone momentum $p_- = 1/R_s$ in the presence of another graviton with momentum $p_- = N/R_s$. The same action is obtained from the matrix theory calculation. For more details of the latter calculation see [289], section 12.2.

Bibliography

[1] Marcos Rigol, Vanja Dunjko, Vladimir Yurovsky, and Maxim Olshanii. Relaxation in a completely integrable many-body quantum system: an ab initio study of the dynamics of the highly excited states of 1d lattice hard-core bosons. *Physical review letters*, 98(5):050405, 2007.

[2] M. Cramer, C. M. Dawson, J. Eisert, and T. J. Osborne. Exact Relaxation in a Class of Nonequilibrium Quantum Lattice Systems. *Phys. Rev. Lett.*, 100:030602, 2008.

[3] Parijat Banerjee, Adwait Gaikwad, Anurag Kaushal, and Gautam Mandal. Quantum quench and thermalization to GGE in arbitrary dimensions and the odd-even effect. *JHEP*, 09:027, 2020.

[4] Shreyoshi Mondal, Diptiman Sen, and K Sengupta. Non-equilibrium dynamics of quantum systems: order parameter evolution, defect generation, and qubit transfer. *Quantum Quenching, Annealing and Computation*, pages 21–56, 2010.

[5] T. W. B. Kibble. Topology of Cosmic Domains and Strings. *J. Phys. A*, 9:1387–1398, 1976.

[6] W. H. Zurek. Cosmological Experiments in Superfluid Helium? *Nature*, 317:505–508, 1985.

[7] Sumit R. Das, Damian A. Galante, and Robert C. Myers. Universal scaling in fast quantum quenches in conformal field theories. *Phys. Rev. Lett.*, 112:171601, 2014.

[8] Sumit R. Das, Damián A. Galante, and Robert C. Myers. Universality in fast quantum quenches. *JHEP*, 02:167, 2015.

[9] Sumit R. Das, Damián A. Galante, and Robert C. Myers. Smooth and fast versus instantaneous quenches in quantum field theory. *JHEP*, 08:073, 2015.

[10] Sumit R. Das, Damian A. Galante, and Robert C. Myers. Quantum Quenches in Free Field Theory: Universal Scaling at Any Rate. *JHEP*, 05:164, 2016.

[11] Pawel Caputa, Sumit R. Das, Masahiro Nozaki, and Akio Tomiya. Quantum Quench and Scaling of Entanglement Entropy. *Phys. Lett. B*, 772:53–57, 2017.

[12] Sinong Liu. Complexity and scaling in quantum quench in $1+1$ dimensional fermionic field theories. *JHEP*, 07:104, 2019.

[13] Sumit R. Das, Shaun Hampton, and Sinong Liu. Quantum Quench in Non-relativistic Fermionic Field Theory: Harmonic traps and 2d String Theory. *JHEP*, 08:176, 2019.

[14] Juan Martin Maldacena. The Large N limit of superconformal field theories and supergravity. *Adv. Theor. Math. Phys.*, 2:231–252, 1998.

[15] Paul M. Chesler and Laurence G. Yaffe. Horizon formation and far-from-equilibrium isotropization in supersymmetric Yang-Mills plasma. *Phys. Rev. Lett.*, 102:211601, 2009.

[16] Sumit R. Das and Antal Jevicki. String Field Theory and Physical Interpretation of $D = 1$ Strings. *Mod. Phys. Lett. A*, 5:1639–1650, 1990.

[17] Joanna L. Karczmarek, Juan Martin Maldacena, and Andrew Strominger. Black hole non-formation in the matrix model. *JHEP*, 01:039, 2006.

[18] Sumit R. Das, Shaun Hampton, and Sinong Liu. Quantum quench in $c = 1$ matrix model and emergent space-times. *JHEP*, 04:107, 2020.

[19] Nathan Seiberg. Emergent spacetime. In *23rd Solvay Conference in Physics: The Quantum Structure of Space and Time*, 1 2006.

[20] Edward A. Mazenc and Daniel Ranard. Target Space Entanglement Entropy. 10 2019.

[21] Sumit R. Das, Anurag Kaushal, Gautam Mandal, and Sandip P. Trivedi. Bulk Entanglement Entropy and Matrices. *J. Phys. A*, 53(44):444002, 2020.

[22] Sumit R. Das, Anurag Kaushal, Sinong Liu, Gautam Mandal, and Sandip P. Trivedi. Gauge invariant target space entanglement in D-brane holography. *JHEP*, 04:225, 2021.

[23] F. Meinert, M. J. Mark, E. Kirilov, K. Lauber, P. Weinmann, A. J. Daley, and H.-C. Nägerl. Quantum quench in an atomic one-dimensional ising chain. *Physical Review Letters*, 111(5), Jul 2013.

[24] S. Trotzky, Y-A. Chen, A. Flesch, I. P. McCulloch, U. Schollwöck, J. Eisert, and I. Bloch. Probing the relaxation towards equilibrium in an isolated strongly correlated one-dimensional bose gas. *Nature Physics*, 8(4):325–330, Feb 2012.

[25] S. Hofferberth, I. Lesanovsky, B. Fischer, T. Schumm, and J. Schmiedmayer. Non-equilibrium coherence dynamics in one-dimensional bose gases. *Nature*, 449(7160):324–327, Sep 2007.

[26] Sumit R. Das. Old and New Scaling Laws in Quantum Quench. *PTEP*, 2016(12):12C107, 2016.

[27] Pasquale Calabrese and John L. Cardy. Time-dependence of correlation functions following a quantum quench. *Phys. Rev. Lett.*, 96:136801, 2006.

[28] Pasquale Calabrese and John Cardy. Quantum Quenches in Extended Systems. *J. Stat. Mech.*, 0706:P06008, 2007.

[29] Spyros Sotiriadis and John Cardy. Quantum quench in interacting field theory: A Self-consistent approximation. *Phys. Rev. B*, 81:134305, 2010.

[30] Johanna Erdmenger. Introduction to Gauge/Gravity Duality. *PoS*, TASI2017:001, 2018.

[31] Edward Witten. Anti-de Sitter space and holography. *Adv. Theor. Math. Phys.*, 2:253–291, 1998.

[32] Ulf H. Danielsson, Esko Keski-Vakkuri, and Martin Kruczenski. Spherically collapsing matter in AdS, holography, and shellons. *Nucl. Phys. B*, 563:279–292, 1999.

[33] Ulf H. Danielsson, Esko Keski-Vakkuri, and Martin Kruczenski. Black hole formation in AdS and thermalization on the boundary. *JHEP*, 02:039, 2000.

[34] Romuald A. Janik and Robert B. Peschanski. Asymptotic perfect fluid dynamics as a consequence of Ads/CFT. *Phys. Rev. D*, 73:045013, 2006.

[35] Romuald A. Janik and Robert B. Peschanski. Gauge/gravity duality and thermalization of a boost-invariant perfect fluid. *Phys. Rev. D*, 74:046007, 2006.

[36] Michal P. Heller, Romuald A. Janik, and R. Peschanski. Hydrodynamic Flow of the Quark-Gluon Plasma and Gauge/Gravity Correspondence. *Acta Phys. Polon. B*, 39:3183–3204, 2008.

[37] Sayantani Bhattacharyya and Shiraz Minwalla. Weak Field Black Hole Formation in Asymptotically AdS Spacetimes. *JHEP*, 09:034, 2009.

[38] David Garfinkle and Leopoldo A. Pando Zayas. Rapid Thermalization in Field Theory from Gravitational Collapse. *Phys. Rev. D*, 84:066006, 2011.

[39] David Garfinkle, Leopoldo A. Pando Zayas, and Dori Reichmann. On Field Theory Thermalization from Gravitational Collapse. *JHEP*, 02:119, 2012.

[40] Elena Caceres, Arnab Kundu, Juan F. Pedraza, and Di-Lun Yang. Weak Field Collapse in AdS: Introducing a Charge Density. *JHEP*, 06:111, 2015.

[41] V. Balasubramanian, A. Bernamonti, J. de Boer, N. Copland, B. Craps, E. Keski-Vakkuri, B. Muller, A. Schafer, M. Shigemori, and W. Staessens. Thermalization of Strongly Coupled Field Theories. *Phys. Rev. Lett.*, 106:191601, 2011.

[42] V. Balasubramanian, A. Bernamonti, J. de Boer, N. Copland, B. Craps, E. Keski-Vakkuri, B. Muller, A. Schafer, M. Shigemori, and W. Staessens. Holographic Thermalization. *Phys. Rev. D*, 84:026010, 2011.

[43] Damian Galante and Martin Schvellinger. Thermalization with a chemical potential from AdS spaces. *JHEP*, 07:096, 2012.

[44] Elena Caceres and Arnab Kundu. Holographic Thermalization with Chemical Potential. *JHEP*, 09:055, 2012.

[45] Walter Baron, Damian Galante, and Martin Schvellinger. Dynamics of holographic thermalization. *JHEP*, 03:070, 2013.

[46] Matthew Headrick. Lectures on entanglement entropy in field theory and holography. 7 2019.

[47] Israel Klich and Leonid Levitov. Quantum Noise as an Entanglement Meter. *Phys. Rev. Lett.*, 102:100502, 2009.

[48] H. Francis Song, Stephan Rachel, Christian Flindt, Israel Klich, Nicolas Laflorencie, and Karyn Le Hur. Bipartite Fluctuations as a Probe of Many-Body Entanglement. *Phys. Rev. B*, 85:035409, 2012.

[49] Shinsei Ryu and Tadashi Takayanagi. Holographic derivation of entanglement entropy from AdS/CFT. *Phys. Rev. Lett.*, 96:181602, 2006.

[50] Veronika E. Hubeny, Mukund Rangamani, and Tadashi Takayanagi. A Covariant holographic entanglement entropy proposal. *JHEP*, 07:062, 2007.

[51] Ro Jefferson and Robert C. Myers. Circuit complexity in quantum field theory. *JHEP*, 10:107, 2017.

[52] Paul H. Ginsparg and Gregory W. Moore. Lectures on 2-D gravity and 2-D string theory. In *Theoretical Advanced Study Institute (TASI 92): From Black Holes and Strings to Particles*, 10 1993.

[53] Igor R. Klebanov. String theory in two-dimensions. In *Spring School on String Theory and Quantum Gravity (to be followed by Workshop)*, 7 1991.

[54] Emil J. Martinec. Matrix models and 2D string theory. In *NATO Advanced Study Institute: Marie Curie Training Course: Applications of Random Matrices in Physics*, 10 2004.

[55] David J. Gross and Nikola Miljkovic. A Nonperturbative Solution of $D = 1$ String Theory. *Phys. Lett. B*, 238:217–223, 1990.

[56] E. Brezin, V. A. Kazakov, and A. B. Zamolodchikov. Scaling Violation in a Field Theory of Closed Strings in One Physical Dimension. *Nucl. Phys. B*, 338:673–688, 1990.

[57] Paul H. Ginsparg and Jean Zinn-Justin. 2-d GRAVITY + 1-d MATTER. *Phys. Lett. B*, 240:333–340, 1990.

[58] Anirvan M. Sengupta and Spenta R. Wadia. Excitations and interactions in d = 1 string theory. *Int. J. Mod. Phys. A*, 6:1961–1984, 1991.

[59] David J. Gross and Igor R. Klebanov. Fermionic string field theory of c = 1 two-dimensional quantum gravity. *Nucl. Phys. B*, 352:671–688, 1991.

[60] Joseph Polchinski. Classical limit of (1+1)-dimensional string theory. *Nucl. Phys. B*, 362:125–140, 1991.

[61] Vladimir Kazakov, Ivan K. Kostov, and David Kutasov. A Matrix model for the two-dimensional black hole. *Nucl. Phys. B*, 622:141–188, 2002.

[62] Joseph Polchinski. Tasi lectures on D-branes. In *Theoretical Advanced Study Institute in Elementary Particle Physics (TASI 96): Fields, Strings, and Duality*, 11 1996.

[63] Washington Taylor. Lectures on D-branes, gauge theory and M(atrices). In *2nd Trieste Conference on Duality in String Theory*, 6 1997.

[64] Edward Witten. Bound states of strings and p-branes. *Nucl. Phys. B*, 460:335–350, 1996.

[65] Anushya Chandran, Amir Erez, Steven S. Gubser, and S. L. Sondhi. Kibble-zurek problem: Universality and the scaling limit. *Physical Review B*, 86(6), Aug 2012.

[66] S. Mondal, D. Sen, and K. Sengupta. Non-equilibrium dynamics of quantum systems: Order parameter evolution, defect generation, and qubit transfer. *Lecture Notes in Physics*, page 21–56, 2010.

[67] Vladimir Gritsev and Anatoli Polkovnikov. Universal Dynamics Near Quantum Critical Points. 10 2009.

[68] Jacek Dziarmaga. Dynamics of a quantum phase transition and relaxation to a steady state. *Advances in Physics*, 59(6):1063–1189, Sep 2010.

[69] Anatoli Polkovnikov, Krishnendu Sengupta, Alessandro Silva, and Mukund Vengalattore. Nonequilibrium dynamics of closed interacting quantum systems. *Rev. Mod. Phys.*, 83:863, 2011.

[70] Austen Lamacraft and Joel Moore. Potential insights into non-equilibrium behavior from atomic physics, 2011.

[71] Diptarka Das, Sumit R. Das, Damián A. Galante, Robert C. Myers, and Krishnendu Sengupta. An exactly solvable quench protocol for integrable spin models. *JHEP*, 11:157, 2017.

[72] Anatoly Dymarsky and Michael Smolkin. Universality of fast quenches from the conformal perturbation theory. *JHEP*, 01:112, 2018.

[73] Mikhail Goykhman, Tom Shachar, and Michael Smolkin. On fast quenches and spinning correlators. *JHEP*, 06:168, 2018.

[74] Mikhail Goykhman, Tom Shachar, and Michael Smolkin. On quantum quenches at one loop. *JHEP*, 01:022, 2019.

[75] Julian Sonner, Adolfo del Campo, and Wojciech H. Zurek. Universal far-from-equilibrium Dynamics of a Holographic Superconductor. *Nature Commun.*, 6:7406, 2015.

[76] Paul M. Chesler, Antonio M. Garcia-Garcia, and Hong Liu. Defect Formation beyond Kibble-Zurek Mechanism and Holography. *Phys. Rev. X*, 5(2):021015, 2015.

[77] Alex Buchel, Luis Lehner, and Robert C. Myers. Thermal quenches in N=2* plasmas. *JHEP*, 08:049, 2012.

[78] Alex Buchel, Luis Lehner, Robert C. Myers, and Anton van Niekerk. Quantum quenches of holographic plasmas. *JHEP*, 05:067, 2013.

[79] Alex Buchel, Robert C. Myers, and Anton van Niekerk. Universality of Abrupt Holographic Quenches. *Phys. Rev. Lett.*, 111:201602, 2013.

[80] Mitsuhiro Nishida, Masahiro Nozaki, Yuji Sugimoto, and Akio Tomiya. Entanglement Spreading and Oscillation. *J. Stat. Mech.*, 1905(5):053102, 2019.

[81] Hugo A. Camargo, Pawel Caputa, Diptarka Das, Michal P. Heller, and Ro Jefferson. Complexity as a novel probe of quantum quenches: universal scalings and purifications. *Phys. Rev. Lett.*, 122(8):081601, 2019.

[82] Leonard Susskind. Computational Complexity and Black Hole Horizons. *Fortsch. Phys.*, 64:24–43, 2016. [Addendum: Fortsch.Phys. 64, 44–48 (2016)].

[83] Douglas Stanford and Leonard Susskind. Complexity and Shock Wave Geometries. *Phys. Rev. D*, 90(12):126007, 2014.

[84] Leonard Susskind and Ying Zhao. Switchbacks and the Bridge to Nowhere. 8 2014.

[85] Leonard Susskind. Entanglement is not enough. *Fortsch. Phys.*, 64:49–71, 2016.

[86] Adam R. Brown, Daniel A. Roberts, Leonard Susskind, Brian Swingle, and Ying Zhao. Holographic Complexity Equals Bulk Action? *Phys. Rev. Lett.*, 116(19):191301, 2016.

[87] Adam R. Brown, Daniel A. Roberts, Leonard Susskind, Brian Swingle, and Ying Zhao. Complexity, action, and black holes. *Phys. Rev. D*, 93(8):086006, 2016.

[88] Dean Carmi, Shira Chapman, Hugo Marrochio, Robert C. Myers, and Sotaro Sugishita. On the Time Dependence of Holographic Complexity. *JHEP*, 11:188, 2017.

[89] Seyed Ali Hosseini Mansoori, Viktor Jahnke, Mohammad M. Qaemmaqami, and Yaithd D. Olivas. Holographic complexity of anisotropic black branes. *Phys. Rev. D*, 100(4):046014, 2019.

[90] Shira Chapman, Michal P. Heller, Hugo Marrochio, and Fernando Pastawski. Toward a Definition of Complexity for Quantum Field Theory States. *Phys. Rev. Lett.*, 120(12):121602, 2018.

[91] Rifath Khan, Chethan Krishnan, and Sanchita Sharma. Circuit Complexity in Fermionic Field Theory. *Phys. Rev. D*, 98(12):126001, 2018.

[92] Lucas Hackl and Robert C. Myers. Circuit complexity for free fermions. *JHEP*, 07:139, 2018.

[93] Minyong Guo, Juan Hernandez, Robert C. Myers, and Shan-Ming Ruan. Circuit Complexity for Coherent States. *JHEP*, 10:011, 2018.

[94] Shira Chapman, Jens Eisert, Lucas Hackl, Michal P. Heller, Ro Jefferson, Hugo Marrochio, and Robert C. Myers. Complexity and entanglement for thermofield double states. *SciPost Phys.*, 6(3):034, 2019.

[95] Arpan Bhattacharyya, Arvind Shekar, and Aninda Sinha. Circuit complexity in interacting QFTs and RG flows. *JHEP*, 10:140, 2018.

[96] Run-Qiu Yang, Yu-Sen An, Chao Niu, Cheng-Yong Zhang, and Keun-Young Kim. Principles and symmetries of complexity in quantum field theory. *Eur. Phys. J. C*, 79(2):109, 2019.

[97] Run-Qiu Yang, Yu-Sen An, Chao Niu, Cheng-Yong Zhang, and Keun-Young Kim. More on complexity of operators in quantum field theory. *JHEP*, 03:161, 2019.

[98] Run-Qiu Yang and Keun-Young Kim. Complexity of operators generated by quantum mechanical Hamiltonians. *JHEP*, 03:010, 2019.

[99] Pawel Caputa, Nilay Kundu, Masamichi Miyaji, Tadashi Takayanagi, and Kento Watanabe. Anti-de Sitter Space from Optimization of Path Integrals in Conformal Field Theories. *Phys. Rev. Lett.*, 119(7):071602, 2017.

[100] Pawel Caputa, Nilay Kundu, Masamichi Miyaji, Tadashi Takayanagi, and Kento Watanabe. Liouville Action as Path-Integral Complexity: From Continuous Tensor Networks to AdS/CFT. *JHEP*, 11:097, 2017.

[101] Arpan Bhattacharyya, Pawel Caputa, Sumit R. Das, Nilay Kundu, Masamichi Miyaji, and Tadashi Takayanagi. Path-Integral Complexity for Perturbed CFTs. *JHEP*, 07:086, 2018.

[102] Alan P. Reynolds and Simon F. Ross. Complexity of the AdS Soliton. *Class. Quant. Grav.*, 35(9):095006, 2018.

[103] Koji Hashimoto, Norihiro Iizuka, and Sotaro Sugishita. Time evolution of complexity in Abelian gauge theories. *Phys. Rev. D*, 96(12):126001, 2017.

[104] Run-Qiu Yang, Chao Niu, Cheng-Yong Zhang, and Keun-Young Kim. Comparison of holographic and field theoretic complexities for time dependent thermofield double states. *JHEP*, 02:082, 2018.

[105] Koji Hashimoto, Norihiro Iizuka, and Sotaro Sugishita. Thoughts on Holographic Complexity and its Basis-dependence. *Phys. Rev. D*, 98(4):046002, 2018.

[106] Jie Jiang and Xiangjing Liu. Circuit Complexity for Fermionic Thermofield Double states. *Phys. Rev. D*, 99(2):026011, 2019.

[107] Daniel W. F. Alves and Giancarlo Camilo. Evolution of complexity following a quantum quench in free field theory. *JHEP*, 06:029, 2018.

[108] Jie Jiang, Jieru Shan, and Jianzhi Yang. Circuit complexity for free Fermion with a mass quench. *Nucl. Phys. B*, 954:114988, 2020.

[109] Lukasz Cincio, Jacek Dziarmaga, Marek M. Rams, and Wojciech H. Zurek. Entropy of entanglement and correlations induced by a quench: Dynamics of a quantum phase transition in the quantum Ising model. *Phys. Rev. A*, 75:052321, 2007.

[110] Frank Pollmann, Subroto Mukerjee, Andrew G. Green, and Joel E. Moore. Dynamics after a sweep through a quantum critical point. *Physical Review E*, 81(2), Feb 2010.

[111] Anna Francuz, Jacek Dziarmaga, Bartlomiej Gardas, and Wojciech H. Zurek. Space and time renormalization in phase transition dynamics. *Phys. Rev. B*, 93(7):075134, 2016.

[112] Elena Canovi, Elisa Ercolessi, Piero Naldesi, Luca Taddia, and Davide Vodola. Dynamics of entanglement entropy and entanglement spectrum crossing a quantum phase transition. *Physical Review B*, 89(10), Mar 2014.

[113] Pallab Basu and Sumit R. Das. Quantum Quench across a Holographic Critical Point. *JHEP*, 01:103, 2012.

[114] Pallab Basu, Diptarka Das, Sumit R. Das, and Tatsuma Nishioka. Quantum Quench Across a Zero Temperature Holographic Superfluid Transition. *JHEP*, 03:146, 2013.

[115] Pallab Basu, Diptarka Das, Sumit R. Das, and Krishnendu Sengupta. Quantum Quench and Double Trace Couplings. *JHEP*, 12:070, 2013.

[116] Sumit R. Das and Takeshi Morita. Kibble-Zurek Scaling in Holographic Quantum Quench : Backreaction. *JHEP*, 01:084, 2015.

[117] Hong Liu and S. Josephine Suh. Entanglement Tsunami: Universal Scaling in Holographic Thermalization. *Phys. Rev. Lett.*, 112:011601, 2014.

[118] Horacio Casini, Hong Liu, and Márk Mezei. Spread of entanglement and causality. *JHEP*, 07:077, 2016.

[119] Márk Mezei and Douglas Stanford. On entanglement spreading in chaotic systems. *JHEP*, 05:065, 2017.

[120] Jordan S. Cotler, Mark P. Hertzberg, Márk Mezei, and Mark T. Mueller. Entanglement Growth after a Global Quench in Free Scalar Field Theory. *JHEP*, 11:166, 2016.

[121] Thomas Hartman and Juan Maldacena. Time Evolution of Entanglement Entropy from Black Hole Interiors. *JHEP*, 05:014, 2013.

[122] Masahiro Nozaki, Tokiro Numasawa, Andrea Prudenziati, and Tadashi Takayanagi. Dynamics of Entanglement Entropy from Einstein Equation. *Phys. Rev. D*, 88(2):026012, 2013.

[123] Pawel Caputa, Gautam Mandal, and Ritam Sinha. Dynamical entanglement entropy with angular momentum and U(1) charge. *JHEP*, 11:052, 2013.

[124] Hong Liu and S. Josephine Suh. Entanglement growth during thermalization in holographic systems. *Phys. Rev. D*, 89(6):066012, 2014.

[125] Tarek Anous, Thomas Hartman, Antonin Rovai, and Julian Sonner. Black Hole Collapse in the 1/c Expansion. *JHEP*, 07:123, 2016.

[126] Tibra Ali, Arpan Bhattacharyya, S. Shajidul Haque, Eugene H. Kim, and Nathan Moynihan. Post-Quench Evolution of Complexity and Entanglement in a Topological System. *Phys. Lett. B*, 811:135919, 2020.

[127] E. H. Lieb and D. W. Robinson. The finite group velocity of quantum spin systems. *Commun. Math. Phys.*, 28:251–257, 1972.

[128] M. Reza Mohammadi Mozaffar and Ali Mollabashi. Entanglement Evolution in Lifshitz-type Scalar Theories. *JHEP*, 01:137, 2019.

[129] Márton Kormos, Mario Collura, and Pasquale Calabrese. Analytic results for a quantum quench from free to hard-core one dimensional bosons. *Phys. Rev. A*, 89(1):013609, 2014.

[130] Bruno Bertini. Approximate light cone effects in a non-relativistic quantum field theory after a local quench. *Phys. Rev. B*, 95(7):075153, 2017.

[131] I. A. Pedrosa. Exact wave functions of a harmonic oscillator with time-dependent mass and frequency. *Phys. Rev. A*, 55:3219–3221, Apr 1997.

[132] Orion Ciftja. A simple derivation of the exact wavefunction of a harmonic oscillator with time-dependent mass and frequency. *Journal of Physics A: Mathematical and General*, 32(36):6385, 1999.

[133] Sang Pyo Kim and Won Kim. Construction of exact Ermakov-Pinney solutions and time-dependent quantum oscillators. *J. Korean Phys. Soc.*, 69(10):1513–1517, 2016.

[134] Sumit R. Das. The one-dimensional matrix model and string theory. In *Spring School on Superstrings*, 4 1992.

[135] Antal Jevicki. Development in 2-d string theory. In *Workshop on String Theory, Gauge Theory and Quantum Gravity*, 9 1993.

[136] Hai Lin, Oleg Lunin, and Juan Martin Maldacena. Bubbling AdS space and 1/2 BPS geometries. *JHEP*, 10:025, 2004.

[137] Gautam Mandal. Fermions from half-BPS supergravity. *JHEP*, 08:052, 2005.

[138] Gautam Mandal and Nemani V. Suryanarayana. Counting 1/8-BPS dual-giants. *JHEP*, 03:031, 2007.

[139] Sumit R. Das, Jeremy Michelson, K. Narayan, and Sandip P. Trivedi. Time dependent cosmologies and their duals. *Phys. Rev. D*, 74:026002, 2006.

[140] Adel Awad, Sumit R. Das, Suresh Nampuri, K. Narayan, and Sandip P. Trivedi. Gauge Theories with Time Dependent Couplings and their Cosmological Duals. *Phys. Rev. D*, 79:046004, 2009.

[141] Adel Awad, Sumit R. Das, Archisman Ghosh, Jae-Hyuk Oh, and Sandip P. Trivedi. Slowly Varying Dilaton Cosmologies and their Field Theory Duals. *Phys. Rev. D*, 80:126011, 2009.

[142] Chong-Sun Chu and Pei-Ming Ho. Time-dependent AdS/CFT duality and null singularity. *JHEP*, 04:013, 2006.

[143] Chong-Sun Chu and Pei-Ming Ho. Spacetime singularity and AdS/CFT for time dependent background. *Prog. Theor. Phys. Suppl.*, 171:133–139, 2007.

[144] Chong-Sun Chu and Pei-Ming Ho. Time-dependent AdS/CFT duality. II. Holographic reconstruction of bulk metric and possible resolution of singularity. *JHEP*, 02:058, 2008.

[145] Neil Turok, Ben Craps, and Thomas Hertog. From big crunch to big bang with AdS/CFT. 11 2007.

[146] Ben Craps, Thomas Hertog, and Neil Turok. On the Quantum Resolution of Cosmological Singularities using AdS/CFT. *Phys. Rev. D*, 86:043513, 2012.

[147] Netta Engelhardt, Thomas Hertog, and Gary T. Horowitz. Holographic Signatures of Cosmological Singularities. *Phys. Rev. Lett.*, 113:121602, 2014.

[148] Netta Engelhardt, Thomas Hertog, and Gary T. Horowitz. Further Holographic Investigations of Big Bang Singularities. *JHEP*, 07:044, 2015.

[149] Netta Engelhardt and Gary T. Horowitz. Holographic Consequences of a No Transmission Principle. *Phys. Rev. D*, 93(2):026005, 2016.

[150] Robert H. Brandenberger, Elisa G. M. Ferreira, Ian A. Morrison, Yi-Fu Cai, Sumit R. Das, and Yi Wang. Fluctuations in a cosmology with a spacelike singularity and their gauge theory dual description. *Phys. Rev. D*, 94(8):083508, 2016.

[151] Gautam Mandal and Takeshi Morita. Quantum quench in matrix models: Dynamical phase transitions, Selective equilibration and the Generalized Gibbs Ensemble. *JHEP*, 10:197, 2013.

[152] Manas Kulkarni, Gautam Mandal, and Takeshi Morita. Quantum quench and thermalization of one-dimensional Fermi gas via phase space hydrodynamics. *Phys. Rev. A*, 98(4):043610, 2018.

[153] Mario Collura, Spyros Sotiriadis, and Pasquale Calabrese. Equilibration of a tonks-girardeau gas following a trap release. *Physical Review Letters*, 110(24), Jun 2013.

[154] Mario Collura, Spyros Sotiriadis, and Pasquale Calabrese. Quench dynamics of a tonks–girardeau gas released from a harmonic trap. *Journal of Statistical Mechanics: Theory and Experiment*, 2013(09):P09025, Sep 2013.

[155] Mario Collura, Márton Kormos, and Pasquale Calabrese. Stationary entanglement entropies following an interaction quench in 1d bose gas. *Journal of Statistical Mechanics: Theory and Experiment*, 2014(1):P01009, Jan 2014.

[156] Marton Kormos, Aditya Shashi, Yang-Zhi Chou, Jean-Sebastien Caux, and Adilet Imambekov. Interaction quenches in the one-dimensional Bose gas. *Phys. Rev. B*, 88(20):205131, 2013.

[157] Paolo P Mazza, Mario Collura, Márton Kormos, and Pasquale Calabrese. Interaction quench in a trapped 1d bose gas. *Journal of Statistical Mechanics: Theory and Experiment*, 2014(11):P11016, Nov 2014.

[158] Mario Collura, Márton Kormos, and Pasquale Calabrese. Quantum quench in a harmonically trapped one-dimensional bose gas. *Physical Review A*, 97(3), Mar 2018.

[159] P. Ruggiero, Y. Brun, and J. Dubail. Conformal field theory on top of a breathing one-dimensional gas of hard core bosons. *SciPost Phys.*, 6(4):051, 2019.

[160] A. Minguzzi and D. M. Gangardt. Exact coherent states of a harmonically confined tonks-girardeau gas. *Physical Review Letters*, 94(24), Jun 2005.

[161] Stefano Scopa, Jéremie Unterberger, and Dragi Karevski. Exact dynamics of a one dimensional bose gas in a periodic time-dependent harmonic trap. *Journal of Physics A: Mathematical and Theoretical*, 51(18):185001, Apr 2018.

[162] Manas Kulkarni and Alexander G. Abanov. Cold Fermi-gas with long range interaction in a harmonic trap. *Nucl. Phys. B*, 846:122–136, 2011.

[163] E. Bettelheim, A. G. Abanov, and P. Wiegmann. Orthogonality catastrophe and shock waves in a nonequilibrium fermi gas. *Physical Review Letters*, 97(24), Dec 2006.

[164] Stefano Scopa and Dragi Karevski. One-dimensional bose gas driven by a slow time-dependent harmonic trap. *Journal of Physics A: Mathematical and Theoretical*, 50(42):425301, 2017.

[165] Supriyo Ghosh, Kumar S. Gupta, and Shashi C. L. Srivastava. Entanglement dynamics following a sudden quench: An exact solution. *EPL*, 120(5):50005, 2017.

[166] Vasilij Petrovich Ermakov. Second-order differential equations: conditions of complete integrability. *Applicable Analysis and Discrete Mathematics*, pages 123–145, 2008.

[167] Edmund Pinney. The nonlinear differential equation $y'' + p(x)y + cy^{-3} = 0$. *Proceedings of the American Mathematical Society*, 1(5):681, 1950.

[168] Avinash Dhar, Gautam Mandal, and Spenta R. Wadia. Classical Fermi fluid and geometric action for c=1. *Int. J. Mod. Phys. A*, 8:325–350, 1993.

[169] Avinash Dhar, Gautam Mandal, and Spenta R. Wadia. Nonrelativistic fermions, coadjoint orbits of W(infinity) and string field theory at c = 1. *Mod. Phys. Lett. A*, 7:3129–3146, 1992.

[170] Avinash Dhar, Gautam Mandal, and Spenta R. Wadia. W(infinity) coherent states and path integral derivation of bosonization of nonrelativistic fermions in one-dimension. *Mod. Phys. Lett. A*, 8:3557–3568, 1993.

[171] Ingo Peschel. Calculation of reduced density matrices from correlation functions. *Journal of Physics A: Mathematical and General*, 36(14):L205–L208, Mar 2003.

[172] Israel Klich. Lower entropy bounds and particle number fluctuations in a fermi sea. *Journal of Physics A: Mathematical and General*, 39(4):L85–L91, jan 2006.

[173] Pasquale Calabrese, Mihail Mintchev, and Ettore Vicari. The entanglement entropy of one-dimensional gases. *Phys. Rev. Lett.*, 107:020601, 2011.

[174] Pasquale Calabrese, Mihail Mintchev, and Ettore Vicari. The Entanglement entropy of 1D systems in continuous and homogenous space. *J. Stat. Mech.*, 1109:P09028, 2011.

[175] Sumit R. Das. Geometric entropy of nonrelativistic fermions and two-dimensional strings. *Phys. Rev. D*, 51:6901–6908, 1995.

[176] Sumit R. Das. Degrees of freedom in two-dimensional string theory. *Nucl. Phys. B Proc. Suppl.*, 45BC:224–233, 1996.

[177] Sean A. Hartnoll and Edward Mazenc. Entanglement entropy in two dimensional string theory. *Phys. Rev. Lett.*, 115(12):121602, 2015.

[178] Pasquale Calabrese, Pierre Le Doussal, and Satya N. Majumdar. Random matrices and entanglement entropy of trapped fermi gases. *Physical Review A*, 91(1), Jan 2015.

[179] M. J. Bhaseen, Jerome P. Gauntlett, B. D. Simons, Julian Sonner, and Toby Wiseman. Holographic Superfluids and the Dynamics of Symmetry Breaking. *Phys. Rev. Lett.*, 110(1):015301, 2013.

[180] Sumit R. Das, Jeremy Michelson, K. Narayan, and Sandip P. Trivedi. Cosmologies with Null Singularities and their Gauge Theory Duals. *Phys. Rev. D*, 75:026002, 2007.

[181] Adel Awad, Sumit R. Das, K. Narayan, and Sandip P. Trivedi. Gauge theory duals of cosmological backgrounds and their energy momentum tensors. *Phys. Rev. D*, 77:046008, 2008.

[182] Thomas Hertog and Gary T. Horowitz. Holographic description of AdS cosmologies. *JHEP*, 04:005, 2005.

[183] Ben Craps, Frederik De Roo, and Oleg Evnin. Quantum evolution across singularities: The Case of geometrical resolutions. *JHEP*, 04:036, 2008.

[184] Ben Craps, Thomas Hertog, and Neil Turok. A Multitrace deformation of ABJM theory. *Phys. Rev. D*, 80:086007, 2009.

[185] Michael Smolkin and Neil Turok. Dual description of a 4d cosmology. 11 2012.

[186] Souvik Banerjee, Samrat Bhowmick, Soumyabrata Chatterjee, and Sudipta Mukherji. A note on AdS cosmology and gauge theory correlator. *JHEP*, 06:043, 2015.

[187] A. Jevicki and B. Sakita. The Quantum Collective Field Method and Its Application to the Planar Limit. *Nucl. Phys. B*, 165:511, 1980.

[188] Joseph Polchinski. Critical Behavior of Random Surfaces in One-dimension. *Nucl. Phys. B*, 346:253–263, 1990.

[189] Makoto Natsuume and Joseph Polchinski. Gravitational scattering in the c = 1 matrix model. *Nucl. Phys. B*, 424:137–154, 1994.

[190] Bruno Balthazar, Victor A. Rodriguez, and Xi Yin. The $c = 1$ string theory S-matrix revisited. *JHEP*, 04:145, 2019.

[191] Bruno Balthazar, Victor A. Rodriguez, and Xi Yin. Long String Scattering in c = 1 String Theory. *JHEP*, 01:173, 2019.

[192] Bruno Balthazar, Victor A. Rodriguez, and Xi Yin. ZZ Instantons and the Non-Perturbative Dual of c = 1 String Theory. 7 2019.

[193] Ashoke Sen. Fixing an Ambiguity in Two Dimensional String Theory Using String Field Theory. *JHEP*, 03:005, 2020.

[194] John McGreevy and Herman L. Verlinde. Strings from tachyons: The c=1 matrix reloaded. *JHEP*, 12:054, 2003.

[195] Igor R. Klebanov, Juan Martin Maldacena, and Nathan Seiberg. D-brane decay in two-dimensional string theory. *JHEP*, 07:045, 2003.

[196] S. Elitzur, A. Forge, and E. Rabinovici. Some global aspects of string compactifications. *Nucl. Phys. B*, 359:581–610, 1991.

[197] Gautam Mandal, Anirvan M. Sengupta, and Spenta R. Wadia. Classical solutions of two-dimensional string theory. *Mod. Phys. Lett. A*, 6:1685–1692, 1991.

[198] Edward Witten. On string theory and black holes. *Phys. Rev. D*, 44:314–324, 1991.

[199] M. Rocek, K. Schoutens, and A. Sevrin. Off-shell WZW models in extended superspace. *Phys. Lett. B*, 265:303–306, 1991.

[200] Herman L. Verlinde. Black holes and strings in two-dimensions. In *6th Marcel Grossmann Meeting on General Relativity (MG6)*, 12 1991.

[201] Jeffrey A. Harvey and Andrew Strominger. Quantum aspects of black holes. In *Spring School on String Theory and Quantum Gravity (To be followed by Workshop on String Theory 8-10 Apr)*, 9 1992.

[202] Larus Thorlacius. Black hole evolution. *Nucl. Phys. B Proc. Suppl.*, 41:245–275, 1995.

[203] VP Ermakov. Transformation of differential equations. *Univ. Izv. Kiev*, 20(1), 1880.

[204] G D'Alessandro, P St J Russell, and AA Wheeler. Nonlinear dynamics of a backward quasi-phase-matched second-harmonic generator. *Physical Review A*, 55(4):3211, 1997.

[205] Gregory W. Moore. Double scaled field theory at c = 1. *Nucl. Phys. B*, 368:557–590, 1992.

[206] Joanna L. Karczmarek and Andrew Strominger. Matrix cosmology. *JHEP*, 04:055, 2004.

[207] Sumit R. Das, Joshua L. Davis, Finn Larsen, and Partha Mukhopadhyay. Particle production in matrix cosmology. *Phys. Rev. D*, 70:044017, 2004.

[208] Joanna L. Karczmarek and Andrew Strominger. Closed string tachyon condensation at c = 1. *JHEP*, 05:062, 2004.

[209] Morten Ernebjerg, Joanna L. Karczmarek, and Joshua M. Lapan. Collective field description of matrix cosmologies. *JHEP*, 09:065, 2004.

[210] Partha Mukhopadhyay. On the problem of particle production in c=1 matrix model. *JHEP*, 08:032, 2004.

[211] Sumit R. Das and Joanna L. Karczmarek. Spacelike boundaries from the c=1 matrix model. *Phys. Rev. D*, 71:086006, 2005.

[212] Sumit R. Das and Luiz H. Santos. Open string descriptions of space-like singularities in two dimensional string theory. *Phys. Rev. D*, 75:126001, 2007.

[213] Raphael Bousso. The Holographic principle. *Rev. Mod. Phys.*, 74:825–874, 2002.

[214] Thomas Faulkner, Aitor Lewkowycz, and Juan Maldacena. Quantum corrections to holographic entanglement entropy. *JHEP*, 11:074, 2013.

[215] Daniel L. Jafferis, Aitor Lewkowycz, Juan Maldacena, and S. Josephine Suh. Relative entropy equals bulk relative entropy. *JHEP*, 06:004, 2016.

[216] Alexandre Belin, Nabil Iqbal, and Sagar F. Lokhande. Bulk entanglement entropy in perturbative excited states. *SciPost Phys.*, 5(3):024, 2018.

[217] Alexandre Belin, Nabil Iqbal, and Jorrit Kruthoff. Bulk entanglement entropy for photons and gravitons in AdS_3. *SciPost Phys.*, 8(5):075, 2020.

[218] Netta Engelhardt and Aron C. Wall. Quantum Extremal Surfaces: Holographic Entanglement Entropy beyond the Classical Regime. *JHEP*, 01:073, 2015.

[219] Gerard 't Hooft. On the Quantum Structure of a Black Hole. *Nucl. Phys. B*, 256:727–745, 1985.

[220] Leonard Susskind. Some speculations about black hole entropy in string theory. 10 1993.

[221] Leonard Susskind and John Uglum. Black hole entropy in canonical quantum gravity and superstring theory. *Phys. Rev. D*, 50:2700–2711, 1994.

[222] Ted Jacobson. Black hole entropy and induced gravity. 4 1994.

[223] Valeri P. Frolov, D. V. Fursaev, and A. I. Zelnikov. Statistical origin of black hole entropy in induced gravity. *Nucl. Phys. B*, 486:339–352, 1997.

[224] Ted Jacobson. Thermodynamics of space-time: The Einstein equation of state. *Phys. Rev. Lett.*, 75:1260–1263, 1995.

[225] Christopher Eling, Raf Guedens, and Ted Jacobson. Non-equilibrium thermodynamics of spacetime. *Phys. Rev. Lett.*, 96:121301, 2006.

[226] Ted Jacobson. Gravitation and vacuum entanglement entropy. *Int. J. Mod. Phys. D*, 21:1242006, 2012.

[227] Eugenio Bianchi and Robert C. Myers. On the Architecture of Spacetime Geometry. *Class. Quant. Grav.*, 31:214002, 2014.

[228] Joseph Polchinski. What is string theory? In *NATO Advanced Study Institute: Les Houches Summer School, Session 62: Fluctuating Geometries in Statistical Mechanics and Field Theory*, 11 1994.

[229] Michael R. Douglas, Daniel N. Kabat, Philippe Pouliot, and Stephen H. Shenker. D-branes and short distances in string theory. *Nucl. Phys. B*, 485:85–127, 1997.

[230] Tom Banks, W. Fischler, S. H. Shenker, and Leonard Susskind. M theory as a matrix model: A Conjecture. *Phys. Rev. D*, 55:5112–5128, 1997.

[231] Daniel N. Kabat and Washington Taylor. Linearized supergravity from matrix theory. *Phys. Lett. B*, 426:297–305, 1998.

[232] Washington Taylor and Mark Van Raamsdonk. Supergravity currents and linearized interactions for matrix theory configurations with fermionic backgrounds. *JHEP*, 04:013, 1999.

[233] Washington Taylor and Mark Van Raamsdonk. Multiple D0-branes in weakly curved backgrounds. *Nucl. Phys. B*, 558:63–95, 1999.

[234] Katrin Becker and Melanie Becker. A Two loop test of M(atrix) theory. *Nucl. Phys. B*, 506:48–60, 1997.

[235] Katrin Becker, Melanie Becker, Joseph Polchinski, and Arkady A. Tseytlin. Higher order graviton scattering in M(atrix) theory. *Phys. Rev. D*, 56:R3174–R3178, 1997.

[236] Washington Taylor. M(atrix) Theory: Matrix Quantum Mechanics as a Fundamental Theory. *Rev. Mod. Phys.*, 73:419–462, 2001.

[237] Nissan Itzhaki, Juan Martin Maldacena, Jacob Sonnenschein, and Shimon Yankielowicz. Supergravity and the large N limit of theories with sixteen supercharges. *Phys. Rev. D*, 58:046004, 1998.

[238] Michael R. Douglas and Washington Taylor. Branes in the bulk of Anti-de Sitter space. 7 1998.

[239] Sumit R. Das. Brane waves, Yang-Mills theories and causality. *JHEP*, 02:012, 1999.

[240] Sumit R. Das. Holograms of branes in the bulk and acceleration terms in SYM effective action. *JHEP*, 06:029, 1999.

[241] Michael R. Douglas, Hirosi Ooguri, and Stephen H. Shenker. Issues in (M)atrix model compactification. *Phys. Lett. B*, 402:36–42, 1997.

[242] Enrico Rinaldi, Evan Berkowitz, Masanori Hanada, Jonathan Maltz, and Pavlos Vranas. Toward Holographic Reconstruction of Bulk Geometry from Lattice Simulations. *JHEP*, 02:042, 2018.

[243] Antal Jevicki, Yoichi Kazama, and Tamiaki Yoneya. Generalized conformal symmetry in D-brane matrix models. *Phys. Rev. D*, 59:066001, 1999.

[244] Yasuhiro Sekino and Tamiaki Yoneya. Generalized AdS / CFT correspondence for matrix theory in the large N limit. *Nucl. Phys. B*, 570:174–206, 2000.

[245] Tom Banks, Michael R. Douglas, Gary T. Horowitz, and Emil J. Martinec. AdS dynamics from conformal field theory. 8 1998.

[246] Alex Hamilton, Daniel N. Kabat, Gilad Lifschytz, and David A. Lowe. Holographic representation of local bulk operators. *Phys. Rev. D*, 74:066009, 2006.

[247] Alex Hamilton, Daniel N. Kabat, Gilad Lifschytz, and David A. Lowe. Local bulk operators in AdS/CFT: A Holographic description of the black hole interior. *Phys. Rev. D*, 75:106001, 2007. [Erratum: Phys.Rev.D 75, 129902 (2007)].

[248] Chandramouli Chowdhury, Olga Papadoulaki, and Suvrat Raju. A physical protocol for observers near the boundary to obtain bulk information in quantum gravity. 8 2020.

[249] Alok Laddha, Siddharth G. Prabhu, Suvrat Raju, and Pushkal Shrivastava. The Holographic Nature of Null Infinity. *SciPost Phys.*, 10:041, 2021.

[250] Piljin Yi. Witten index and threshold bound states of D-branes. *Nucl. Phys. B*, 505:307–318, 1997.

[251] Savdeep Sethi and Mark Stern. D-brane bound states redux. *Commun. Math. Phys.*, 194:675–705, 1998.

[252] Savdeep Sethi and Mark Stern. Invariance theorems for supersymmetric Yang-Mills theories. *Adv. Theor. Math. Phys.*, 4:487–501, 2000.

[253] Naoyuki Kawahara, Jun Nishimura, and Shingo Takeuchi. Phase structure of matrix quantum mechanics at finite temperature. *JHEP*, 10:097, 2007.

[254] Gautam Mandal, Manavendra Mahato, and Takeshi Morita. Phases of one dimensional large N gauge theory in a 1/D expansion. *JHEP*, 02:034, 2010.

[255] Daniel N. Kabat and Gilad Lifschytz. Approximations for strongly coupled supersymmetric quantum mechanics. *Nucl. Phys. B*, 571:419–456, 2000.

[256] Daniel N. Kabat, Gilad Lifschytz, and David A. Lowe. Black hole thermodynamics from calculations in strongly coupled gauge theory. *Int. J. Mod. Phys. A*, 16:856–865, 2001.

[257] Simon Catterall and Toby Wiseman. Black hole thermodynamics from simulations of lattice Yang-Mills theory. *Phys. Rev. D*, 78:041502, 2008.

[258] Simon Catterall and Toby Wiseman. Extracting black hole physics from the lattice. *JHEP*, 04:077, 2010.

[259] Masanori Hanada, Yoshifumi Hyakutake, Goro Ishiki, and Jun Nishimura. Numerical tests of the gauge/gravity duality conjecture for D0-branes at finite temperature and finite N. *Phys. Rev. D*, 94(8):086010, 2016.

[260] Evan Berkowitz, Enrico Rinaldi, Masanori Hanada, Goro Ishiki, Shinji Shimasaki, and Pavlos Vranas. Supergravity from D0-brane Quantum Mechanics. 6 2016.

[261] Evan Berkowitz, Enrico Rinaldi, Masanori Hanada, Goro Ishiki, Shinji Shimasaki, and Pavlos Vranas. Precision lattice test of the gauge/gravity duality at large-N. *Phys. Rev. D*, 94(9):094501, 2016.

[262] Masanori Hanada, Jun Nishimura, Yasuhiro Sekino, and Tamiaki Yoneya. Monte Carlo studies of Matrix theory correlation functions. *Phys. Rev. Lett.*, 104:151601, 2010.

[263] Masanori Hanada, Jun Nishimura, Yasuhiro Sekino, and Tamiaki Yoneya. Direct test of the gauge-gravity correspondence for Matrix theory correlation functions. *JHEP*, 12:020, 2011.

[264] A. Joseph A. Kaushal S. Liu G. Mandal E. Rinaldi S. R. Das, M. Hanada and S. P. Trivedi. in progress.

[265] G. Mandal S. R. Das and S. P. Trivedi. Unpublished notes.

[266] Atish Dabholkar. Quantum corrections to black hole entropy in string theory. *Phys. Lett. B*, 347:222–229, 1995.

[267] Atish Dabholkar. Strings on a cone and black hole entropy. *Nucl. Phys. B*, 439:650–664, 1995.

[268] Song He, Tokiro Numasawa, Tadashi Takayanagi, and Kento Watanabe. Notes on Entanglement Entropy in String Theory. *JHEP*, 05:106, 2015.

[269] Edward Witten. Open Strings On The Rindler Horizon. *JHEP*, 01:126, 2019.

[270] Usman Naseer. Entanglement Entropy in Closed String Theory. 2 2020.

[271] C. Robin Graham and Andreas Karch. Minimal area submanifolds in AdS x compact. *JHEP*, 04:168, 2014.

[272] Ali Mollabashi, Noburo Shiba, and Tadashi Takayanagi. Entanglement between Two Interacting CFTs and Generalized Holographic Entanglement Entropy. *JHEP*, 04:185, 2014.

[273] Andreas Karch and Christoph F. Uhlemann. Holographic entanglement entropy and the internal space. *Phys. Rev. D*, 91(8):086005, 2015.

[274] M. Reza Mohammadi Mozaffar and Ali Mollabashi. On the Entanglement Between Interacting Scalar Field Theories. *JHEP*, 03:015, 2016.

[275] Vijay Balasubramanian, Borun D. Chowdhury, Bartlomiej Czech, and Jan de Boer. Entwinement and the emergence of spacetime. *JHEP*, 01:048, 2015.

[276] Vijay Balasubramanian, Ben Craps, Tim De Jonckheere, and Gábor Sárosi. Entanglement versus entwinement in symmetric product orbifolds. *JHEP*, 01:190, 2019.

[277] Johanna Erdmenger and Marius Gerbershagen. Entwinement as a possible alternative to complexity. *JHEP*, 03:082, 2020.

[278] Masanori Hanada, Antal Jevicki, Cheng Peng, and Nico Wintergerst. Anatomy of Deconfinement. *JHEP*, 12:167, 2019.

[279] Fabien Alet, Masanori Hanada, Antal Jevicki, and Cheng Peng. Entanglement and Confinement in Coupled Quantum Systems. *JHEP*, 02:034, 2021.

[280] Tarek Anous, Joanna L. Karczmarek, Eric Mintun, Mark Van Raamsdonk, and Benson Way. Areas and entropies in BFSS/gravity duality. *SciPost Phys.*, 8(4):057, 2020.

[281] Harsha R. Hampapura, Jonathan Harper, and Albion Lawrence. Target space entanglement in Matrix Models. 12 2020.

[282] Ronak M Soni and Sandip P. Trivedi. Aspects of Entanglement Entropy for Gauge Theories. *JHEP*, 01:136, 2016.

[283] Karel Van Acoleyen, Nick Bultinck, Jutho Haegeman, Michael Marien, Volkher B. Scholz, and Frank Verstraete. The entanglement of distillation for gauge theories. *Phys. Rev. Lett.*, 117(13):131602, 2016.

[284] Mthokozisi Masuku and Joao P. Rodrigues. Laplacians in polar matrix coordinates and radial fermionization in higher dimensions. *J. Math. Phys.*, 52:032302, 2011.

[285] Mthokozisi Masuku, Mbavhalelo Mulokwe, and João P. Rodrigues. Large N Matrix Hyperspheres and the Gauge-Gravity Correspondence. *JHEP*, 12:035, 2015.

[286] Mark Van Raamsdonk. Building up spacetime with quantum entanglement. *Gen. Rel. Grav.*, 42:2323–2329, 2010.

[287] Nima Lashkari, Michael B. McDermott, and Mark Van Raamsdonk. Gravitational dynamics from entanglement 'thermodynamics'. *JHEP*, 04:195, 2014.

[288] Thomas Faulkner, Monica Guica, Thomas Hartman, Robert C. Myers, and Mark Van Raamsdonk. Gravitation from Entanglement in Holographic CFTs. *JHEP*, 03:051, 2014.

[289] Katrin Becker, Melanie Becker, and John H Schwarz. *String theory and M-theory: A modern introduction*. Cambridge university press, 2006.

VITA

Sinong Liu

EDUCATION

University of Kentucky, U.S.A. *August 2016 – Present*
Ph.D. Candidate in Physics

Fudan University, P.R.China *September 2011 – July 2015*
B.Sc in Physics

PROFESSIONAL EXPERIENCE

- Graduate Teaching Assistant
  Department of Physics and Astronomy, University of Kentucky
  August 2017 – July 2020

- Graduate Research Assistant
  Department of Physics and Astronomy, University of Kentucky
  May 2018, May 2019, May 2020 and May 2021

PUBLICATIONS

- Sumit R. Das, Anurag Kaushal, **Sinong Liu**, Gautam Mandal and Sandip P. Trivedi, *"Gauge Invariant Target Space Entanglement in D-Brane Holography," Journal of High Energy Physics* **04**, 225 (2021).

- Sumit R. Das, Shaun Hampton and **Sinong Liu**, *"Quantum quench in $c = 1$ matrix model and emergent space-times," Journal of High Energy Physics* **04**, 107 (2020).

- Sumit R. Das, Shaun Hampton and **Sinong Liu**, *"Quantum Quench in Non-relativistic Fermionic Field Theory: Harmonic traps and 2d String Theory," Journal of High Energy Physics* **08**, 176 (2019).

- **Sinong Liu**, *"Complexity and scaling in quantum quench in $1+1$ dimensional fermionic field theories," Journal of High Energy Physics* **07**, 104 (2019).

- Arpan Bhattacharyya, Ling-Yan Hung, Pak Hang Chris Lau and **Si-Nong Liu**, *"Inspecting non-perturbative contributions to the Entanglement Entropy via wave-functions,". Entropy* **19**, no.12, 671 (2017)

- Arpan Bhattacharyya, Zhe-Shen Gao, Ling-Yan Hung and **Si-Nong Liu**, *"Exploring the Tensor Networks/AdS Correspondence," Journal of High Energy Physics* **08**, 086 (2016).

- Long Cheng, Ling-Yan Hung, **Si-Nong Liu** and Hong-Zhe Zhou, *"First law of entanglement entropy in topologically massive gravity," Physical Review* **D 94**, no.6, 064063 (2016).

AWARDS & HONORS

2020 – 2021	Keith B. MacAdam Graduate Excellence Fellowship in Physics and Astronomy, Department of Physics and Astronomy, University of Kentucky
Fall 2020	Graduate Fellowship, Kavli Institute for Theoretical Physics, University of California, Santa Barbara
Fall 2020	Max Steckler Fellowship, University of Kentucky
2016 – 2017	Huffaker Fellowship, Department of Physics and Astronomy, University of Kentucky
July 2015	Honored Graduated Student in Physics in National Top Talent Undergraduate Training Program, Department of Physics, Fudan University
2011 – 2015	Undergraduate Scholarship of Fudan University, Fudan University